

**MOLECULAR STUDIES OF CROSS-TALK
BETWEEN M₂ AND M₃ MUSCARINIC
ACETYLCHOLINE RECEPTOR SUBTYPES**

Thesis submitted for the degree of Doctor of
Philosophy at the University of Leicester

By

David Charles Hornigold

Department of Cell Physiology and Pharmacology,
University of Leicester, U.K

June 2001

UMI Number: U143671

All rights reserved

INFORMATION TO ALL USERS

The quality of this reproduction is dependent upon the quality of the copy submitted.

In the unlikely event that the author did not send a complete manuscript and there are missing pages, these will be noted. Also, if material had to be removed, a note will indicate the deletion.



UMI U143671

Published by ProQuest LLC 2013. Copyright in the Dissertation held by the Author.
Microform Edition © ProQuest LLC.

All rights reserved. This work is protected against
unauthorized copying under Title 17, United States Code.



ProQuest LLC
789 East Eisenhower Parkway
P.O. Box 1346
Ann Arbor, MI 48106-1346

Molecular studies of cross-talk between M₂ and M₃ muscarinic acetylcholine receptors

David C. Hornigold

Many cell-types in the body express mixed populations of muscarinic acetylcholine (mACh) receptors. For example, various types of smooth muscle express both M₂ and M₃ mACh receptors. While the M₃ mACh receptor sub-population is implicated in pharmacomechanical coupling in smooth muscle, the role of the M₂ mACh receptor remains unclear. The aim of the studies described here was to investigate if there is 'cross-talk' between the signalling pathways regulated by M₂ and M₃ mACh receptors, co-expressed in either model (CHO) cells, or a smooth muscle tissue preparation.

Based on [³H]-NMS radioligand binding, cyclic AMP and inositol 1,4,5-trisphosphate (IP₃) mass measurements, and single cell Ca²⁺-imaging experiments, stable and functional co-expression of M₂ and M₃ mACh receptors was demonstrated in two CHO-m2m3 cell lines. Initial experiments provided little evidence for M₂/M₃ mACh receptor cross-talk in CHO-m2m3 cells, as co-stimulation of the M₂ receptor had no discernible effect on M₃ receptor-mediated phospholipase C activation, assessed at the level of IP₃ and [Ca²⁺]_i. Although both M₂ and M₃ mACh receptor stimulation modulated adenylyl cyclase activity, the biphasic modulation of cyclic AMP concentration in the CHO-m2m3 cells could be explained as additivity between the responses observed in CHO-m2 and -m3 cells. M₂ and M₃ mACh receptor stimulation caused essentially opposite effects on cell proliferation, assessed by measuring [³H]-thymidine incorporation into DNA, in CHO-m2 and CHO-m3 cells. In CHO-m2m3 cells, the inhibitory M₃ mACh receptor-mediated effect appeared to dominate with respect to cell growth, however, a proliferative M₂ mACh receptor-mediated effect could be 'unmasked' using the subtype-selective mACh receptor antagonist, darifenacin.

Evidence for M₂/M₃ mACh receptor cross-talk was obtained at the level of extracellular signal-regulated protein kinase (ERK) regulation. In CHO-m2m3 cells, ERK activity increases were more sustained (>60 min), and the EC₅₀ for ERK activation by a mACh receptor agonist was approx. 50 fold lower (pEC₅₀, 7.17 ± 0.07) compared to both CHO-m2 (pEC₅₀, 5.58 ± 0.09) and CHO-m3 (pEC₅₀, 5.69 ± 0.27) cells. In contrast, agonist-stimulated c-Jun N-terminal kinase (JNK) activities were similar, in terms of both the time-course of activation and the concentration-dependency of the response, in CHO-m3 and CHO-m2m3 cells, with CHO-m2 cells showing only minimal agonist-stimulated JNK activity. In bovine tracheal smooth muscle (BTSM) slices, which co-express M₂ and M₃ mACh receptors, mACh receptor agonist stimulation produced an ERK activation profile consistent with that observed in the CHO-m2m3 cells (sustained response activated by low agonist concentrations). Further investigations of the potential cross-talk between M₂ and M₃ mACh receptors in regulating ERK activity in CHO-m2m3 cells, using pertussis toxin to inactivate G_{i/o} proteins, and receptor subtype-selective antagonists, to date have proved inconclusive.

In conclusion, this study has provided the first evidence for a facilitatory interaction between M₂ and M₃ mACh receptor signalling pathways in the regulation of both the duration and concentration-dependency of ERK activation. Further work is required (i) to establish the precise contribution(s) of each mACh receptor subtype in this cross-talk, (ii) to assess what the downstream consequences are with respect to cell fate, and (iii) to establish whether what has been learned in CHO cells provides a paradigm for tissues co-expressing M₂ and M₃ mACh receptors.

Acknowledgements

The work contained within this thesis was funded by Roche Bioscience, Palo Alto, CA, USA.

Firstly, I would like to thank my supervisor Dr R.A. John Challiss for his guidance and help throughout my three years. Also I would like to acknowledge the kind help and enthusiasm of Dr Jonathan L Blank and Don Daniels (USA).

I would like to thank all of the members of labs 324 and 347 past and present for their friendship, technical assistance and help, Raj Mistry (cAMP experiments), Helen Sherriffs, Ruth Saunders, Liz Akam, Rick Davis (single cell Ca²⁺ imaging), Paul Wylie, Karl Deacon, Drew Burdon, Ian Brockhurst and Donna Boxall. I would like to thank Dr Gary Willars for statistical analysis advice. Thanks must also be expressed to all the members of the laboratory in Palo Alto, CA, (where FLIPR analysis reported in Chapter 4 was performed), especially Bryan Wylie, Joel Gever and Don (I now understand the importance of always walking fast in the corridor!).

I would like to thank my family: Mum, Dad, Sarah, Lucy, Nick, Grandma, Grandpa, Pop and Michael for encouragement and support. I would also like to thank Kirsti for her continual encouragement and support. Many thanks to all of my other friends especially Ian B, Steve, Hazel, Gus, Sam, Dayle, Mark and the rest of the Leeds bunch.

Contents

	Page
Abstract	i
Acknowledgements	ii
Contents	iii
Abbreviations	viii
<u>Chapter One: Introduction</u>	1
1.1 Muscarinic acetylcholine receptors	1
1.1.1 Muscarinic acetylcholine receptors subtypes	2
1.1.2 G proteins	2
1.2 Muscarinic receptor signal transduction pathways	4
1.2.1 Phosphoinositide hydrolysis	6
1.2.2 Inhibition of Adenylyl Cyclase	6
1.2.3 Coupling of M ₂ and M ₃ mACh receptors to other signalling pathways	7
1.2.4 M ₂ /M ₃ receptor regulation	7
1.3 Profile of muscarinic receptor subtype distribution in smooth muscle tissues and commonly used antagonists	8
1.4 Muscarinic gene-knockout studies	8
1.5 Mitogen-activated protein kinases (MAPKs)	11
1.5.1 The mitogen-activated protein kinase cascade	11
1.5.2 Downstream targets of MAPKs	15
1.5.3 Activation of the mitogen-activated protein kinase cascade	18
1.5.3.1 Receptor tyrosine kinase (RTK) activation of MAPK	18
1.5.3.2 GPCR-mediated MAPK activation	21
1.5.3.2.1 G _i - and G _q - protein-mediated MAPK activation	21
1.5.3.2.2 G _s , G _o - protein and cAMP protein kinase-mediated	25
1.5.3.2.3 Role of PI3 Kinase in MAPK signalling	26
1.5.3.2.4 GPCR-mediated activation of JNK and p38 pathways	26
1.5.3.2.5 Transactivation	27
1.5 Aims of project	29
<u>Chapter Two: Experimental methodology</u>	31
2.1 General cell culture and transfection procedure	31
2.1.1 Cell culture	31
2.1.2 Transfection procedures	31
2.2 N-methyl-[³ H]-scopolamine (NMS) binding	32
2.2.1 Membrane preparation	32
2.2.2 [³ H]-NMS saturation binding	32
2.2.3 [³ H]-NMS displacement binding	33
2.3 Inositol 1,4,5-trisphosphate (IP ₃) mass accumulation	33
2.3.1 Cell preparation	33
2.3.2 Sample generation	33
2.3.3 IP ₃ mass assay	34
2.4 Measurement of total [³ H]-IP _x accumulation	34
2.4.1 Cell preparation and radio-labelling	34

2.4.2	Sample preparation	35
2.4.3	[³ H]-InsP _x sample separation	35
2.5	Cyclic AMP accumulation	35
2.5.1	Cell preparation	35
2.5.2	Sample generation	36
2.5.3	Cyclic AMP determination	36
2.6	Single cell calcium Imaging Experiments	36
2.7	Measurement of [Ca ²⁺] _i using fluorimetric imaging plate reader (FLIPR)	37
2.7.1	Cell preparation	37
2.7.2	Measurement of [Ca ²⁺] _i for a population of cells	37
2.8	[³ H]-Thymidine incorporation	38
2.8.1	Cell preparation	38
2.8.2	Measurement of [³ H]-thymidine incorporation	38
2.9	Mitogen Activated Protein Kinase (MAPK) Assays	39
2.9.1	Cell preparation	39
2.9.2	Extracellular-signal regulated kinase (ERK) activation	39
2.9.2.1	Sample generation	39
2.9.2.2	ERK Activation Assay	40
2.9.3	JNK Activation	40
2.9.3.1	Sample generation	40
2.9.3.2	Preparation of GST-c-Jun fusion protein	41
2.9.3.3	JNK activation assay	41
2.10	Bovine tracheal smooth muscle	42
2.10.1	BTSM slice preparation	42
2.10.2	BTSM slice stimulation	42
2.10.3	Phosphorylated ERK western blot analysis	43
2.11	Protein determinations	44
2.11.1	Lowry protein assay	44
2.11.2	Bradford protein assay	44
2.12	Data analysis	44
	Materials	46

Chapter Three: General characterisation of receptor populations and second messenger signalling in CHO cells expressing or co-expressing M₂- and M₃- mAChRs. 47

3.1	Introduction	47
3.2	Results	48
3.2.1	Determination of total receptor populations in CHO-m2, CHO-m3 and CHO-m2m3 (B2) cells by [³ H]-N-methyl-[³ H]-scopolamine (NMS) binding.	48
3.2.2	[³ H]-NNMS displacement binding in CHO-m2, CHO-m3 and CHO-m2m3 (B2) cells	49
3.2.3	Measurement of mACh receptor agonist induced [³ H]-cAMP accumulation in CHO-m2, CHO-m3 and CHO-m2m3 cells	56
3.2.4	Pharmacological characterisation of [³ H]-cAMP accumulation in CHO-m2, CHO-m3 and CHO-m2m3 cells	64
3.2.5	Measurement of mAChR agonist stimulated [³ H]-IP ₃ accumulation in CHO-m2, CHO-m3 and CHO-m2m3 (B2) cells	67

3.2.6	Assessment of single-cell calcium responses in a field of CHO-m2m3 (B2) cells	70
3.3	Discussion	70
Chapter Four: Characterisation of phosphoinositide and Ca²⁺ responses in CHO-m2, CHO-m3 and CHO-m2m3 (B2) cells		78
4.1	Introduction	78
4.2	Results	79
4.2.1	Comparison of agonist-stimulated [³ H]-IP _x accumulation in CHO-m2, CHO-m3 and CHO-m2m3 (B2) cells	79
4.2.2	Analysis of calcium-release profiles in CHO-m2, CHO-m3 and CHO-m2m3 (B2) cells	83
4.2.3	Inhibition of MCh-stimulated Ca ²⁺ responses by mACh receptor antagonists	89
4.2.4	Involvement of extracellular Ca ²⁺ on Ca ²⁺ response profiles in CHO-m2, CHO-m3 and CHO-m2m3 (B2) cells	89
4.2.5	Investigating the coupling mechanism between M ₂ mACh receptor activation and the Ca ²⁺ response in CHO-m2 cells	102
4.3	Discussion	106
Chapter Five: Comparison of [³H]-Thymidine incorporation in CHO-m2, CHO-m3 and CHO-m2m3 cells		117
5.1	Introduction	117
5.2	Method	118
5.3	Results	120
5.3.1	Effects of serum on [³ H]-thymidine incorporation into DNA in serum-starved CHO-m2, CHO-m3 and CHO-m2m3 cells	120
5.3.2	Effects of mAChR agonists on [³ H]-thymidine incorporation in serum-starved CHO-m2, CHO-m3 and CHO-m2m3 cells	120
5.3.3	Agonist effects on [³ H]-thymidine incorporation in serum-replete CHO-m2, CHO-m3 and CHO-m2m3 cells	127
5.3.4	Inhibition of muscarinic receptor-mediated effects on [³ H]-thymidine incorporation by a subtype-selective antagonist	134
5.4	Discussion	141
Chapter Six: Characterisation of ERK and JNK activation by M₂ and M₃ mAChRs in CHO cells and BTSM tissue preparations		146
6.1	Introduction	146
6.2	Methods	148
6.3	Results	149
6.3.1	Time-course profiles of ERK activation in CHO-m2, CHO-m3 and CHO-m2m3 cell lines	149
6.3.2	Concentration-dependency of MCh-stimulated ERK activation in CHO-m2, CHO-m3 and CHO-m2m3 (B2) cells	149
6.3.3	Time-course measurement of JNK activation in CHO-m2, CHO-m3 and CHO-m2m3 (B2) cells	153

6.3.4	Concentration-dependency of MCh stimulated JNK activation in CHO-m3 and co-expressing CHO-m2m3 (B2) cells	153
6.3.5	Measurement of mACh receptor agonist-stimulated ERK and JNK activation in BTSM slice preparations	160
6.4	Discussion	160
<u>Chapter Seven: Dissection of synergistic ERK activation through co-stimulation of M₂- and M₃-receptors in CHO-m2m3 cells and BTSM tissue preparations</u>		165
7.1	Introduction	165
7.2	Results	
7.2.1	Effects of pertussis toxin pretreatment on concentration-dependency of ERK activation in CHO-m2, CHO-m3 and CHO-m2m3 (B2) cells	166
7.2.2	Pharmacological dissection of M ₂ - and M ₃ - receptor components of MCh-stimulated ERK activation in CHO-m2, CHO-m3, CHO-m2m3 (B2) cells and BTSM tissue slices	172
7.2.3	Measurement effects of co-stimulating mACh receptors and endogenous P2Y receptors on ERK activation in CHO-m2 cells	180
7.3	Discussion	183
<u>Chapter Eight: Final discussion</u>		191
<u>Appendix</u>		200
	Materials	200
	SDS-PAGE gel compositions	204
<u>References</u>		205

Abbreviations

AC	Adenylyl Cyclase
ACh	Acetylcholine
AChR	Acetylcholine Receptor
ATP	Adenosine 5'triphosphate
ATR	Atropine
B_{max}	Maximal specific binding
cAMP	Adenosine 3', 5'-cyclic monophosphate
CCh	Carbachol
CHO	Chinese Hamster Ovary
DNA	Deoxyribonucleic Acid
DAG	sn-1,2-diacylglycerol
DAR	Darifenacin
DPM	Disintegrations per minute
EC₅₀	[Agonist] to produce 50 % maximal response (M)
EC₁₂₀	Supra-maximal [Agonist]
EGF	Epidermal Growth Factor
EGFR	Epidermal Growth Factor Receptot
EGTA	Ethylene glycol bis(β-aminoethyl ether)-N',N',N',N'-tetraacetate
ERK	Extracellular signal Regulated protein Kinase
FCS	Foetal Calf Serum
FK	Forskolin
FLIPR	Fluorimetric Imaging Plate Reader
GAP	GTPase-activating protein
GDP	Guanosine-diphosphate
GPCR	G-protein Coupled Receptor
G-protein	Guanine-nucleotide binding protein
GRB2	Growth-factor-Receptor Binding protein 2
GST	Glutathione S-transferase
GTP	Guanosine-triphosphate
IC₅₀	[Ligand] to inhibit maximal response by 50 % (M)
IP_x	Total Inositol Phosphates
IP₃	Inositol 1,4,5-trisphosphate
IP₃R	Inositol 1,4,5-trisphosphate Receptor
JIP-1	JNK-Interacting binding Protein-1
JNK	c-Jun NH ₂ -terminal kinase
K_D	Equilibrium dissociation constant
KHB	Krebs-Henseleit Buffer
mAChR	Muscarinic Acetylcholine Receptor
M₂-AChR	M ₂ -Muscarinic Acetylcholine Receptor
M₃-AChR	M ₃ -Muscarinic Acetylcholine Receptor
MAPK	Mitogen-Activated Protein Kinase
MAPKK	Mitogen-Activated Protein Kinase Kinase
MAPKKK	Mitogen-Activated Protein Kinase Kinase Kinase
MCh	Methacholine

MEK	MAPK / ERK Kinase
MEKK	MAPK / ERK Kinase Kinase
MEM-α	Minimum Essential Medium- α
METH	Methoctramine
MLK	Mixed Lineage Kinase
NBCS	Newborn Calf Serum
NMS	N-methyl scopolamine
NSB	Non-specific binding
PDE	Phosphodiesterase
PDGF	Platelet-Derived Growth Factor
pEC₅₀	$-\log_{10}(EC_{50})$
pIC₅₀	$-\log_{10}(IC_{50})$
PI	Phosphatidylinositol
PIP₂	Phosphatidylinositol 4,5-bisphosphate
PI3 K	Phosphoinositide 3-Kinase
PIP₂	Phosphatidyl 4,5-bisphosphate
PKA	Protein kinase A
PKC	Protein kinase C
PLA₂	Phospholipase A ₂
PLC	Phospholipase C
PLD	Phospholipase D
PTX	Pertussis Toxin
RTK	Receptor Tyrosine Kinase
SAPK	Stress-Activated Protein Kinase
SDS PAGE	Sodium Dodecyl Sulfate Polyacrylamide Gel Electrophoresis
SH2	Src-homology domain
SOS	Son-Of-Sevenless
TCA	Trichloroacetic acid
TRIP	Tripitramine

Chapter One: Introduction

The research contained within this thesis studies cross-talk between M₂- and M₃-muscarinic acetylcholine receptors co-expressed in both recombinant model cell lines and in smooth muscle tissue.

The release of acetylcholine by parasympathetic nerves is believed to be important in regulating the contractile state of smooth muscle in both health and disease. Acetylcholine mediates its intracellular effects by acting on nicotinic and muscarinic cholinergic receptor subtypes. Mixed populations of muscarinic receptors are found in many tissue types and both M₂ and M₃ receptor subtypes are found in smooth muscle. Initial functional studies indicated that the M₃ receptor population was responsible for regulating the contraction of most types of smooth muscle. However, using radioligand binding it was revealed, with only a few exceptions, that the M₂ receptor subtype was predominant over the M₃ receptor. It was found that M₂ receptors constitute between 70 and 90% of the muscarinic receptor population in many types of smooth muscle with the remainder being M₃ receptors (reviewed by Eglen et al., 1996a). This interesting phenomenon of nearly all smooth muscle tissue types conserving a co-expressed mixed population of M₂ and M₃ receptors is the basis of this thesis and raises the question: “Does cross-talk exist between the two receptors and what function does the M₂ receptor population fulfil in tissues?”. Muscarinic receptors belong to the seven transmembrane-spanning domain superfamily of receptors coupling to conventional second messenger pathways as well as activating mitogen-activated protein kinases. The following discusses muscarinic receptors and their downstream signalling pathways in detail.

1.1 Muscarinic acetylcholine receptors

In 1914, Dale classified the effects of acetylcholine into two types of response, one which is mimicked by muscarine, and inhibited by atropine, and one which is mimicked by nicotine. However, it was not until long after this that it became evident that there was more than one subtype of muscarinic receptor.

1.1.1 Muscarinic acetylcholine receptors subtypes

Muscarinic acetylcholine (mACh) receptors were initially sub-divided pharmacologically, using pirenzepine, into two subtypes (M_1 -neural and M_2 -heart; Hammer et al., 1980), then later into three subtypes (M_1 -neural, M_2 -cardiac and M_3 -glandular /smooth muscle; Birdsall et al., 1983) by using such ligands as 4-diphenylacetoxy-n-methylpiperidine (4-DAMP). Human mACh receptors have more recently been defined into five subtypes (M_1 - M_5) through cloning techniques (Kubo et al., 1986; Bonner et al., 1987, 1988; for reviews see Caulfield, 1993; Eglen et al., 1996a; Eglen and Nahorski, 2000)

All muscarinic receptors belong to the guanine-nucleotide binding protein (G-protein) coupled receptor superfamily. All G protein-coupled receptors (GPCRs) are characterised by a single polypeptide chain with seven hydrophobic transmembrane spanning regions linked alternatively by intracellular and extracellular loops (Wess, 1993). The five muscarinic receptor subtypes have a high amino acid sequence similarity within the seven hydrophobic transmembrane spanning domains ($\approx 90\%$). However, there is little sequence similarity in the hydrophilic cytoplasmic and extracellular loops and tails (Wess, 1993). Molecular characterisation of the five human receptor subtypes revealed their lengths to be 460, 466, 590, 479 and 532 for m_1 - m_5 , respectively. The large third intracellular (i3) loop is believed to be critically involved in G protein-coupling (for reviews see Hulme et al., 1990; Wess, 1993; Felder 1995).

1.1.2 G proteins

G protein-coupled receptors are integral membrane proteins involved in the transmission of signals from the extracellular environment to the cytoplasm through interaction with heterotrimeric G proteins. Heterotrimeric G proteins are complexes consisting of three subunits (existing as an α -GDP bound (inactive form) and $\beta\gamma$ complex).

The signalling pathway observed with GPCRs, following the binding of the agonist (e.g. acetylcholine) to its specific receptor (e.g. muscarinic M_2 receptors) on the cell surface, is initially a conformational change in the receptor allowing it to interact with a heterotrimeric G protein (e.g. G_i). The receptor-G protein complex facilitates guanine nucleotide exchange on the α subunit and the GTP-bound α subunit (active) and $\beta\gamma$ complex dissociate from the receptor complex to initiate intracellular signalling responses respectively (See Figure 1.1;

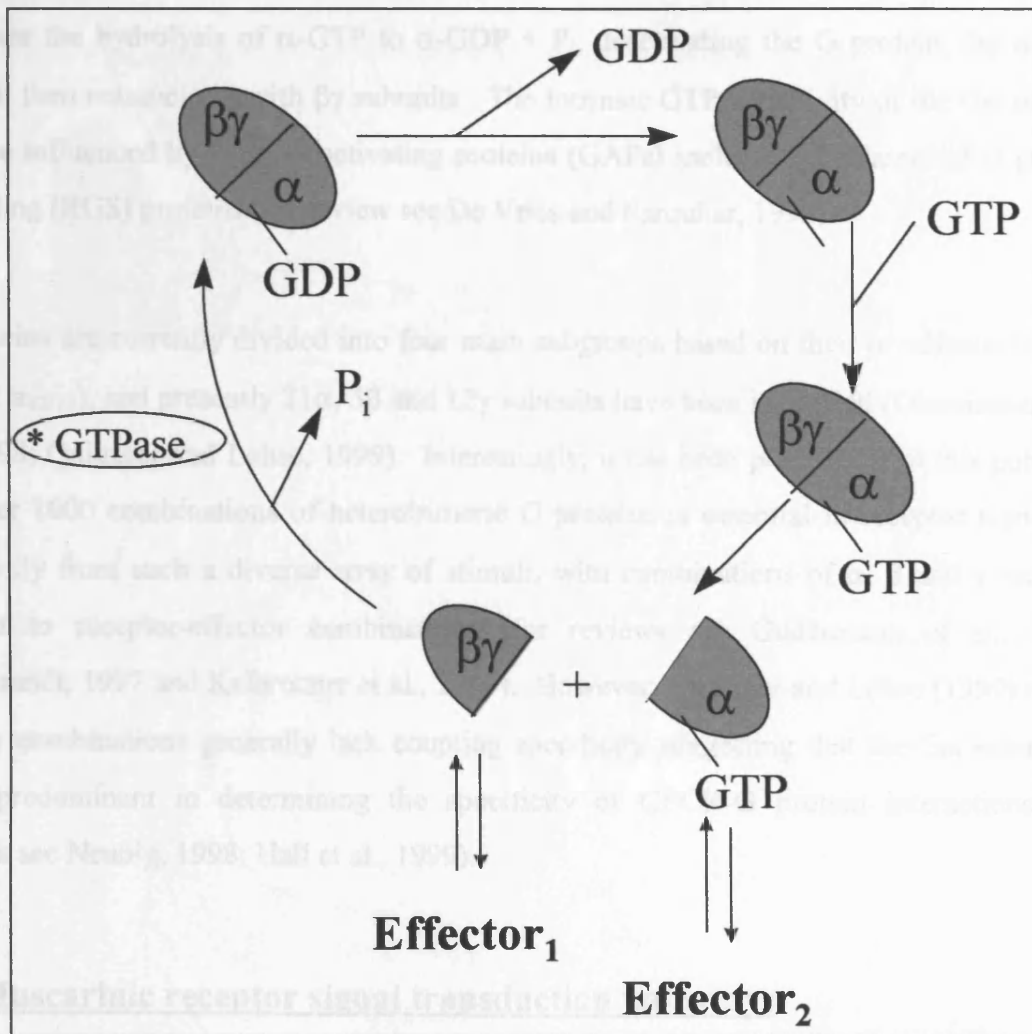


Figure 1.1 Summary diagram of heterotrimeric G protein activation cycle (see text for details).

The muscarinic receptors (M_1 , M_2 and M_4) preferentially couple via $G_{i/o}$ proteins to the inhibition of adenylyl cyclase (Carroll, 1993; see Figure 1.2). A simple example illustrating the combination of these two preferred signal transduction mechanisms is the effect of co-stimulating M_1 and M_2 mACh receptors in some smooth muscle preparations. M_2 mACh receptor stimulation causes the generation of inositol 1,4,5-trisphosphate (IP_3) and 1,2-dioleoylglycerol (DAG) initiating muscle contraction, and contributing to the sustained phase of contraction, respectively (see 1.2.1 Phosphoinositide hydrolysis section below). The contribution made by M_1 mACh receptors to the contractile response appears to be more indirect, perhaps involving a decrease in cyclic AMP concentration (and a decrease in cyclic AMP-dependent protein kinase activity; see 1.2.2 Inhibition of adenylyl cyclase below) and providing an inhibitory signal to prevent adenylyl cyclase activation by agonists causing muscle relaxation (e.g. β -adrenoceptor agonists). Although some studies have demonstrated a role for the M_2 mACh receptor in the smooth muscle contractile response (Fernandes et al., 1992; Sawyer and Ebner, 1999), others

also see Birnbaumer et al., 1990 for review). The intrinsic GTPase activity of the α subunit catalyses the hydrolysis of α -GTP to α -GDP + P_i , deactivating the G protein, the α -GDP subunit then reassociates with $\beta\gamma$ subunits. The intrinsic GTPase activity of the $G\alpha$ subunit may be influenced by GTPase activating proteins (GAPs) including regulators of G protein signalling (RGS) proteins (for review see De Vries and Farquhar, 1999).

G proteins are currently divided into four main subgroups based on their α subunits (α_s , α_i , α_q and $\alpha_{12/13}$), and presently 21 α , 5 β and 12 γ subunits have been identified (Dhanasekaran et al., 1998; Quitterer and Lohse, 1999). Interestingly, it has been proposed that this potential for over 1000 combinations of heterotrimeric G proteins is essential in receptor signalling specificity from such a diverse array of stimuli, with combinations of α , β and γ proteins distinct to receptor-effector combinations (for reviews see Gudermann et al., 1996; Hildebrandt, 1997 and Kalbrenner et al., 1999). However, Quitterer and Lohse (1999) report that $\beta\gamma$ combinations generally lack coupling specificity suggesting that the $G\alpha$ subunit is often predominant in determining the specificity of GPCR-G protein interactions (for reviews see Neubig, 1998; Hall et al., 1999).

1.2 Muscarinic receptor signal transduction pathways

The muscarinic receptors M_1 , M_3 and M_5 preferentially couple, via $G_{q/11}$ proteins, to phospholipase C-mediated phosphoinositide hydrolysis, while M_2 and M_4 preferentially couple, via $G_{i/o}$ proteins, to the inhibition of adenylyl cyclase (Caulfield, 1993; see Figure 1.2). A simple example illustrating the coordination of these two preferred signal transduction mechanisms is the effect of co-stimulating M_2 and M_3 mACh receptors in some smooth muscle preparations. M_3 mACh receptor stimulation causes the generation of inositol 1,4,5-trisphosphate (IP_3) and 1,2-diacylglycerol (DAG) initiating muscle contraction, and contributing to the sustained phase of contraction, respectively (see 1.2.1 Phosphoinositide hydrolysis section below). The contribution made by M_2 mACh receptors to the contractile response appears to be more indirect, perhaps involving a decrease in cyclic AMP concentration (and a decrease in cyclic AMP-dependent protein kinase activity; see 1.2.2 Inhibition of adenylyl cyclase below) and providing an inhibitory input to prevent adenylyl cyclase activation by agonists causing muscle relaxation (e.g. β -adrenoceptor agonists). Although some studies have demonstrated a role for the M_2 mACh receptor in the smooth muscle contractile response (Fernandes et al., 1992; Sawyer and Ehlert, 1999), others

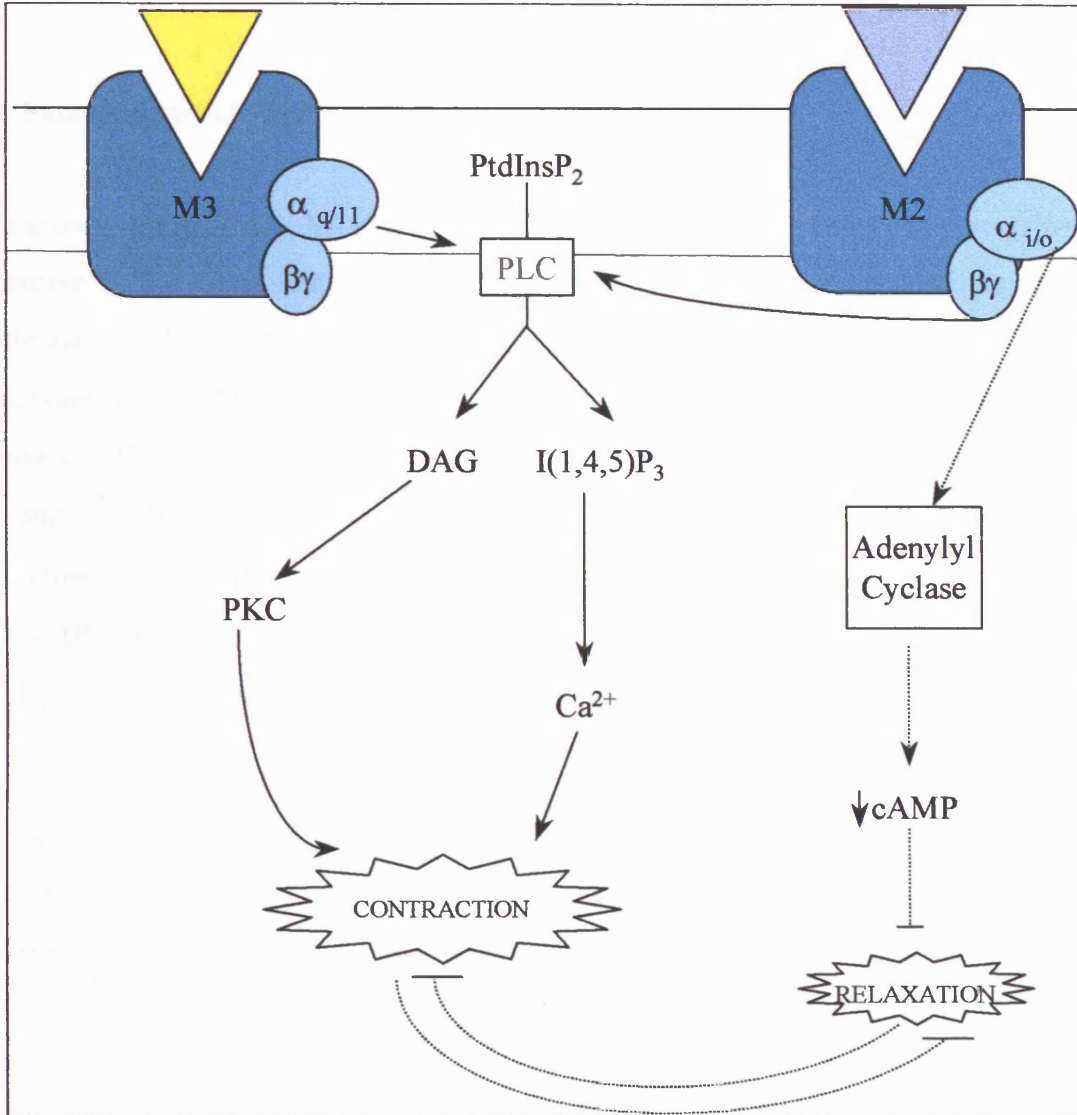


Figure 1.2 A Schematic representation of the signal transduction pathways from M₂ and M₃ muscarinic receptors, both coupling via G proteins (M₃ preferentially with G_{q/11} and M₂ with G_i) to their downstream second messengers. Dotted lines represent inhibitory mechanisms. See text for details.

have suggested that M₂ mACh receptor stimulation plays little or no role under normal physiological conditions (Roffel et al., 1995; see Eglen et al., 1996a for further discussion).

1.2.1 Phosphoinositide hydrolysis

As is shown in Figure 1.2, M₃ muscarinic receptors preferentially couple to pertussis-toxin-insensitive G_{q/11} G proteins (Caulfield, 1993) which lead to increased activation of the membrane bound phosphoinositide-specific phospholipase C (PLC). There are a number of isoenzymic forms (almost 20) of PLC, divided into PLC β , PLC γ and PLC δ subtypes, (for reviews see Rhee and Dennis 1996; Exton, 1996). It is the PLC- β isoenzymes that have been shown to be involved in signalling via G $\alpha_{q/11}$ proteins (Exton, 1996). PLC has also been shown to be activated by G $\beta\gamma$ subunits of pertussis toxin-sensitive or -insensitive G proteins (Blank et al., 1992; Camps et al., 1992), although whether $\beta\gamma$ -subunits can activate PLC- β *per se*, or require G α_q remains uncertain (Chan et al., 2000).

The activation of PLC- β leads to increased hydrolysis of phosphatidylinositol 4,5-bisphosphate (PIP₂) producing inositol 1,4,5-trisphosphate (IP₃) and *sn*-1,2-diacylglycerol (DAG) (Nahorski et al., 1997). The increased production of IP₃ leads to the initiation of contraction in smooth muscle via the release of endoplasmic reticular Ca²⁺ stores (Berridge, 1993). Increased production of DAG within the membrane leads to the activation of a number of types of protein kinase C (PKC), which in smooth muscle are believed to be involved in the maintenance phase of contraction (Rasmussen, 1987) as the direct activation of PKC with phorbol esters has been shown to cause a slowly developing contractile response (Rasmussen, 1987).

1.2.2 Inhibition of Adenylyl Cyclase

The M₂ receptor preferentially links via pertussis toxin-sensitive G_i subtypes of G proteins to inhibit the activity of adenylyl cyclase (Caulfield, 1993). The family of adenylyl cyclase isoenzymes is now known to contain at least nine types, each with 12 transmembrane spanning domains, and they are differentially regulated, e.g. stimulated or inhibited by Ca²⁺ or G $\beta\gamma$ subunits (for reviews see Cooper et al. 1995; Sunahara et al., 1996; Simmonds, 1999). The inhibition of adenylyl cyclase activity reduces levels of cyclic AMP (cAMP) production, and decreases protein kinase A (PKA) activity, which can then have an inhibitory influence

on effects caused by G_s-linked receptors, for example β-adrenoceptors, therefore putatively counteracting smooth muscle relaxation mediated by the latter (Eglen et al., 1994).

1.2.3 Coupling of M₂ and M₃ mACh receptors to other signalling pathways

M₂ mACh receptors have been shown to signal via both Gα (inhibition of cAMP accumulation) and Gβγ subunits. G_i-derived βγ-subunits may regulate PLC, Phospholipase A₂ (PLA₂), sphingosine kinase and PI3-kinase, which has been suggested to be a requirement of G_i signalling to MAPK activation (Lopez-Illasca et al., 1997; also see Section 1.6). Gβγ are known to be important in regulation of ion channels including G protein-dependent inwardly-rectifying K⁺ channels (GIRKs, Leaney and Tinker, 2000); N- and P/Q-type voltage-operated Ca²⁺ channels (VOCCs) and non-selective cation channels (see Eglen et al., 1996a; Wang et al., 1997; Zholos and Bolton, 1998; Wang et al., 1999)

M₃ mACh receptors have been shown to regulate a variety of cellular effector targets in addition to PLC activity, however there has been difficulty in distinguishing whether the particular pathways are independent or downstream of IP₃/Ca²⁺ release or DAG/PKC activation (PLC inhibitors e.g. U73122 have proven to be poor pharmacological tools). M₃ receptors couple efficiently to PLA₂ and phospholipase D (PLD) as well as PLC activities. M₂ and M₃ receptor function has also been shown to include regulation of ion channels and the MAPK pathway (for reviews see Caulfield, 1993; Gutkind, 1995 and see Section 1.6). Recent reports have suggested muscarinic receptor activation in smooth muscle causes cytoskeletal changes, which may be brought about via a G_q (or G_{12/13}, see Kozasa et al., 1998) -dependent activation of the Rho small GTPase family (Hirshman and Emala, 1999; Linesman et al., 2000).

1.2.4 M₂ / M₃ receptor regulation

Upon chronic exposure to agonist GPCRs, including muscarinic receptors, have been shown to be phosphorylated by G protein receptor kinases (GRKs) or PKC as well as other kinases including PKA and perhaps casein kinase 1α (Wess, 1993; Tobin et al. 1996). Subsequent to phosphorylation GPCRs have been demonstrated to internalise in clathrin-coated pits, involving the binding of arrestin and dynamin (for reviews see Lefkowitz, 1998; Ceresa and

Schmid, 2000; Ferguson, 2001). Phosphorylation with GRKs has been associated with homologous desensitisation and PKC with heterologous desensitisation (Wess, 1993). However, M₂ receptors differ from M₃ muscarinic receptors and classical GPCRs as they can internalise by a dynamin-insensitive, as yet unclassified pathway (Roseberry et al., 2001).

1.3 Profile of muscarinic receptor subtype distribution in smooth muscle tissues and commonly used antagonists

Mixed populations of muscarinic receptors are found in many tissue types and both M₂ and M₃ receptor subtypes are found in smooth muscle. Although the muscarinic receptors have been the focus of many signalling pathway studies, these have often been frustrated by the lack of subtype-specific or -selective ligands. Due to the lack of subtype-specific agonists, antagonists are used to discriminate between the receptor subtypes. Profiles of the limited 'selectivity windows' of some commonly used muscarinic antagonists are summarised in Table 1.1 below. Table 1.1 shows that tripitramine (M₂>M₃) and darifenacin (M₃>M₂) have the 'greatest selectivity window' for discriminating between M₂ and M₃ receptors, with the former compound exhibiting >100 fold selectivity. Pharmacological dissection of mACh receptor distribution has been characterised by comparing relative affinity profiles using the antagonists mentioned above. Initial functional studies had indicated that the M₃ population is responsible for regulating the contraction of most types of smooth muscle. However, using radioligand binding it was revealed, with only a few exceptions, that in fact the M₂ subtype population was predominant over the M₃. It was found that M₂ receptors made up between 70 and 90% of the muscarinic receptor population in smooth muscle with the remainder being M₃ receptors (Eglen et al., 1996a). For example, Eglen et al., (1996a), reported M₂ receptor populations in lung tissue of young guinea-pigs making up 73% of the muscarinic receptor population (and the M₃ 23%). However, it should be noted that isolated rat uterus studies disclosed a tissue type demonstrating a predominant M₃ (≈ 65 %) over M₂ (≈35 %) receptor population (Choppin et al., 1999). Examples of receptor ratios in typical smooth muscle tissues are given in Table 1.2 below.

1.4 Muscarinic gene-knockout studies

Using pharmacological dissection profiles and receptor antibodies it has been possible to establish muscarinic receptor distributions and some function significance. However, with the recent advancement of gene knockout methodologies (Offermans, 1999) it has become

<u>Antagonist</u>	<u>M₁</u>	<u>M₂</u>	<u>M₃</u>	<u>M₄</u>	<u>M₅</u>
Atropine ¹	9.1	8.9	9.5	9.2	9.1
Pirenzepine ¹	8.0	6.3	6.8	7.0	6.9
Methoctramine ¹	6.6	7.6	6.1	6.9	6.4
Tripitramine ²	8.8	9.5	7.4	8.2	7.5
Darifenacin ¹	7.8	7.0	8.9	7.7	8.1

Table 1.1 Antagonist profiles in radioligand binding assays at muscarinic receptors recombinantly expressed in Chinese hamster ovary (CHO) cells. Affinity profiles are shown as pK_i (pK_i = - log K_i) (Adapted from ¹Table 3 Hedge et al., 1997 and ²Table 1 Maggio et al., 1994).

<u>Tissue</u>	<u>Species</u>	<u>ratio of M₂:M₃ mACh receptors</u>	<u>reference</u>
Ileum	Guinea Pig	65:35 %	Michel & Whiting 1987
Stomach	Human	79:21%	Bellido et al, 1995
Colon	Human	76:24 %	Gomez et al., 1992
Trachea	Cow	74:26%	Roffel et al., 1988
	Guinea-pig	52:48 %	Haddad et al, 1991
	Rabbit	83:17 %	Mahesh et al., 1992
Bladder	Rat	87:13 %	Monferini et al., 1988

Table 1.2 Examples of mACh receptor subtype distributions in smooth muscle tissues determined in competition radioligand binding studies (adapted from Table 8; Eglen et al., 1996a)

possible to investigate unambiguously the physiological roles of the individual muscarinic receptors (for review see Birdsall et al., 2001). M₂ muscarinic receptor gene knockout studies showed M₂ to play a key role in mediating muscarinic receptor-dependent movement, temperature control and antinociceptive responses (Gomez et al., 1999). Stengel and colleagues (2000) found no effect of M₄ receptor knockout on stomach fundus, urinary bladder or tracheal contractility in mice. In contrast studies of M₂ receptor knockout mice were shown to have somewhat different contractile profiles in stomach fundus, urinary bladder and trachea as well as inducing bradycardia. Studies on the PLC-linked mACh receptors showed M₁ receptor knockout mice to have no behavioral or histological defects, but M₁ receptors were shown to modulate M current (K⁺ current) in sympathetic neurons (Hamilton et al, 1997). M₃ receptor knockout studies showed their important role in salivary secretion, papillary constriction, bladder detrusor contraction and receptor-mediated facilitation of food intake (Matsui et al., 2000, Yamada et al., 2001).

Although the M₂ ‘knockout’ studies provide some insight into M₂-mACh receptor function *in vivo*, questions remain as to what is the true function of the M₂ receptor population in smooth muscle, as it has little apparent direct effect on the contraction of smooth muscle *per se*, and why are M₂ receptors present at such high levels in smooth muscle tissue? A clear understanding of the cellular physiology of smooth muscle is desired since dysfunction of the smooth muscle may be important in disorders such as asthma, urge incontinence and irritable bowel syndrome. It is therefore important to understand the physiological significance of the co-expression of M₂ and M₃ receptors in smooth muscle cells. Although as described above M₂ and M₃ receptors may be involved in the contraction of smooth muscle they may both also influence cell proliferation and differentiation, and potentially other cellular responses that involve mitogen-activated protein kinases.

1.5 Mitogen-activated protein kinases

1.5.1 The mitogen-activated protein kinase (MAPK) cascade

Since the late 1980s there has been many advances in the area of research of mitogen-activated protein kinases (MAPKs) and how extracellular signals can result in nuclear signalling events controlling such important cell consequences as proliferation, differentiation or apoptosis. The first MAPK to be discovered was microtubule-associated protein 2 (MAPK-2, later to be called ERK2) by Ray and Sturgill in 1987, which they

isolated from insulin-stimulated 3T3-L1 adipocytes (Ray and Sturgill, 1987). Following the initial discovery of ERK2 in 3T3-L1 adipocytes this kinase has been shown to be ubiquitously expressed in eukaryotic cells, and can be activated by receptor tyrosine kinases and G protein coupled receptors (both of which are discussed below). A number of related proteins have now also been isolated and constitute a family of mitogen-activated protein kinases divided into subfamilies, that are categorised through their sequence similarity, mechanisms of upstream regulation and downstream substrates. Initially mitogen-activated protein kinase (MAPK) was a title used to describe only extracellular-signal regulated kinases (ERKs), but following the discovery and analysis of other closely related protein-directed serine/threonine kinases, MAPK was more widely used to describe the whole group of kinases including c-Jun N-terminal kinase (SAPK/JNK) and p38 homologues. The MAPK family now consists of at least 12 members which are grouped into five subfamilies, of which the best characterised are the Extracellular signal-Regulated protein Kinases (ERK), the c-Jun NH₂-terminal Kinases (JNK) and p38 subfamilies.

The MAPKs are serine/threonine kinases and are themselves situated in a phosphorylation cascade of three kinases acting sequentially (for reviews see Davis, 1993; Blenis, 1993; Cobb and Goldsmith, 1995; Robinson and Cobb, 1997). MAPKs are activated by the dual phosphorylation of a threonine and a tyrosine residue within the protein kinase subdomain VIII (Davis, 1993). This activation was shown, by Anderson and co-workers, not to be due to two upstream protein kinases, but due to a single, dual specificity kinase which catalyses phosphorylation of both residues (Anderson et al., 1990). The dual specificity kinases are known as MAPK kinases (MAPKK, MKK or MAPK Kinase/ERK kinase, MEK) and the first to be identified was MEK1 (45kDa). MEKs are themselves in turn activated through phosphorylation on serine and threonine residues by a MAP kinase kinase kinase (MAPKKK, MKKK or MEKK).

The best studied and understood MAPK activation pathway is that leading to the activation of ERK 1/2 (see Figure 1.3). The ERKs belong to a family of protein-serine/threonine kinases of which there are two original members ERK 1 (44 KDa) and ERK 2 (42 KDa) which have 90% identity, more recently there has been the discovery of a further four isoenzymes of ERK, and a splice variant of ERK1 (ERK1b) has also been reported by Yung and colleagues (Yung et al., 2000).

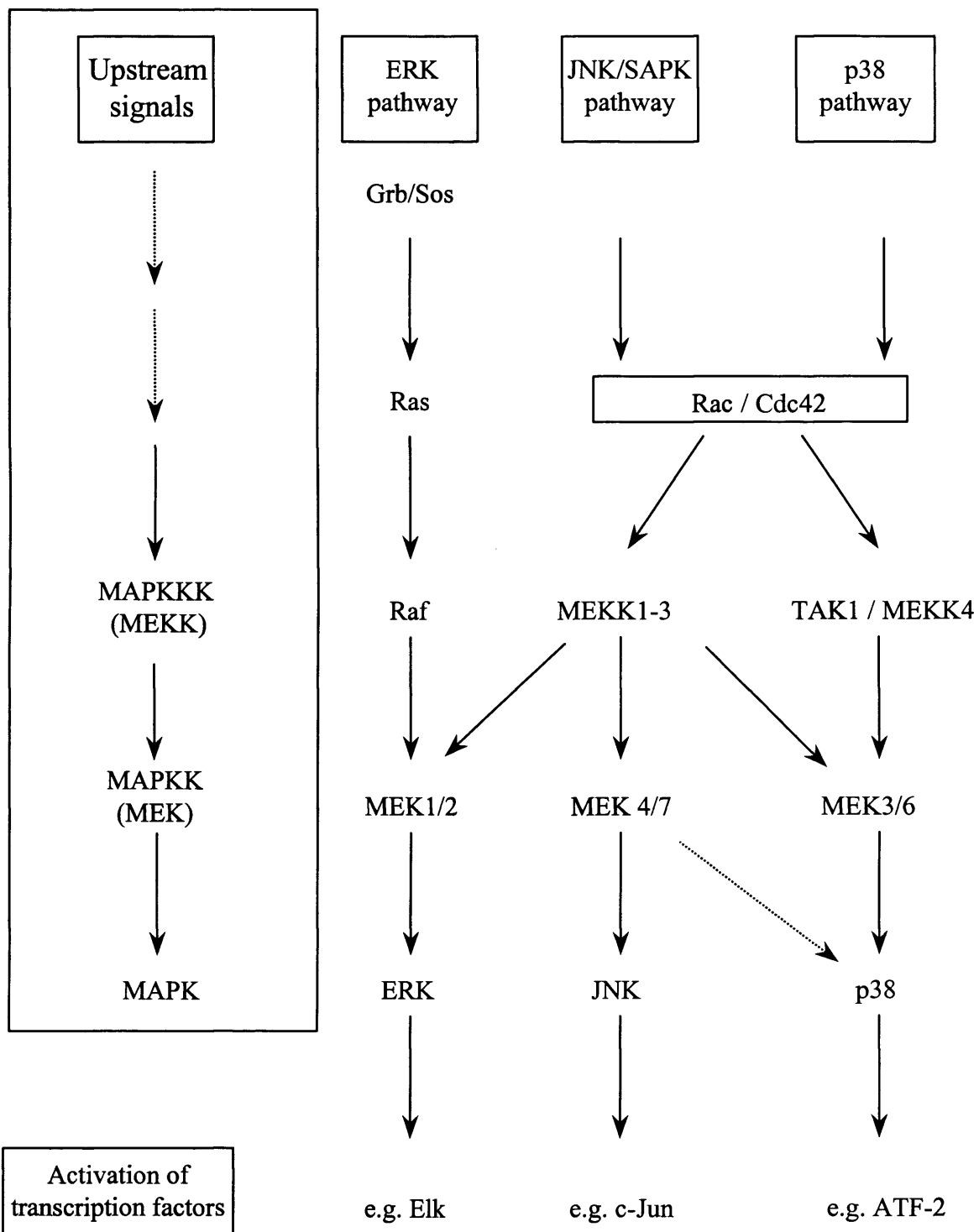


Figure 1.3 A schematic diagram showing the MAPKs pathways. Boxed on the left is the generic MAPK pathway (Adapted from Robinson and Cobb, 1997).

ERK 1/2 isoforms are specifically activated enzymatically by MEK1 and MEK2. MEK1/2 in turn has been shown, by Kyriakis and colleagues (1992), to be activated immediately upstream by c-raf-1 (a MAPKKK) through phosphorylation of serine residues 218 and 222 (Kyriakis et al., 1992; Dent et al., 1992; Zheng and Guan, 1994). There are three known isoforms of raf (c-raf-1, A-raf and B-raf, for review see Kolch, 2000). Although unclear in all cell systems, the activation of Raf has been linked to the integration of a number of mitogenic signals, including those from PKC and the monomeric G protein Ras. It is believed that activated Ras acts to recruit Raf to the plasma membrane, through its amino terminal region, where it is subsequently activated (Stokoe et al., 1994).

The c-Jun NH₂-terminal kinases (JNKs) of which there are two best characterised isoforms JNK1 (46kDa) and JNK2 (55KDa) were identified by their phosphorylation of serine residues 63 and 73 in the amino terminal of the transcription factor c-Jun (Dérjard et al., 1994; Gupta et al., 1996). These kinases were initially known as the stress-activated protein kinases (SAPKs) due to their activation by cellular stress, UV light, osmotic shock, γ -radiation and inflammatory cytokine stimulation. Whereas the threonine and tyrosine residue sequence for activation of ERK 1/2 is separated by a glutamic acid residue (TEY), JNK and p38 isoforms also have the TXY sequence conserved in subdomain VIII of the catalytic domain, however the separating residue is proline (TPY) and glycine (TGY) respectively (Robinson and Cobb, 1997). The two best characterised JNKs, JNK1 and JNK2 are activated specifically by MEK 4 (MKK4) (Waskiewicz and Cooper, 1995), however MEK 4 itself can also phosphorylate some p38 isoforms. Recently, MEK 7 (MKK7) has also been identified as a specific activator of JNKs (Moriguchi et al., 1997; Tournier et al., 1997). Work by Deacon and Blank has shown that both MEKK2 and MEKK3 can activate the MEK4 (MKK4) and MEK7 (MKK 7), leading to JNK activation (Deacon and Blank, 1999). MEKK activation in the JNK and p38 pathways has been shown to involve two Ras-related proteins, namely Rac and Cdc42 (Minden et al., 1995, Coso et al., 1995a) and does not involve Raf (Minden et al., 1994). Candidate MAPKKKs in the JNK pathway that are activated by Rac and Cdc42 include the mixed-lineage kinases (MLKs) (for reviews see Robinson and Cobb, 1997; Garrington and Johnson, 1999; Chang and Karin, 2001; Davis, 2000).

Four isoforms of p38 MAPKs, p38 α , β , γ and δ have been identified (also known as SAPK2a, 2b, 3 and 4) which have all been shown to be activated by the upstream kinases MKK3 and MKK6 (for review see Nebreda and Porras, 2000). Substrates for p38 MAPKs

have been shown to include transcription factors, such as ATF2, and other protein kinases such as MAPKAPK2.

As reviewed by Robinson and Cobb, there can be cross-talk between the ERK, JNK and p38 MAPK signalling modules (Robinson and Cobb, 1997; see Figure 1.3). However, while Raf is the MEK kinase specific to the ERK activation MEKK1-3 may activate MEKs of the ERK, JNK or p38 pathways (see Figure 1.3).

ERK5 (predicted to contain 815 amino acids) is approximately twice the size of other known ERKs and does not interact with MEK1 or MEK2, but was identified following the report of a new MEK, termed MEK5 by Zhou and colleagues (Zhou et al., 1995). The finding that MEK5 contains unique amino acid sequences in its N terminus led them to suggest that MEK5 may interact with GTPases such as Cdc42. Also sequences in the C terminus of ERK5 may target this kinase to cytoskeletal elements, however direct supporting evidence for this idea is presently lacking.

The ability of different MAPK pathways to be selectively regulated is thought to be achieved, in part, through their association with scaffolding and anchoring proteins which have also been suggested to facilitate the kinase activation cascade by holding the kinases in a conformation which enhances their interactions. Examples of MAPK cascade scaffolds are MAPK kinase (MEK) partner 1 (MP1), JNK interacting protein (JIP1), and JNK/SAPK activating kinase suppressor of Ras (KSR) (for review see Burack and Shaw, 2000). Dickens et al. (1997) have shown JIP1, a cytoplasmic protein, to bind to JNK, but not ERK or p38, and in a later study by the same group (Whitmarsh et al., 1998) using co-precipitation showed JIP1 to bind mixed lineage kinase 3 (MLK3, member of the group of MEKKs) and MKK7 (JNK activator) and to facilitate JNK activation, but not MKK3 or MKK6 (p38 activators) or c-Raf1 or MEK1 (ERK activators). Therefore, although there are an increasing number of MAPK scaffolding candidate proteins much has yet to be learnt about this fascinating recent development.

1.5.2 Downstream targets of MAPKs

The activation of extracellular signal-regulated kinases (ERKs) can occur in response to mitogenic stimulation. ERKs appear to play an important role in mitogenic signalling, as blocking their activation can prevent cell proliferation, and constitutive activation of the

MAPK pathway is sufficient for tumorigenesis in a wide range of cell-types (Pagès et al., 1993; Gutkind, 1998b). In their activated (phosphorylated) form the MAPKs can directly regulate gene expression by phosphorylating a large number of substrates including cytosolic enzymes (e.g. cPLA₂), membrane-associated proteins (e.g. epidermal growth factor (EGF) receptor, Northwood et al., 1991) and the nuclear transcription factors, c-Jun, c-Fos and c-Myc (by phosphorylated JNK), ATF-2 (p38) and Elk (ERK, Gille et al., 1992). After mitogenic stimulation MAPKs translocate from the cytoplasm to the nucleus (Khokhlatchev et al., 1998) which is a requirement for cell cycle entry (Brunet et al., 1999). The first target of JNK to be studied was c-Jun, which is phosphorylated on the serine residues 73 and 63 (Dérijard et al., 1994), and is part of the AP-1 transcription factor that regulates key genes involved in cell proliferation (Bohmann et al., 1987). Pagès et al. (1993) showed a requirement for ERK activation to induce fibroblast proliferation. Fukuda et al. (1997) demonstrated how MAPK is localised to the cytoplasm through its specific association with MEK (MAPKK) and that the nuclear accumulation of MAPK, following its activation through dual phosphorylation, is accompanied by dissociation of a complex between MAPK and MEK. Interestingly, recent reports have commented on how phosphorylation of ERK2 causes it to dimerise with phosphorylated or unphosphorylated ERK2, which is thought to promote nuclear localisation of ERK2 (Khokhlatchev et al., 1998; Cobb and Goldsmith, 2000). It appears that the nuclear translocation of MAPKs represents a crucial step in the regulation of its transcription factor substrates and therefore gene expression. The regulation of gene transcription by MAPKs is reviewed by Hill and Treisman (1995), Karin and Hunter (1995) and Triesman (1996).

Marshall (1995) has emphasised that the duration, as well as the magnitude, of the MAPK activation is probably critical to cell signalling decisions. The duration of ERK activation is likely to be important in determining the amount of ERK which translocates to the nucleus in order to phosphorylate transcription factors and alter gene expression. Therefore, it is likely that not only the magnitude of the MAPK activation, but also its longevity, is decisive in determining the phenotypic outcome of MAPK activation. It has been found in PC12 cells that when ERK activation is transient it is not associated with cell differentiation, whereas sustained activation of ERKs produced differentiation (reviewed Marshall, 1995). Alblas et al. (1996) have shown also that sustained MAP kinase activity (induced by nerve growth factor) influences neurite outgrowth and differentiation, whereas transient activation (induced by epidermal growth factor) initiates a mitogenic signal.

Substrates for MAPKs include nuclear transcription factors, non-nuclear substrates such as the protein serine/threonine kinase p90^{tsk}, cytoskeletal proteins and cytosolic PLA₂ (cPLA₂). cPLA₂ catalyses the release of arachidonic acid from phospholipids in membranes and is one of the rate-limiting steps in the synthesis of prostaglandins, thromboxanes and leukotrienes. Some members of the MAPK cascade have also been shown to act as substrates for activated MAPKs suggesting potential complex feedback modulation. For example Anderson and colleagues showed that Raf-1 may be a substrate for MAP kinase *in vivo* (Anderson et al. 1991), MEK has also been shown to be a MAPK substrate and proposed to be involved in negative feedback control of the MAPK cascade (Brunet et al., 1994). Also Bornfeldt et al. (1997) reported MAPK activation either stimulating cell proliferation or inhibiting cell proliferation through activation of cPLA₂ and subsequent PKA inhibition of cell cycle progression depending on availability of specific downstream enzyme targets.

Having realised the importance of MAPK activation in cell survival and cell death, and the varied downstream targets of MAPKs, it is important to consider how the magnitude and duration of their signalling may be regulated, especially as the activation of transcription factors has been linked to prolonged activation of MAPKs leading to their translocation from the cytoplasm to the nucleus. The determinants of this biological effect are the critical balance between the upstream activators and the complex regulatory network of protein phosphatases (for reviews see Denhardt, 1996, Keyse, 2000). Phosphatases may inactivate MAPKs by dephosphorylating either or both the threonine and tyrosine residues required for activation, through tyrosine specific phosphatases, serine/threonine-specific phosphatases or by dual specificity (threonine/tyrosine) protein phosphatases. There are at least nine members of the MAPK phosphatases which can specifically target different members of the MAPK superfamily and these are reviewed by Keyse (2000). The pathways leading from extracellular signal to MAPK activation are complicated and involve many stages, at each of which there can be the potential for regulation, which can affect the final MAPK signal. For example, the influence of Ras GTPases upon duration of Ras activation and hence Ras-dependent MAPK activation, or the GTPase activity of the heterotrimeric G-protein linking to the receptor in GPCR-mediated MAPK activation.

1.5.3 Activation of the mitogen-activated protein kinase cascade

1.5.3.1 Receptor tyrosine kinase (RTK) activation of MAPK

MAPKs can be activated by stimuli such as growth factors, hormones and neurotransmitters either, via agonist stimulation of G protein-coupled receptors (GPCRs) or tyrosine kinase receptors (Faure et al., 1994).

The original and best understood pathways to be studied leading to MAPK activation was through receptor protein tyrosine kinase (RTK) activation (for reviews see Van der Geer et al., 1994; Pronk and Bos, 1994, see Figure 1.4 for a diagram of RTK activation of MAPK cascade). Receptor protein kinases include growth factor receptors such as epidermal growth factor receptor (EGFR) and platelet-derived growth factor receptor (PDGFR) which signal through p21Ras and the MAPK cascade (see above) leading to differentiation or proliferation. RTKs, with some exceptions (e.g. the insulin receptor), are single polypeptide chains which traverse the cell membrane once, and contain a tyrosine kinase domain within the intracellular portion of the protein. Upon stimulation, RTKs (e.g. EGFR) dimerise, which causes the receptors to transphosphorylate tyrosine residues in their C-terminal tail (Heldin, 1995), and this is presumed to occur by a ligand-induced conformational change. It is believed that this autophosphorylation causes a secondary conformational change and phosphotyrosine residues on the dimerised receptor act as docking sites for substrates containing Src homology-2 (SH2) domains. These substrates include adaptor proteins (e.g. growth-factor-receptor binding protein 2 (Grb2), or Shc, a non-enzymatic adaptor protein), which are intermediates between RTKs and downstream signalling molecules, and effector molecules (e.g. PLC γ 1, Ras-GAP) whose activity can be altered directly by phosphorylation (Van der Geer et al., 1994).

Many studies have focused on the downstream signalling from the EGF receptor and have shown that stimulation of this receptor leads to the recruitment of a complex between Grb2 and mammalian Son of Sevenless (mSos) to the autophosphorylated receptor and the subsequent phosphorylation of mSos (Batzer et al., 1993). Grb2 contains a SH2 domain, which binds it to the autophosphorylated EGFR, and two SH3 domains, which bind to the proline rich sequences of mSos (Rozakis-Adcock et al., 1993). mSos is a guanine-nucleotide exchange factor (GNEF) and once recruited it catalyses the exchange of GDP for GTP on

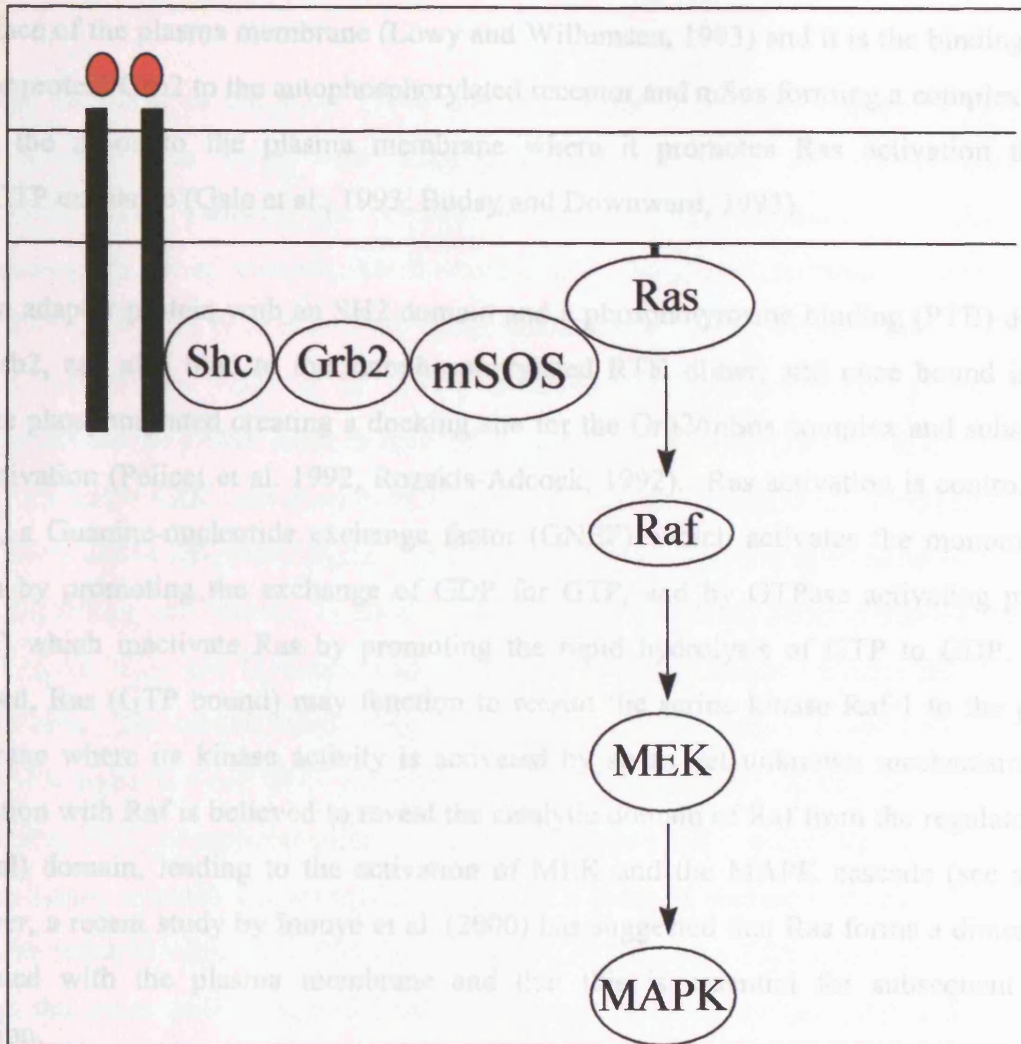


Figure 1.4. A diagram showing RTK-mediated activation of a MAPK.

The discovery that either growth factor or oncogene was activation of MAPKs could be attenuated following expression of a dominant-negative form of c-ras1 and the knowledge of Raf activating MEKs in the MAPK cascade (see above) showed Ras to be positioned upstream of Raf activation (see Mahoney et al., 1994, for review). c-Src, a non-receptor tyrosine kinase has also been linked to the activation of the MAPK cascade through Ras, by binding to the autophosphorylated receptor. c-Src phosphorylated c-Src can activate Ras possibly through phosphorylation of Shc and subsequent activation of the Grb2/mSOS complex (Gould and Hunter, 1998) and is thought to be important in GPCR signaling to MAPK through transactivation of a RTK (see below).

While most studies have centred on RTKs leading to activation of the MAPK cascade, JNK and p38 subfamilies have also been shown to be activated by receptor tyrosine kinases, via a Ras-dependent pathway (Minden et al., 1994).

Ras (a monomeric G-protein) leading to its activation. The Ras protein is associated with the inner face of the plasma membrane (Lowy and Willumsen, 1993) and it is the binding of the adaptor protein Grb2 to the autophosphorylated receptor and mSos forming a complex which brings the mSos to the plasma membrane where it promotes Ras activation through GDP/GTP exchange (Gale et al., 1993; Buday and Downward, 1993).

Shc, an adaptor protein with an SH2 domain and a phosphotyrosine binding (PTB) domain, like Grb2, can also bind to the autophosphorylated RTK dimer, and once bound is itself tyrosine phosphorylated creating a docking site for the Grb2/mSos complex and subsequent Ras activation (Pelicci et al. 1992, Rozakis-Adcock, 1992). Ras activation is controlled by mSOS, a Guanine-nucleotide exchange factor (GNEF), which activates the monomeric G protein by promoting the exchange of GDP for GTP, and by GTPase activating proteins (GAPs) which inactivate Ras by promoting the rapid hydrolysis of GTP to GDP. Once activated, Ras (GTP bound) may function to recruit the serine kinase Raf-1 to the plasma membrane where its kinase activity is activated by an as yet unknown mechanism. Ras interaction with Raf is believed to reveal the catalytic domain of Raf from the regulatory (N-terminal) domain, leading to the activation of MEK and the MAPK cascade (see above). However, a recent study by Inouye et al. (2000) has suggested that Ras forms a dimer when associated with the plasma membrane and that this is essential for subsequent Raf-1 activation.

The subsequent activation of the MAPK cascade has been the centre of much research and the discovery that either growth factor or oncogenic *ras* activation of MAPKs could be attenuated following expression of a dominant-negative form of c-raf-1 and the knowledge of Raf activating MEKs in the MAPK cascade (see above) showed Ras to be positioned upstream of Raf activation (see Malarkey et al., 1995, for review). c-Src, a non-receptor tyrosine kinase has also been linked to the activation of the MAPK cascade through Ras, by binding to the autophosphorylated receptor. Once phosphorylated c-Src can activate Ras possibly through phosphorylation of Shc and subsequent activation of the Grb2/mSos complex (Gould and Hunter, 1998) and is thought to be important in GPCR signalling to MAPK through transactivation of a RTK (see below).

While most studies have centred on RTKs leading to activation of the ERK cascade, JNK and p38 subfamilies have also been shown to be activated by receptor tyrosine kinases, via a Ras-dependent pathway (Minden et al., 1994).

1.5.3.2 GPCR-mediated MAPK activation

Since the discovery in the early 1990s that stimulation of GPCRs can signal to MAPK activation, and thus have wide ranging effects, including cell proliferation and differentiation, this pathway has become the basis of intense study and, despite the accumulating amount of research, is still only partially understood (for reviews see Malarkey et al., 1995; Gutkind, 1998a and 1998b; Dhanasekaran et al., 1998; Lopez-Illasca, 1998). For example, research by Faure et al. (1994) in COS-7 cells demonstrated a $G\alpha_s$ -protein-mediated increase in cAMP leads to ERK activation, Vossler et al. (1997) also demonstrated a cAMP-mediated ERK activation in PC12 cells. However, Crespo et al. (1995) show $G\alpha_s$ -cAMP an mediated inhibitory signal to ERK activation (for further discussion of cAMP to MAPK signalling, see below). In addition, Williams et al. (1998) showed that activation of MAPKs by G_i , $G_{q/11}$ and G_s -coupled adrenoceptors is very different between fibroblast and neuronal cells. The overall theme from the accumulation of research in the field is that the final MAPK signal is a cell type-, receptor- and G protein-specific pathway, and may proceed via Ras, Raf, PKC, phosphoinositide 3-kinase (PI3 kinase) and involve $G\alpha$ - or $G\beta\gamma$ -subunits and non-ligand induced phosphorylation of RTKs (termed transactivation). I will now summarise research relevant to this thesis, with an emphasis on ERK activation by GPCRs, which is the most widely studied MAPK pathway regulated by G_i - (M_2) and G_q - (M_3) coupled receptors.

1.5.3.2.1 G_i - and G_q - protein-mediated MAPK activation

It has been shown in COS-7 cells expressing M_1 (G_q -coupled) or M_2 (G_i -coupled) muscarinic receptors that agonist stimulation of either G_i -coupled (pertussis toxin-sensitive) and $G_{q/11}$ -coupled (pertussis toxin-insensitive) receptors can activate MAPK activity (Crespo et al., 1994b; see also Figure 1.5).

While G_i - and G_q - coupled receptors appear to initiate very different signalling cascades proximal to the receptor (inhibition of adenylyl cyclase, or hydrolysis of PIP_2) they have been shown to have similar or related MAPK activation effects. For example, it has been reported recently by Wylie et al. (1999) that muscarinic M_2 and M_3 receptors stably expressed in CHO cells show an identical ERK activation profile in terms of time-course, magnitude and concentration-dependency. However, the pathways linking receptor activation to ERK have been shown to be very distinct with G_i signalling proceeding through $G\beta\gamma$ -subunit activation

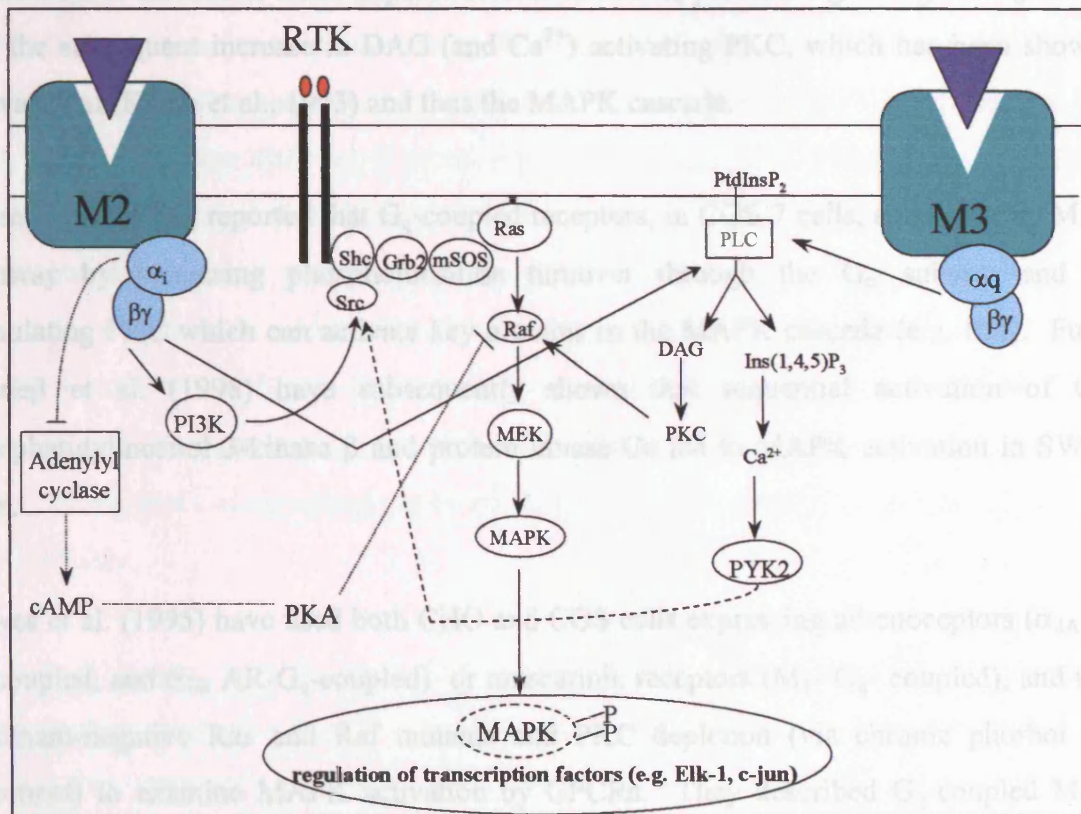


Figure 1.5 Diagram summarising the pathways linking GPCR (G_i and G_q coupled) activation to MAPK activation, including transactivation of RTKs. Dotted lines indicate inhibitory mechanisms and dashed lines indicate proposed pathways. See text for details.

Contrary to the findings of Hawes et al (1995) in COS and CHO cells, Della Rocca et al (1997) suggested that in HEK 293 cells expressing α_{1A} adrenergic receptors (G_{i1} -coupled) and β_1 cells expressing α_{2A} receptors (G_q -coupled) the signals converge at PLC (as shown in Figure 1.5) and proceed via a Ras-dependent pathway, involving the calcium-dependent activation of Src family kinases and a sequence of events leading to the activation of MEKs, possibly by transactivation of a tyrosine kinase receptor (see below).

of the MAPK cascade in a Ras-dependent manner and G_q proteins signalling via G_α subunits and the subsequent increase in DAG (and Ca^{2+}) activating PKC, which has been shown to activate Raf (Kolch et al., 1993) and thus the MAPK cascade.

Faure et al. (1994), reported that G_q -coupled receptors, in COS-7 cells, stimulate the MAPK pathway by increasing phosphoinositide turnover through the G_α subunit and thus stimulating PKC which can activate key proteins in the MAPK cascade (e.g. Raf). Further Graneß et al. (1998) have subsequently shown that sequential activation of $G_{q/11}$, phosphatidylinositol 3-kinase β and protein kinase C ϵ led to MAPK activation in SW-480 cells.

Hawes et al. (1995) have used both CHO and COS cells expressing adrenoceptors (α_{2A} AR- G_i -coupled, and α_{1B} AR- G_q -coupled) or muscarinic receptors (M_1 - G_q - coupled), and using dominant-negative Ras and Raf mutants and PKC depletion (via chronic phorbol ester treatment) to examine MAPK activation by GPCRs. They described G_q -coupled MAPK activation to be mediated by the $G\alpha_q$ subunit in a PKC-dependent and Ras-independent pathway that could not be dissociated from its activation of PLC, with PKC activating the MAPK cascade at the level of Raf. However, the pathway they described linking G_i coupled receptors to MAPK activation was Ras-dependent, PKC-independent, dissociable from its activation of PLC, and mediated by $G_{\beta\gamma}$ subunits. However, Crespo et al. (1994a) showed M_1 muscarinic receptor-mediated Raf-1 activation, in NIH 3T3 cells, was not via a PKC-dependent pathway. Other studies have also shown that the activation of ERK by G_i protein-coupled receptors may occur through the $\beta\gamma$ -subunit complex of heterotrimeric G-proteins acting on a Ras-dependent pathway (Crespo et al., 1994b, Winitz et al., 1993). However, Crespo et al. (1994b) showed M_2 muscarinic receptors (G_i) activated ERK by $\beta\gamma$ subunits, by over-expression of the α subunit of transducin (α_t) to sequester free $\beta\gamma$ dimers and inhibit the ERK activation, and also found this to be the case for M_1 (G_q) receptors.

Contrary to the findings of Hawes et al. (1995) in COS and CHO cells, Della Rocca et al. (1997) suggested that in HEK 293 cells expressing α_{1B} adrenoceptors ($G_{q/11}$ -coupled) and cells expressing α_{2A} receptors (G_i -coupled) the signals converge at PLC (as shown in Figure 1.5) and proceed via a Ras-dependent pathway, involving the calcium-dependent activation of Src family kinases and a sequence of events leading to the activation of MAPKs, possibly by transactivation of a tyrosine kinase receptor (see below).

Interestingly the idea that MAPK signalling by GPCRs is dependent on cell background was vividly shown by some elegant work by Williams and colleagues (Williams et al., 1998), where they studied the coupling of three different adrenoceptors inducibly expressed in PC12 cells, coupled to three different G proteins ($\alpha_{1A}/G_{q/11}$, α_2/G_i , and β/G_s) to the activation of MAPKs. They showed that all three receptors coupled to their respective classical second messenger pathways and while the $G_{q/11}$ and G_s -coupled receptors did activate ERK, G_i did not. Since Hawes et al. (1995) and Della Rocca et al. (1997) observed G_i -mediated ERK responses, whereas Williams did not, they proposed that this may be explained by the expression of $G\alpha_o$ in neuronal cells, such as PC12 cells. This speculation was based on the recent finding that $G_{\beta\gamma}$ signalling can be inhibited by expression of $G\alpha_o$ -subunits (Yamauchi et al., 1997a).

Interestingly recent work by Slack (2000) in HEK cells stably expressing M_3 muscarinic receptors (G_q) reported a MAPK activation which was mediated by two pathways; one of which is PKC-dependent and one which is transduced through the EGF receptor and Src (see transactivation section below). Luttrell and colleagues also showed with LPA stimulation that pertussis toxin-sensitive GPCR activation of MAPK in COS-7 cells is $G_{\beta\gamma}$ subunit-mediated, proceeding via a Shc-Src complex, mSOS, Ras and Raf (Luttrell et al., 1996). It has also been shown that stimulated G_i -coupled muscarinic receptors (M_2) cause rap1GAPII (a Rap1 GTPase activating protein) to translocate from the cytosol to the plasma membrane and to decrease the amount of GTP bound to Rap1 (Mochizuki et al., 1999). Rap 1 is thought to inhibit MAPK activation through antagonising Ras (Cook et al., 1993a), and therefore this is another mechanism of $G\alpha_i$ -subunit-mediated enhancement of ERK activation.

Indeed, it has been shown recently that both G_i - and G_q -coupled receptors in COS-7 cells (lysophosphatidic acid (LPA) and M_1 mACh receptors respectively) cause transactivation of the EGF receptor upstream of MAPK activation (see below and Daub et al., 1997). It is apparent that GPCR signalling to MAPK involves multiple components, including components of the RTK signalling, Ras, non-receptor tyrosine kinases such as Src and PYK2, as well as PKC isoforms and PI3 kinase (PI3 kinase, Duckworth and Cantley, 1997).

1.5.3.2.2 G_s, G_o- protein and cAMP protein kinase-mediated MAPK activation

As mentioned above, the study by Williams and colleagues (Williams et al., 1998) in PC12 cells reported G_s-coupled receptor (β -adrenoceptor) activation of ERK, JNK and p38. G α_o proteins have been shown to activate MAPK in CHO cells through a PKC-dependent, but Ras-independent signalling pathway (van Biesen et al., 1996), as well as to inhibit MAPK activation through G $\beta\gamma$ subunits from other (G_i) G protein activation (Yamauchi et al., 1997a). Since M₃ receptors have been shown to promiscuously couple to G α_s -proteins (Burford and Nahorski, 1996; Boxall 1998; Akam et al., 2001) causing an increase in cAMP levels, it is also important to consider the possible pathways mediating G_s stimulation of MAPK pathways.

Receptors acting through G_s proteins (e.g. β adrenoceptors) have been proposed to have a dual effect on MAPK activation, thus while G_s-derived $\beta\gamma$ subunits may cause MAPK activation, the G α_s subunit through stimulation of adenylyl cyclase activity and the subsequent increase in cAMP, causes inhibition of MAPK activation (Crespo et al., 1995). Recently, it has been shown by Daaka and colleagues that G-protein coupled receptor kinases (GRKs) and β -arrestins, which uncouple GPCRs and target them for internalisation, function as important components in the β_2 -adrenoceptor-mediated activation of MAP kinase in HEK293 cells (Daaka et al., 1998, reviewed by Lefkowitz, 1998). However, it has been shown by Budd et al. (1999) that this phenomenon is probably both cell-type and receptor-specific, as by using both inhibitors of endocytosis and a M₃-muscarinic receptor mutant that does not internalise they showed receptor endocytosis in CHO-m3 cells is not essential for ERK activation. However, G_s signalling may be more complicated than originally thought, as Daaka and colleagues have reported 'switching' of G protein coupling of the β adrenoceptor via a G α_s /PKA -mediated mechanism to G α_i ERK activation (Daaka et al., 1998).

As mentioned above the cell background may greatly influence the signalling pathway, since research by Faure et al. (1994) in COS-7 cells demonstrated that a G α_s -protein-mediated increase in cAMP leads to ERK activation, (as did Vossler et al., 1997, in PC12 cells), however Crespo et al. (1995) showed a G α_s -cAMP-mediated inhibitory signal to MAPK activation. It has been proposed that cAMP activation of PKA causes it to phosphorylate c-Raf-1 within the regulatory domain preventing its binding to Ras (Hordijk et al., 1994), or

PKA phosphorylation of Rap-1 causes it to compete with Ras for Raf (Cook et al., 1993b). MAPK activation by G_q-coupled receptors, in rat airway smooth muscle cells was reported to be significantly inhibited by activation of PKA, and elevation of cAMP (by forskolin) attenuated proliferation, as measured by [³H]-thymidine incorporation (Shapiro et al., 1996).

1.5.3.2.3 Role of PI3-Kinase in MAPK signalling

Using COS-7 cells and overexpression of PI3K- γ , Lopez-Illasaca et al. (1997) showed PI3K- γ signalling to ERK activation occurred through a tyrosine kinase, Shc, Grb2, Sos, Ras and Raf mediated pathway (see Transactivation section below). They also went on to demonstrate that M₂-muscarinic receptor activation of ERK was mediated by G _{$\beta\gamma$} subunits and PI3K- γ . It is possible that the G _{$\beta\gamma$} subunits recruit PI3K- γ to the plasma membrane, enhancing the activity of a Src-like kinase. Bondeva et al. (1998) have also suggested that PI3K γ must be liberated from the plasma membrane to enhance its protein kinase activity to leading to MAPK activation as opposed to its PIP₂ phosphorylation kinase activity.

An elegant study by Duckworth and Cantley (1997) in both Swiss 3T3 cells and Chinese hamster ovary (CHO) cells showed that PI3-kinase involvement in ERK activation was both cell type- and ligand-specific. In their study PI3K was blocked, using wortmannin, and this inhibited the PDGF-induced Raf-1 and ERK activation in CHO cells (containing few PDGF receptors) but not in Swiss 3T3 cells (which expressed high levels of PDGF receptors). However ERK activation by low concentrations of PDGF could be blocked by wortmannin in Swiss 3T3 cells. They concluded that a PI3K-dependent mechanism provides an efficient pathway for ERK activation, but when more receptors are activated a redundant pathway can be recruited which is independent of PI3K. (See Malarkey et al., (1995) for review of PI3 kinase involvement in MAPK signalling).

1.5.3.2.4 GPCR-mediated activation of JNK and p38 pathways

In addition to ERK, both JNK and p38 have also been shown to be activated following stimulation of GPCRs. However, less is known about the pathways linking these receptors to JNK and p38 activation. As previously highlighted for ERK regulation by GPCRs cell background may also be an important determinant for JNK activation by G_i-coupled receptors. For example, Williams et al. (1998) found no G_i-mediated JNK activation in

PC12 cells, whereas Lopez-Illasca et al. (1998) report JNK activation from G_i -coupled receptors in COS-7 cells through a PI3K γ -dependent pathway. Williams et al., (1998) also showed that G_q and G_s are coupled to JNK activation in PC12 cells and G_q to p38. In this context it is important to note that Coso et al. (1995b) have shown that G protein-coupled M_1 -muscarinic receptors in NIH 3T3 cells can activate pathways leading to the phosphorylation of the NH₂-terminus of the protein c-Jun, whereas tyrosine kinase receptor (PDGF receptor) stimulation does not. Coso et al. (1996) went on to demonstrate, that stimulation of JNK activity by M_1 or M_2 muscarinic receptors in COS-7 cells was mediated by $G_{\beta\gamma}$ subunits through a Ras and Rac1-dependent pathway. Mitchell et al. (1995) found that Rat 1a fibroblasts, expressing either M_1 - (G_q) or M_2 - (G_i) muscarinic receptors, both exhibited a Ca^{2+} -dependent JNK activation compared with a calcium-independent ERK activation upon agonist challenge. Wylie et al. (1999) also reported a G_q -linked, Ca^{2+} -dependent receptor (M_3) activation of JNK in CHO cells, which they showed to be negatively regulated by PKC. However, Coso et al. (1995b) reported M_1 -mediated JNK activation which did not correlate with PKC stimulation. Studies by Yamauchi et al. (1997), in HEK293 cells, reported both M_1 and M_2 receptor-mediated activation of p38 and this appeared to occur via a $G_{\beta\gamma}$, PKC and Src family kinase-dependent pathway (Nagao et al., 1998). Clearly further work is required to fully elucidate the pathways mediating GPCR activation of JNK and p38.

1.5.3.2.5 Transactivation

The discovery of MAPK activation by GPCRs, and reports that the pathway resembled that originally discovered from RTKs, at least for some GPCR / cell-types, led to the concept of transactivation of RTKs by GPCRs. Thus, it has been proposed by Ullrich and co-workers that GPCR signalling to MAPK activation involves a pathway transactivating tyrosine kinase receptors, mediated by cytosolic non-receptor tyrosine kinases such as PYK2 and Src (Daub et al. 1996; Dikic et al. 1996; also see Figure 1.5). Initially Daub et al. (1996) suggested that transactivation of the EGF receptor was involved in linking the GPCR pathway to the activation of the MAPK cascade. Many studies since then have investigated this transactivation phenomena (for review see Leserer et al., 2000 and references therein).

As has been found in general with GPCR signalling to MAPK cascades, transactivation has been shown to be both PKC-dependent and PKC-independent. Following earlier evidence implicating tyrosine kinases and adaptor protein phosphorylation (Shc) in the GPCR

activation of ERK (Chen et al., 1996), Daub and colleagues (1997) followed up their earlier finding of EGFR transactivation via G protein signalling cascades (Daub et al., 1996) by specifically investigating both G_i - and G_q -mediated transactivation pathways leading to MAPK activation in COS-7 cells. Using transiently transfected M_2 -muscarinic receptors (G_i -coupled) or M_1 -muscarinic and bombesin receptors (G_q -coupled) they found EGF receptor transactivation may occur through both PTX-sensitive (G_i) and PTX-insensitive (G_q) receptor activation. As reported above, G_i protein activation of the MAPK pathway is believed to occur via $G_i\alpha$ or $G\beta\gamma$ subunit signal transduction and has been shown to involve Src family kinases. Recent studies by Luttrell et al. (1997) have shown that Src is necessary for both $G\beta\gamma$ -subunit mediated and $G_i\alpha$ -coupled receptor-mediated phosphorylation of both EGFR and the adaptor protein Shc. Studies by Dikic and colleagues (Dikic et al., 1996) found that downstream of G protein activation (both G_i and G_q) phosphorylation of PYK2 (a calcium-activated tyrosine kinase) leads to it binding to the SH2 domain of Src and subsequent activation of Src. While transactivation through PYK2 is not relevant to all physiological environments, as it is predominantly expressed only in neuronal cells, it offers an insight into possible pathways connecting GPCRs to the activation of the MAPK cascade, and it is possible that other members of this focal adhesion kinase (FAK) family are utilised in other cellular environments. Dikic and colleagues went on to demonstrate that dominant-negative mutants of Grb2 or mSOS inhibited the MAPK activation by G_i - and G_q -coupled receptors. Blaukat et al. (1999) later reported specific pathways from PYK2 to JNK activation and PYK2 to ERK activation in HEK293 cells. Once PYK2 has been activated by various transmembrane receptors through increases in intracellular calcium and the activation of PKC, PYK2 associates with Src. Src then phosphorylates PYK2 and adjacent Shc and $p130^{Cas}$ (a docking protein), creating direct binding sites for Grb2 and Crk (adaptor proteins) respectively. Blaukat et al. went on to show that Crk then recruits Crk effectors (e.g. C3G or DOCK180) to the Pyk2 / $p130^{Cas}$ / Crk complex, which leads to JNK activation, whereas Grb2 translocates mSOS leading eventually to ERK activation.

Another study, also downstream of G_i - and G_q -coupled receptors, in HEK293 cells provided evidence that G_i (α_{2A} adrenoceptor) and G_q (α_{1B} adrenoceptor)-mediated ERK responses converge at the level of PLC β ($G_q\alpha$ and $G\beta\gamma$ release from G_i -protein) and proceed through a Ras-, calcium- and tyrosine kinase-dependent pathway, suggesting PYK2 as the link to the activation of Src (Della Rocca et al., 1997). This conclusion was based on the use of the PLC inhibitor U73122, dominant-negative forms of Ras, dominant-negative forms of PYK2 and the calcium chelating agent BAPTA to attenuate the ERK activation through

adrenoceptor stimulation. Once activated, PYK2 can bind Src which can in turn tyrosine phosphorylate Shc, an adaptor protein which itself can go on to bind and form a Shc/Grb2/mSOS complex (see RTK signalling above) and lead to an activation of Ras and the MAPK cascade. Whereas work from this same group expressing the same G protein-coupled adrenoceptors in a different cell background, COS-7 cells, (Hawes et al., 1995) found that G_q (α_{1B} -AR) activation of ERK was Ras-dependent, whereas G_i (α_{2A} -AR) was Ras-independent.

However, a recent study by Adomeit et al. (1999), using COS-7 cells transiently transfected with bradykinin receptors (G_q -coupled), reported a PKC- and EGFR transactivation-dependent activation of ERK which was Src kinase-independent. When using wortmanin, a specific inhibitor of PI3K, and PP-1, a src kinase inhibitor, they reported no effect on GPCR to MAPK activation, whereas AG1478, a specific inhibitor of EGFR tyrosine kinase activity attenuated the ERK activation, as did PKC inhibitors (Ro 31-8220 and bisindolylmaleimide).

In summary, transactivation of RTKs has been shown to be very important for GPCR signal transduction to MAPKs. However, it is not a universal pathway employed by all GPCRs since for example it has been shown that the P2Y (G_q) signalling pathway does not involve cross-activation of a RTK (Short et al., 2000).

1.6 Aims of project

As discussed above M_2 -mACh receptors constitute the majority (typically 60-90%) of muscarinic receptors found within most smooth muscle tissues and as this appears to be a conserved phenomena within virtually all mammalian species so far studied, it is important to identify the function of these receptors within the context of smooth muscle physiology.

It is interesting to address the question as to what is the function of the M_2 receptor population in smooth muscle, as it has only subtle effects on the contraction of smooth muscle *per se* (Sawyer and Ehlert, 1999; Stengel et al., 2000), and why M_2 receptors are present at such high levels in smooth muscle tissue. A clear understanding of the cellular physiology of smooth muscle is desired since dysfunction of the smooth muscle may be important in disorders such as asthma, urge incontinence and irritable bowel syndrome. It is therefore important to understand the physiological significance of the co-expression of M_2 and M_3 receptors in smooth muscle cells. Although model cell systems expressing either M_2

or M₃ muscarinic receptors have been characterised, the receptor functions in isolation do not necessarily predict what will happen when both are expressed in the same cell, as occurs *in vivo* in a variety of tissues. Therefore, these studies involving CHO-m2m3 cells provide a relatively simple experimental paradigm to examine the consequences of receptor co-expression.

We chose to carry out the studies in a model cell system where the recombinant receptors were stably expressed because previous experiments using cultured smooth muscle cells have shown that M₃ receptors are rapidly lost *in vitro*, resulting in a homogenous M₂ population (Widdop et al., 1993; Yang et al., 1990). For this study Chinese hamster ovary (CHO) cells expressing M₂-, M₃- or co-expressing M₂- and M₃- muscarinic receptors have been used. Evidence for cross-talk between the receptors could then be validated through experiments in smooth muscle tissues. Initial experiments were designed to confirm that the receptors, in the CHO cell model, were coupling to their respective pathways, and this was achieved through radioligand binding techniques with the specific muscarinic antagonist [³H]-NMS, second messenger accumulation (IP₃ and cAMP) assays and intracellular Ca²⁺ single cell imaging in co-expressing CHO-m2m3 cells. Further studies investigated the effects of M₂- and M₃- receptor co-expression upon second messenger generation and calcium signalling. In addition, following studies showing that, both M₂ and M₃ receptors may be involved in the contraction of smooth muscle and more recently many GPCRs, including muscarinic receptors, are involved in membrane to nucleus signal transduction the effects of M₂- and M₃- receptor co-expression upon both MAPK activation (at the level of ERK and JNK) and DNA synthesis (as measured by [³H]-thymidine incorporation) were analysed. Any evidence for cross-talk between the co-expressed receptors was then also investigated in the more physiological situation of airway smooth muscle tissue maintained under conditions designed to preserve M₂/M₃ co-expression.

Chapter Two: Experimental Methodology

2.1 General cell culture and transfection procedures

2.1.1 Cell culture

Chinese hamster ovary (CHO) cells transfected with m2 or m3 human muscarinic receptor cDNA (CHO-m2 obtained from Dr S. Lazareno and CHO-m3 obtained from Dr N. Buckley, National Institute for Medical Research, Mill Hill, London) were cultured in minimal essential medium-alpha (MEM α) supplemented with new-born calf serum (NBCS, 10% v/v), penicillin (50 units ml⁻¹), streptomycin (100 μ g ml⁻¹) and fungizone (amphotericin B) (2.5 μ g ml⁻¹) in 175cm² tissue culture flasks. CHO-m2 cells co-transfected with m3 muscarinic receptor cDNA (CHO-m2m3, see below) were cultured in MEM α supplemented with NBCS (10% v/v), penicillin (50 units ml⁻¹), streptomycin (100 μ g ml⁻¹), fungizone (amphotericin B) (2.5 μ g ml⁻¹) and hygromycin B (400 μ g ml⁻¹). The cells were routinely passaged by washing the cell monolayer with HEPES buffered saline (HBS, composition: 154 mM NaCl, 10 mM HEPES, pH 7.4), detaching with trypsin (0.5 g l⁻¹)-EDTA (0.2 g l⁻¹), and splitting into fresh flasks (175cm²) containing 30 ml medium. Cells maintained in this manner kept the same doubling time and morphology. Experiments were carried out only on cells between passages eight and twenty-five. Cells were maintained at 37 °C in 5% CO₂: humidified air.

2.1.2 Transfection procedures

Boxall and colleagues generated a number of co-expressing cell lines by transfecting human m3 cDNA into parent CHO-m2 cells using a mammalian expression vector (p-CEP-hygro) (Boxall, 1998). The calcium phosphate-DNA co-precipitation procedure was used, as described by Sambrook et al. (1989), which increases the uptake of cDNA into cultured cells by presenting the nucleic acid to the cells as a calcium phosphate-DNA precipitate. Hygromycin B resistant stable transformants were selected, screened using western blotting and assessment of [³H]-InsP and cyclic AMP responses (see below) to agonist and m2m3-positive clones identified. CHO-m2m3 clones B2 and B7 were chosen for further study because they demonstrated both a

functional M3 receptor population through Western blotting and increases in total [³H]-inositol accumulation with similar magnitude and profile to CHO-m3 cells, as well as decreases in forskolin stimulated cAMP accumulation as observed in CHO-m2 cells (Boxall, 1998).

Experiments were performed on CHO-m2, CHO-m3, CHO-m3(vt-9), CHO-m2m3 (B2) and CHO-m2m3 (B7) cell lines unless otherwise stated.

2.2 N-methyl-[³H]-scopolamine (NMS) binding

2.2.1 Membrane preparation

The required number of large (175 cm²) flasks were grown to confluence and the medium removed before the cell monolayer was rinsed with HBS-EDTA (10 mM HEPES, 0.9% NaCl, 0.2% EDTA, pH 7.4). The cells were then lifted with 10ml HBS-EDTA per flask. The cells were centrifuged at 200×g for 5 min, at 4°C, and the supernatant discarded. The cells were then homogenised in wash buffer A (10 mM HEPES, 10 mM EDTA, pH 7.4; 2 ml buffer per confluent flask of cells), using a Polytron homogeniser (speed 5, 4 × 5 s bursts separated by 30 s on ice), in Sorvall centrifuge tubes. The tubes were then centrifuged at 40,000×g in a Sorvall RC-5 centrifuge (rotor SS-34) for 15 min at 4°C. The supernatant was discarded and the pellet re-homogenised, as above, in buffer B (10 mM HEPES, 0.1 mM EDTA, pH 7.4). The tubes were again centrifuged at 40,000×g in Sorvall RC-5 centrifuge for 15 min at 4°C, the supernatant discarded and the pellet dispersed in wash buffer B, (1 ml per confluent flask of cells), using the Polytron homogeniser. The protein concentration of the membranes was determined by Lowry assay, the membrane samples were either aliquoted or diluted with wash buffer B to the desired concentration (≈1 mg ml⁻¹) and then snap frozen in Eppendorf tubes in liquid nitrogen and stored at -80 °C.

2.2.2 [³H]-NMS saturation binding

[³H]- NMS binding was performed on membrane samples (prepared as described above) as described by Lambert et al. (1989). Two total binding and one non-specific binding samples were prepared for each concentration of [³H]-NMS. Each sample was prepared in a test tube with a final assay volume of 200 µl. Total binding samples were 140 µl wash/assay buffer (10

mM HEPES, 10 mM MgCl₂, 100 mM NaCl), 40 µl of [³H]-NMS at stated concentration and 20 µl of the membranes (added last). Non-specific binding samples were 100 µl wash/assay buffer, 40 µl 5 µM atropine (1 µM final), 40 µl stated concentration of [³H]-NMS and 20 µl cell membranes (added last). [³H]-NMS concentrations were prepared from 0.05 nM to 3 nM, in wash/assay buffer, two 40 µl samples of the standards were taken at each concentration in order to calculate precisely the concentration of [³H]-NMS added to each sample. The samples were incubated in a shaking water-bath after membrane addition for 60 min at 37°C. The samples were then rapidly filtered through Whatman GF/B filter paper with 3 × 3 ml washes with ice cold wash/assay buffer. The filter discs were then placed into vials, 4 ml Emulsifier Safe scintillant was added and they were left overnight before being counted.

2.2.3 [³H]-NMS displacement binding

Displacement of [³H]-NMS from cell membranes preparations by tripitramine, methoctramine or darifenacin was performed as described for saturation binding with final assay volume of 200 µl, 100 µl wash/assay buffer, 40 µl of [³H]-NMS (approximately 1.5 nM [³H]-NMS), 40 µl antagonist (prepared in the wash/assay buffer) and 20 µl cell membranes.

2.3 Inositol (1,4,5) - trisphosphate (IP₃) mass accumulation

2.3.1 Cell preparation

Confluent cells in twenty-four well plates (surface area 1.9 cm²/ well) were washed twice in 1 ml freshly gassed (95% CO₂, 5% O₂) Krebs Henseleit buffer (KHB) (composition in mM: HEPES 10, NaCl 118, KCl 4.7, MgSO₄ 1.2, KH₂PO₄ 1.2, NaHCO₃ 28.1, CaCl₂ 1.3, D-glucose 11, pH 7.4) and allowed to stabilise in 450 µl KHB for 15 min at 37°C.

2.3.2 Sample generation

Cells were stimulated by addition of 1 mM methacholine (MCh) at 37°C. The reaction was terminated by aspiration of the KHB/drug solution and the addition of 300 µl 0.5 M trichloroacetic acid (TCA) to each well. The plate was then left on ice for 30 min after which all 300 µl in each well was transferred to Eppendorf tubes. 3 ml of blank buffer for the mass assay

was prepared by the same protocol as for the samples. 75 μ l 10 mM EDTA (pH 7.0) was then added to each tube, the samples were vortexed and 600 μ l of a 1:1 (v/v) solution of Tri-n-octylamine and trichlorotrifluoroethane (Freon) added and vortexed again. These samples were then left for 15 min at room temperature, vortexed and centrifuged for 2 min in a bench centrifuge at full speed (12000 \times g). 200 μ l of supernatant was then transferred to a fresh Eppendorf tube and 50 μ l NaHCO₃ was added, samples were re-vortexed and stored at 4°C.

2.3.3 IP₃ mass assay

The Ins(1,4,5) P₃ (IP₃) binding assay was performed as described by Challiss et al. (1990), with competition of radiolabeled IP₃ and sample/standard IP₃ for IP₃ binding sites in bovine adrenal cortical membranes. 30 μ l TRIS (100 mM)/EDTA (4 mM) buffer (pH 8.0) was added to 30 μ l of sample/standard on ice. 30 μ l [³H]-IP₃ (at a concentration where 30 μ l gives approximately 8000 d.p.m.; this is approximately 10 μ l [³H]-IP₃: 1 ml H₂O) was then added before 30 μ l binding protein. Standards were prepared in the range 1.2 nM to 1.2 μ M IP₃, using a 40 μ M IP₃ standard diluted with blank buffer. The samples were then vortexed and left on ice for 40 min before rapid filtration on manifolds using 3 \times 3 ml washes with ice-cold wash buffer (25mM TRIS, 1mM EDTA, 5mM NaHCO₃, pH 8.0) onto GF/B Whatman filter discs which were then placed in vials with 4.2 ml Scintillant Plus and left overnight before counting.

2.4 Measurement of total [³H]-IP_x accumulation

2.4.1 Cell preparation and radio-labelling

Cells were plated out in culture medium containing 1 μ Ci ml⁻¹ [³H]-*myo*-inositol for 48 h prior to experiment. Confluent cells on twenty-four well plates, were washed twice in 1 ml freshly gassed (95% CO₂, 5%O₂) KHB (composition above). Cells were placed in 450 μ l KHB containing 10 mM LiCl and allowed to stabilise for 15 min at 37°C. Lithium has been shown to prevent inositol recycling by uncompetitive inhibition of inositol monophosphatase (Nahorski et al. 1991) and to allow accumulation of inositol phosphates (IP_x). Where indicated, calcium was omitted from the KHB buffer and EGTA (100 μ M) was included.

2.4.2 Sample preparation

Cells were challenged with agonist for the stated time (15 min for concentration-response experiments) and reactions were terminated by aspiration of the drug/KHB solution and addition of 500 μ l ice-cold TCA (0.5 M) to each well. Plates were then left on ice for 20 min and neutralised by oil extraction as described under section 2.3.2 above, (200 μ l EDTA was added to each 500 μ l sample prior to oil extraction.). 500 μ l of neutralised supernatant was then transferred to a fresh tube and 200 μ l NaHCO₃ (60 mM) was added. Samples were re-vortexed and stored for 24-96 h at 4°C before [³H]-IP_x separation (see below).

2.4.3 [³H]-IP_x sample separation

Separation was performed as described by Challiss et al. (1992). Samples were removed from 4°C storage and vortexed at room temperature. Samples were loaded, with 5 ml water, onto glass columns containing 0.5 ml bed-volume Dowex AG1-X8 anion exchange resin (formate form, 50-100 mesh). Columns were then washed with 10 ml ammonium formate (CH₂O₂H₃N) (60 mM) / Na₂B₄O₇ (5 mM) to remove [³H]-glycerophosphoinositol. Bound [³H]-InsPx fractions were eluted with 10 ml of ammonium formate (0.75 M) / HCOOH (0.1 M). 10 ml FloScint IV was added to 5 ml of each fraction which were then vortexed before liquid scintillation counting. Columns were 'regenerated' by addition of 10 ml ammonium formate (2 M) / HCOOH (0.1 M) followed by 20 ml water, and stored at 4°C until further use. Total cell protein was determined by Lowry method (see below).

2.5 Cyclic AMP accumulation

2.5.1 Cell preparation

Following the removal of the medium, confluent cells in twenty-four well plates were washed twice in 1 ml freshly gassed Krebs Henseleit buffer (KHB, composition above). Cells were placed in 450 μ l KHB and allowed to stabilise for 15 min at 37°C.

2.5.2 Sample generation

Confluent cells were stimulated with methacholine at the stated concentration in a final volume of 500 μl for 10 min before being challenged with forskolin (10 μM) for 10 min. Reactions were terminated by aspirating the drug solution and adding 250 μl of trichloroacetic acid (TCA; 0.5 M). The plates were then left for 15 min on ice, before the solution was removed to polycarbonate tubes. 600 μl of a 1:1 solution of Tri-n-octylamine and trichlorotrifluoroethane was added and the samples were vortexed. 150 μl of the upper phase was removed and neutralised with 60 mM NaHCO_3 to pH 7.4. The samples were stored at 4°C and analysed for cAMP. Lowry protein assay was performed on the cell debris left in the wells of the plate.

2.5.3 Cyclic AMP determination

Cyclic AMP was quantified as described by Brown et al. (1971). 50 μl of sample or a standard concentration of cAMP (2.5-200 nM, made up in 50 μl of assay buffer containing 50 mM Tris-HCl and 4 mM EDTA, pH 7.5; NSB 250 pmol cAMP) was added to 100 μl of [^3H]-cAMP (approximately 4 nM; specific activity 28.9 Ci/mmol) in microfuge tubes. 150 μl binding protein was then added to the tubes to start the reaction, tubes were vortexed and incubated 90 min at 4°C. Bound and free [^3H]-cAMP was separated by addition of 250 μl of an ice-cold suspension of activated charcoal (0.25 g / 50 ml) in bovine serum albumin solution (0.1 g / 50 ml of assay buffer), followed by vigorous mixing. The samples were then left on ice for 7 min prior to centrifugation at 14,000 \times g for 4 min. 0.4 ml of the supernatant was then counted by liquid scintillation counting.

2.6 Single cell calcium imaging experiments

CHO-m2m3 cells were thinly seeded on flame-sterilised coverslips (380 mm^2) in culture dishes (35 \times 10 mm) in MEM α medium at 37°C for 24 h. The coverslips were then washed twice with Krebs-Henseleit buffer before the addition of 5 μM fura-2/AM. Cover slips were incubated for 30 min in the dark at room temperature. The coverslips were again washed twice with KHB and mounted onto the stage of a Nikon Diaphot inverted epifluorescence microscope (\times 40 objective). A field of approximately 10-15 cells was selected. KHB or agonist was

continuously perfused over the cells at a rate of 5 ml/min. Methacholine was applied to the co-expressing cells at concentrations of 0.1, 1, and 100 μM . Background fluorescence images at wavelengths above 510 nm were subtracted from all results. Fluorescent images were obtained after excitation at 340 and 380 nm (four consecutive images over 1.6 s averaged) with a xenon arc lamp. The emission signal was measured at 510 nm using an intensified charge-coupled device camera (Photonic Science). The ratiometric values obtained were converted to approximate $[\text{Ca}^{2+}]_i$ using a previously obtained calibration curve and the equation,

$$[\text{Ca}^{2+}]_i = K_d \times \{(R - R_{\min}) / (R_{\max} - R)\} \times \{F_{\min}(380\text{nm}) / F_{\max}(380\text{nm})\}$$

where K_d is the dissociation constant of Ca^{2+} for fura-2/AM (224nM at 37°C), R_{\min} and R_{\max} are the minimal and maximal fluorescent ratios obtained by permeabilising the cells with 0.1% Triton-X-100 for R_{\max} followed by the addition of an excess of EGTA at 5 mM for R_{\min} . F_{\min} (380 nm) and F_{\max} (380 nm) are the fluorescent intensities after excitation at 380 nm, in the absence and presence of Ca^{2+} , respectively.

2.7 Measurement of $[\text{Ca}^{2+}]_i$ responses using fluorimetric imaging plate reader (FLIPR)

2.7.1 Cell preparation

CHO-m2, CHO-m3 and CHO-m2m3 (B2) cells were seeded in black-walled clear-base 96 well plates (Costar, UK) at 30,000 cells per well 24 h prior to experiment in culture medium supplemented as described above.

2.7.2 Measurement of $[\text{Ca}^{2+}]_i$ for a population of cells

The confluent wells of cells were then washed twice with FLIPR buffer (composition Hanks balanced salt solution (HBSS, calcium free, Gibco/Life Technologies, UK) supplemented with 200 mM CaCl_2 , 1 M HEPES, 250 mM probenecid) before being incubated for 1 h at 37°C in FLIPR buffer containing the calcium indicator Fluo-3AM (4 μM , Teflabs, Texas, USA). In some studies calcium was omitted from the experiments and EGTA (100 μM) added but FLIPR

buffer for the incubation with the dyes always contained calcium. The cells were then washed three times in FLIPR buffer (\pm calcium/EGTA) using a COSTAR plate washer to remove excess dye. The plates were then incubated in FLIPR buffer (75 μ l) at room temperature for 30 min with or without antagonists / signal transduction modifying agents. The plates were then loaded into a FLIPR (Molecular Devices, UK) to monitor fluorescence (λ_{ex} =488 nm, λ_{EM} = 540 nm) before and after the addition of the relevant drug / vehicle. Responses were measured as peak fluorescence intensity (FI) minus basal FI. Agonists were added 10 s after measurements started to establish baseline recording, with the exception of Ca^{2+} free experiments (Section 4.2.4), where fluorescence measurements were made throughout the 30 min equilibration period. Ionomycin (5 μ M) was routinely added for the last 30 s of each time-course.

2.8 [3 H]-Thymidine incorporation

2.8.1 Cell preparation

[3 H]-thymidine incorporation method was based on that by Levine et al. (1997). Confluent flasks of cells were lifted with trypsin/EDTA and plated into 24 well plates at a density of 50,000 cells/well in 1 ml of medium (MEM α + NBCS, supplemented with penicillin, streptomycin and fungizone as for normal tissue culture) and incubated at 37°C for 24 h to allow cells to adhere. The media was then removed by aspiration and replaced with 1 ml/well of either serum free media (MEM α -NBCS, for serum-starved experiments) or normal serum containing culture media (MEM α +NBCS, for serum-replete experiments) and the cells incubated for a further 24 h. This was then replaced with either serum-free or serum containing media prior to treatment with agonist /antagonist /control solutions for 24 h.

2.8.2 Measurement of [3 H]-thymidine incorporation

2 μ Ci of [3 H]-thymidine was added to each well for the final 2 h of the drug treatment and the experiment was then terminated by aspirating the media from the cells, followed by washing them three times with serum-free medium. The cells were then incubated for 1 h, at 4°C, in 2 ml / well 5% ice cold TCA. The cells were then washed in a further 2 ml of 5% TCA and incubated for 5 min at 4°C with ice-cold ethanol (containing 200 μ M potassium acetate). This was then

followed by two 15 min incubations, at 4°C, with 2 ml of a 1:3 mix of ether:ethanol. The cells were left to air dry for approximately 45 min before being scraped into 1 ml of 0.1 % NaOH. The samples were added to scintillation vials with 9 ml Emulsifier Safe scintillant and counted.

2.9 Mitogen-activated protein kinase (MAPK) assays

2.9.1 Cell preparation

Following the removal of the medium, confluent cell monolayers in six well plates (surface area 9.6 cm²/ well) were twice washed in 3 ml freshly gassed (95% CO₂, 5%O₂) Krebs-Henseleit buffer (KHB, composition above). 3 ml KHB was then added and cells allowed to stabilise for 30 min at 37°C.

2.9.2 Extracellular-signal regulated kinase (ERK) Activation

2.9.2.1 Sample generation

Cells were routinely stimulated with MCh (at stated concentrations for indicated times) at 37°C, with antagonists being applied 30 min prior to initial agonist addition. The reaction was terminated by aspirating the KHB/drug solution and washing each well with ice-cold phosphate-buffered saline (PBS, composition: 140 mM NaCl, 2.68 mM KCl, 8.1 mM Na₂HPO₄, 1.47 mM KH₂PO₄, pH 7.4). Cells were then lysed with 500 µl ice-cold lysis buffer per well (20 mM Tris-HCl (pH 8.0), 0.5% NP-40, 250 mM NaCl, 3 mM EDTA, 3 mM EGTA, 1 mM phenylmethylsulfonyl fluoride (PMSF), 2 mM Na₃VO₄, 20 µg/ml aprotinin, 5 µg/ml leupeptin, 1 mM dithiothreitol (DTT), pH 7.6). Each well was scraped and the samples transferred to Eppendorf tubes. Samples were centrifuged at 20,000 r.p.m. for 10 min at 4°C, and a 200 µl aliquot of supernatant taken for activity assay.

2.9.2.2 ERK Activation Assay

ERK activity was assayed as described by Wylie et al. (1999). 2 µl rabbit anti-ERK1 polyclonal antibody (Santa Cruz) was added to the 200 µl aliquot of lysate, the samples were vortexed and

left on ice for 90 min. 70 μ l Protein A Sepharose (15% slurry) was then added to the samples and they were left on a bottle roller at 4°C, for 90 min. The samples were then pulse spun, at 14,000 r.p.m., to pellet the beads which were then washed four times, twice in lysis buffer and twice in kinase buffer (20 mM HEPES (pH 7.2), β -glycerophosphate (pH7.2), 10 mM MgCl₂, 1 mM DTT, 50 μ M Na₃VO₄) and the supernatant removed. 40 μ l of assay solution (kinase buffer containing 20 μ M cold ATP, 1 μ Ci [γ -³²P]-ATP, 0.2 mM of synthetic peptide substrate corresponding to amino acids 662-681 of the epidermal growth factor receptor (EGFR), see appendix) was then added to each sample, samples were vortexed and incubated at 30°C for 20 min. The samples were re-vortexed every 5 min throughout the incubation. The reaction was stopped by the addition of 10 μ l 25% TCA. The samples were then pulse spun at 14,000 r.p.m. and 40 μ l of each sample was blotted onto Whatman p81 chromatography paper. Papers were washed for 4 \times 5 min, in 400 ml 0.5% orthophosphoric acid and then 1 \times 3 min in 400 ml acetone. After this final wash the papers were laid on tissue paper at room temperature and, once dry, placed in scintillation vials with 5 ml Scintillation Plus and then counted.

2.9.3 c-Jun NH₂-terminal kinase (JNK) activation

2.9.3.1 Sample generation

Confluent monolayers of cells were stimulated by addition of MCh (at stated concentrations) and incubated for the indicated times at 37°C. As for the ERK activity assay the reaction was terminated by aspirating the KHB/drug solution, each well being washed with ice-cold PBS, and then lysed with 500 μ l ice-cold lysis buffer per well. Each well was scraped and the samples transferred to Eppendorf tubes. Samples were spun at 20,000 r.p.m. for 10 min at 4°C, and a 400 μ l aliquot of supernatant taken for activity assay.

2.9.3.2 Preparation of GST-c-Jun fusion protein

A Glutathione S-transferase (GST) - c-Jun fusion protein was produced in bacteria using a GST-c-Jun gene fusion system (Pharmacia Biotech) for assaying the JNK activation in cell lysates. The fusion protein was prepared using the pGEX plasmid vector which contains the laq I^q gene (to induce expression), an AMP^r gene (for selection) and the GST gene upstream of a multiple

cloning site into which the c-Jun cDNA encoding amino acids 1-79 of the gene had been inserted. *E. Coli* transformed with the plasmid (previously stored at -80°C) were scraped in to 10 ml Luzziula Broth (LB) (170 mM NaCl, 10 g.L⁻¹ tryptone and 5 g.L⁻¹ yeast extract) containing ampicillin (50 µg ml⁻¹) and left in a shaking incubator at 30°C overnight. The following day, the culture was added to 500 ml of LB containing ampicillin (50 µg ml⁻¹) and left to grow at 37°C for approximately 3 h until the OD, measured at 600 nm, reached 0.5 units. Expression of GST-c-Jun was induced by incubation with 1mM IPTG for 3 h in a shaking incubator at 37°C. The culture was then centrifuged for 5 min at 10,000 r.p.m. and the bacterial pellet resuspended in 5 ml PBS, containing 1% Triton X100 (PBS/Triton) and aprotinin (4 µg ml⁻¹). The resuspended pellets were then stored at -20°C overnight. The resuspended culture was thawed and sonicated for 30 s on ice. The sample was then spun for 15 min at 10,000 r.p.m. the supernatant retained and added to 2 ml of glutathione-sepharose beads that had been prewashed twice in 50 ml of ice-cold PBS/Triton. The samples were then incubated with the sepharose beads for 4 hours at 4°C on a roller. The beads were then washed twice in 50 ml of PBS/Triton, and resuspended in 2 ml PBS/Triton before being dispensed into aliquots. Proteins were analysed by boiling 5 µl of beads in Laemmli sample buffer containing 50 mM DTT and running them on a 12% SDS PAGE gel (for gel composition see appendix) using a BioRad minigel apparatus with low weight molecular markers and Coomassie Blue staining.

2.9.3.3 JNK activation assay

JNK activation was assayed as described by Wylie et al. (1999). The buffer was removed from the GST-c-Jun beads and they were diluted 1 in 4 with lysis buffer. 20 µl of the 1 in 4 bead solution was then added to each sample and they were placed on a bottle roller for one hour. The samples were then pulse spun, at 14,000 r.p.m., to retain the beads which were then washed four times, twice in lysis buffer and twice in kinase buffer and the supernatant removed. 40 µl of assay solution (kinase buffer containing 20 µM ATP, and 1 µCi [γ -³²P]ATP) was then added to each sample. Samples were vortexed and incubated at 30°C for 20 min. The samples were re-vortexed every 5 min throughout the incubation. The reaction was stopped by the addition of 40 µl 2X Laemmli sample buffer, containing 5% DTT. The samples were then heated at 100°C for 5 min and centrifuged at 14,000 r.p.m. for 5 min.

70 μ l of the samples was loaded onto a 12% SDS-PAGE gel (for gel composition see appendix) along with 20 μ l of a commercial low molecular weight marker preparation. The gels were run at 18 mA/gel through the stacking gel and 24 mA through the resolving gel or 5 mA/gel overnight. The gel it was stained with 0.25% Coomassie blue containing 50% methanol and 10% acetic acid solution to detect GST-c-Jun. The gels were then destained with a 40% methanol, 10% acetic acid and 1% glycerol solution, and dried at 80°C under vacuum for one hour. The dried gels were then exposed to Hyperfilm MP using an intensifying screen. Following autoradiography, each lane on the gel was excised and placed in a scintillation vial with 5 ml Scintillation Plus and counted.

2.10 Bovine tracheal smooth muscle (BTSM)

2.10.1 BTSM slice preparation

Bovine trachea was supplied by a local abattoir, and transported to the laboratory in ice-cold KHB, pH7.4 (for composition see IP₃ mass accumulation protocol above). The smooth muscle tissue was washed in ice-cold KHB following dissection of the trachea and removal of the epithelial layer, submucosa and connective tissue. A McIlwain tissue chopper, set at maximum blade force, was used to cut the tissue into 300 \times 300 μ m cubes. The slices were then washed 2-3 times in warm, gassed, KHB (37°C). Washed slices were allowed to settle and 10 ml of packed slices were transferred to a 175cm² tissue culture flask (see below). Packed BTSM slices were cultured overnight (18-22h), at 37°C in 95% air / 5% CO₂, in MEM α medium supplemented with streptomycin (100 μ g ml⁻¹) and penicillin (50 units ml⁻¹).

2.10.2 BTSM slice stimulation

Following overnight culture the slice preparation from each flask was transferred to 30 ml sterile tubes and repeatedly washed with KHB (37°C). 75 μ l of packed BTSM slices were then added to individual insert vials containing 325 μ l of gassed KHB/antagonist, placed in a shaking waterbath, and allowed to equilibrate for 30 min. The slices were then challenged with the appropriate agonist for the desired time and the reaction was terminated with 2 ml ice-cold KHB and the samples were placed on ice. The samples were immediately centrifuged at 4°C at 3000

r.p.m for 10 min. The supernatant was removed, and 1 ml of ice-cold lysis buffer was added to each vial, which were kept on ice until homogenisation. Each sample was homogenised using a Polytron homogeniser and then centrifuged as before. The supernatant was then placed into a 1.5 ml Eppendorf tube prior to assay (by western blotting).

2.10.3 Phosphorylated ERK Western blot analysis

An equal volume of BTSM slice lysate was added to 2X Laemmli buffer (containing 50 mM DTT) and the samples were boiled at 100°C for 5 min before 10 µl of each sample was run on a 10% SDS PAGE gel (for gel composition see appendix) with an appropriate marker at 200mV for 1 h. Gels were then placed onto nitrocellulose membranes between Whatman 3MM filter paper pre-soaked in transfer buffer (48 mM Tris-HCl, 39 mM glycine, 1.3 mM SDS, 20% methanol, pH 8.0) and transferred using a semi-dry transfer apparatus (Bio-Rad), at 12V for 30 min. Proteins were then visualised for equal loading by staining with Ponceau S red stain and protein standards marked. Ponceau S stain was then removed by washing with Tween/Tris-buffered saline (TTBS: 50 mM Tris/HCl buffer, 150 mM NaCl, 0.1% Tween 20, pH 8.0). Nitrocellulose paper was then placed in blocking buffer (1% bovine serum albumin (BSA), in TTBS) for 1 h at room temperature. Blocking buffer was removed by one 5 min TTBS wash. The nitrocellulose membranes were then incubated overnight at 4°C on a roller with the primary phospho-ERK antibody (anti-ACTIVE MAPK pAb; Promega, UK) at a dilution of 1:500 in TTBS. Following the incubation with the primary antibody the membranes were washed three times for 5 min in TTBS to remove excess antibody. The nitrocellulose membranes were then incubated with the secondary antibody (ant-rabbit IgG, Sigma, UK, 1:1000 dilution in TTBS) at room temperature for 1 h. The blots were then washed 5 X 5 min with TTBS to remove unbound secondary antibody. The immunoblots were then developed using the enhanced chemiluminescence (ECL; Amersham) technique and exposed to Hyperfilm MP using an intensifying screen for between 1 and 5 min and the film developed on a hyperprocessor.

2.11 Protein determinations

2.11.1 Lowry protein assay

Protein assays for IP₃ mass accumulation and cAMP accumulation experiments were carried out in quadruplicate on 500 µl of sample by the method of Lowry (Lowry et al. 1951). The samples were obtained by removing the protein from four randomly chosen wells on the 24 well plates using 250 µl 0.1 M NaOH left for 20 min to solubilise then another 250 µl to rinse the well and transferred to test tubes. The standards were made up to 500 µl, in duplicate, in 0.1M NaOH. To each tube 1 ml assay solution was added (made in ratio 100:1:1, 2% Na₂CO₃, 0.4% NaOH : 2% K⁺/Na⁺ tartrate : 1% CuSO₄) and the tubes vortexed and left for 10 min. Then 100 µl 3-fold diluted Folin & Ciocalteu's Phenol reagent was added and each tube revortexed and left for 15 min before 1 ml water added to each sample (vortexed again) and their absorbance was measured at 750 nm.

2.11.2 Bradford protein assay

Protein assays for the MAPK assays were carried out using the Bradford protein assay (Bradford, 1976). The blank was made up of lysis buffer (10 µl), the standards were diluted with lysis buffer to a final volume of 10 µl, and 5 µl of each sample was made to a final volume of 10 µl with 5 µl lysis buffer. To each of these 10 µl samples, 10 µl H₂O and 50 µl 1 M NaOH was added and the tubes vortexed. 1 ml of dye reagent (0.01% Serva Blue G, 8.5% phosphoric acid, 4.75% ethanol, filtered through Whatman No1 filter paper) was added to the samples which were then left for 5 min before being vortexed. Absorbance of the samples was measured at 595 nm and 465 nm. The difference between the readings at the two wavelengths was calculated and plotted against protein concentration.

2.12 Data analysis

Unless otherwise stated, data are expressed as means ± standard error of the mean (S.E.M.) from at least 3 separate experiments performed on different days with fresh drug dilutions and

solutions. Curve fitting and parameter estimations were carried out using Graphpad Prism version 2.0 or 3.0 (Graphpad Software INC., Sam Diego, CA, USA).

cAMP curve fitting

Where the response to MCh was biphasic (Figure 3.9), the agonist mediating inhibition at low, and potentiation at high concentrations, concentration-response relationships were fitted by a sum of two logistic equations:

$$f = I_{\max} + F_s \left\{ \frac{C^{n_1}}{C^{n_1} + K_1^{n_1}} \right\} + S_{\max} \left\{ \frac{C^{n_2}}{C^{n_2} + K_2^{n_2}} \right\}$$

where I_{\max} is the maximum inhibition of the forskolin-stimulated adenylyl cyclase activity by MCh (F_s) with dissociation constant K_1 and Hill coefficient n_1 ; S_{\max} is the maximum stimulation of cAMP accumulation by high concentrations of MCh with dissociation constant and Hill coefficient K_2 and n_2 , respectively, and c is the concentration of MCh. Fitting was done by least squares minimization using the above equation and Prism 3.0.

Cheng-Prusoff equation

Antagonists activities are reported as pK_i values.

K_i can be calculated from IC_{50} value using the Cheng-Prusoff equation (Cheng and Prusoff, 1973).

$$K_i = \frac{IC_{50}}{1 + \frac{[\text{ligand}]}{K_d}}$$

Where IC_{50} is the experimentally derived concentration of antagonist needed to inhibit the response (e.g. binding) by 50 %, $[\text{ligand}]$ is the concentration of agonist or radio-labelled ligand added and K_d in the case of binding is the affinity of the radioligand for the receptor or in the case of ERK activation assays is the EC_{50} value for the agonist.

$$pK_i = -\log_{10} K_i$$

Concentration response curve analysis

Concentration response relationships were reported as pEC₅₀ where

$$\text{pEC}_{50} = -\log_{10} \text{EC}_{50}$$

(EC₅₀ measured in M)

2.13 Materials

For a list of reagents and suppliers see appendix.

Chapter Three: General characterisation of receptor expression and coupling in CHO cells singularly expressing or co-expressing M₂- and M₃- mACh receptors

3.1 Introduction

Many tissue types express a mixed population of muscarinic receptors, with most smooth muscle tissues expressing a predominant M₂ over M₃ muscarinic receptor population. Thus, it has been established that M₂ receptors predominated over M₃ in an approx. 3:1 ratio in many smooth muscle types (see Eglen et al., 1996a and Introduction to this thesis). Muscarinic receptors are G-protein coupled receptors and M₂ classically couple to G_{i/o} proteins, while M₃ couple to G_{q/11} (Caulfield, 1993). Hence, activation of M₂ receptors inhibits adenylyl cyclase activity, decreasing cAMP production, and activation of M₃ receptors activates PLC to increase hydrolysis of PIP₂ increasing the production of IP₃ and DAG.

So the question is raised as to whether the M₂ and M₃ receptor signalling pathways interact in smooth muscle, and why are M₂ receptors present at such high levels in smooth muscle tissue? It is important to understand the physiological significance of the co-expression of M₂ and M₃ receptors in smooth muscle cells. Although model cell systems expressing either M₂ or M₃ muscarinic receptors have been characterised, observation of the receptor functions in isolation do not necessarily predict what will happen when both are co-expressed in the same cell, as occurs *in vivo* in a variety of tissues. Therefore, it is hoped that these studies will provide a relatively simple experimental paradigm in which to study M₂ / M₃ interactions at the level of their respective signalling pathways, and hopefully to establish possible cross-talk mechanisms to explore further in smooth muscle preparations.

Previous experiments, using cultured smooth muscle cells, have shown that M₃ receptors are often lost from an initial heterologous population of muscarinic receptors, resulting in a homogenous M₂ population (Yang et al. 1990; Widdop et al., 1993). Chinese hamster ovary (CHO) cells, which lack endogenously expressed mACh receptors (Peralta, 1987), expressing M₂ (CHO-m2) or M₃ (CHO-m3) human muscarinic receptors were obtained from Dr S.

Lazareno and Dr N. Buckley respectively (National Institute for Medical Research, Mill Hill, London). A number of co-expressing CHO-m2m3 cell lines were generated previously by Donna Boxall, in this Department, by co-transfection of human M₃ receptor cDNA into CHO cells already expressing M₂ receptors (CHO-m2).

Using CHO-m2, CHO-m3 and CHO-m2m3 cell lines, the aims of this Chapter were to characterise the receptor populations and their second messenger signalling in the co-expressing clones to show successful generation of a functioning/viable model for mixed mACh receptor populations. By comparing the responses observed in co-expressing (CHO-m2m3) cells to those in CHO-m2 and CHO-m3 cells it would also be possible to study potential interactions/cross-talk between co-expressed M₂ and M₃ receptors. Receptor populations were characterised by radioligand saturation and displacement experiments, and second messenger assays to assess functional coupling (cAMP and IP₃ for M₂ and M₃ receptors, respectively) and potential cross-talk between the respective signalling pathways for the M₂ and M₃ receptors within the co-expressing cells. It will be shown that the receptors are co-expressed homologously in the CHO-m2m3 clones, by observation of single cell Ca²⁺ responses within the cells.

3.2 Results

3.2.1 Determination of total receptor populations in CHO-m2, CHO-m3 and CHO-m2m3 (B2) cells by N-methyl-[³H]-scopolamine (NMS) binding.

N-methyl-[³H]-scopolamine saturation binding data from CHO cell membranes were analysed using both an iterative non-linear curve fitting procedure of binding isotherms (GraphPad Prism 3.0) and according to the method of Scatchard (Scatchard, 1949). There were no significant differences in estimates of K_d or B_{max} by each of these methods. pK_i values were calculated according to the method of Cheng & Prusoff (1973). Saturation and displacement binding was routinely performed at early, middle and late passages and no significant differences were observed.

Saturation binding of cell membrane preparations with [³H]-NMS revealed the varied receptor populations shown in Figures 3.1-3.3 and summarised in Table 3.1. The [³H]-NMS saturation binding studies on membrane preparations revealed total mACh receptor populations for the cell

lines studied of 617 ± 51 , 3962 ± 409 and 1694 ± 456 fmol/mg protein and similar K_d values for CHO-m2, CHO-m3 and CHO-m2m3 (B2 clone) cells respectively. Binding isotherms showed clear saturation and thus knowing the protein concentrations of membrane preparations (Lowry protein assays see Chapter 2) it was possible to calculate B_{max} (total number of specific binding sites for NMS) see Table 3.1.

Characterisation of receptor numbers within a second cell line expressing M_3 -receptors (CHO-m3 VT-9) at a lower expression level revealed expression levels of 160 ± 8 fmol receptors/mg protein. A second co-expressing clone, CHO-m2m3 (B7), expressed a smaller total receptor population (1395 ± 123 fmol/mg protein) than CHO-m2m3 (B2) cells (Table 3.1).

3.2.2 [3 H]-NMS displacement binding in CHO-m2, CHO-m3 and CHO-m2m3 (B2) cell membranes

Antagonist displacements of [3 H]-NMS binding in CHO-m2, CHO-m3 and CHO-m2m3 (B2) cell membranes are shown in Figures 3.4 - 3.7 and summarised in Tables 3.2 and 3.3. A concentration of [3 H]-NMS approximately equal to the K_d was displaced from mACh receptors by increasing concentrations of the M_2/M_3 'selective' antagonists methoctramine, tripitramine and darifenacin.

Displacement binding has been performed on membrane preparations for the three main cell lines studied initially using tripitramine as the M_2 over M_3 selective muscarinic antagonist. However, due to a lack of a commercial source of tripitramine, and it no longer being produced by Melchiorre and colleagues, methoctramine has also been characterised in displacement experiments to establish whether it shows selectivity approaching that of tripitramine; this is shown in Figure 3.4. These experiments were initially performed on CHO-m2 and CHO-m3 membranes and these antagonists were then used to dissect the receptor populations within the co-expressing CHO-m2m3 (B2) clone. As can be seen from Figure 3.4 and Table 3.2, while tripitramine is the M_2 over M_3 selective antagonist of choice (395 fold selectivity), methoctramine also shows a large selectivity window (251 fold).

Displacement binding has also been performed using the M_3 over M_2 selective compound darifenacin; characterisation of this compound using CHO-m2 and CHO-m3 membranes is

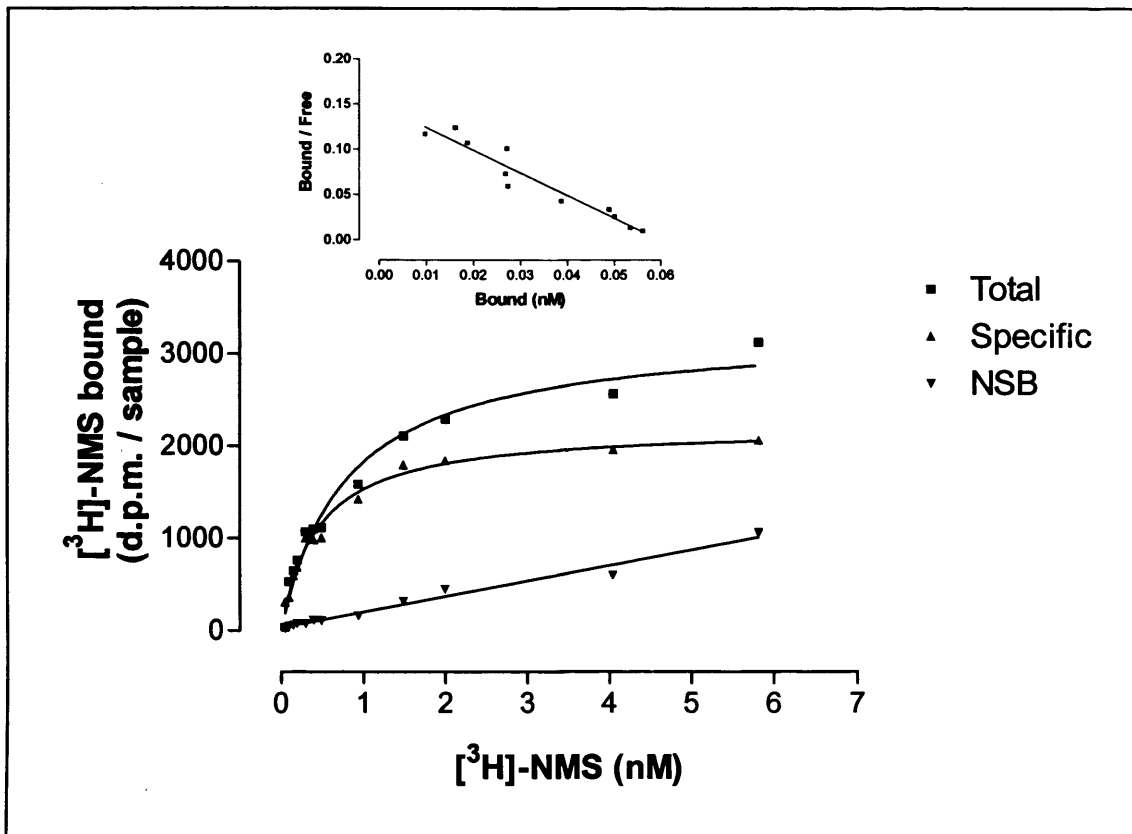


Figure 3.1 $[^3\text{H}]\text{-NMS}$ saturation binding in CHO-m2 cell membrane preparations. Data are shown as means of a representative experiment performed in duplicate and repeated at least three times. The inset shows Scatchard analysis for the same data. Non-specific binding was assessed in the presence of 1 μM atropine.

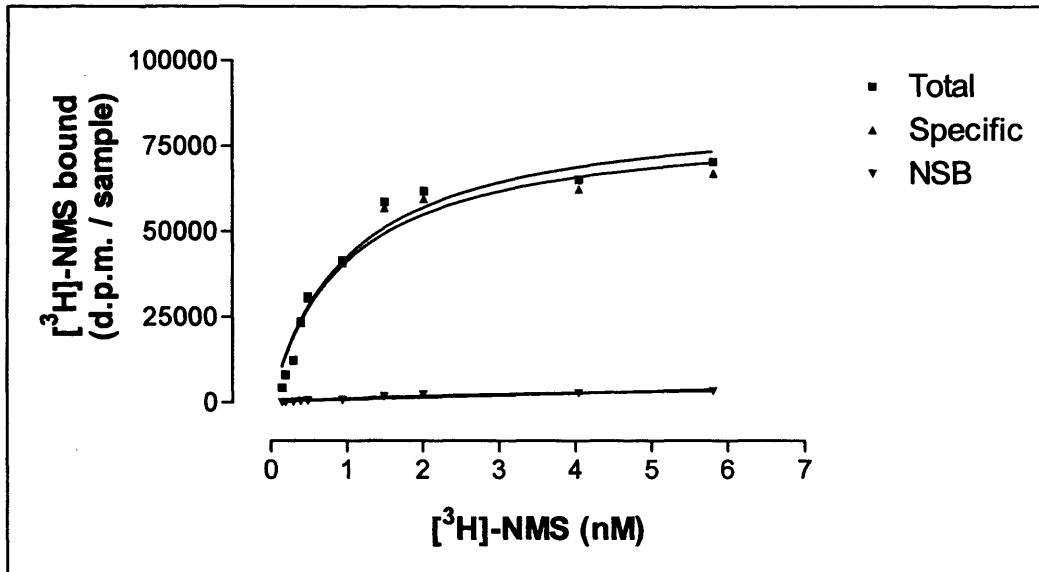


Figure 3.2 [³H]-NMS saturation binding in CHO-m3 cell membrane preparations. Data are shown as means of a representative experiment performed in duplicate and repeated at least three times showing total, specific and non-specific binding.

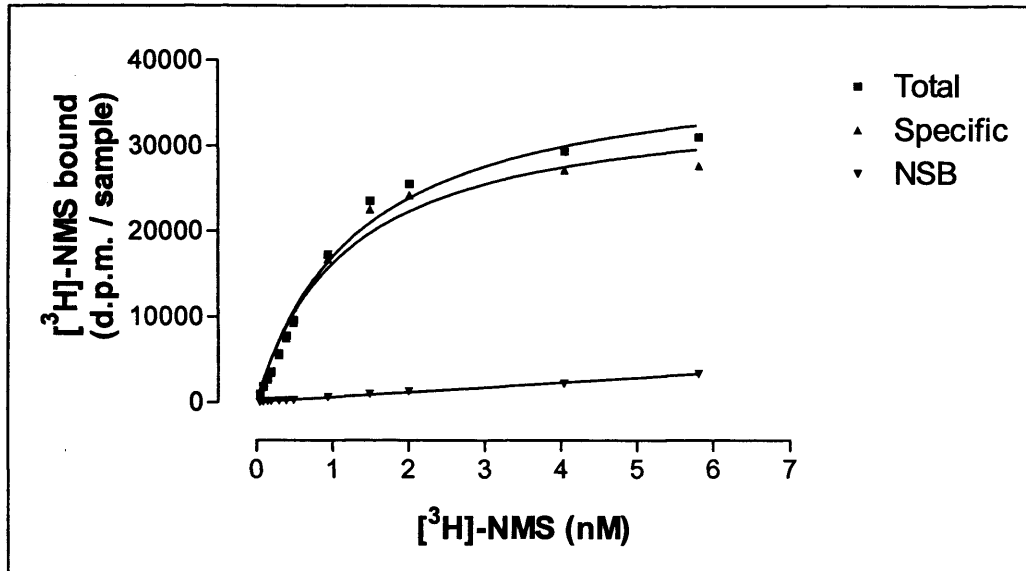


Figure 3.3 [³H]-NMS saturation binding in CHO-m2m3 (B2) cell membrane preparations. Data are shown as means of a representative experiment performed in duplicate and repeated at least three times showing non-specific, specific and total binding.

Cell Line	K_d (nM)	B_{max} (fmol / mg protein)	N
CHO-m2	0.35 ± 0.13	617 ± 51	3
CHO-m3	0.35 ± 0.16	3692 ± 409	3
CHO-m2m3 (B2)	0.18 ± 0.004	1694 ± 456	3
CHO-m2m3 (B7)	0.20 ± 0.045	1395 ± 123	3
CHO-m3 VT-9	0.16 ± 0.02	160 ± 8	3

Table 3.1 Summary of [³H]-NMS saturation binding analysis of the five cell lines studied.

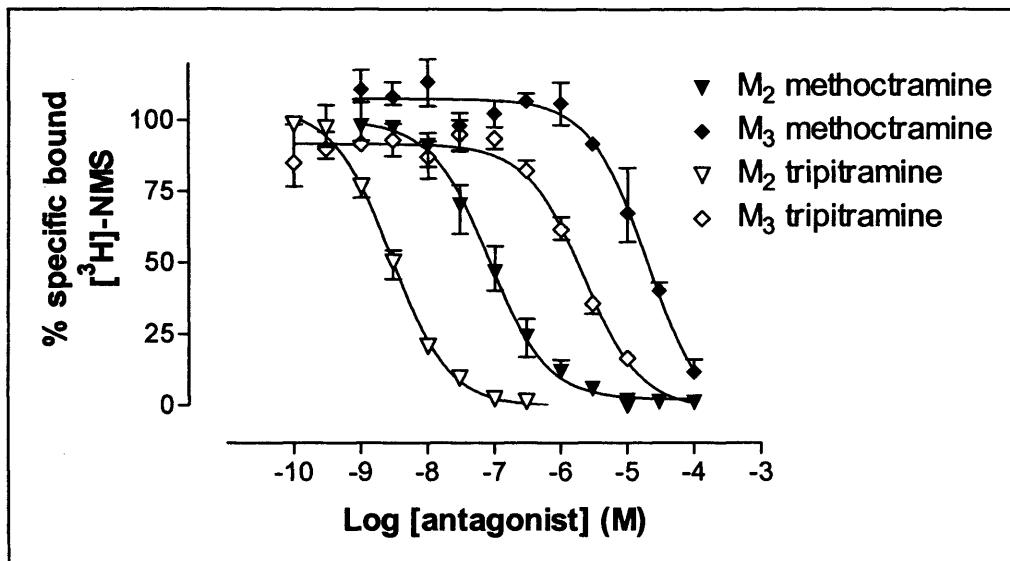


Figure 3.4 Displacement of [³H]-NMS (specific) binding by tripitramine and methoctramine from CHO-m2 and CHO-m3 cell membranes. Data are shown as means ± range for a representative experiment performed in triplicate.

	Tripitramine	Methoctramine	Darifenacin
M₂	9.35 ± 0.15	8.00 ± 0.18	7.30 ± 0.15
M₃	6.75 ± 0.25	5.60 ± 0.21	8.34 ± 0.04
M₃/M₂ selectivity ratio	395	251	0.1

Table 3.2. Summary of pK_i values for three antagonists at muscarinic receptors on CHO-m2 and CHO-m3 membranes (n=3). pK_i values were calculated using the Cheng-Prusoff equation.

shown in Figure 3.5. Table 3.2 reveals that both methoctramine and tripitramine have large selectivity windows for M_2 over M_3 receptors which will make them useful pharmacological tools for dissecting the M_2 and M_3 components of the co-expressing CHO-m2m3 cells. Here, displacement of [3 H]-NMS from membranes using tripitramine revealed $-\log IC_{50}$ values of 8.5 and 5.6 for CHO-m2 and CHO-m3 cells respectively which correlates with studies by Chiarini et al. (1995) who also found tripitramine to have an approx. 1000 fold selectivity for M_2 receptors over M_3 , ($-\log IC_{50}$ values of 9.6 and 6.2 for M_2 and M_3 receptors, respectively).

The relative M_2 and M_3 receptor levels within the co-expressing cell lines were profiled through displacement binding studies on the CHO-m2m3 membranes; these are represented in Figures 3.6 and 3.7, and Table 3.3. Using competition analysis (GraphPad Prism) it is possible to fit a two-site competition isotherm to these data. Displacement binding with tripitramine (the best tool) revealed the high affinity binding site (M_2) to be 27 ± 2.3 % of the total muscarinic receptor population. From Table 3.1, saturation binding on CHO-m2m3 (B2) cell membranes revealed B_{max} value of 1694 ± 456 fmol/mg protein correlating to approx. 450 and 1250 fmol/mg protein of M_2 and M_3 receptors respectively, a proportion ($\approx 3:1$, $M_3:M_2$ ratio) confirmed using both methoctramine and darifenacin to 'dissect' M_2/M_3 receptor populations (see Table 3.3). As predicted [3 H]-NMS displacement by darifenacin revealed the converse high and low affinity receptor populations of the sites compared to tripitramine or methoctramine, still with a predominant M_2 receptor population (Table 3.3). However, although this result must be treated with some caution considering the marginal M_3/M_2 selectivity of this agent (approx. 10-fold) in our hands it is noteworthy that statistical analysis of the darifenacin (as well as methoctramine and tripitramine) results showed two-site modelling of the displacement binding to provide a better fit than one-site analysis ($P < 0.05$, F-test comparison of the fit of two equations using, Graphpad Prism).

3.2.3 Measurement of mACh receptor agonist-induced cAMP accumulation in CHO-m2, CHO-m3 and CHO-m2m3 cells

Having transfected M_3 mACh receptors into parent CHO-m2 cells and shown that clones have been generated which co-express a mixed population of these receptors it was important to demonstrate that both receptors were functionally expressed at the cell surface, coupling to their

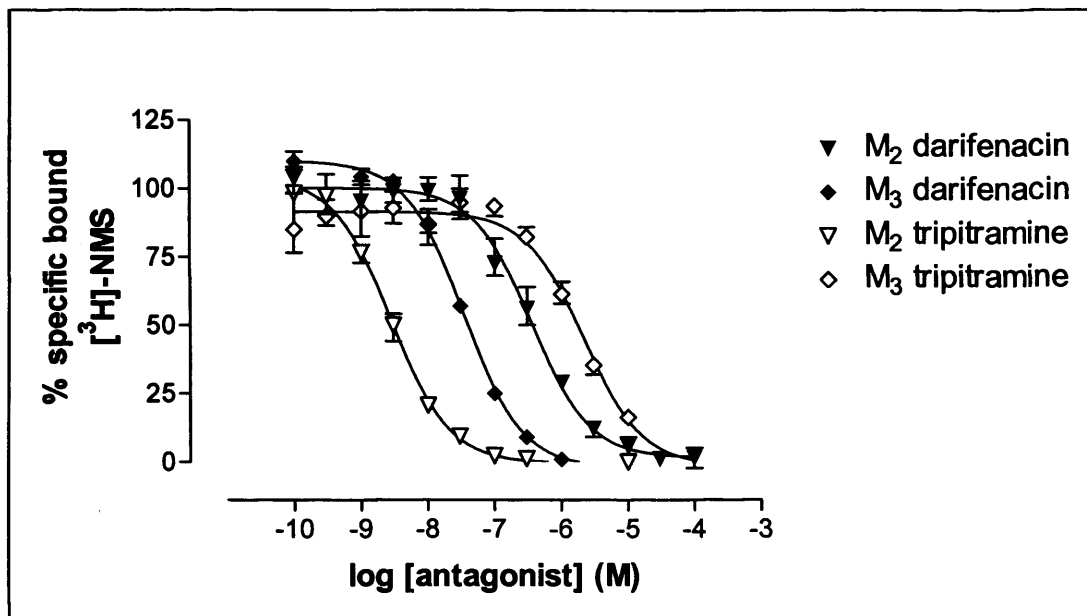


Figure 3.5 Displacement of $[^3\text{H}]\text{-NMS}$ (specific) binding by tripitramine and darifenacin from CHO-m2 and CHO-m3 cell membranes. Data are shown as means \pm range for one representative experiment performed in triplicate.

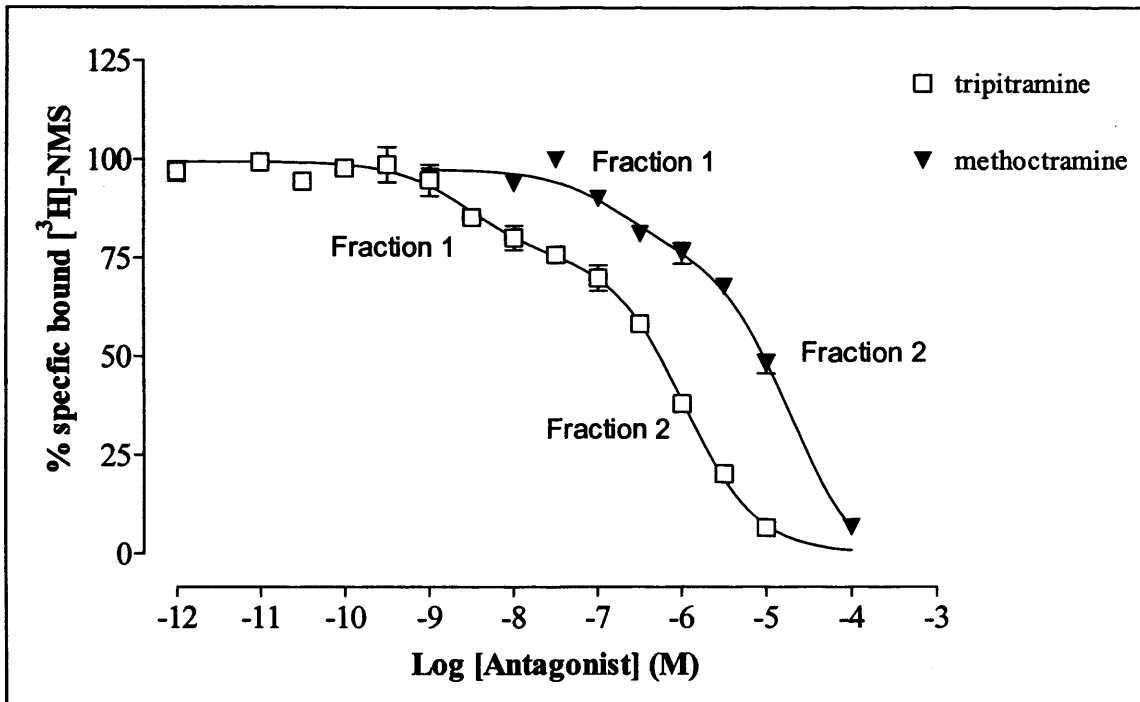


Figure 3.6 Displacement of [³H]-NMS from CHO-m2m3 (B2) membranes by methoctramine and tripitramine. Data are shown as means for one experiment performed in triplicate, which is representative of at least three separate experiments. In the example shown displacement with tripitramine revealed fraction 1 (high affinity, the M₂ receptor population) as 24% and methoctramine gave an estimate of 19% for this receptor population.

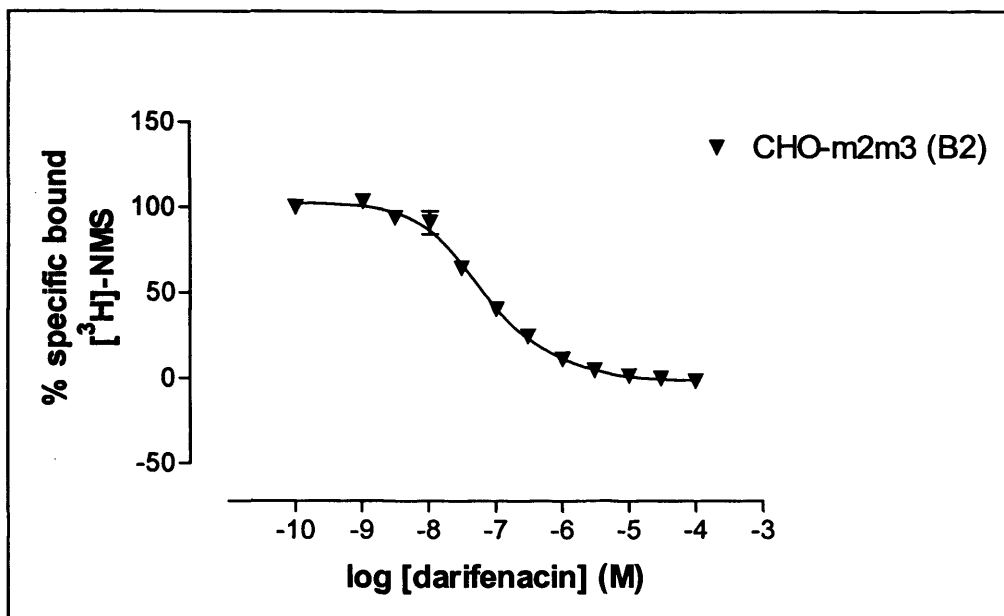


Figure 3.7 A representative graph of experiments performed on CHO-m2m3 (B2) membranes displacing [³H]-NMS by darifenacin. Data are shown as means for one experiment performed in triplicate, which is representative of three separate experiments. Two-site analysis of this example displacement, by darifenacin, reveals a high affinity receptor population (the M₃ receptor population) of 84%.

	Tripitramine (n=5)	Methoctramine (n=3)	Darifenacin (n=3)
pK_i (M) M₂	9.43 ± 0.07	7.90 ± 0.11	7.11 ± 0.06
pK_i (M) M₃	6.97 ± 0.15	5.80 ± 0.20	8.38 ± 0.01
Fraction 1	27 ± 2.3 %	20.5 ± 3.1%	82 ± 0.7%
M2 receptor population (fmol/mg protein)	457	347	305
M3 receptor population (fmol/mg protein)	1237	1347	1389

Table 3.3 Summary of displacement binding of [³H]-NMS by tripitramine, methoctramine and darifenacin on CHO-m2m3 (B2) membranes, each experiment was performed in triplicate. pK_i values were calculated from IC₅₀ values by using the Cheng-Prusoff equation.

respective preferred second messenger pathways (i.e. phosphoinositide hydrolysis and inhibition of adenylyl cyclase). Initial studies defining the effects of mACh receptor stimulation upon adenylyl cyclase activity through measurement of cyclic AMP accumulation demonstrated that M₂-receptor populations within the CHO-m2m3 cells were unaffected by the transfection procedure. However, they could also be used to reveal if there was any evidence of cross-talk between M₂- and M₃-receptors and their respective signalling pathways at the level of adenylyl cyclase regulation.

As can be observed from Figure 3.8, addition of forskolin (FK, 10 μ M, 10 min) caused a large elevation in cAMP above basal (100 fold) in all cell lines studied. As has been reported previously (Griffin & Ehlert, 1992; Caulfield, 1993; Boxall, 1998) MCh stimulation of CHO-m2 cells causes a concentration-dependent inhibition of cAMP accumulation, $pIC_{50} = 6.60 \pm 0.02$ (n=4), with maximal inhibition $\geq 95\%$ (at 100 μ M MCh). MCh-stimulation of CHO-m3 and CHO-m2m3 (B2) cells gave a biphasic modulation of cAMP accumulation (see Figure 3.8). Surprisingly, MCh at low concentrations inhibited FK-stimulated cAMP accumulation in CHO-m3 cells (max inhibition 39%; $pIC_{50} 7.43 \pm 0.08$, n=5), but stimulatory effects were seen at high agonist concentrations (max. stimulation 1.95 fold over FK alone; $pEC_{50} 4.35 \pm 0.12$, n=5).

The effects of MCh on the FK-stimulated cAMP response in CHO-m2m3 (B2) cells are shown in Figure 3.8 (panel B). In common with the agonist-stimulated responses observed in CHO-m2 and CHO-m3 cells, low concentrations of MCh (3-300 nM) caused a pronounced inhibition of cAMP accumulation that was maximal at 0.3 μ M MCh (70% inhibition). The pIC_{50} value for the inhibitory phase of the response (7.66 ± 0.06 ; n=5) was much closer to the comparable value obtained in CHO-m3 cells and at least a log unit lower than that observed for CHO-m2 cells (see Figure 3.8, panel A). The pIC_{50} value, and the magnitude of the inhibition seen, strongly suggests that both M₂ and M₃ mACh receptor stimulations contribute to the inhibitory phase of the cAMP response. In contrast, the marked stimulatory effect of MCh seen at higher concentrations (1-100 μ M) was essentially similar in CHO-m2m3 (B2) cells (max. stimulation 2.0 fold over FK only response; $pEC_{50} 4.95 \pm 0.10$; n=5). Thus, these studies provided little evidence for an effective antagonism of the cAMP stimulatory effect of the M₃ mACh receptor stimulation by simultaneous stimulation of the M₂ receptor population. Similar modulations of FK-stimulated cAMP accumulation by MCh were observed in a preliminary experiment in a second CHO-m2m3 clone (#B7) as shown in Figure 3.9, although the high agonist M₃-mediated

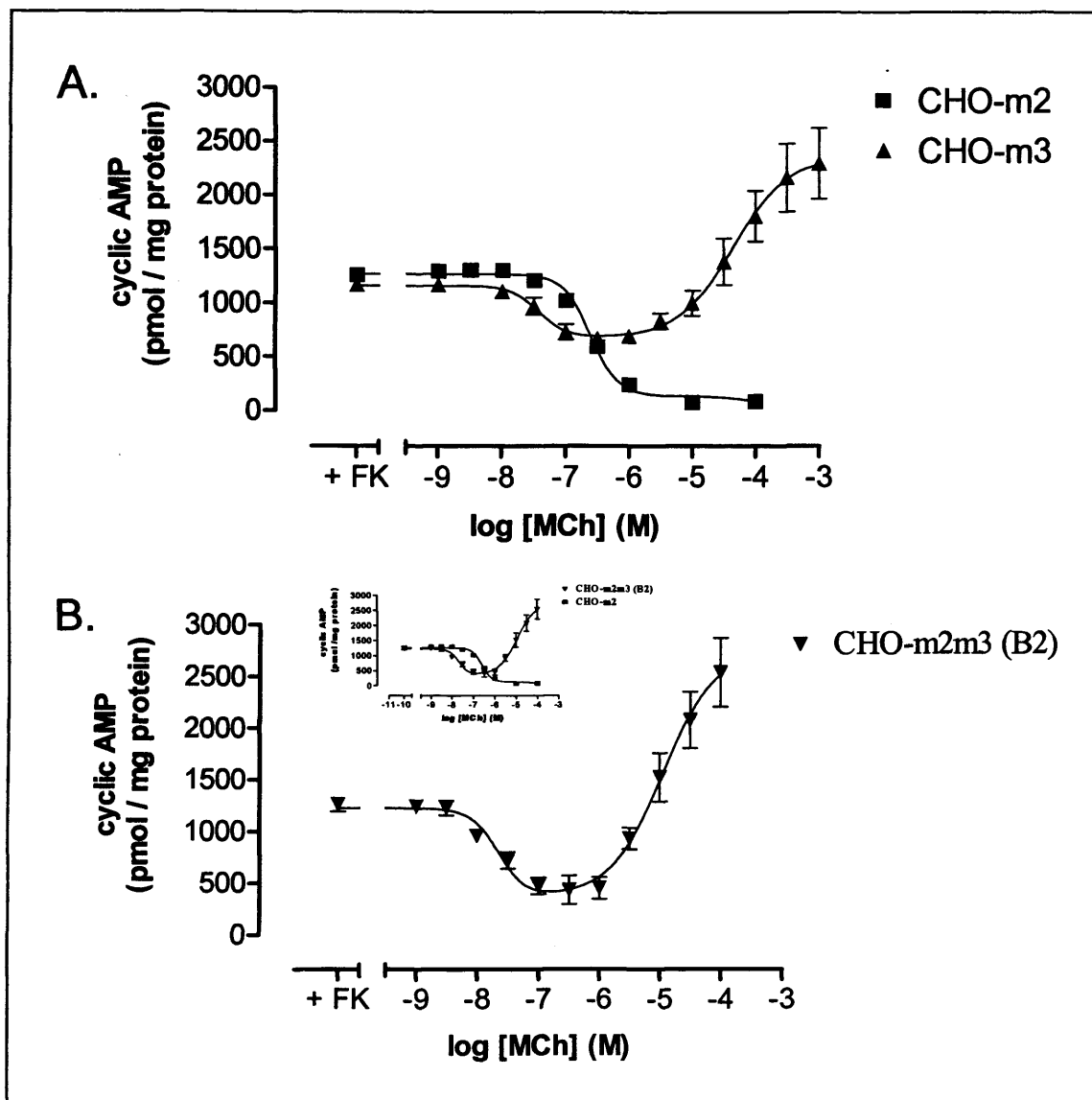


Figure 3.8 Concentration-dependent modulation of forskolin-stimulated cyclic AMP accumulation by MCh in CHO-m2, CHO-m3 and CHO-m2m3 (B2) cells. The effects of increasing concentrations of MCh on cAMP accumulation in CHO-m2 (panel A), CHO-m3 cells (panel A) and CHO-m2m3 (B2) (panel B) cells are shown, with the inset to panel B bringing together CHO-m2 and CHO-m2m3 (B2) cell results on the same axis. Data are shown as means \pm S.E.M. for four separate experiments performed in duplicate.

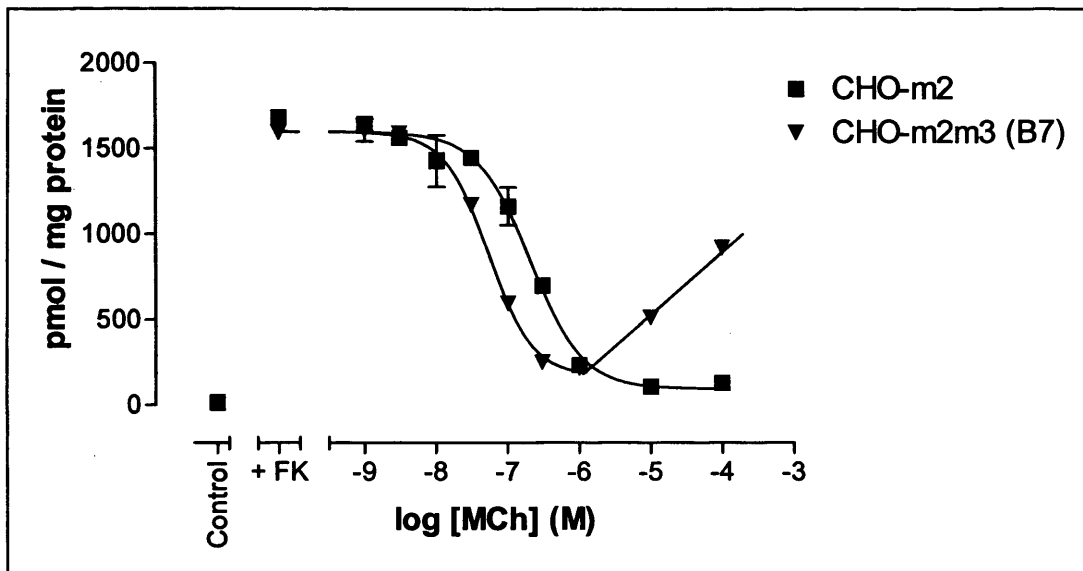


Figure 3.9 Comparison of concentration-dependent modulation of forskolin-stimulated cyclic AMP accumulation by MCh in CHO-m2 and CHO-m2m3 (B7) cells. Data are shown as means \pm range for one experiment performed in duplicate.

stimulatory phase was less pronounced.

3.2.4 Use of subtype-selective antagonists to establish M₂ and M₃ mACh receptor-mediated cAMP responses in CHO-m2m3 cells

In binding studies, the mACh receptor-selective antagonists, triptiramine and methoctramine, were shown to possess sufficient M₂-over-M₃ selectivity to allow delineation of the mACh receptor sub-populations, whereas the M₃-over-M₂ selective antagonist darifenacin showed only approx. 10 fold selectivity with respect to [³H]-NMS displacement for a mixed M₂/M₃ mACh receptor population (see Section 3.2.2). Here, the 'functional' selectivity of darifenacin was examined by assessing the ability of this antagonist to inhibit M₃- and M₂- mediated cAMP effects in CHO-m2m3 cells. 'Functional' selectivity of darifenacin was examined by assessing the ability of this antagonist to inhibit M₃- and M₂- mediated cAMP effects in CHO-m2m3 cells.

Initial studies assessed the antagonism of the M₃ mACh receptor-mediated (low agonist concentration) inhibition of FK-stimulated cAMP accumulation in CHO-m3 cells. A concentration of MCh (0.3 μM) which maximally inhibited FK-stimulated cAMP accumulation was concentration-dependently antagonised by increasing concentrations of darifenacin and triptiramine (see Figure 3.10). As can be seen, much lower concentrations of darifenacin (pK_i, 8.97) were needed to inhibit the MCh-mediated effect compared to triptiramine (pK_i, 6.99) consistent with the M₃ mACh receptor mediation of this response.

In CHO-m2m3 cells the picture is somewhat more complicated. Addition of a relatively high concentration of MCh (10 μM) results in a small increase in cAMP accumulation over that caused by FK alone. Under these circumstances it is assumed that the M₃-mediated stimulatory effect is just dominating over a M₂-driven inhibitory effect (see Figure 3.11). Pre-incubation (≥ 30 min) with increasing concentrations of darifenacin initially inhibits the M₃-driven adenylyl cyclase stimulatory effect and the M₂-driven inhibitory effect is increasingly unmasked. As can be seen from Figure 3.11, at a concentration of darifenacin of 0.3 μM the MCh stimulation of the M₃ receptor-mediated stimulation is maximally suppressed and the full inhibitory effect mediated by the M₂ receptor is revealed. However, as darifenacin concentration is increased further then inhibition of the M₂-mediated effect is seen and at 30 μM darifenacin both M₂ and M₃ mediated effects are completely blocked (see Figure 3.11). It can also be observed from

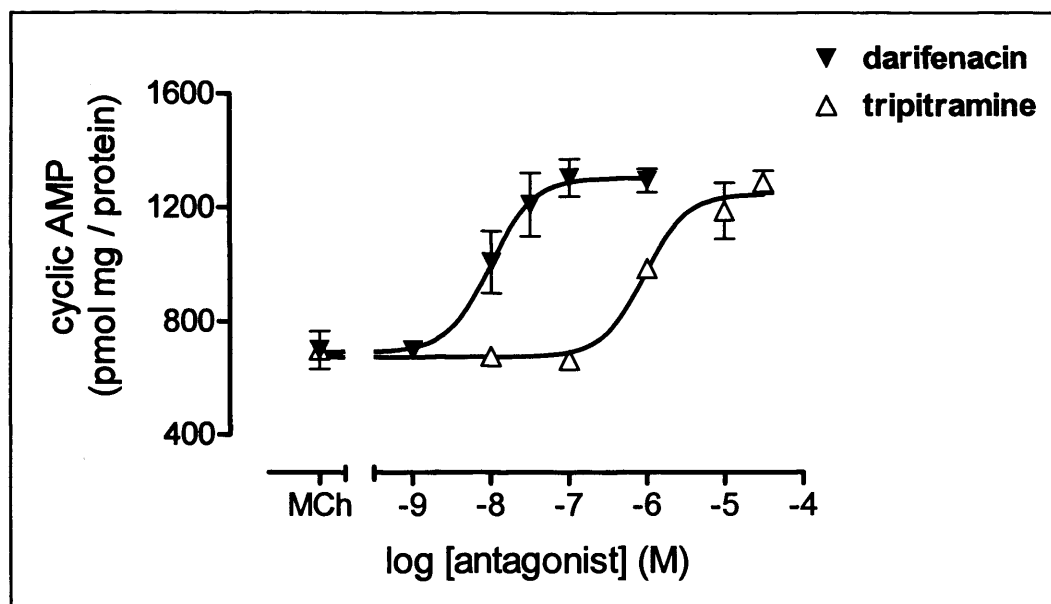


Figure 3.10 Reversal of the inhibitory effect of MCh (0.3 μ M) on FK-stimulated cyclic AMP accumulation in CHO-m3 cells by darifenacin and tripitramine. Data are shown as means \pm S.E.M. for three separate experiments.

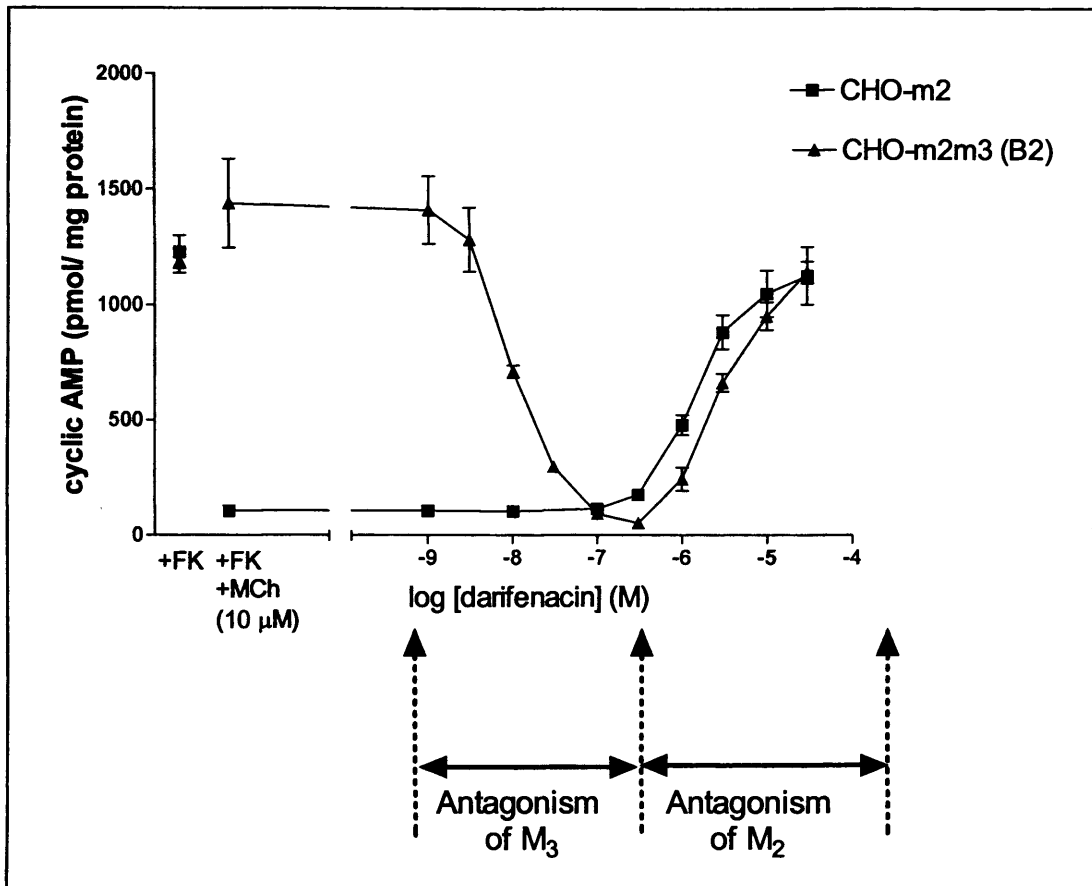


Figure 3.11 Darifenacin blockade of MCh (10 μM) stimulated cAMP accumulation in CHO-m2 and CHO-m2m3 (B2) cells. Data are means ± S.E.M. from three separate experiments performed in duplicate. CHO-m2 and CHO-m2m3 cell monolayers were preincubated in the absence or presence of the indicated concentrations of darifenacin for 30 min. This was followed by addition of MCh (10 μM) or vehicle and 10 min later by FK (10 μM) and terminated 10 min subsequent to this.

Figure 3.11, that the darifenacin inhibition of the M_2 -mediated inhibitory component of FK-stimulated cAMP accumulation in CHO-m2m3 (B2) cells overlies that in CHO-m2 cells.

3.2.5 Measurement of mACh receptor agonist-stimulated IP_3 accumulation in CHO-m2, CHO-m3 and CHO-m2m3 (B2) cells

Once it was established that the M_2 receptors had been unaffected by the transfection procedure and coupled functionally to adenylyl cyclase modulation it was necessary to demonstrate that the M_3 receptors within the model CHO-m2m3 cells, detected by displacement binding, were functionally coupled to activation of the phosphoinositide (PI) signal transduction pathway. Previous studies from this Department have reported a concentration-dependent MCh-stimulated IP_3 response in CHO-m3 cells, with an $EC_{50} \approx 2 \mu M$, evoking maximal stimulation with 1 mM MCh (Boxall, 1998; Wylie et al., 1999). The IP_3 mass accumulation time-course in CHO-m3 cells, following maximal agonist stimulation with MCh (1 mM), is shown in Figure 3.12. The basal level of IP_3 in the CHO-m3 cells was 80 ± 19 pmol/mg protein. Initially following agonist stimulation, the IP_3 mass accumulation increased very sharply to a peak of 416 ± 36 pmol/mg protein, after 15 s, which was then followed by a decrease to an elevated sustained plateau response (≈ 200 pmol/mg protein) which was observable beyond 10 min (data not shown). There was no apparent change in the basal level of IP_3 mass in the unstimulated cells throughout the time-courses for any of the three cell lines studied.

MCh (1 mM) stimulation of the CHO-m2 cells did not cause a detectable change in IP_3 mass accumulation (data not shown), the basal level in these cells was 120 ± 12 pmol/mg protein (n=3, in duplicate).

Demonstrating the properties of a functioning M_3 -receptor, the co-expressing CHO-m2m3 (B2) cell line showed a similar MCh-induced time-course profile of IP_3 mass accumulation to the CHO-m3 cells with a peak after 15s (Figure 3.13). The peak after 15 s was 358 ± 15 pmol/mg protein, although the basal IP_3 level in these cells was lower than in CHO-m3 cells at 32 ± 8 pmol/mg protein.

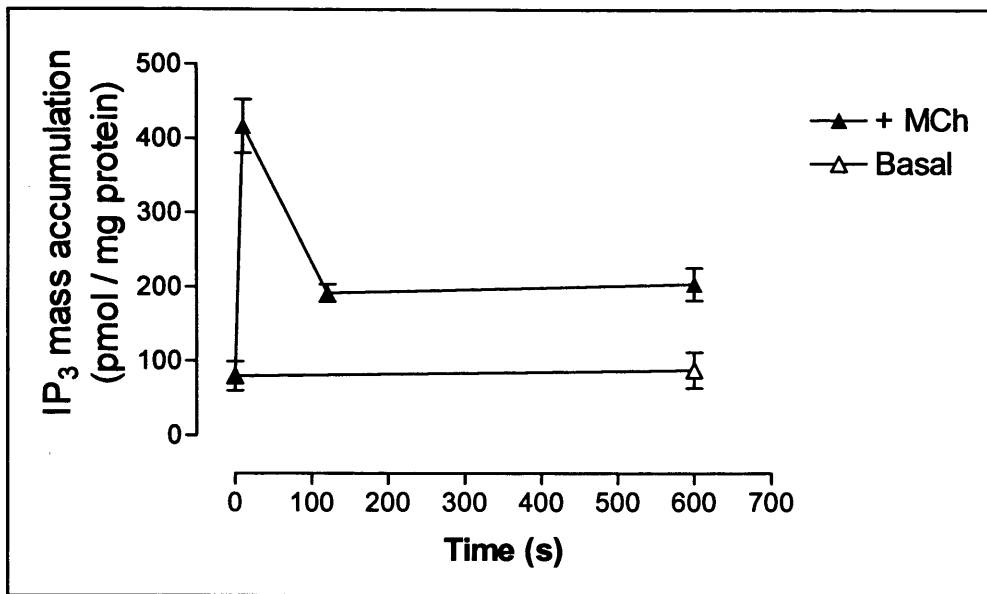


Figure 3.12 Time-course profile of MCh (1 mM) stimulated IP₃ mass accumulation in CHO-m3 cells. Data are shown as means \pm S.E.M. for three separate experiments.

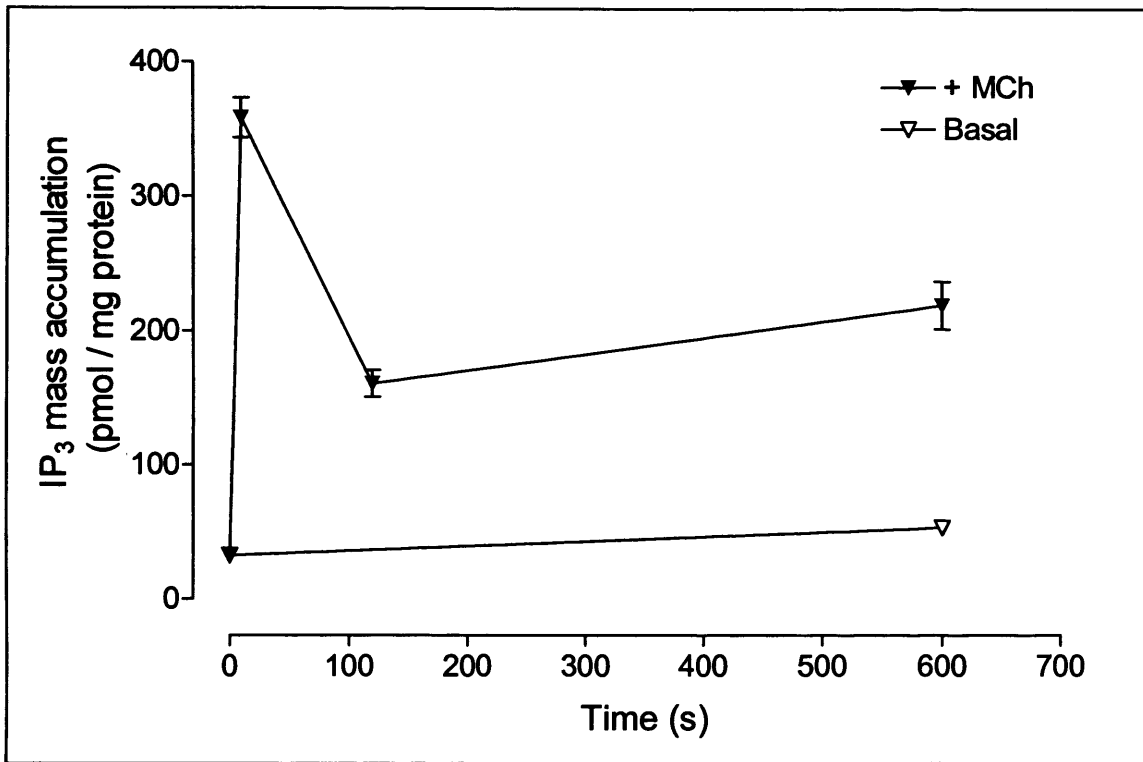


Figure 3.13 Time-course profile of MCh (1 mM) stimulated IP₃ mass accumulation in CHO-m2m3 (B2) cells. Data are shown as means \pm S.E.M. for three separate experiments.

3.2.6 Assessment of single-cell Ca^{2+} responses in a field of CHO-m2m3 (B2) cells

It was also considered important to establish that each of the co-expressing CHO-m2m3 (B2) cells, is genuinely, individually co-expressing M_2 and M_3 receptors and, in particular, that we have not created a mixed population of CHO-m2 and CHO-m2m3 cells. The M_3 -receptor population was shown to be ubiquitous in the co-expressing CHO-m2m3 cells by single cell Ca^{2+} analysis.

As can be observed from Figure 3.14, CHO-m2m3 (B2) cells showed a rapid and robust increase in $[\text{Ca}^{2+}]_i$ following application of MCh (100 μM). Also this response was robust and pronounced in all of the cells with addition of 1 μM MCh. These responses are represented by example time-course profiles in Figure 3.14 which shows a peak and plateau response beyond 5 min. Figure 3.15, showing the pseudo-colour image of the populations of cells as different concentrations of MCh are perfused across the CHO-m2m3 cells, demonstrates that all of the cells show an increase in $[\text{Ca}^{2+}]_i$ within 1 s of agonist application for 1 μM and 100 μM MCh.

3.3 Discussion

Initially in this investigation into the potential cross-talk between muscarinic acetylcholine receptors in cells transfected to co-express M_2 - and M_3 - mACh receptors, I performed radioligand binding studies, and measured second messenger production at the level of IP_3 , cAMP and Ca^{2+} in order to determine whether the co-expression of M_2 and M_3 mACh receptors results in responses different to simple summation of the effects of the two receptors expressed in isolation.

The [^3H]-NMS saturation binding studies on membrane preparations revealed total mACh receptor populations for the cell lines studied of 617 ± 51 , 3962 ± 409 and 1694 ± 456 fmol / mg protein, and similar K_d values for CHO-m2, CHO-m3 and CHO-m2m3 (B2 clone) cells, respectively. Displacement binding with tripitramine revealed the receptor populations within the co-expressing cells to be 457 and 1237 fmol/mg protein for M_2 and M_3 receptors, respectively, a ratio confirmed using both methoctramine and darifenacin to 'dissect' M_2/M_3 receptor populations.

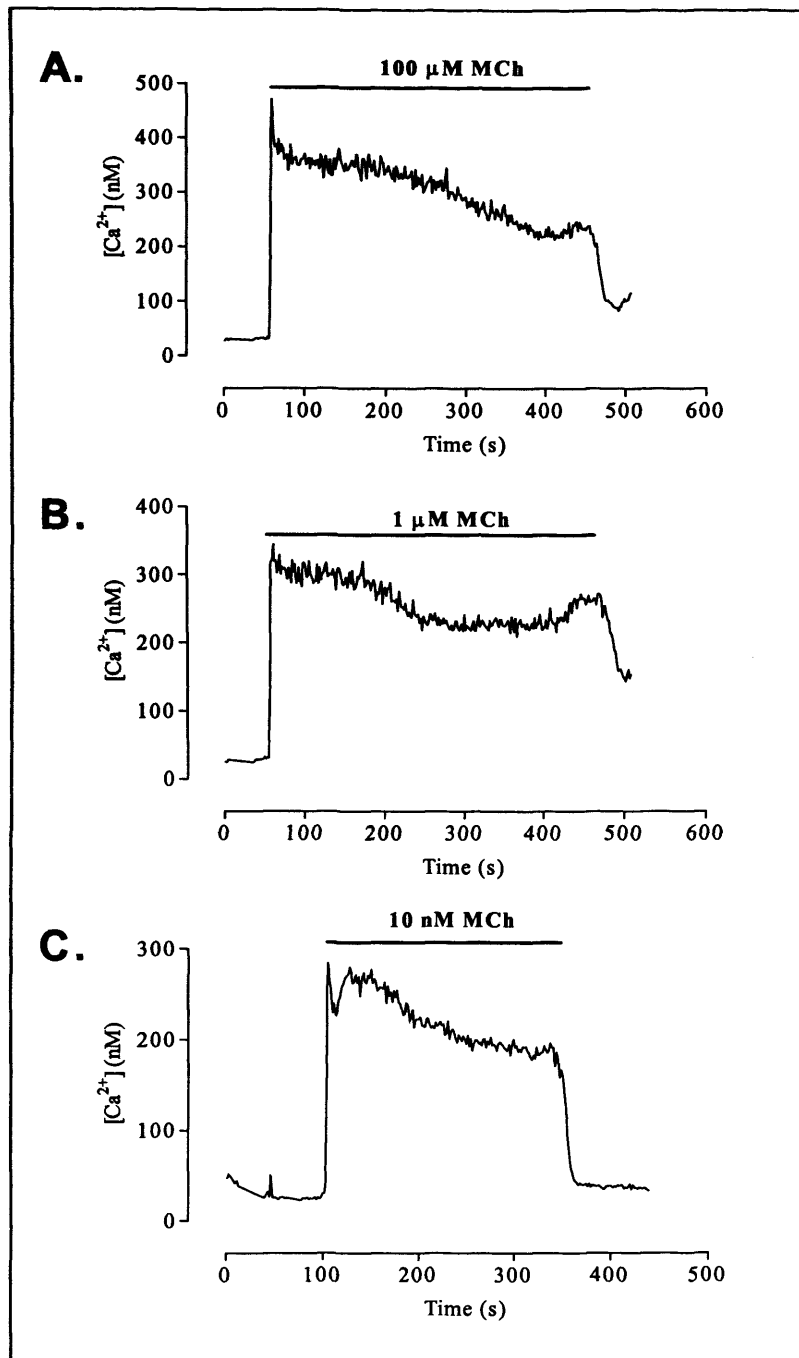


Figure 3.14 Single cell traces, representative of a population of cells (10 - 15 cells) in three separate experiments, showing the change in intracellular Ca^{2+} concentrations following agonist stimulation at $100 \mu\text{M}$, $1 \mu\text{M}$ and 10 nM MCh in CHO-m2m3 (B2) cells in panels a, b and c respectively.

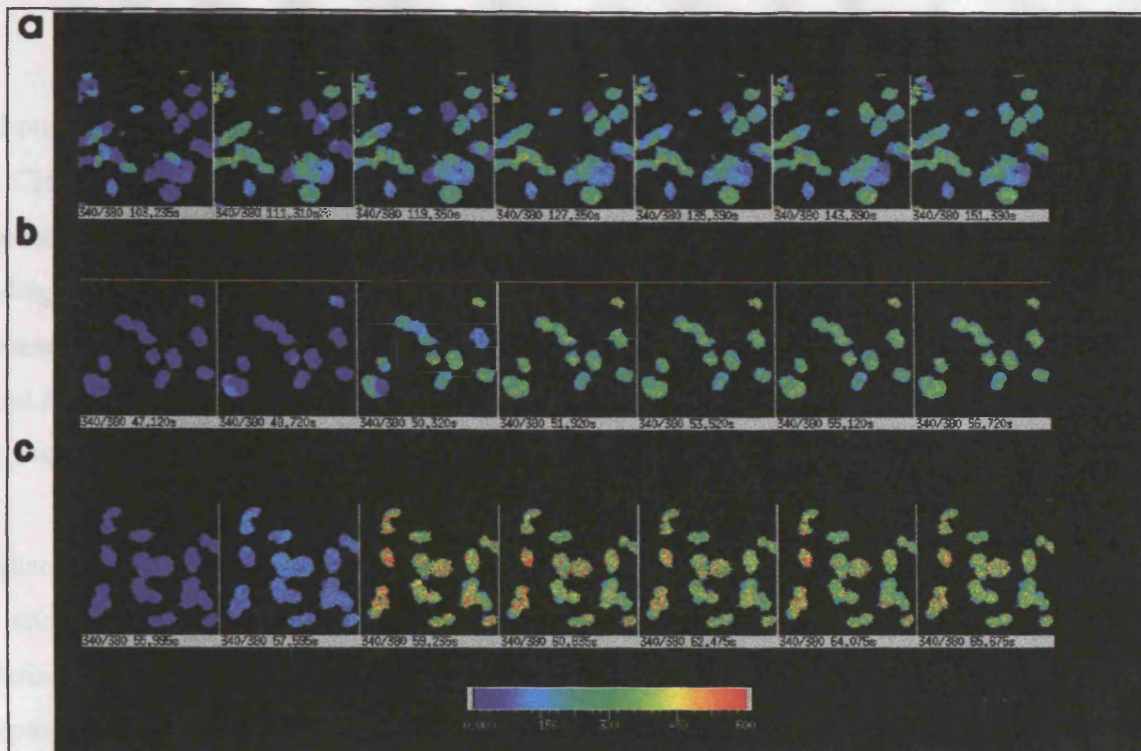


Figure 3.15 Pseudo-colour images representing the levels of intracellular Ca^{2+} following addition of MCh at 0.01, 1 and 100 μM MCh in CHO-m2m3 (B2) cells in panels a, b and c respectively. Each frame is 1.6 s later than the previous one with the exception of the last frame of panel a (0.01 μM MCh) which is 22.5s later than the previous frame. The colour scale at the bottom of the figure represents $[\text{Ca}^{2+}]$ in nM. Representative experiment of three separate experiments.

The displacement binding studies were performed with ^{125}I -MCh as well as topography due to the lack of experimental power of triplicate. It is worth to observe from Figure 3.4 that there is a sufficiently large window of selectivity between M_2 and M_3 receptors using imphocromin to suggest that our agent can adequately discriminate the up/down in subsequent studies.

The receptor populations in a second overexpressing CHO-m2m3 (B2) clone were also profiled. However, cultures of these cells tended to grow more slowly and were dependent on medium that showed non-pulsate characteristics compared to the other CHO cell lines tested. Following the initial overexpression, ^{125}I -MCh and cell images (IP) screened potential α -expressing clones for IP₃ response and cell-activated in response to IP₃ mass accumulation in CHO-m2m3 (B2) cells similar to original and three other profiles in CHO-m3 cells. However, maximal MCh

Although the M_2 receptor population in the CHO-m2 and CHO-m2m3 cell lines are comparable, the CHO-m3 cells over-express the M_3 receptor relative to the co-expressing clone. Hence another low M_3 expressing cell line, CHO-m3VT-9 cells, were also characterised. Saturation binding studies on CHO-m3VT-9 membranes revealed that this clone had a much lower expression level with $B_{max}=159$ fmol/mg protein, (see Table 3.1), which is somewhat less than found in other studies using CHO-m3VT-9 cells, for example Burford et al. (1995) who reported $B_{max}=450$ fmol/mg protein.

Displacement of [3 H]-NMS from membranes using tripitramine revealed $-\log IC_{50}$ (M) values of 8.5 and 5.6 for CHO-m2 and CHO-m3 cells, respectively, which correlate with studies by Chiarini et al. (1995) who also found that tripitramine had a 1000 fold selectivity for M_2 receptors over M_3 ($-\log IC_{50}$ (M) values of 9.6 and 6.2 for M_2 and M_3 receptors, respectively). The two-site competition analysis of the displacement binding with tripitramine, methoctramine or darifenacin revealed that the proportion of M_2 to M_3 receptors in the co-expressing cells was approx. 1:3. While this diverges from the ratio seen in most smooth muscle tissues, where the M_2 receptor population is predominant, it should provide a satisfactory model for identifying potential interactions between the two receptors. It should also be noted that isolated rat uterus contain a predominant M_3 ($\approx 65\%$) over M_2 ($\approx 35\%$) receptor population (Choppin et al., 1999), giving the model cell $M_2:M_3$ ratio a 'real' tissue counterpart.

The displacement binding studies were performed with methoctramine as well as tripitramine due to the lack of a commercial source of tripitramine. It is possible to observe from Figure 3.4 that there is a sufficiently large window of selectivity between M_2 and M_3 receptors using methoctramine to suggest that this agent can adequately substitute for tripitramine in subsequent studies.

The receptor populations in a second co-expressing CHO-m2m3 (B7) clone were also profiled. However, culture of these cells revealed them to grow more slowly, and visual inspection of these cells showed non-uniform shape compared to the other CHO cell lines studied. Following the initial co-transfection, Boxall and colleagues (1998) screened potential co-expressing clones for IP_3 responses, and MCh evoked an increase in IP_3 mass accumulation in CHO-m2m3 (B2) cells similar in magnitude and time-course profile to CHO-m3 cells. However, maximal MCh-

evoked IP₃ mass accumulation in CHO-m2m3 (B7) was only approx. 30-50 % of that seen in CHO-m3 cells. Hence CHO-m2m3 (B7) cells were used to reinforce observations made in the CHO-m2m3 (B2) cells, whilst their growth and second messenger response differences were always borne in mind.

Characterisation of cAMP and IP₃ accumulations within the CHO-m2m3 cells would show whether the mixed population of M₂ and M₃ receptors, revealed by radioligand binding experiments, effectively couple to their respective G protein-linked signalling pathways. The cAMP accumulation experiments confirm that the M₂ receptors within the co-expressing cells efficiently couple through G_i to adenylyl cyclase leading to an inhibition of forskolin-stimulated cAMP accumulation (Figure 3.8). Further confirmation of the presence of M₃-receptors within the co-expressing cells coupling successfully to their signal transduction pathways is seen at higher methacholine concentrations (>1 μM) as the forskolin-stimulated (10 μM) cAMP accumulation curve essentially overlies that observed for CHO-m3 cells (1 μM to 1 mM MCh Figure 3.8). The increase in cAMP accumulation above the level stimulated by forskolin (10 μM) *per se* has been observed previously in CHO-m3 (Boxall, 1998) and CHO-m1 (Burford and Nahorski, 1996) cells and is believed to be due to 'promiscuous' coupling of M₃ receptors to G_s-proteins leading to increased adenylyl cyclase activity and therefore an increase in cAMP accumulation.

The cAMP accumulation studies revealed an interesting difference between the MCh-induced inhibition observed in CHO-m2m3 (B2) and CHO-m2 cells with the concentration-response curve in the co-expressing cells lying substantially to the left of that for the CHO-m2 cells. This observation of an apparent augmentation of the M₂ inhibitory response upon co-stimulation of M₃ receptors, at least over a particular agonist concentrations, was also seen in a second co-expressing clone (CHO-m2m3 #B7). The inhibitory response observed with low concentrations of MCh in CHO-m3 cells was shown to be mediated by M₃ receptor activation as both tripitramine and darifenacin reversed the MCh (300 nM) induced inhibition of FK-stimulated cAMP accumulation, with estimated affinities for M₃ receptors as reported previously (Eglen and Nahorski, 2000; pK_i 8.97 and 6.99 for darifenacin and tripitramine respectively, see Figure 3.10). Darifenacin blockade of the MCh-induced cAMP accumulation response in CHO-m2m3 (B2) cells is somewhat more complicated (Figure 3.11). 10 μM MCh causes an elevation of FK-stimulated cAMP accumulation in CHO-m2m3 (B2) cells. Darifenacin (300 nM) blocking the

M₃-mediated stimulatory effect on cAMP accumulation unmasks the M₂ inhibitory effect which is blocked by concentrations of darifenacin above 300 nM. However, the slope of the concentration-dependent darifenacin (1 nM- 300 nM) blockade of M₃-mediated stimulatory signal (10 μM MCh) is made up of summation of the unmasked M₂- and M₃-mediated inhibitory components (see Figure 3.11)

If it is assumed that the inhibitory component of the biphasic curve (Figure 3.11) is attributable to darifenacin inhibition of M₃ mACh receptors (IC₅₀ 10 nM) and the rising arm to inhibition of M₂ mACh receptors (IC₅₀ 3.6 μM), then the 'functional' selectivity of darifenacin appears to be approx. 400 fold (i.e. 40 fold greater than was observed in [³H]-NMS displacement studies).

Another study within our laboratory has since demonstrated that the inhibitory effect observed though M₃-receptor stimulation at low agonist concentrations is due to inhibition of adenylyl cyclase (AC) isoenzymes by Ca²⁺ entering the cell via a capacitative Ca²⁺ influx pathway. AC subtypes V and VI can be inhibited by increases in Ca²⁺ (Sunahara et al., 1996). Thus, the apparent additive inhibitory effects (approx. 10 leftward shift) of co-activation of M₂ and M₃-receptors in CHO-m2m3 (B2) cells may be inhibited by M₃-selective concentrations of darifenacin (300 nM), or via removal of extracellular calcium. In addition, thapsigargin (2 μM) in calcium-containing experiments will also evoke a similar inhibition of FK-stimulated cAMP accumulation to that evoked by low concentrations of MCh (Mistry et al., 2001).

The cAMP experiments (see Section 3.2.3 above) suggested that coupling of M₂-receptors to G_i-proteins, in CHO-m2m3 (B2) cells had been unaffected by the transfection procedure, but also implied that the activation of the co-expressed M₃ receptors had the same characteristics as in CHO-m3 cells (i.e. inhibition at low [MCh], and stimulation at high [MCh] of cAMP accumulation).

IP₃ mass accumulation studies revealed the G_q-mediated signal transduction from M₃ receptors in both CHO-m3 and the co-transfected CHO-m2m3 (B2) cells to be similar, while also revealing if there are any apparent effects of co-stimulation of M₂ receptors within these same cells. Agonist stimulation of CHO-m2 cells caused no apparent change in IP₃ mass accumulation. The time-course profile of maximal MCh (1 mM) induced IP₃ mass accumulation in the co-expressing CHO-m2m3 cell was similar to that of the cells expressing M₃-receptors

alone (see Figures 3.12 and 3.13). This time-course profile correlates with previously published data in CHO-m3 cells, an initial peak after 10 s of 8-10 fold over basal which falls to 3-4 fold within 1 min (Tobin et al., 1992).

The radioligand binding analysis, cAMP accumulation, IP₃ mass accumulation experiments (see sections 3.2.1, 3.2.3 and 3.2.6 above) and survival in hygromycin B selection medium, all imply successful transfection of M₃-receptors into the parent CHO-m2 cell population to create co-expressing clones. However, it was important to prove CHO-m2m3 cells were a homogeneous cell population with all cells expressing both muscarinic receptor subtypes, and not just a mixed population of CHO-m2 and CHO-m3 cells and CHO-m2m3 cells. The M₃-receptor population within CHO-m2m3 cells was shown to be ubiquitously expressed in the co-expressing CHO-m2m3 cells using single cell Ca²⁺ imaging (see Figure 3.15).

The profile of this Ca²⁺ release is similar to that observed in CHO-m3 cells (Boxall, 1998), indicating that the co-transfected M₃ receptors in the CHO-m2m3 cells couple appropriately to their signal transduction pathway. Although there have been studies showing increases in [Ca²⁺]_i following agonist stimulation of CHO-m2 cells (Schmidt et al., 1995; Boxall, 1998; Wylie et al., 1999) this has a distinct profile which is characterised by a smaller and a more gradual increase in [Ca²⁺]_i. Boxall (1998) also found Ca²⁺ responses in CHO-m2 cells only at high concentrations of MCh, whereas the studies presented here show a robust response at 1 μM MCh in all the CHO-m2m3 (B2) cells, and a rapid increase is observed in over 80% of the cells challenged with 10 nM MCh. This provides compelling evidence that all the co-expressed cells contained M₃ receptors and not just a proportion of the population. However, further characterisation of Ca²⁺ signalling within CHO-m2 and CHO-m3 cells was performed (where 0.1 μM MCh failed to induce a Ca²⁺ response in CHO-m2 cells, see Chapter 4, Figure 4.5) to consolidate these observations in the CHO-m2m3 cells.

This Chapter has verified that the recombinant cell model being studied co-expresses M₂ and M₃ muscarinic receptors in the proportion 1:3 (M₂:M₃ respectively), and these receptors functionally couple to their respective signalling pathways (G_i to AC and G_q to PLC, see Figure 1.2) on agonist stimulation. Therefore, this model can be used to study possible interactions/cross-talk between these receptors and their signalling pathways. Agonist-stimulated second messenger

generation (IP₃ and cAMP) in CHO-m2m3 cells was investigated for evidence of cross-talk, because adenylyl cyclases are known to be regulated by effectors downstream of G_q-linked receptor activation, Ca²⁺ (inhibition of AC subtypes V and VI) and PKC (stimulation of AC subtypes II and V), as reviewed by Sunahara et al. (1996). Also G_i-derived βγ-subunits have been shown to stimulate some PLC isoforms (Blank et al., 1992), as well as G_i-protein activation being implicated in augmentation of G_q activation of PLC hydrolysis (for review see Selbie and Hill, 1998; also see Chapter 4).

While there is evidence for a M₃ receptor influence upon M₂-mediated inhibition of adenylyl cyclase activity, preliminary IP₃ mass accumulation experiments revealed no influence of co-stimulation of M₂ receptors upon the M₃-mediated response. However, this is more thoroughly investigated in Chapter 4 using fluorimetric imaging plate reader (FLIPR) techniques to analyse Ca²⁺ signalling within the co-expressing model.

Chapter Four: Characterisation of phosphoinositide and Ca²⁺ responses in CHO-m2, CHO-m3 and CHO-m2m3 (B2) cells

4.1 Introduction

Traditionally the signal transduction pathways from M₂ and M₃ muscarinic receptors have been classified as independent pathways, coupling through G_i and G_q proteins to inhibition of adenylyl cyclase and stimulation of phosphoinositide hydrolysis, respectively (See Figure 1.2). Activation of G_q proteins causes the stimulation of β isoforms of PLC which increases the hydrolysis of PIP₂ to produce IP₃ and DAG, causing release of Ca²⁺ from intracellular stores, and activation of PKC, respectively (for review see Berridge et al., 2000).

However, more recently it has been shown that receptors which traditionally activate G_i- or G_q-mediated pathways are not necessarily independent, as evidence for promiscuity and cross-talk leading to overlap between their respective pathways has become more common. Many studies have investigated cross-talk between G_i and G_q pathway activation in modulating PLC hydrolysis (for review see Selbie and Hill, 1998). Activation of G_i proteins has been shown to activate PLC-β isoforms via Gβγ subunits (Blank et al., 1992; Camps et al., 1992). Megson and colleagues have shown simultaneous activation of G_i- and G_q- mediated pathways (through activation of adenosine A1 and P2-purinoceptors, respectively) produced a large augmentation of phospholipid hydrolysis as measured by accumulation of [³H]-inositol phosphates (Megson et al., 1995). G_i augmentation of G_q-mediated stimulation of PLC has been shown to be mediated by Gβγ subunits (Selbie et al., 1997) and, in some cases, is dependent on pre-activation of PLC by Gα_q subunits (Chan et al., 2000). Watkins and colleagues also have shown G_i interaction with PLC, however, they demonstrated that suppression of Gα_{i2} signalling raised basal PLC activity and augmented agonist-induced [³H]-IP_x accumulation responses (Watkins et al., 1994), suggesting a possible negative coupling to PLC.

Modulation of PLC by cross-talk between G proteins is important because the modulation of IP₃-stimulated mobilisation of Ca²⁺ from intracellular stores and subsequent influx from extracellular environment via Ca²⁺ channels (for reviews see Berridge, 1993; 2000) are known to be important in modulating many signalling pathways. Ca²⁺ signalling has been implicated in

both direct and indirect modulation of such wide ranging cellular molecules and processes as adenylyl cyclase, PLC (Del Río et al., 1994; Berridge, 1998; Masgrau et al., 2000), PKC, Ca^{2+} channels, MAPKs (Mitchell et al., 1995; Gutkind, 1998a; Wylie et al., 1999), tyrosine kinases (PYK2, Dikic et al., 1996), as well as contraction, fertilisation, growth and apoptosis (reviewed by Berridge et al., 1998; 2000).

With these known interactions between G_i - and G_q -coupled receptor pathways, this Chapter investigates if there is evidence for cross-talk between co-expressed M_2 and M_3 receptors at the level of phosphoinositide hydrolysis, through [^3H]-IP $_x$ accumulation measurements and the use of FLIPR technology for the measurement of intracellular [Ca^{2+}] changes.

4.2 Results

4.2.1 Comparison of agonist-stimulated [^3H]-IP $_x$ accumulation in CHO-m2, CHO-m3 and CHO-m2m3 (B2) cells

MCh (1 mM) caused a robust time-dependent increase in [^3H]-IP $_x$ accumulation in both [^3H]-inositol-labelled CHO-m3 and CHO-m2m3 (B2) cells (see Figure 4.1, panel B). As can be observed from Figure 4.1 (panel B) an approx 5 fold increase could be detected at 5 min after agonist challenge and the response peaked at ≥ 30 fold over basal beyond 30 min. In contrast, [^3H]-inositol-labelled CHO-m2 cells showed only a modest increase in [^3H]-IP $_x$ accumulation with 1 mM MCh of only 1.85 fold over basal at 30 min (Figure 4.1, panel A). Also, the concentration-dependencies (assessed at 15 min) of these observed responses varies greatly with CHO-m3 and CHO-m2m3 (B2) cells having sub-micomolar EC_{50} values and CHO-m2 cells having an EC_{50} value of approx. 50 μM (pEC_{50} , 4.30 ± 0.07 , 6.24 ± 0.13 and 6.55 ± 0.16 for CHO-m2, CHO-m3 and CHO-m2m3 (B2) cells respectively, $n=3$, see Figure 4.2 and Table 4.1).

Thus, although mACh receptor stimulation in CHO-m2 cells can cause [^3H]-IP $_x$ accumulation, higher agonist concentrations are required to evoke responses which are maximally only approx. 5 % of those observed in CHO-m3 or CHO-m2m3 (B2) cells.

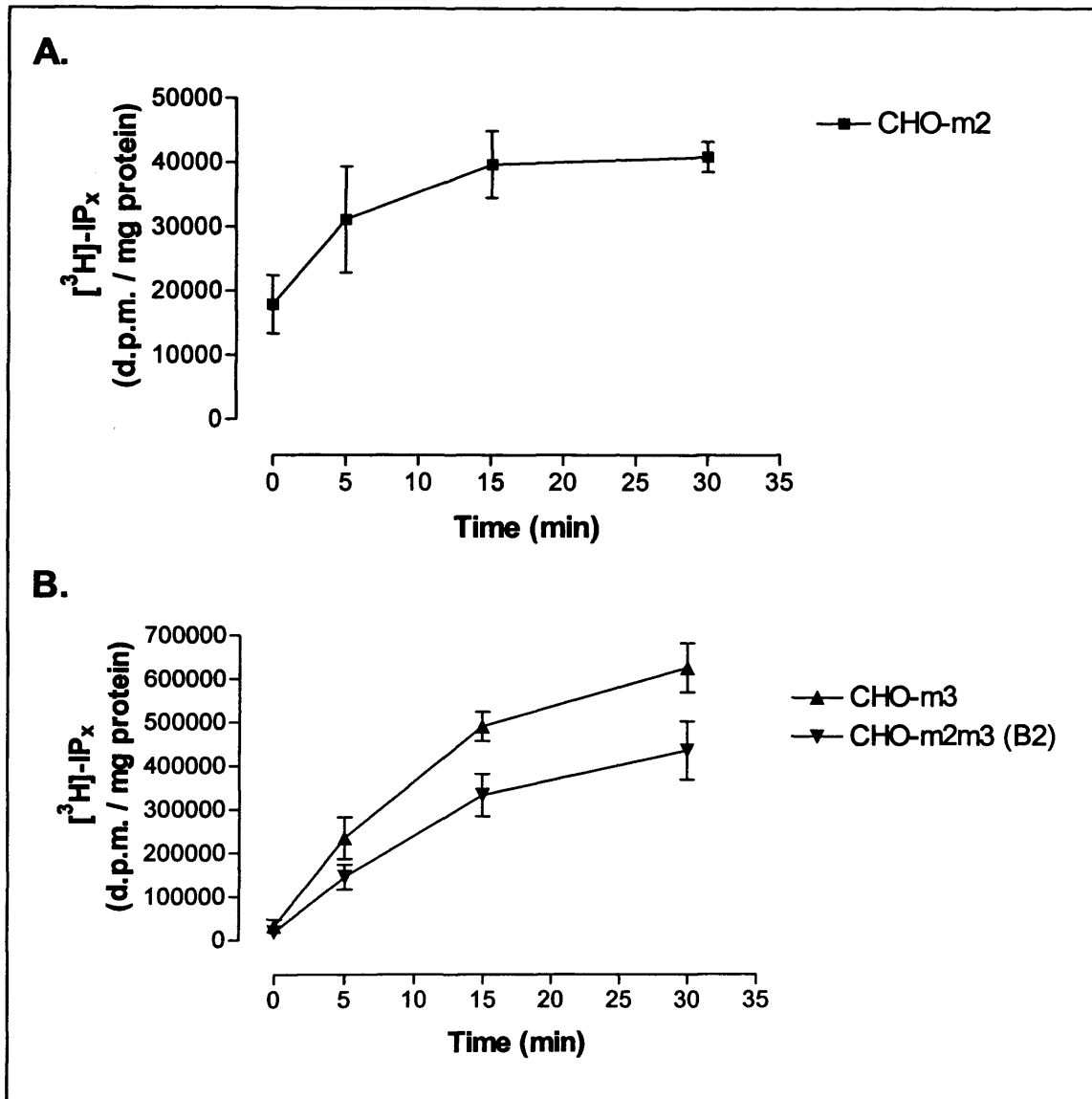


Figure 4.1 Time-course profiles of 1 mM MCh-stimulated [³H]-IP_x accumulation in [³H]-inositol pre-labelled CHO-m2 (panel A), CHO-m3 (panel B) and CHO-m2m3 (B2) (panel B) cells. Data are shown as means ± S.E.M. of three separate experiments performed in duplicate. Note differences in y-axis scales between panels A and B.

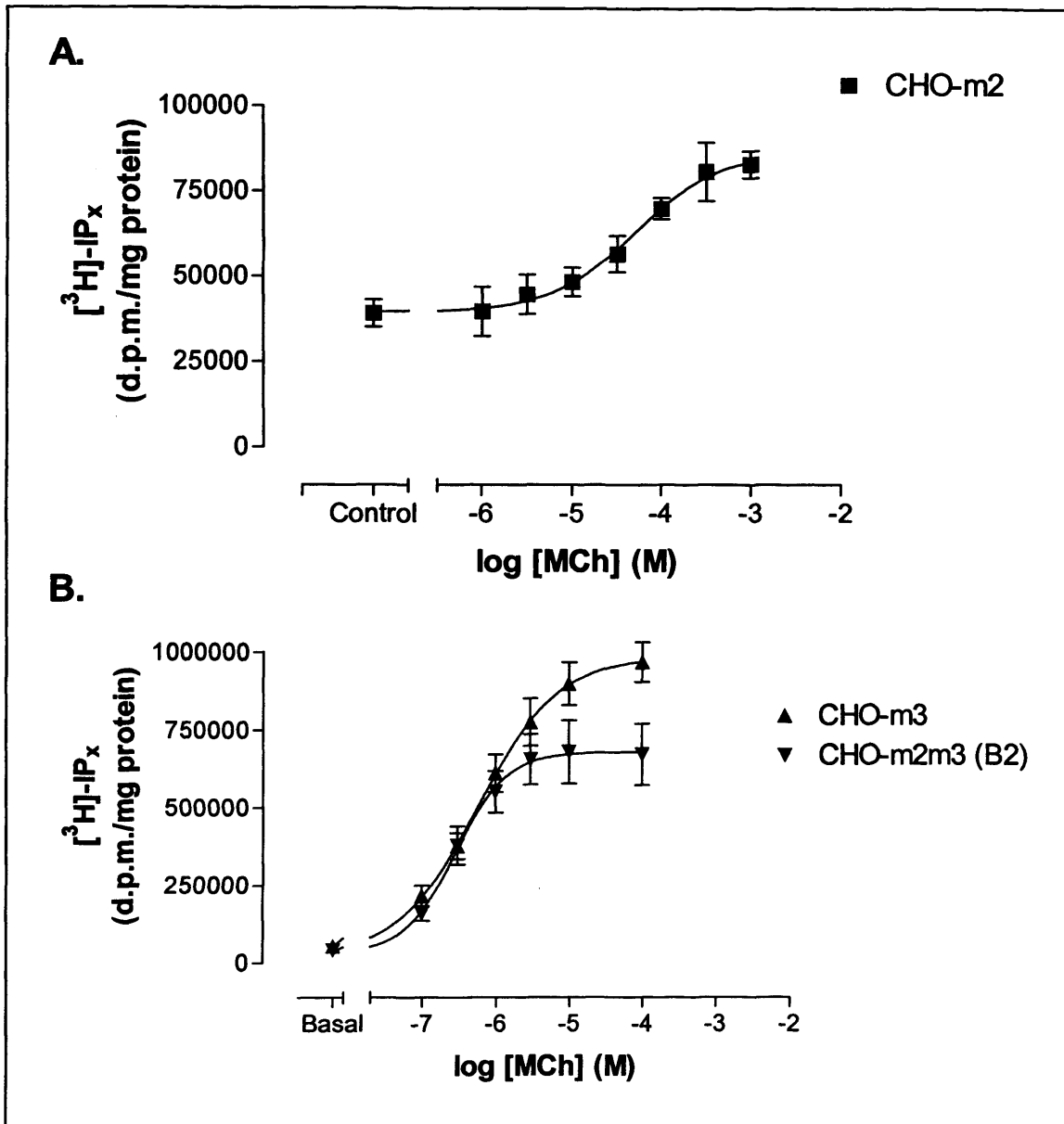


Figure 4.2 Concentration-dependencies of MCh-stimulated (15 min time-point at stated concentrations) $[^3\text{H}]\text{-IP}_x$ accumulation in $[^3\text{H}]\text{-inositol}$ pre-labelled CHO-m2 (n=4) CHO-m3 (n=3) and CHO-m2m3 (B2) (n=3) cells. Data are shown as means \pm S.E.M. Panel A shows CHO-m2 cells and Panel B shows CHO-m3 and CHO-m2m3 (B2) cells. Note difference in scale y-axis between panels A and B.

Cell Line	pEC₅₀ (± S.E.M.)	E_{max} (± S.E.M.)
CHO-m2 (n=4)	4.30 ± 0.07	1.8 ± 0.2
CHO-m3 (n=3)	6.24 ± 0.13	17.9 ± 1.2
CHO-m2m3 (B2) (n=3)	6.55 ± 0.16	16.2 ± 2.4

Table 4.1 A summary of MCh-stimulated (at 15 min) [³H]-IP_x accumulation in [³H]-inositol pre-labelled CHO-m2, CHO-m3 and CHO-m2m3 (B2) cells. Data represent means ± S.E.M. for at least three separate experiments performed in duplicate. Basal [³H]-IP_x accumulations were 43054 ± 8335, 54203 ± 11586 and 41552 ± 10909 for CHO-m2 , CHO-m3 and CHO-m2m3 respectively.

4.2.2 Analysis of Ca^{2+} -release profiles in CHO-m2, CHO-m3 and CHO-m2m3 (B2) cells

MCh stimulation of all three cell lines studied (CHO-m2, CHO-m3 and CHO-m2m3 (B2)) caused a time-dependent and concentration-dependent increase in $[\text{Ca}^{2+}]_i$. In CHO-m2 cells, as shown in Figures 4.3 (panel A), 4.4 and 4.5, concentrations of MCh above 1 μM evoked concentration-dependent increases in intracellular Ca^{2+} levels (pEC_{50} 5.98 ± 0.30 , $n=3$, Figure 4.5 and Table 4.2) which peaked ≈ 14 s after agonist addition and returned to basal within 120 s. In contrast, both CHO-m3 and CHO-m2m3 (B2) cells exhibited much larger and more rapid Ca^{2+} responses upon agonist stimulation, compared to CHO-m2 cells, which peaked ≈ 3 s after agonist addition with similar maximal stimulations (Figure 4.3 panels B and C). 10 nM MCh elicited maximal responses in CHO-m3 and CHO-m2m3 (B2) cells, which were approx. 5 fold larger than the maximal response observed in CHO-m2 cells and occurred at concentrations 100 fold lower than that which elicited the maximal response in CHO-m2 cells (pEC_{50} (M) 8.80 ± 0.17 ; 8.57 ± 0.21 for CHO-m3 and CHO-m2m3 (B2) cells, respectively Figure 4.5 and Table 4.2).

The concentration-response relationships for the agonist-induced peak response in the three cell lines are summarised in Figure 4.5 panel A and Table 4.2. In both CHO-m3 and CHO-m2m3 (B2) cells, 10 nM MCh elicited a rapid peak response which then declined to a plateau level (≈ 40 % of peak) at 90 s and remains elevated beyond 4 min. It is interesting to note from the example time-course traces in Figures 4.3-4.5 that the plateau phase of the agonist-induced Ca^{2+} response in CHO-m3 and CHO-m2m3 (B2) cells *decreased* in a concentration-dependent manner with supra-maximal agonist concentrations (above 30 nM MCh). This phenomenon of a bell-shaped plateau concentration-response curve is highlighted in Figure 4.5 panel B with the same EC_{50} values for maximal $[\text{Ca}^{2+}]_i$ elevation at 180 s as for peak response (≈ 3 s, see Table 4.2).

It was also noteworthy that the time taken to achieve a peak increase in $[\text{Ca}^{2+}]_i$ in CHO-m3 and CHO-m2m3 (B2) cells following agonist addition decreased with increasing agonist concentration. Thus, at a sub-maximal (threshold) concentration of MCh (1 nM) the peak rise in $[\text{Ca}^{2+}]_i$ was similar in time-course (approx. 16 s to peak) and magnitude to that elicited by a much higher concentration of MCh in CHO-m2 cells (see Figure 4.3 cf. panels A & C).

Figure 4.3 Time-course profile of MCh-stimulated Ca^{2+} responses in CHO-m2 (panel A), CHO-m3 (panel B) and CHO-m2m3 (B2) (panel C) cells. MCh was added at $t = 10$ s of baseline. Data are shown for a representative experiment repeated at least three times in quadruplicate.

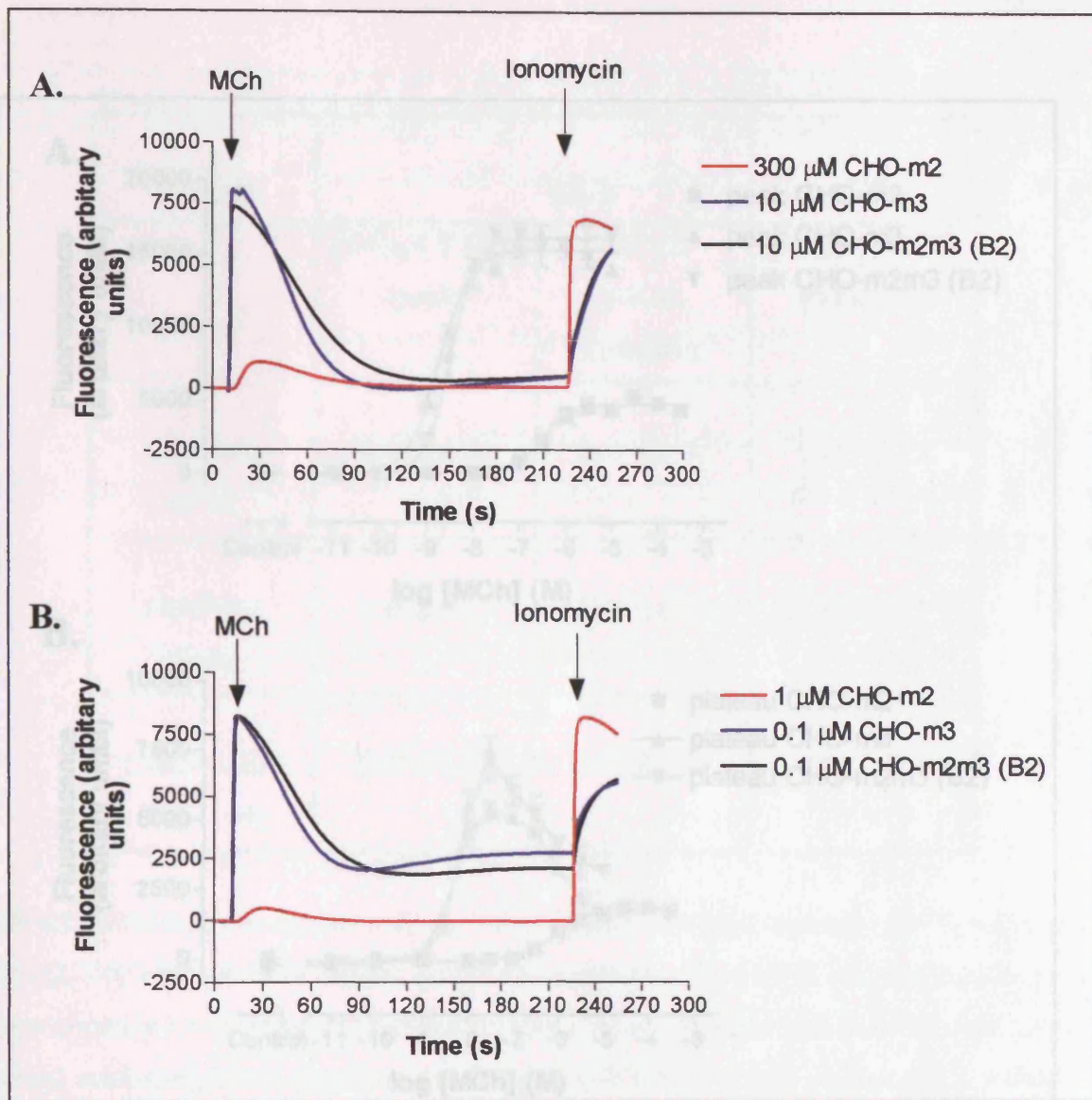


Figure 4.4 Time-course profiles of MCh-stimulated Ca^{2+} responses in CHO-m2, CHO-m3 and CHO-m2m3 (B2) cells. MCh was added after 10 s of baseline recording. Panel A shows Ca^{2+} responses to supra-maximal MCh concentrations, and panel B shows Ca^{2+} responses to sub-maximal MCh concentrations. Data are shown as mean fluorescence of a representative experiment repeated at least three times in quadruplicate.

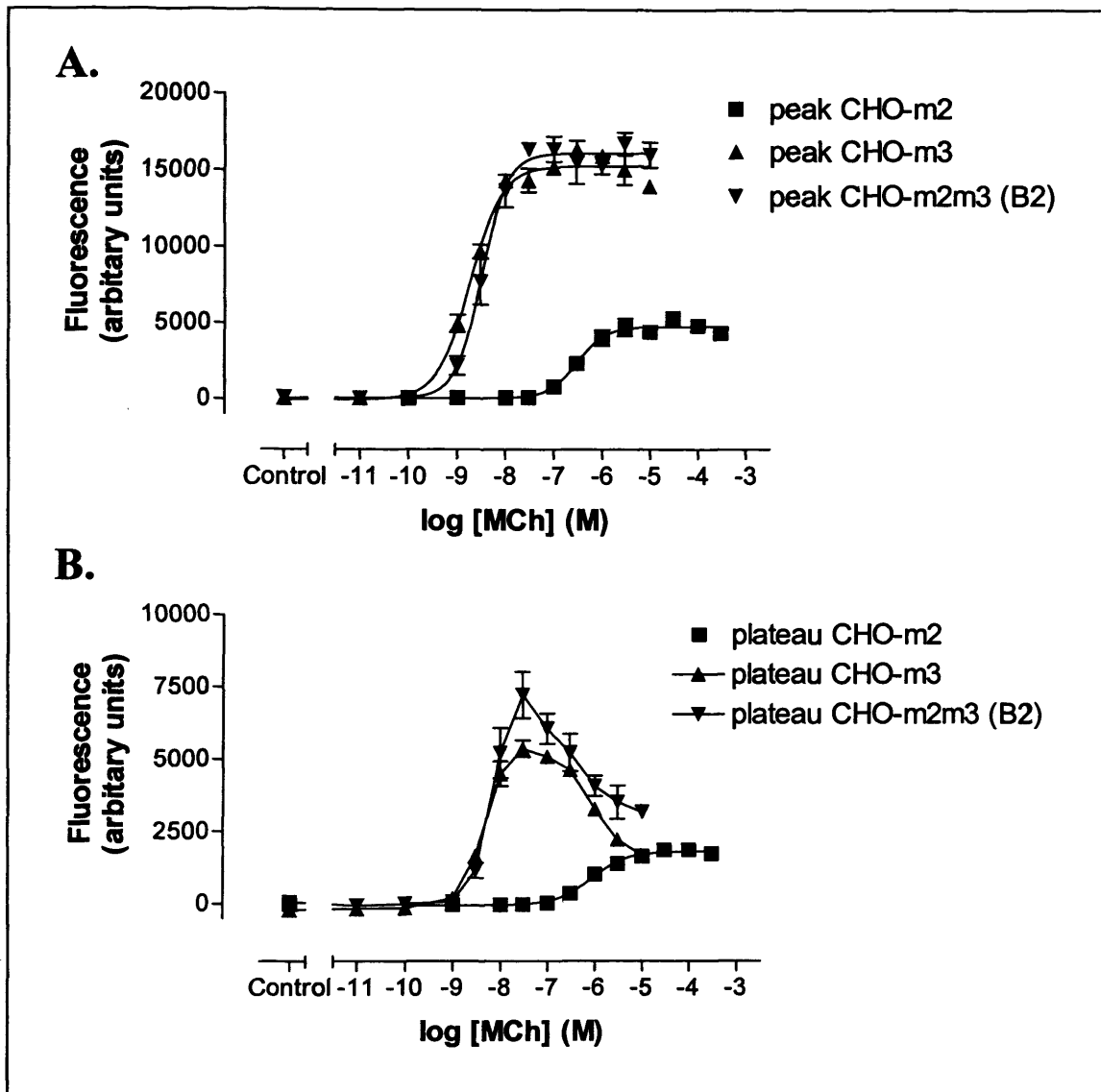


Figure 4.5 Concentration-effect curves for peak (A) and plateau (B) agonist-stimulated intracellular Ca^{2+} responses in CHO-m2, CHO-m3 and CHO-m2m3 (B2) cells as measured by FLIPR. Peak response is approximately 3 s after agonist addition for CHO-m3 and CHO-m2m3 (B2) cells and 15 s for CHO-m2 cells, the plateau phase was measured at 180 s (see Figure 4.3). Data are shown as means \pm S.E.M. for at least three separate experiments performed in quadruplicate.

<u>Cell Line</u>	<u>MCh</u>		<u>CCh</u>
	pEC₅₀ ± S.E.M. (peak)	pEC₅₀ ± S.E.M. (plateau)	pEC₅₀ ± S.E.M. (peak)(n=6)
CHO-m2 (n=4)	5.98 ± 0.30	6.51 ± 0.07	5.91 ± 0.14
CHO-m3 (n=4)	8.80 ± 0.17	8.51 ± 0.38	8.85 ± 0.11
CHO-m2m3 (B2) (n=4)	8.57 ± 0.21	8.52 ± 0.49	8.64 ± 0.16

Table 4.2 A summary of agonist (MCh or CCh) stimulated peak and plateau $[Ca^{2+}]_i$ response in CHO-m2, CHO-m3 and CHO-m2m3 (B2) cells as measured by FLIPR analysis. Peak response is approximately 3 s after agonist addition for CHO-m3 and CHO-m2m3 (B2) cells and 15 s for CHO-m2 cells, the plateau phase was measured at 180 s. To estimate plateau pEC₅₀ values for CHO-m3 and CHO-m2m3 (B2) cells data between 10⁻¹¹ - 10⁻⁷ M were analysed (see Figure 4.5).

Concentration-dependency profiles for CCh-stimulated $[Ca^{2+}]_i$ responses were also established in CHO-m2, CHO-m3 and CHO-m2m3 (B2) cells. CCh demonstrated a similar efficacy and potency to MCh ($pEC_{50} = 5.91 \pm 0.14$, 8.85 ± 0.11 and 8.64 ± 0.16 for CHO-m2, CHO-m3 and CHO-m2m3 (B2) respectively, as summarised in Table 4.2).

4.2.3 Inhibition of MCh-stimulated Ca^{2+} responses by mACh receptor antagonists

The activities of the mACh receptor antagonists, triptiramine, darifenacin and atropine in inhibiting MCh-stimulated Ca^{2+} responses in CHO-m2, CHO-m3 and CHO-m2m3 cells were assessed. Triptiramine is M_2 -over- M_3 -selective, darifenacin is M_3 -over- M_2 -selective, and atropine is a non-selective mACh receptor antagonist. In each cell-line a concentration of MCh was chosen to elicit an approx. EC_{80} response (CHO-m2, 10 μ M; CHO-m3 and CHO-m2m3, 10 nM) and antagonists pre-incubated with cells for 30 min prior to agonist addition. None of the antagonists used had any effect on basal (or auto) fluorescence.

As illustrated in Figure 4.6, triptiramine showed selectivity for inhibition of the M_2 -mediated Ca^{2+} response (pK_i , 9.3 ± 0.5) compared to the response observed in either CHO-m3 or CHO-m2m3 cell-lines (pK_i , 7.6 ± 0.5 ; 7.9 ± 0.3 , respectively), although the absolute level of selectivity (20-50 fold) was less than would have been predicted from radioligand binding studies. Darifenacin showed little M_3 selectivity (≈ 5 fold) in FLIPR experiments (pK_i ; 8.5 ± 0.1 ; 9.0 ± 0.5 ; 8.9 ± 0.3 , for CHO-m2, -m3 and -m2m3 cells, respectively, Figure 4.7). The non-selective mACh receptor antagonist atropine inhibited both M_2 and M_3 -mediated Ca^{2+} responses (Figure 4.8) with similar activity. Antagonist profiles are summarised in Table 4.3.

4.2.4 Contribution of extracellular Ca^{2+} influx to Ca^{2+} response profiles in CHO-m2, CHO-m3 and CHO-m2m3 (B2) cells

The initial peak Ca^{2+} response has previously been shown to be caused predominantly by release of Ca^{2+} from intracellular Ca^{2+} stores, while the sustained plateau phase observed in CHO-m3 cells is caused by Ca^{2+} influx into the cell (Berridge et al., 2000). It was important therefore to investigate if the observed Ca^{2+} response in CHO-m2 cells was evoked by the same mechanism as the more traditionally studied G_q -linked PLC/ IP_3 / Ca^{2+} response (CHO-m3 cells).

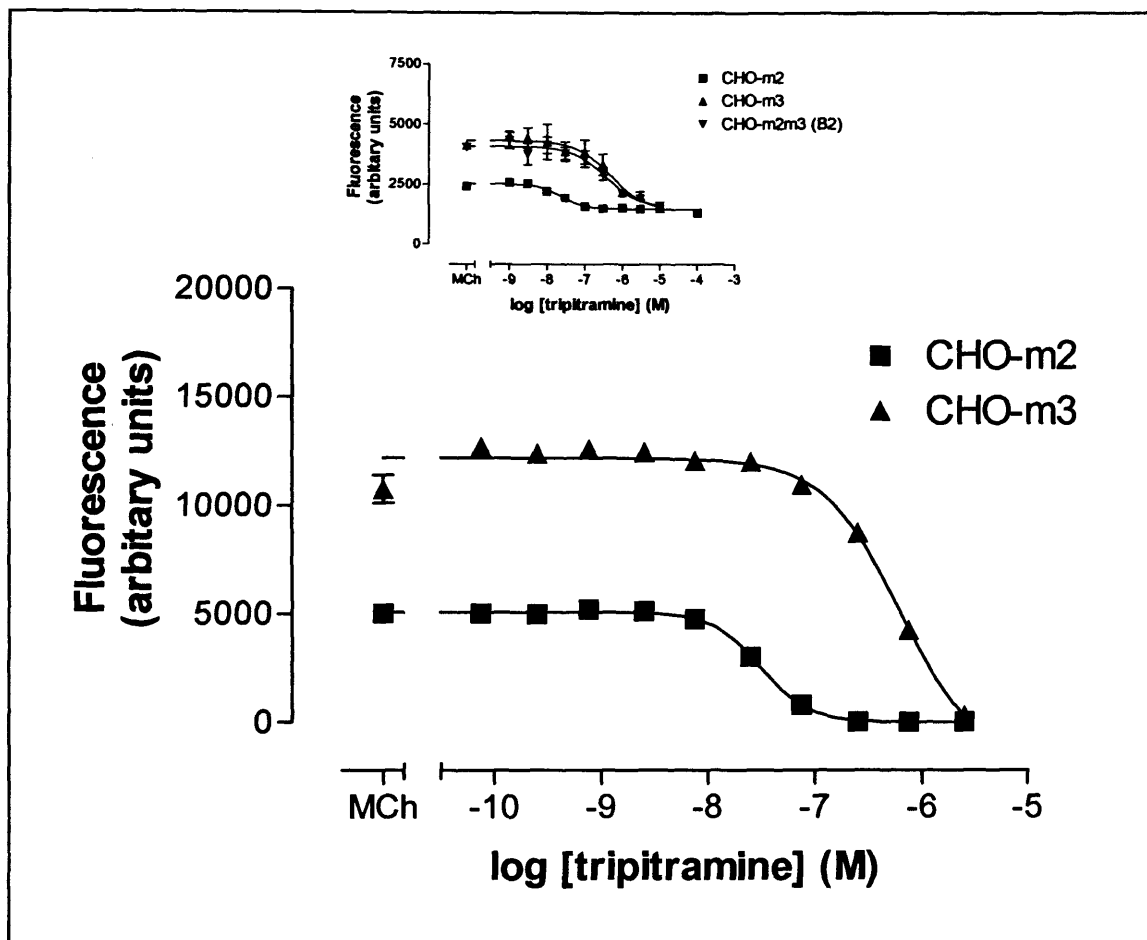


Figure 4.6 Tripitramine inhibition of the MCh-stimulated Ca^{2+} response in CHO-m2, CHO-m3 and CHO-m2m3 (B2) cells. MCh = 10 μM in CHO-m2 cells, and 10 nM in CHO-m3 and CHO-m2m3 (B2) cells. Data are shown as means \pm S.E.M. for one representative experiment performed in quadruplicate, and repeated three times. The inset shows a second representative experiment with all three cell lines analysed within the same experiment. See Table 4.3 for composite data from multiple separate experiments.

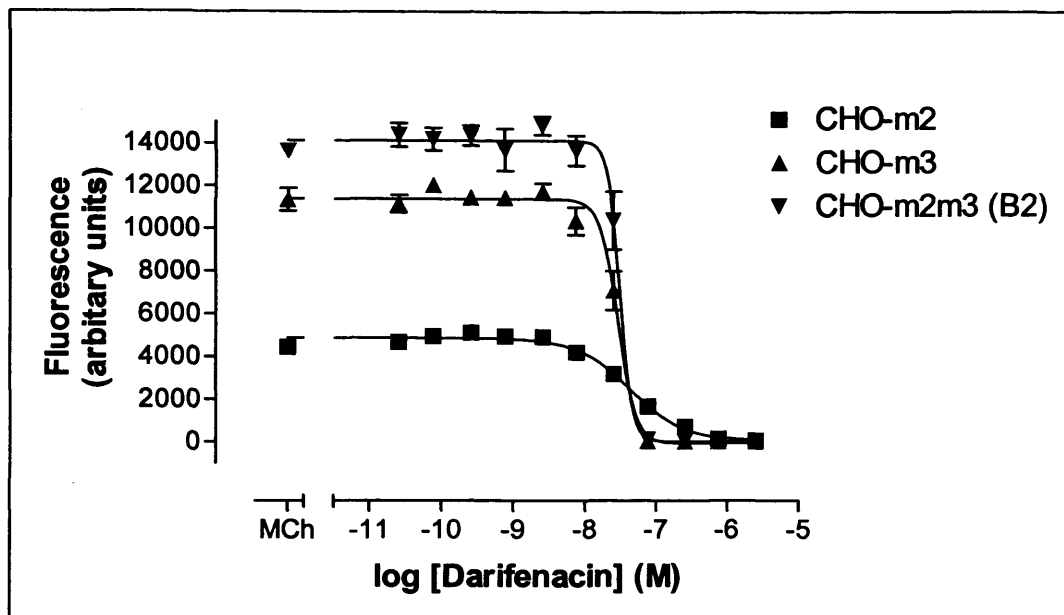


Figure 4.7 Darifenacin inhibition of MCh-stimulated $[Ca^{2+}]$ responses in CHO-m2, CHO-m3 and CHO-m2m3 (B2) cells. MCh = 10 μ M in CHO-m2 cells, and 10 nM in CHO-m3 and CHO-m2m3 (B2) cells. Data are shown as means \pm S.E.M. for one representative experiment performed in quadruplicate, and repeated three times. See Table 4.3 for composite data from multiple separate experiments.

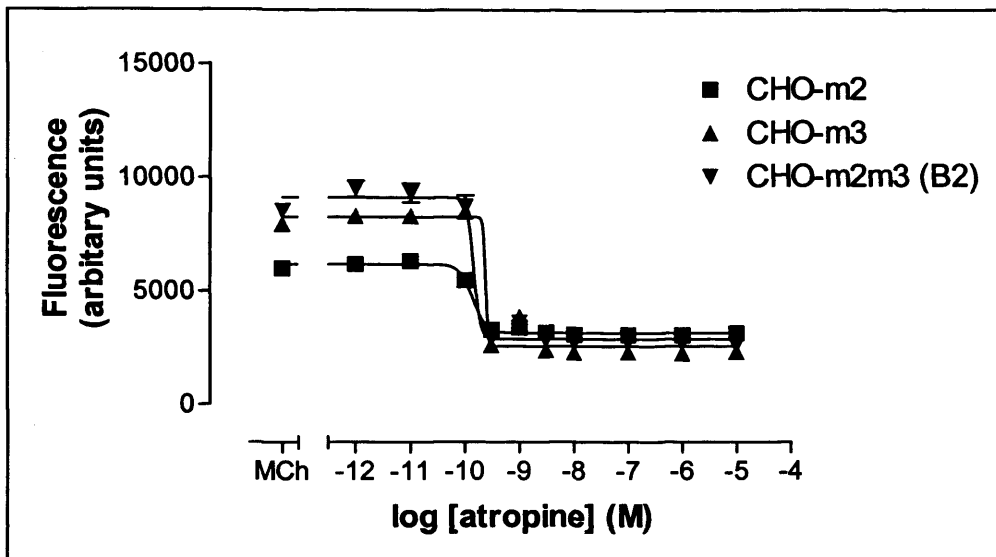


Figure 4.8 Atropine inhibition of MCh stimulated $[Ca^{2+}]$ response in CHO-m2 and CHO-m3 and CHO-m2m3 (B2) cells. MCh = 10 μ M in CHO-m2 cells and 10 nM in CHO-m3 and CHO-m2m3 (B2) cells. Data are shown as means \pm S.E.M. for one representative experiment performed in quadruplicate and repeated three times. See Table 4.3 for composite data from multiple separate experiments.

	CHO-m2	CHO-m3	CHO-m2m3 (B2)
Tripitramine pK _i (n=3)	9.25 ± 0.47	7.59 ± 0.54	7.94 ± 0.33
Darifenacin pK _i (n=3)	8.48 ± 0.1	8.98 ± 0.54	8.85 ± 0.25
Atropine pK _i (n=3)	10.76 ± 0.61	10.09 ± 0.42	10.57 ± 0.38

Table 4.3. Summary of inhibition profiles of various mACh receptor antagonists on MCh-stimulated $[Ca^{2+}]_i$ responses in CHO-m2, CHO-m3 and CHO-m2m3 (B2) cells. pK_i values were calculated by Cheng-Prusoff analysis (see Methods). Inhibition profiles to 10 μ M MCh in CHO-m2 cells, and 10 nM MCh in CHO-m3 and CHO-m2m3 (B2) cells.

Extracellular Ca^{2+} was removed by omission of Ca^{2+} from the FLIPR buffer and addition of EGTA (100 μM) to further reduce extracellular Ca^{2+} to approx. 100 nM. Surprisingly, under calcium-free conditions in CHO-m2 cells, MCh caused a stimulation of intracellular Ca^{2+} release *greater* than that observed in normal Ca^{2+} -containing experiments, as shown in Figure 4.9. There was no change in potency of MCh under Ca^{2+} -free compared to Ca^{2+} -containing experimental conditions but the maximal MCh-induced fluorescence change was 1.46 ± 0.12 fold greater than under Ca^{2+} -containing conditions, as shown in Figure 4.10, and Table 4.4.

In contrast to CHO-m2 cells, removal of extracellular Ca^{2+} caused an inhibitory effect upon MCh-stimulated $[\text{Ca}^{2+}]_i$ responses in both CHO-m3 and CHO-m2m3 (B2) cells (Figures 4.11 - 4.14, Table 4.4). The peak increase in fluorescence in the absence of extracellular Ca^{2+} was 79 ± 6 and 79 ± 3 % of the maximal $[\text{Ca}^{2+}]_i$ response in the presence of extracellular Ca^{2+} . Removal of extracellular Ca^{2+} completely abolished the plateau phase elicited by both maximal and sub-maximal agonist concentrations. As for CHO-m2 cells, removal of extracellular Ca^{2+} did not affect the agonist concentration-dependencies in CHO-m3 or CHO-m2m3 (B2) cells (Table 4.4).

As can be observed from Figures 4.9 - 4.14, the addition of thapsigargin (2 μM) 20 min prior to agonist addition depleted intracellular Ca^{2+} stores and completely abolished agonist-induced $[\text{Ca}^{2+}]_i$ responses in all three cell lines.

In all cases, the observed agonist-induced Ca^{2+} response in CHO-m2m3 (B2) cells mimicked that observed in CHO-m3 cells and there was no evidence of any 'crosstalk' through an M_2 -receptor-mediated component, presumably because any effect is masked by the large magnitude of the M_3 -mediated Ca^{2+} response. However, it was considered important to establish whether the mechanism of the agonist-induced Ca^{2+} response in CHO-m2 cells is mediated by "promiscuous" coupling of M_2 -receptors to G_q -proteins or G_i -derived $\text{G}_{\beta\gamma}$ activation of PLC causing the modest IP_x and Ca^{2+} responses. One fascinating aspect, not easily explained by either of these possibilities, is the apparent enhancement of the agonist-stimulated increase in $[\text{Ca}^{2+}]_i$ under Ca^{2+} -free conditions. Therefore, an additional objective was to attempt to establish a mechanism for this phenomenon.

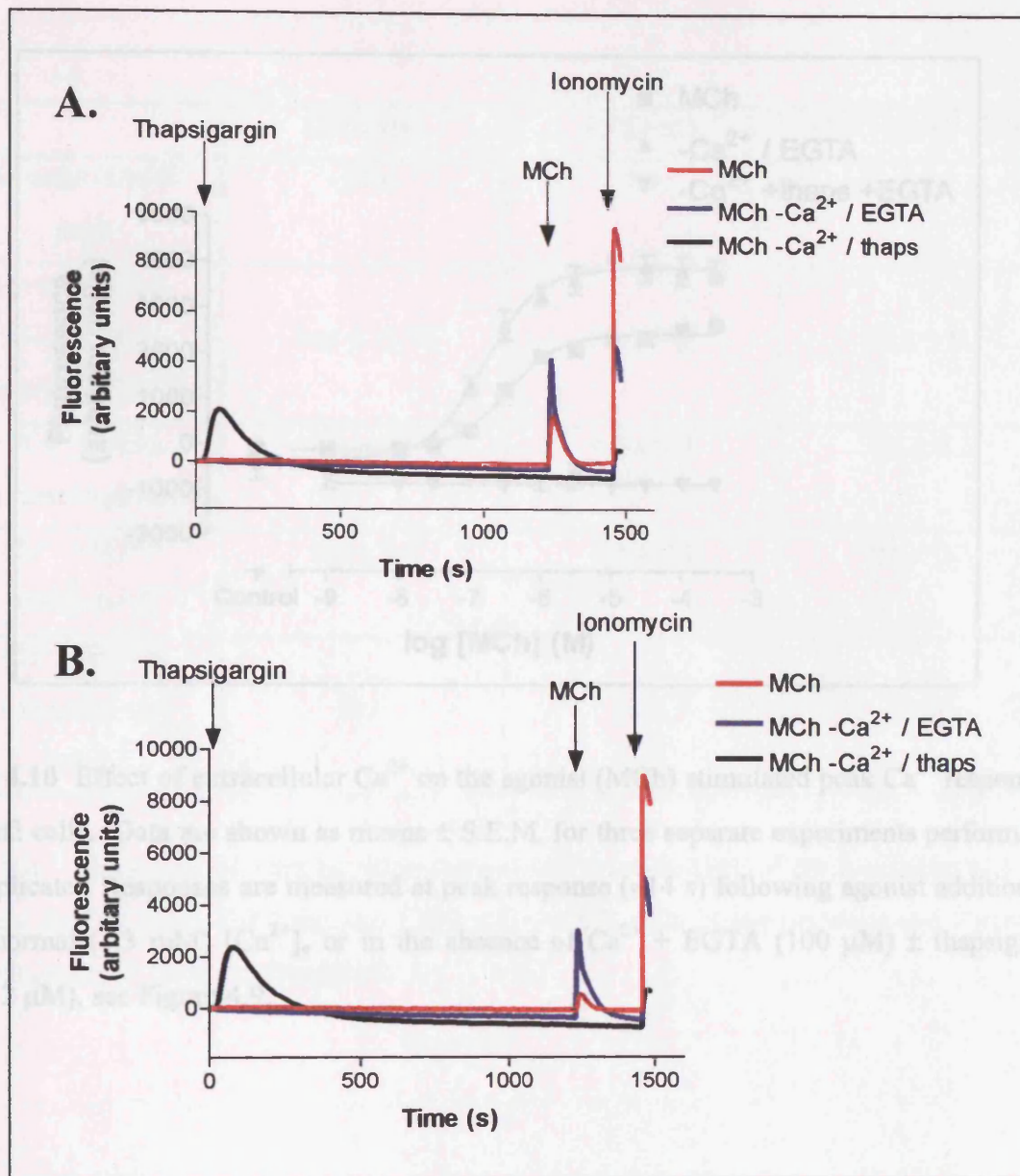


Figure 4.9 Effect of extracellular Ca^{2+} on the agonist (MCh) stimulated Ca^{2+} response in CHO-m2 cells at maximal (100 μM , panel A) and sub-maximal (1 μM , panel B) agonist concentrations. Thapsigargin (2 μM) was added for 20 min in Ca^{2+} -free + EGTA (100 μM) medium (black trace). Data are shown for one representative experiment (performed in quadruplicate) from data for three separate experiments.

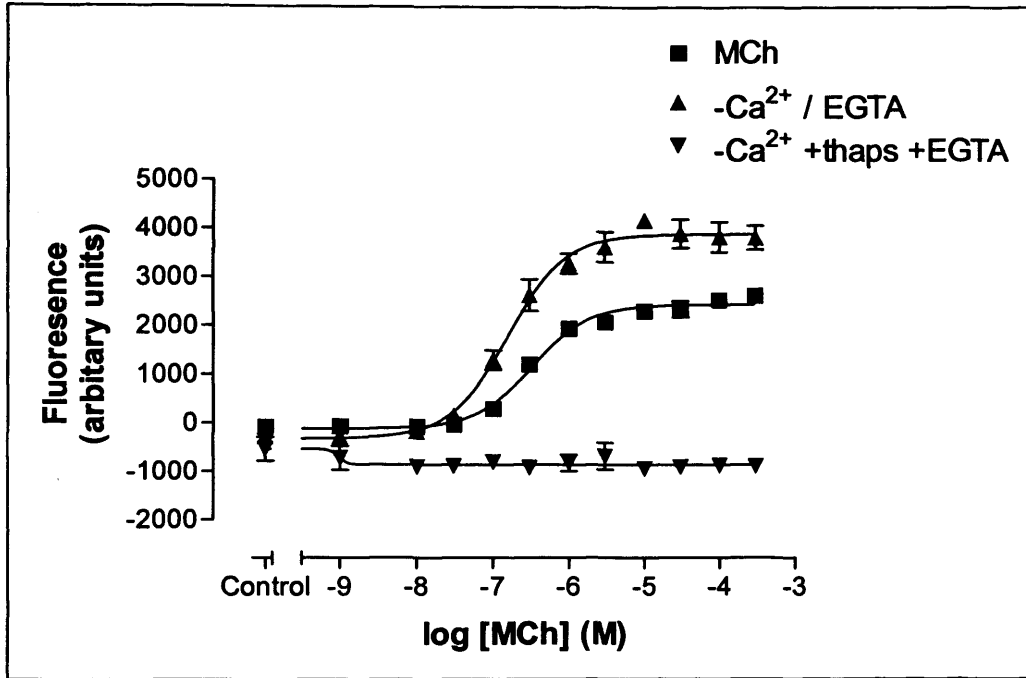


Figure 4.10 Effect of extracellular Ca^{2+} on the agonist (MCh) stimulated peak Ca^{2+} response in CHO-m2 cells. Data are shown as means \pm S.E.M. for three separate experiments performed in quadruplicate. Responses are measured at peak response (≈ 14 s) following agonist addition, in either normal (1.3 mM) $[\text{Ca}^{2+}]_e$ or in the absence of Ca^{2+} + EGTA (100 μM) \pm thapsigargin (thaps; 2 μM), see Figure 4.9.

	CHO-m2	CHO-m3	CHO-m2m3 (B2)
Average time to peak	14 s	3 s	3 s
Average peak (% of max in presence of $[Ca^{2+}]_e$)	$146 \pm 13 \%$	$79 \pm 6 \%$	$79 \pm 3 \%$
+ $[Ca^{2+}]_e$ pEC ₅₀ (on same day) (n=3)	6.1 ± 0.3	9.0 ± 0.2	8.6 ± 0.2
-Ca ²⁺ +EGTA pEC ₅₀ (n=3)	6.6 ± 0.1	8.8 ± 0.1	8.5 ± 0.2
-Ca ²⁺ +EGTA + thapsigargin (n=3)	N/A	N/A	N/A

Table 4.4 Summary of concentration-dependency relationships of MCh-stimulated $[Ca^{2+}]_i$ responses in CHO-m2, CHO-m3 and CHO-m2m3 (B2) cells in the presence and absence of extracellular Ca^{2+} . N/A = no response.

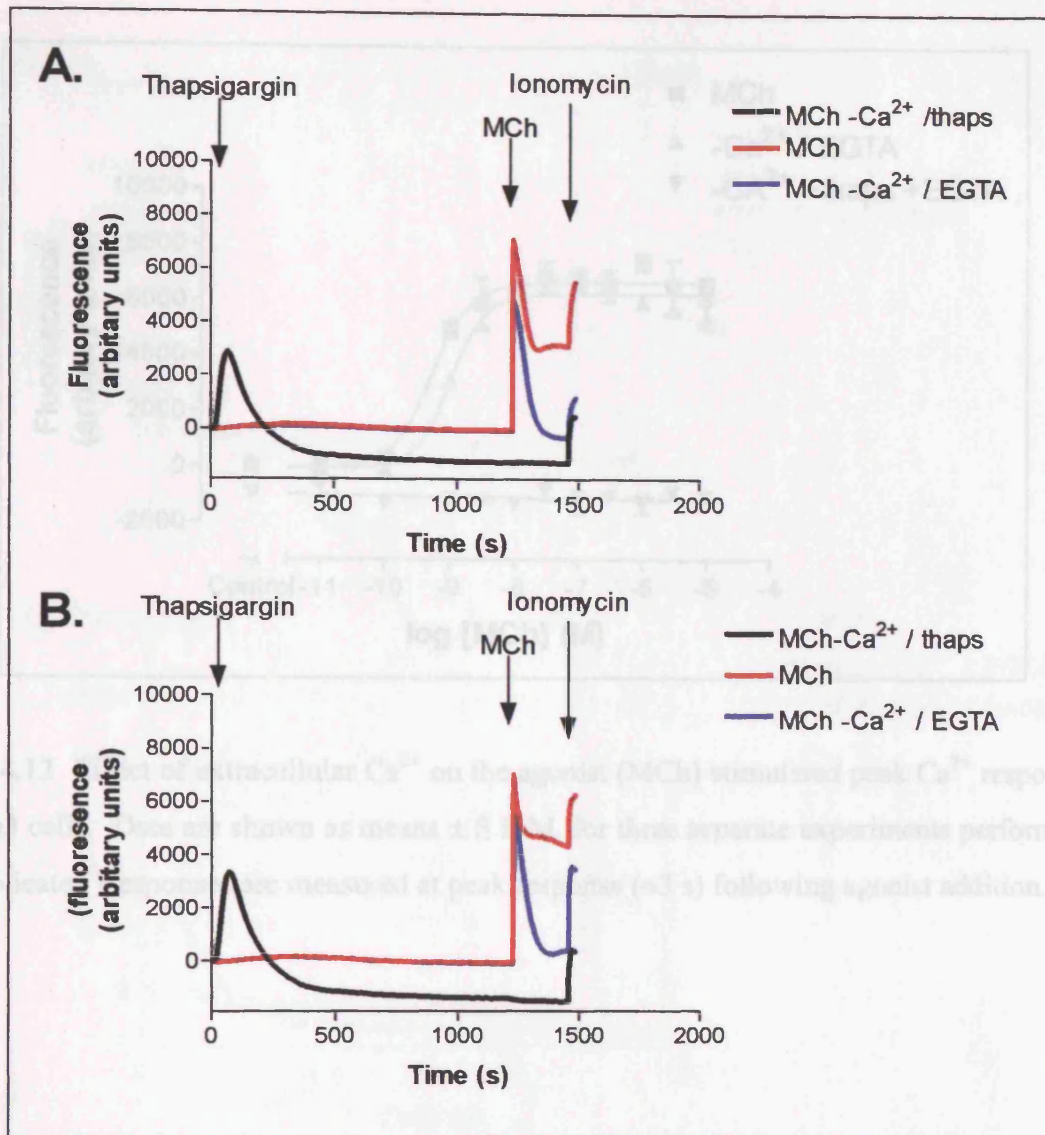


Figure 4.11 Effect of extracellular Ca²⁺ on the agonist (MCh) stimulated Ca²⁺ response in CHO-m3 cells at maximal (10 μM, panel A) and sub-maximal (10 nM, panel B) agonist concentrations. Data are shown for one representative experiment (performed in quadruplicate) from data for three separate experiments.

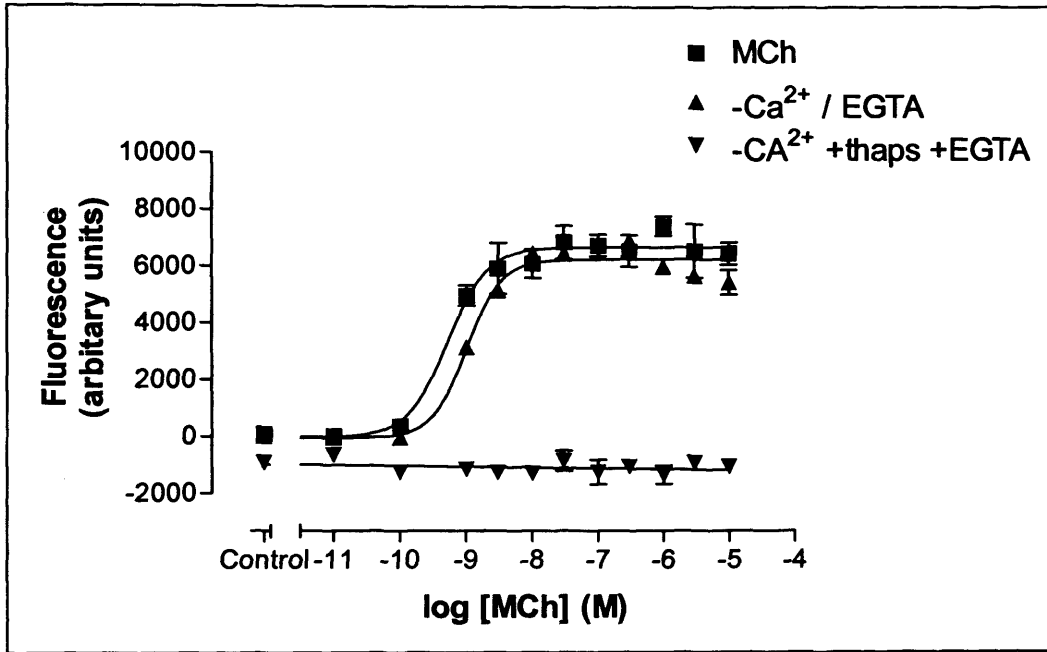


Figure 4.12 Effect of extracellular Ca^{2+} on the agonist (MCh) stimulated peak Ca^{2+} response in CHO-m3 cells. Data are shown as means \pm S.E.M. for three separate experiments performed in quadruplicate. Responses are measured at peak response (≈ 3 s) following agonist addition.

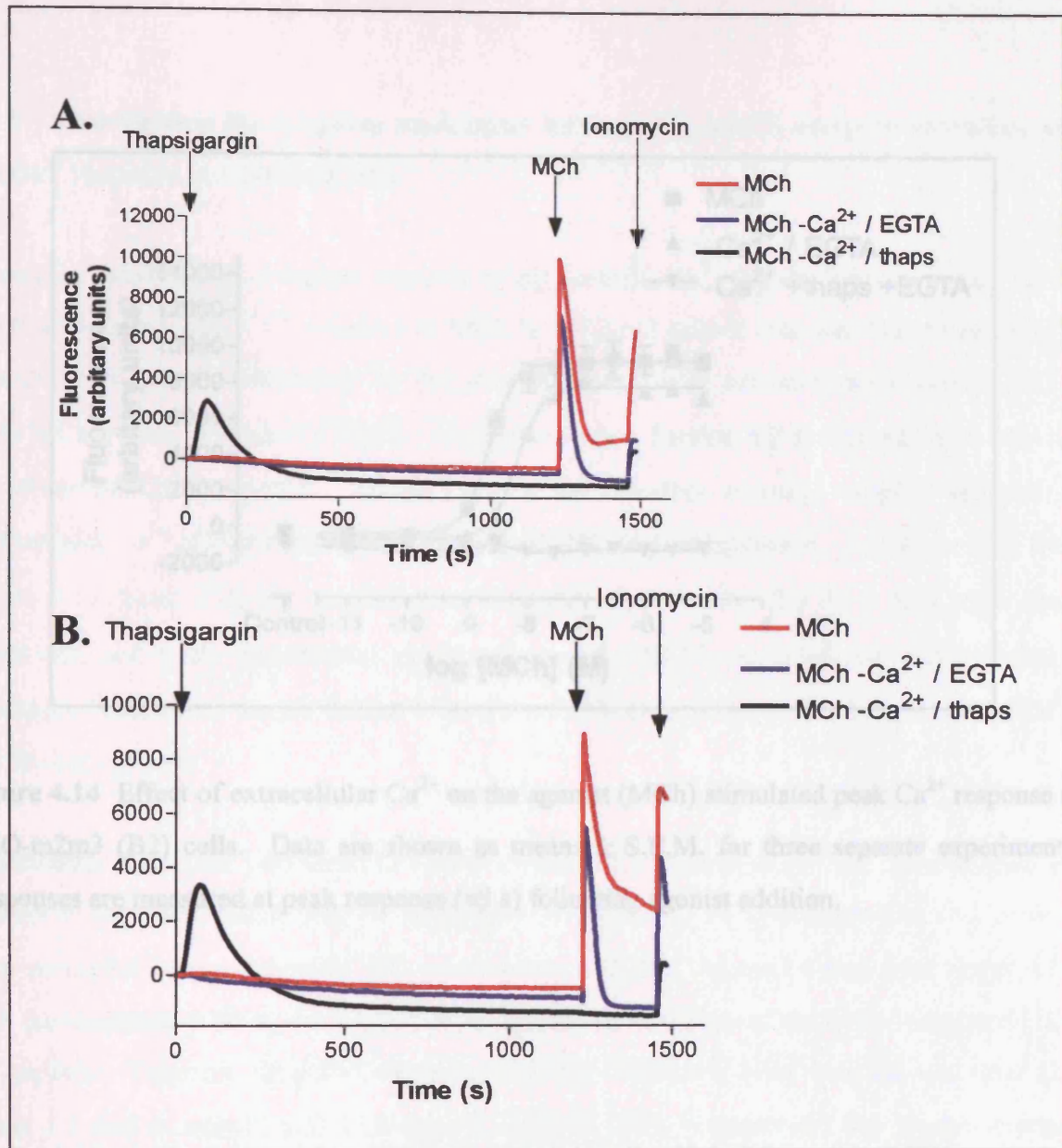


Figure 4.13 Effect of extracellular Ca^{2+} on the agonist (MCh) stimulated Ca^{2+} response in CHO-m2m3 (B2) cells at maximal ($10 \mu\text{M}$, panel A) and sub-maximal (10nM , panel B) agonist concentrations. Data are shown for one representative experiment (performed in quadruplicate) from data for three separate experiments.

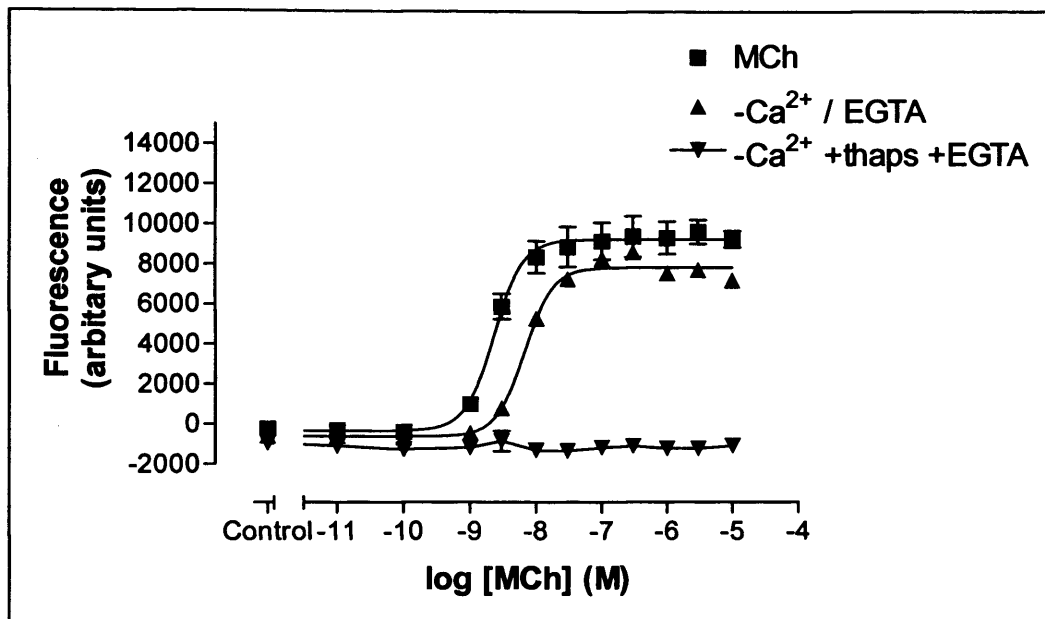


Figure 4.14 Effect of extracellular Ca^{2+} on the agonist (MCh) stimulated peak Ca^{2+} response in CHO-m2m3 (B2) cells. Data are shown as means \pm S.E.M. for three separate experiments. Responses are measured at peak response (≈ 3 s) following agonist addition.

4.2.5 Investigating the coupling mechanism between M₂ mACh receptor activation and the Ca²⁺ response in CHO-m2 cells

Having established that complete removal of extracellular Ca²⁺ (by Ca²⁺ omission and EGTA addition) increases the Ca²⁺ response to MCh in CHO-m2 cells it was considered important to attempt to establish a mechanism for this phenomenon. Under normal conditions (Ca²⁺_e = 1.3 mM) MCh evoked a modest [³H]-IP_x accumulation (see Section 4.2.1) that might account for the observed Ca²⁺ response. Initial experiments therefore assessed whether removal of extracellular Ca²⁺ affected the agonist-stimulated [³H]-IP_x accumulation. As can be seen from Figure 4.15, basal [³H]-IP_x accumulation was somewhat reduced (by 34 ± 5%) under these conditions, and more importantly, agonist-stimulated [³H]-IP_x accumulation was completely abolished. These data suggest that, at least under Ca²⁺-free conditions, IP₃ may not be the Ca²⁺-mobilizing stimulus.

Experiments were then performed to assess whether PLC activation and Ca²⁺ mobilisation are dependent upon M₂ mACh receptor coupling to G_{i/o} proteins. To investigate this, G_{i/o} proteins were uncoupled by pre-treatment with pertussis toxin (PTX). As can be seen from Figure 4.16, PTX pre-treatment (100 ng ml⁻¹; 16 h) caused a modest inhibition of the MCh-stimulated [³H]-IP_x response. However, the effect, when expressed as a fold-over-basal increase, was small (2.2 versus 1.9 fold in control and PTX-treated CHO-m2 cells, respectively) and a concentration-dependent increase in MCh-stimulated [³H]-IP_x accumulation could still be observed following toxin pre-treatment (pEC₅₀ values 4.7 ± 0.6; 4.4 ± 0.5 for control and PTX-treated CHO-m2 cells, respectively).

The effects of extracellular Ca²⁺ removal and PTX pre-treatment were also assessed with respect to the [³H]-IP_x response evoked by the ionophore ionomycin. This agent was maximally effective at a concentration of 1 μM (with higher concentrations perhaps causing a loss of cell viability; see Figure 4.17A) stimulating a [³H]-IP_x response similar to that caused by 1 mM MCh. Under Ca²⁺-free conditions the ionomycin stimulation of PLC was completely abolished. Further experiments demonstrated that PTX pre-treatment had little effect on ionomycin-

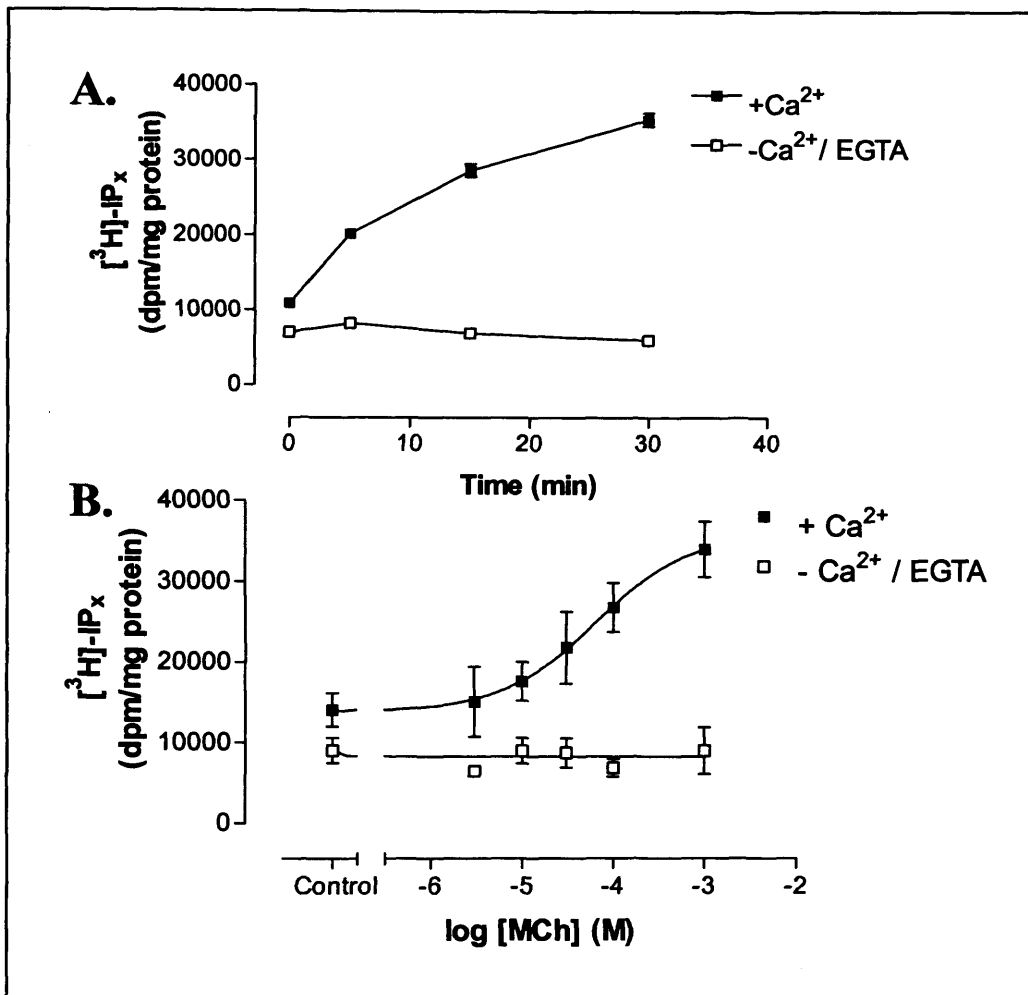


Figure 4.15 Agonist-stimulated $[^3\text{H}]\text{-IP}_x$ accumulation in the presence and absence of Ca^{2+} in $[^3\text{H}]\text{-inositol}$ pre-labelled CHO-m2 cells. Cells were washed into Ca^{2+} free (FLIPR buffer minus Ca^{2+} plus EGTA 100 μM) or normal FLIPR, and were then left to equilibrate for 30 min in the presence of LiCl (10 mM). Panel A is a time-course profile, data are shown as means \pm range for one experiment performed in duplicate. Panel B shows the concentration-dependency of the agonist-induced stimulation in the presence and absence of calcium, data are shown as means \pm S.E.M for three separate experiments.

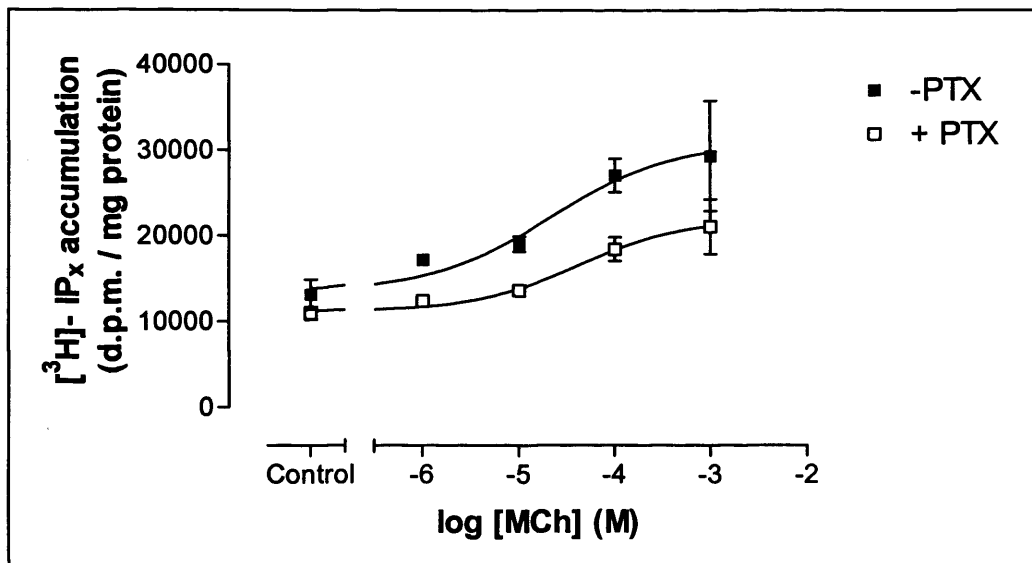


Figure 4.16 Effect of pertussis-toxin (PTX) upon MCh stimulated $[^3\text{H}]\text{-IP}_x$ accumulation in $[^3\text{H}]\text{-inositol}$ pre-labelled CHO-m2 cells. Data are shown as means \pm S.E.M for three separate experiments.

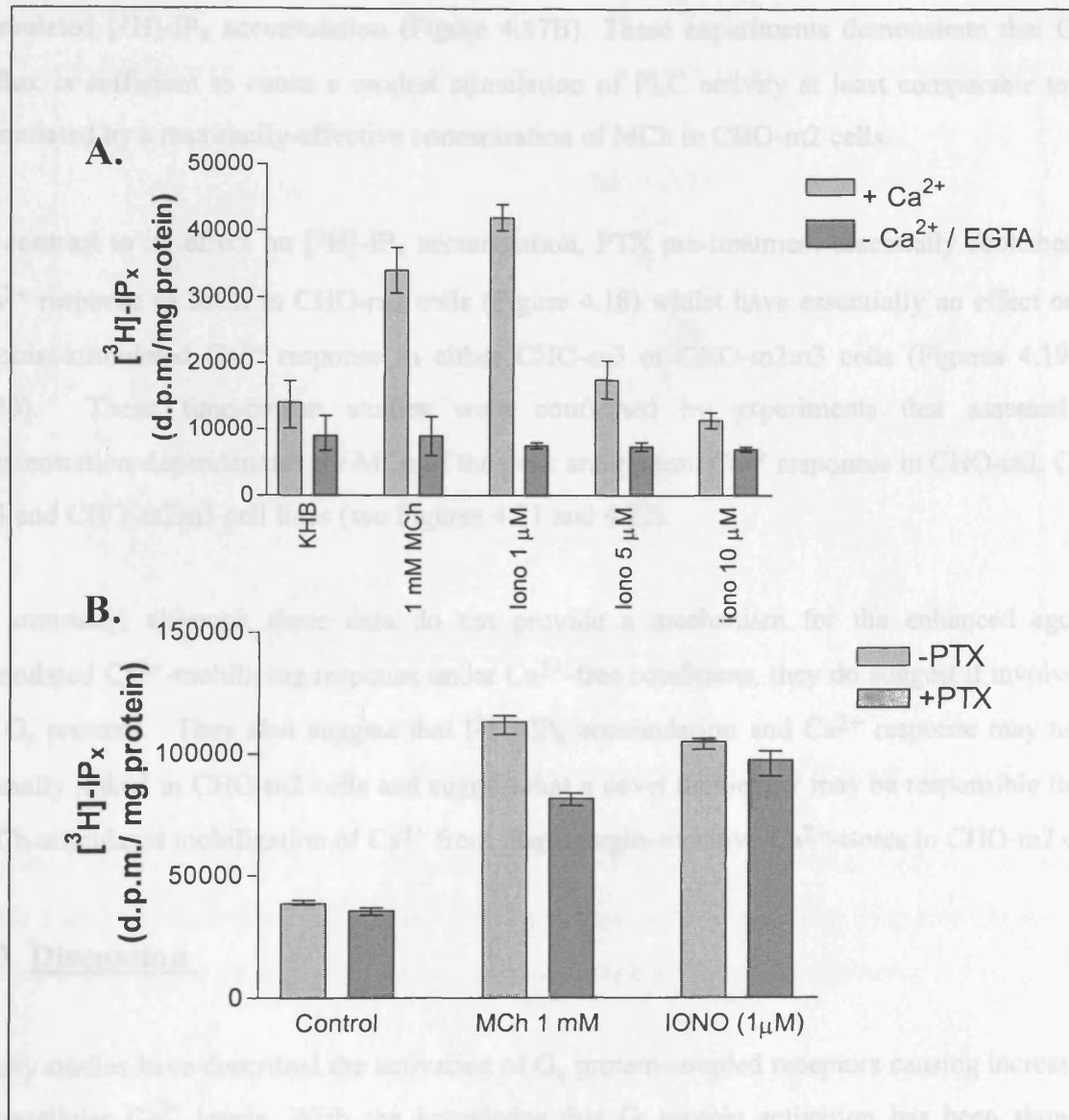


Figure 4.17 Effects of ionomycin on [³H]-IP_x accumulation [³H]-inositol pre-labelled CHO-m2 cells. Panel A Shows the effects of MCh (1 mM) or increasing concentrations of ionomycin in the presence and absence of extracellular Ca²⁺. Panel B shows the effect of PTX pretreatment on MCh and ionomycin stimulated [³H]-IP_x accumulation. Data are shown as means ± range for two experiments performed in duplicate.

stimulated [^3H]-IP $_x$ accumulation (Figure 4.17B). These experiments demonstrate that Ca $^{2+}$ -influx is sufficient to cause a modest stimulation of PLC activity at least comparable to that stimulated by a maximally-effective concentration of MCh in CHO-m2 cells.

In contrast to its effect on [^3H]-IP $_x$ accumulation, PTX pre-treatment essentially abolished the Ca $^{2+}$ response to MCh in CHO-m2 cells (Figure 4.18) whilst have essentially no effect on the agonist-stimulated Ca $^{2+}$ response in either CHO-m3 or CHO-m2m3 cells (Figures 4.19 and 4.20). These time-course studies were confirmed by experiments that assessed the concentration-dependencies for MCh of the peak and plateau Ca $^{2+}$ responses in CHO-m2, CHO-m3 and CHO-m2m3 cell lines (see Figures 4.21 and 4.22).

In summary, although these data do not provide a mechanism for the enhanced agonist-stimulated Ca $^{2+}$ -mobilizing response under Ca $^{2+}$ -free conditions, they do suggest it involves G $_i$ or G $_o$ proteins. They also suggest that [^3H]-IP $_x$ accumulation and Ca $^{2+}$ response may not be causally linked in CHO-m2 cells and suggest that a novel messenger may be responsible for the MCh-stimulated mobilization of Ca $^{2+}$ from thapsigargin-sensitive Ca $^{2+}$ -stores in CHO-m2 cells.

4.3 Discussion

Many studies have described the activation of G $_q$ protein-coupled receptors causing increases in intracellular Ca $^{2+}$ levels. With the knowledge that G $_i$ protein activation has been shown to interact with the G $_q$ signalling pathway, and G $\beta\gamma$ subunits released by G $_i$ activation stimulating PLC, it was important to research possible cross-talk at the level of IP $_x$ accumulation and Ca $^{2+}$ release (Blank et al., 1992; Selbie and Hill, 1998). MCh induced a robust concentration-dependent increase in [^3H]-IP $_x$ accumulation in CHO-m3 and CHO-m2m3 (B2) cells (Figure 4.2), this result and the observed peak and plateau IP $_3$ response (Chapter 3, Figures 3.12 and 3.13) correlated with the measured peak and plateau Ca $^{2+}$ response ([Ca $^{2+}$] $_i$ EC $_{50}$ \approx 100 fold lower than IP $_x$ EC $_{50}$; Figure 4.3 panels B and C). It is assumed that the initial [Ca $^{2+}$] $_i$ rise is due to mobilisation of stores and the latter plateau is due to Ca $^{2+}$ influx (Berridge et al., 2000). MCh also stimulated a concentration-dependent increase in both [^3H]-IP $_x$ accumulation and [Ca $^{2+}$] $_i$ in CHO-m2 cells, although these responses were modest and required much higher concentrations of agonist in comparison to both CHO-m3 and CHO-m2m3 (B2) cells. In addition, the

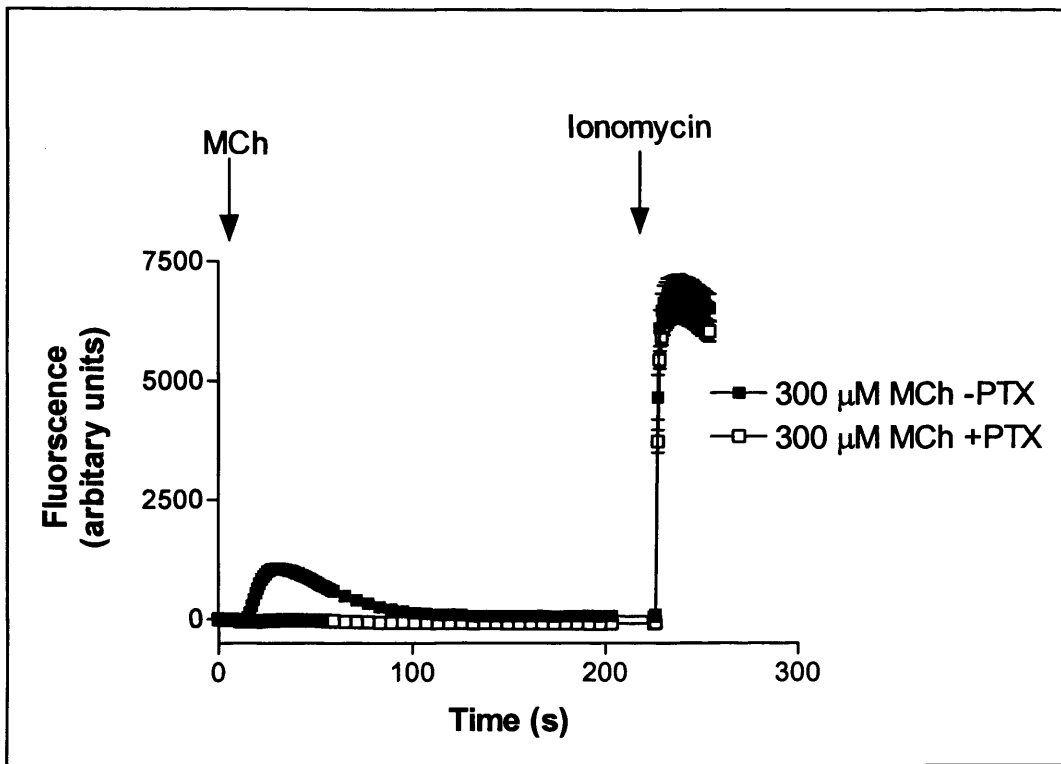


Figure 4.18 Effect of PTX pre-treatment (100 ng/ml, 20 h) on time-course profiles of maximal MCh (300 μ M)-stimulated intracellular Ca^{2+} response in CHO-m2 cells. The data are shown as means \pm S.E.M. from a representative experiment performed in quadruplicate.

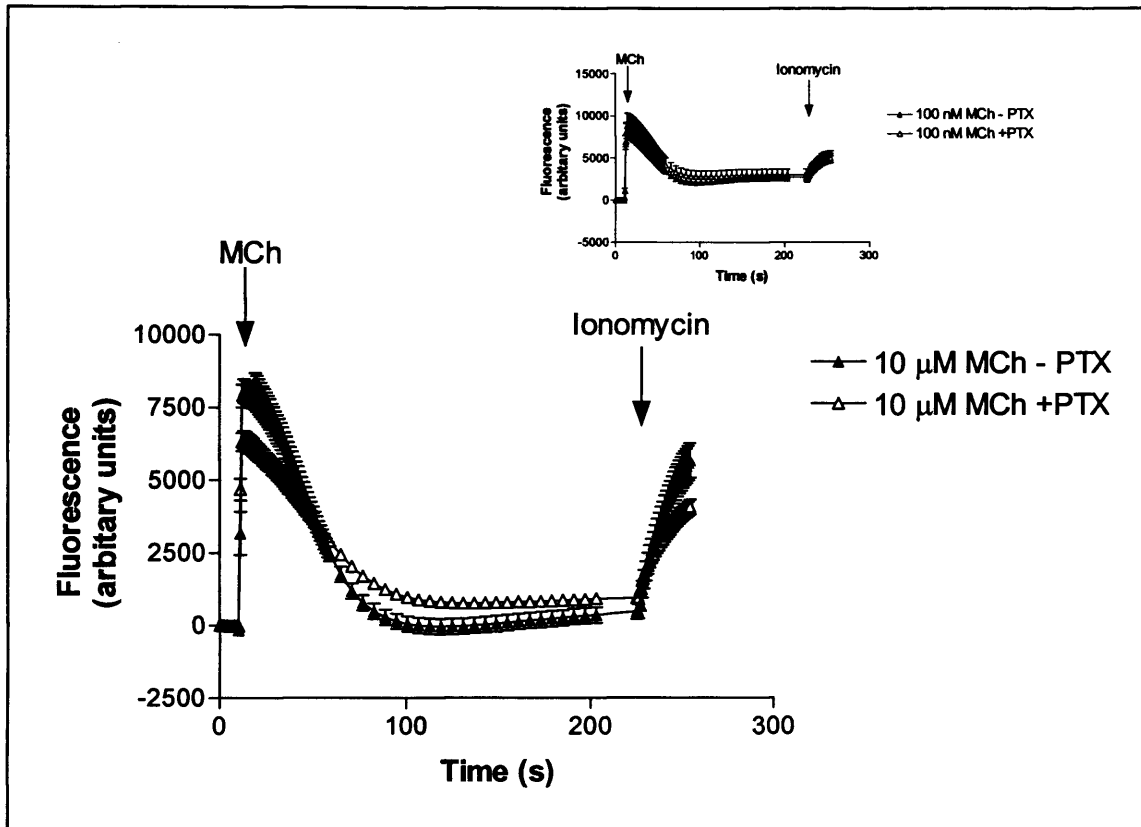


Figure 4.19 Effect of PTX pre-treatment on (100 ng/ml, 20 h) time-course profile of agonist-stimulated intracellular Ca^{2+} response in CHO-m3 cells. The data are shown as means \pm S.E.M. from a representative experiment performed in quadruplicate. The main graphs shows PTX effect on maximal agonist stimulation (10 μM MCh,) and the inset shows sub-maximal (0.1 μM MCh).

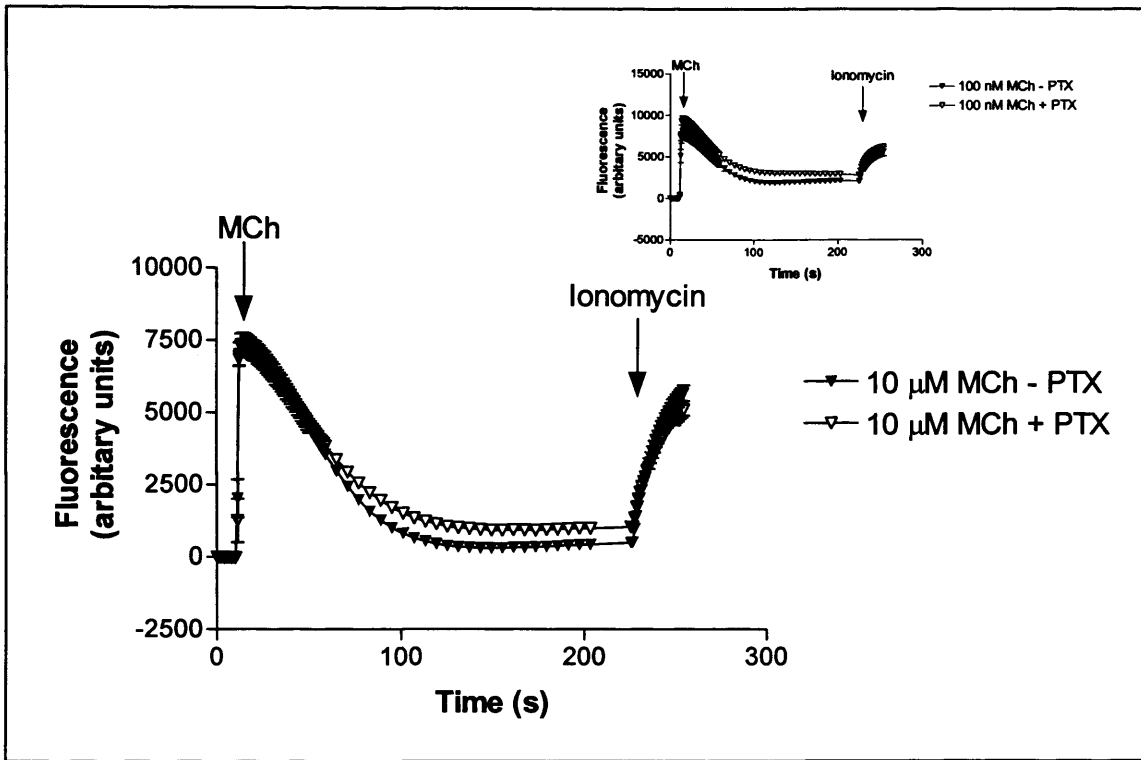


Figure 4.20 Effect of PTX pre-treatment (100 ng/ml, 20 h) on time-course profile of agonist-stimulated intracellular Ca^{2+} response in CHO-m2m3 (B2) cells. The data are shown as means \pm S.E.M. from a representative experiment performed in quadruplicate. The main graphs shows PTX effect on maximal agonist stimulation (10 μM MCh,) and the inset shows sub-maximal (0.1 μM MCh).

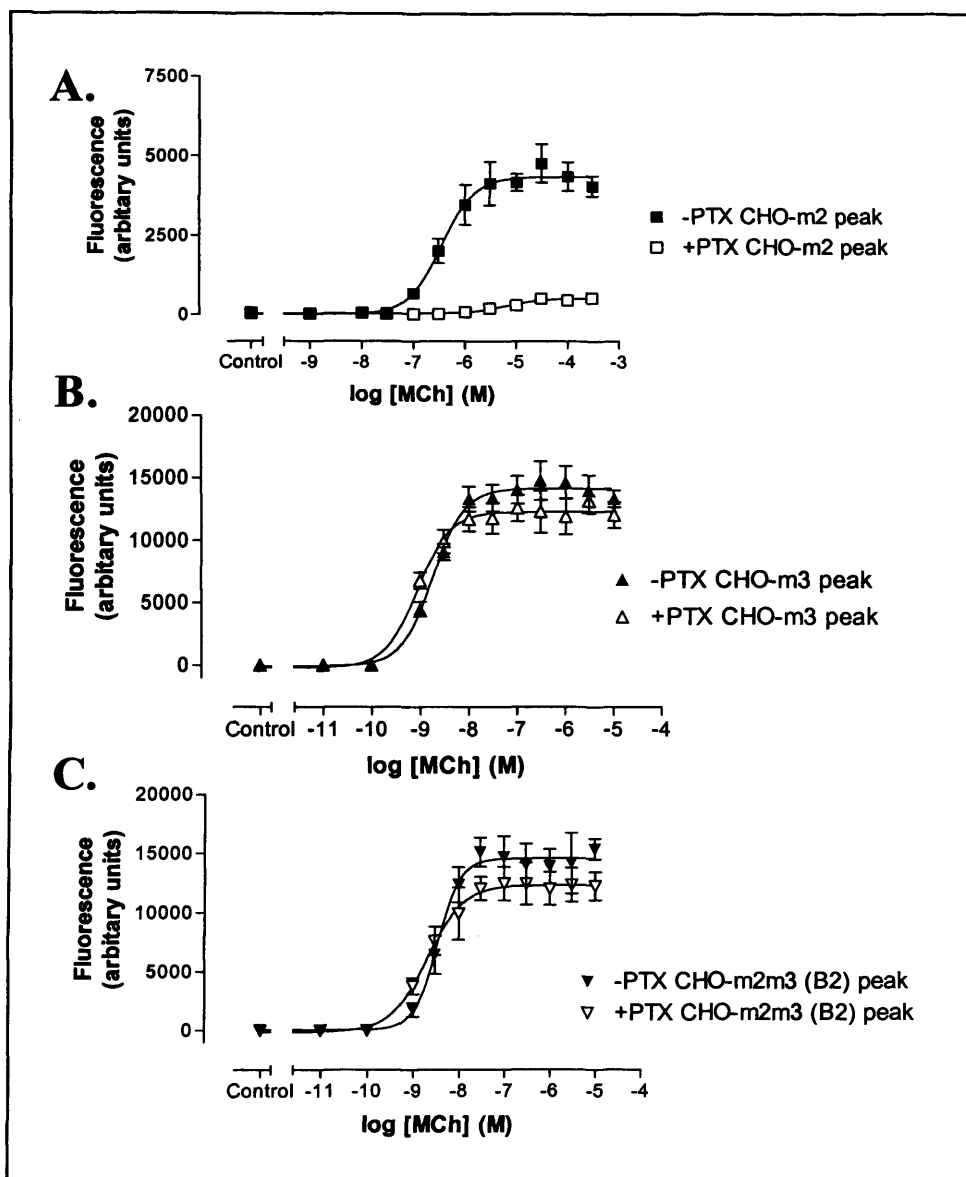


Figure 4.21 Effect of PTX pre-treatment on MCh concentration-effect curves for MCh-stimulated $[Ca^{2+}]_i$ increases measured at the peak response in CHO-m2 (Panel A), CHO-m3 (panel B) and CHO-m2m3 (B2) (panel C) cells. Responses were measured 3 s, 3 s and 14 s after agonist addition for CHO-m2, CHO-m3 and CHO-m2m3 (b2) cells respectively. Data are shown as means \pm S.E.M. of three separate experiments performed in quadruplicate.

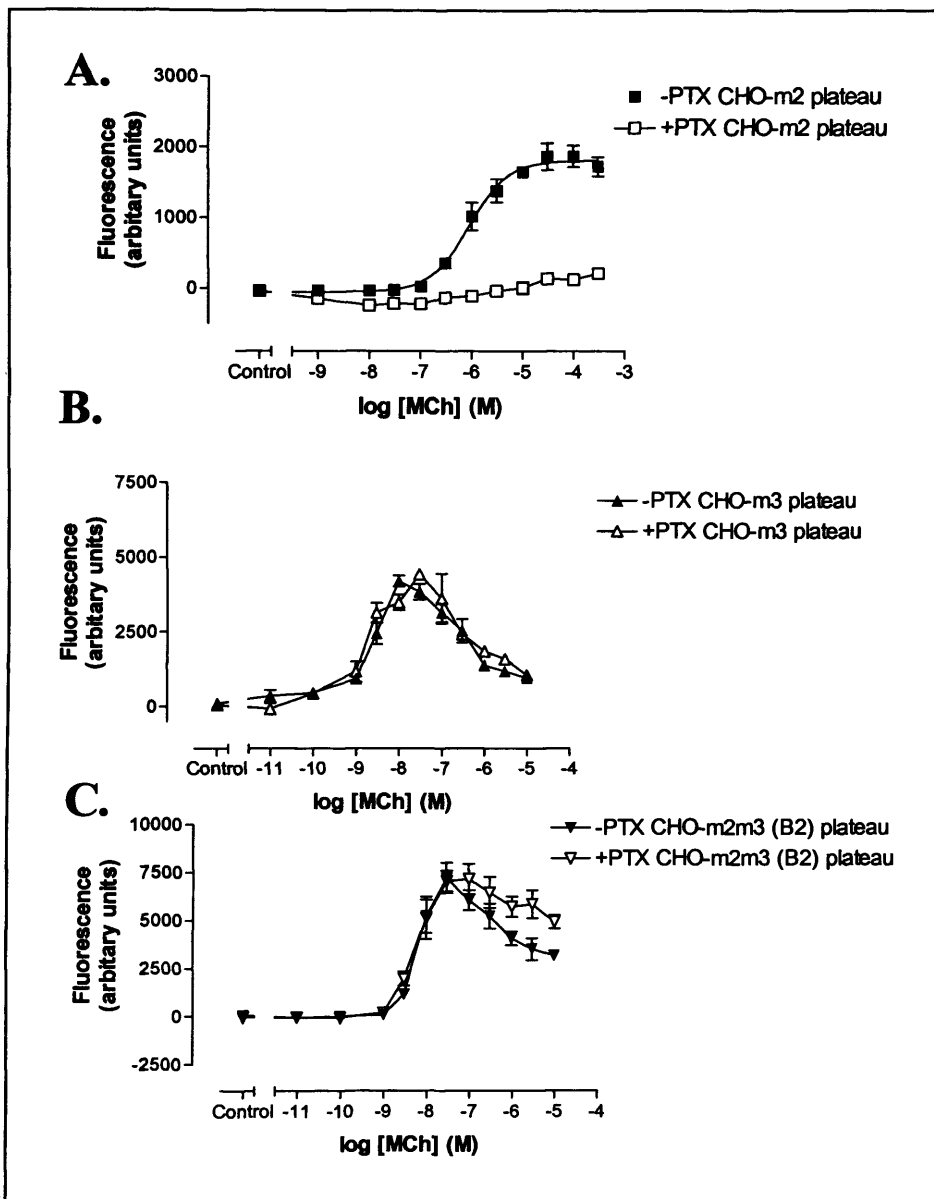


Figure 4.22 Effect of PTX pre-treatment on MCh concentration-effect curves for MCh-stimulated $[Ca^{2+}]_i$ increases measured at the plateau response phase (180 s after agonist addition) in CHO-m2 (Panel A), CHO-m3 (panel B) and CHO-m2m3 (B2) (panel C) cells. Data are shown as means \pm S.E.M. of three separate experiments performed in quadruplicate.

amplification between the [^3H]-IP $_x$ and [Ca^{2+}] $_i$ responses in CHO-m2 cells appeared to be less (only ≈ 30 fold) compared to that seen in CHO-m3 cells.

Similarities in MCh-evoked EC $_{50}$ values for [^3H]-IP $_x$ accumulation and [Ca^{2+}] $_i$ release in CHO-m3 and CHO-m2m3 (B2) cells did not provide any evidence for cross-talk from co-activation of M $_2$ and M $_3$ receptors, either because there was no interaction, or because the M $_2$ -mediated influence was so small it was masked by the robust M $_3$ /G $_q$ -driven signal. The present findings did not provide evidence for augmentation of [^3H]-IP $_x$ accumulation by co-stimulation of G $_i$ - and G $_q$ -coupled receptors as has been reported previously in some cases (Megson et al., 1995; for review see Selbie and Hill, 1998). Thus, Megson and colleagues stimulated G $_i$ -coupled adenosine A $_1$ and G $_q$ -coupled P $_2$ Y receptors and both produced increases in [^3H]-IP $_x$ accumulation, but when co-stimulated they produced an augmented [^3H]-IP $_x$ accumulation response. However, it has been reported that G $_i$ activation, may inhibit PLC activity (Watkins et al., 1994), at least in some cell backgrounds, and since maximal MCh (100 μM) evoked only approx. 70% of maximal response in CHO-m2m3 (B2) cells compared to that observed in CHO-m3 cells, it would be interesting to study the effects of PTX on [^3H]-IP $_x$ accumulation in CHO-m2m3 (B2) cells. However, it is noteworthy that PTX pre-treatment had no effect on [Ca^{2+}] $_i$ release in CHO-m2m3 (B2) cells and MCh caused a modest increase in [^3H]-IP $_x$ accumulation in CHO-m2 cells in this study.

With such different concentration-dependencies between the agonist-induced M $_2$ - and M $_3$ -mediated [Ca^{2+}] $_i$ increases, it was important to establish if these responses were mediated through the same mechanism. The MCh-induced [Ca^{2+}] $_i$ release observed in CHO-m2 appears to be independent of the modest [^3H]-IP $_x$ accumulation, as the [Ca^{2+}] $_i$ response is completely attenuated by PTX pre-treatment, but the [^3H]-IP $_x$ accumulation was only partly PTX-sensitive (Figure 4.16). Hence, the MCh-induced [Ca^{2+}] $_i$ response in CHO-m2 may not be mediated by either G α_i or G β_γ subunit activation of PLC, or through promiscuous coupling of M $_2$ receptors to activation of G $_q$ proteins. Schmidt et al. (1995) studied Ca $^{2+}$ signalling by M $_2$ and M $_3$ receptors in HEK cells, and demonstrated similar concentration-dependencies to those observed in this study (IP $_x$ EC $_{50}$ s = 20 μM and 2 μM , Ca $^{2+}$ EC $_{50}$ s = 7 μM and 30 nM for HEK-m2 and HEK-m3 cells, respectively), but opposite to the findings in this Chapter their M $_2$ -mediated Ca $^{2+}$ response was only partially PTX-sensitive, while IP $_x$ -accumulation was completely attenuated by PTX pre-treatment. It has been proposed that one pathway in which GPCR, PLC-independent,

signalling to Ca^{2+} responses may be regulated is by the sphingosine kinase / sphingosine 1-phosphate pathway (Meyer et al., 1998; Young et al., 1999). Thus, Meyer et al. blocked agonist-induced $[\text{Ca}^{2+}]_i$ responses in HEK-m2 cells by using sphingosine kinase inhibitors (e.g. N,N-dimethylsphingosine (DMS), or DL-*threo*-dihydrosphingosine (DHS)). Here, studies were also performed using the PLC inhibitor U73122 (10 μM) and its inactive control U73343 (10 μM), to demonstrate the PLC dependence of the observed $[\text{Ca}^{2+}]_i$ response. However, whereas PLC inhibition blocked $[\text{Ca}^{2+}]_i$ responses in all three cell lines, the inactive control also acted as an antagonist right-shifting the MCh-evoked $[\text{Ca}^{2+}]_i$ concentration response curve (data not shown).

FLIPR analysis of time-to-peak maximal MCh-induced $[\text{Ca}^{2+}]_i$ responses differed between CHO-m2 (≈ 15 s) and CHO-m3 (≈ 3 s) cells. However, it is noteworthy that at low (threshold) MCh concentrations (0.1 nM) time-to-peak in CHO-m3 cells is ≈ 15 s, the same as maximal Ca^{2+} responses in CHO-m2. This could be due to M_3 activation of Ca^{2+} at low agonist concentrations acting through a distinct mechanism to that utilised at high agonist concentrations, or the modest Ca^{2+} responses observed with low MCh concentrations ($\approx 10\%$ of maximal Ca^{2+} elevation) in CHO-m3, and maximal MCh concentrations in CHO-m2 cells, being buffered within the cell leading to a slower rate of rise.

Experiments studying Ca^{2+} release under Ca^{2+} -free conditions provided some interesting results. As has been reported previously, M_3 -mediated $[\text{Ca}^{2+}]_i$ increases in normal Ca^{2+} -containing conditions are seen as a peak-and-plateau relationship (SH-SY5Y cells, Lambert and Nahorski, 1990; CHO cells, Tobin et al., 1992). It is assumed that initial Ca^{2+} rise is due to emptying of intracellular stores and then the latter plateau is due to Ca^{2+} influx (Edelman et al., 1994). Removal of extracellular Ca^{2+} abolished the plateau phase of the $[\text{Ca}^{2+}]_i$ response in CHO-m3 and CHO-m2m3 (B2) cells (Figure 4.11 and 4.13). Removal of extracellular Ca^{2+} led to an inhibition of the peak MCh-stimulated $[\text{Ca}^{2+}]_i$ response in CHO-m3 and CHO-m2m3 (B2) cells, but an *augmentation* of response in CHO-m2 cells. This could be brought about because removal of extracellular Ca^{2+} removes an inhibitory mechanism acting on Ca^{2+} release, or because M_2 -mediated Ca^{2+} release is by different mechanisms in Ca^{2+} -containing and Ca^{2+} -free experiments. Removal of extracellular Ca^{2+} completely abolished the modest MCh induced $[\text{H}^3\text{H}]\text{-IP}_x$ accumulation observed in the presence of Ca^{2+} in CHO-m2 cells. Therefore M_2 -mediated Ca^{2+} release under Ca^{2+} -free conditions appears to be PLC-independent and not mediated by generation of IP_3 . However further work is necessary to confirm these observations

were not due to an insensitive IP₃ mass measurement and to elucidate the possible mechanism of this Ca²⁺ release. As speculated for Ca²⁺-containing experiments, MCh-induced [Ca²⁺]_i release in Ca²⁺-free conditions may be through a sphingosine kinase / sphingosine 1-phosphate mechanism. Ca²⁺-free experiments on PTX pre-treated CHO-m2 cells might have revealed if this augmentation is still solely G_i driven and not due to a switch in receptor-coupling to alternative G protein partners.

Ca²⁺-free experiments demonstrated that the plateau phase of the MCh-induced [Ca²⁺]_i release in CHO-m3 and CHO-m2m3 (B2) was mediated by extracellular Ca²⁺ influx. Figures 4.3, 4.4 and 4.5 show how increases in MCh caused a bell-shaped concentration-response relationship for plateau phase [Ca²⁺]_i release in CHO-m3 and CHO-m2m3 (B2) cells, in [Ca²⁺]_e-containing conditions, peaking at agonist concentrations of 10 -100 nM. Carroll and Peralta (1998) also reported an agonist-induced bell-shaped concentration-response in CHO-m3 cells (peaking at 1-10 μM CCh). They showed the influx of Ca²⁺ to be voltage-sensitive and therefore inhibited by membrane depolarisation. M₃ receptors appear to activate inward monovalent cation channels which inhibit the influx of extracellular Ca²⁺ by causing a depolarisation of the cell membrane, thus decreasing the driving force for Ca²⁺ entry, and hence inhibiting the plateau, but not peak, phases of the observed response (see Figure 4.23).

Since there was an agonist-induced [Ca²⁺]_i release in all three cell lines studied it was possible to use the high throughput capabilities of FLIPR equipment to characterise potential pharmacological tools which will become important in subsequent M₂- and M₃- mediated dissection experiments in CHO-m2m3 (B2) cells. Tripitramine, darifenacin and atropine all inhibited MCh-stimulated [Ca²⁺]_i increases in a concentration-dependent manner. However, whereas tripitramine showed good selectivity for M₂ over M₃ receptor-mediated [Ca²⁺]_i increases (≈50 fold, Table 4.3) correlating with published pK_i values (Maggio et al., 1994), darifenacin showed little or no selectivity for the M₃ over M₂-mediated [Ca²⁺]_i increases. Calculated pK_i values (8.48-8.85) for the three cell lines were typical of published M₃ pK_i values (Hedge et al.,1997). This may be contrasted to cAMP accumulation and displacement binding experiments in CHO-m2m3 (B2) cells, reviewed in Chapter 3, where darifenacin showed greater selectivity for M₂ over M₃-mediated responses. These differences in selectivity are presumed to be due to the very different experimental conditions, since in binding studies antagonist displacement equilibrates over a 1 h period and cAMP experiments have a 30 min antagonist

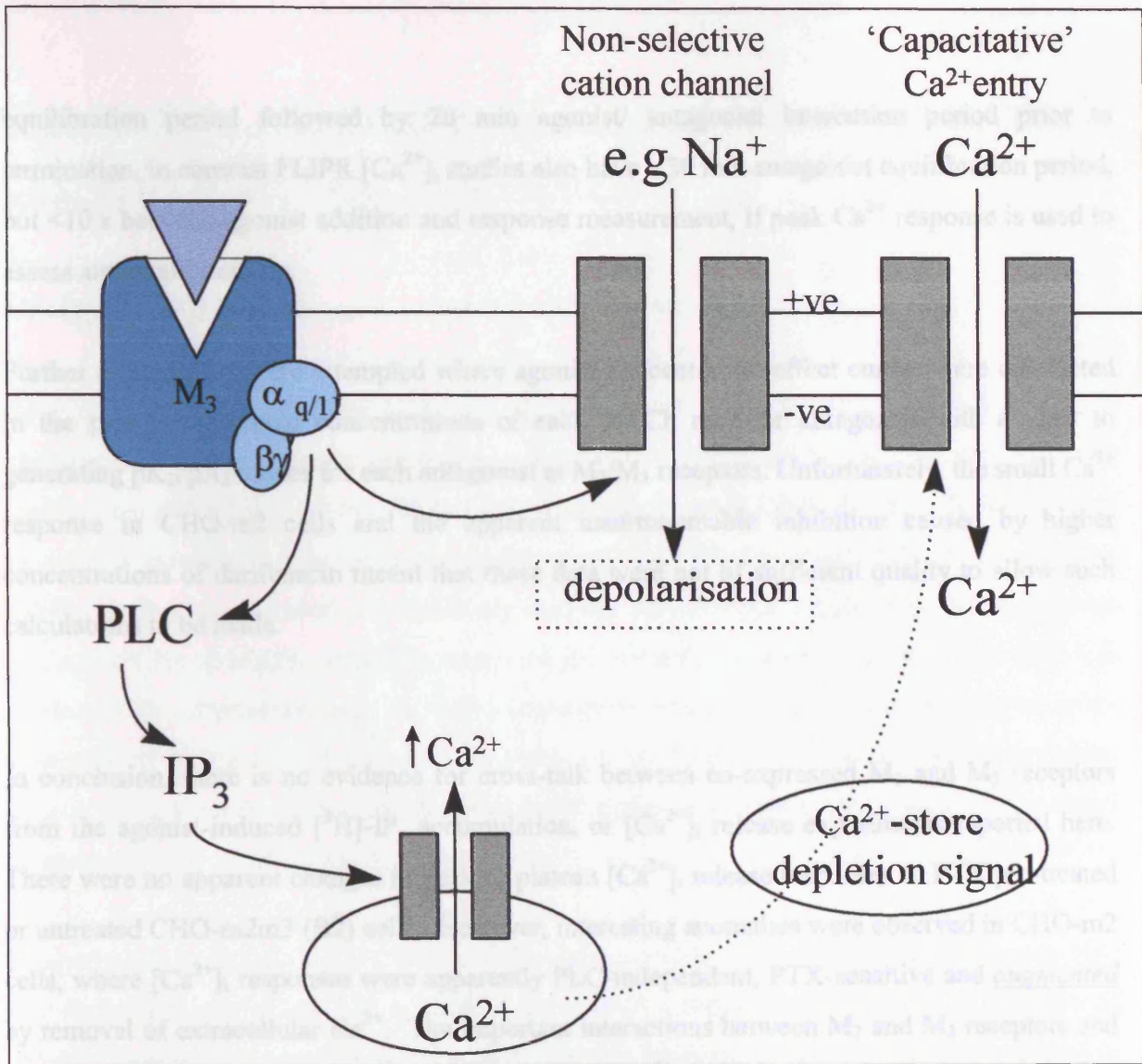


Figure 4.23. A diagram of M_3 -mediated non-selective cation channel inhibition of Ca^{2+} influx via membrane depolarisation as described by Carroll and Peralta (1998).

equilibration period followed by 20 min agonist/ antagonist interaction period prior to termination, in contrast FLIPR $[Ca^{2+}]_i$ studies also have a 30 min antagonist equilibration period, but <10 s between agonist addition and response measurement, if peak Ca^{2+} response is used to assess antagonist activity.

Further experiments were attempted where agonist concentration-effect curves were conducted in the presence of fixed concentrations of each mACh receptor antagonist with a view to generating pK_B/pA_2 values for each antagonist at M_2/M_3 receptors. Unfortunately, the small Ca^{2+} response in CHO-m2 cells and the apparent insurmountable inhibition caused by higher concentrations of darifenacin meant that these data were not of sufficient quality to allow such calculations to be made.

In conclusion, there is no evidence for cross-talk between co-expressed M_2 and M_3 receptors from the agonist-induced $[^3H]$ -IP_x accumulation, or $[Ca^{2+}]_i$ release experiments reported here. There were no apparent changes in peak or plateau $[Ca^{2+}]_i$ release responses in PTX pre-treated or untreated CHO-m2m3 (B2) cells. However, interesting anomalies were observed in CHO-m2 cells, where $[Ca^{2+}]_i$ responses were apparently PLC-independent, PTX-sensitive and *augmented* by removal of extracellular Ca^{2+} . The important interactions between M_2 and M_3 receptors and the fact that they both couple to pathways activating $[Ca^{2+}]_i$ release is highlighted by Kotlikoff et al. (1999) as M_2 stimulation results in the gating of non-selective cation channels in smooth muscle, and is mediated by M_3 receptor-driven $[Ca^{2+}]_i$ release. Subsequent interactions between M_2 - and M_3 -mediated Ca^{2+} mobilisation may prove to be important in numerous diverse cellular processes including smooth muscle contraction and cell growth. Ca^{2+} mobilisation has also been deemed important in expression of certain transcription factors during the G1 phase of the cell cycle (Cook et al., 1999), and hence in cell growth.

Chapter Five: Comparison of [³H]-thymidine incorporation in CHO-m2, CHO-m3 and CHO-m2m3 cells

5.1 Introduction

Since the late 1980s there has been evidence linking the stimulation of GPCRs not only to traditional second messenger production but also to nuclear events and effects upon cell proliferation and differentiation. With the discovery in the early 1990s that MAPK activation is an essential component in proliferative signalling pathways (Pagès et al., 1993) GPCR activation of MAPKs has become even more intensely studied. However, the signal transduction pathway linking GPCRs to MAPK activation or to cell growth are still not fully defined (see Gutkind, 1998a, 1998b; Dhanasekaran et al., 1998; Gudermann et al., 2000). Such reviews cover many examples of GPCRs activating MAPK pathways via both PTX-sensitive and -insensitive heterotrimeric G proteins in a variety of cell backgrounds, which have now been shown to signal to changes in cell proliferation in certain cases.

The pathways leading from GPCRs to cell growth are not fully defined, however by measuring [³H]-thymidine incorporation as an indication of DNA synthesis, and therefore an indicator of cell proliferation, it is possible to observe differences between M₂ and M₃ receptor potential to cause cell proliferation. Thus, the same experiments measuring [³H]-thymidine incorporation in co-expressing CHO-m2m3 cells have been used as an end-point assay to discover possible evidence for interactions or cross-talk between these two receptors when they are co-expressed.

Following publications from this department showing MAPK activation, including ERK activation by M₃ receptors in CHO cells (Wylie et al., 1999, and Budd et al., 1999), it was interesting to see if stimulation of either M₂ or M₃ receptors caused a change in rates of DNA synthesis. While both receptors have been shown to have similar ERK activation profiles when expressed in CHO cells, there is a marked difference in coupling to JNK activation as only M₃ receptors appear to activate this pathway (Wylie et al., 1999). It will be interesting therefore to compare and correlate the known MAPK activation profiles with changes in cell growth. As reviewed by Marshall (1995) it is the duration as well as the magnitude of the MAPK activation which is probably critical to cell signalling decisions.

There has also been a putative link between PI hydrolysis and DNA synthesis (Ashkenazi et al., 1989, Gutkind et al., 1991) which may discriminate between the agonist-stimulated [³H]-thymidine incorporation levels between these cell lines, since traditionally M₃ muscarinic receptors efficiently couple to PLC activation and M₂ inhibit adenylyl cyclase activity. However M₂ receptors are G_{α_i}-coupled and PLC has been shown to be activated by G_{βγ} subunits of pertussis toxin-sensitive or -insensitive G proteins (Blank et al., 1992; Camps et al., 1992) so M₂ receptors have been proposed to activate PLCβ through βγ subunits. However, as reported in Chapter 3, M₂ receptors in the CHO model cells utilised here did not appear to activate PLC as measured by IP₃ mass accumulation or total inositol phosphate accumulation.

Interestingly, a recent report by Nicke et al. (1999), using [³H]-thymidine incorporation methodology, found that DNA synthesis following stimulation of M₃ receptors with carbachol, in NIH3T3 cells, was influenced by the initial cell cycle state of the cells. Thus, carbachol caused an increase in [³H]-thymidine incorporation in serum-starved cells, but a decrease in serum-replete cells. Therefore the initial experiments described in this Chapter are performed after serum-starvation for 24 h prior to agonist challenge in order for the cells to initially all be at a similar stage of the cell cycle (i.e. quiescent, G₀). This was followed by serum-replete experiments to see if the same phenomenon as reported by Nicke et al. (1999), of opposite effects depending on whether the cells are initially in a growing phase or quiescent, was also observable in CHO cells.

5.2 Methods

Serum-starved and serum replete [³H]-thymidine incorporation methods were performed as detailed in Chapter 2 (see Figure 5.1 for a simple diagram of the method), with antagonists (darifenacin and atropine) added 30 min prior to agonist / vehicle addition (therefore 24 ½ h preceding termination of experiment). CHO-m2m3 (B2) cells were plated and initially cultured (first 24 h, while plating down) in routine medium (MEM α + NBCS, fungizone and pen /strep see Chapter 2.1) containing selection agent hygromycin B (400 µg. ml⁻¹). After 24 h, this medium was replaced with either serum-free or serum-containing medium without hygromycin B.

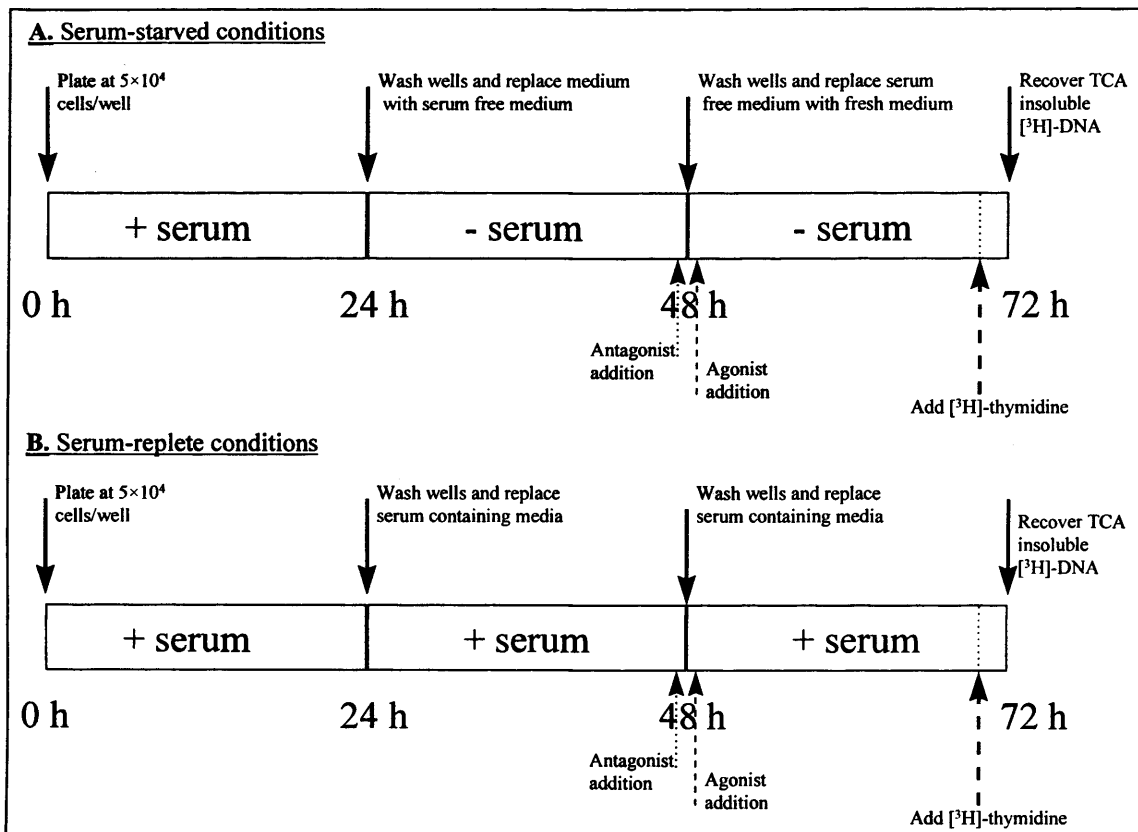


Figure 5.1. Time-bar diagram illustration of the method for $[^3\text{H}]\text{-thymidine}$ incorporation for either serum-starved or serum-replete conditions. For full method see Chapter 2.

5.3 Results

5.3.1 Effects of serum on [³H]-thymidine incorporation into DNA in serum-starved CHO-m2, CHO-m3 and CHO-m2m3 cells

As described, in Methods (Chapter 2) and above in 5.2, cells were serum-starved for 24 h prior to agonist addition, with [³H]-thymidine (2 μ Ci / well) being added for the final 2 h of the subsequent 24 h period with agonist (see Figure 5.1). 10 % foetal calf serum (FCS) was used as a positive control for the cell lines studied. As shown in Figure 5.2 (panel B), all cell lines showed increases in [³H]-thymidine incorporation following stimulation with 10% FCS for 24 h, giving 1.83 ± 0.27 (n=8 in triplicate), 4.06 ± 0.49 (n=6 in triplicate), 4.93 ± 0.90 (n=12 in triplicate) and 3.07 (n=2 in triplicate, data not shown) fold over basal for CHO-m2, CHO-m3, CHO-m2m3 (B2) and CHO-m2m3 (B7) cells, respectively. However, as is also shown in Figure 5.2, panel A, the basal level of [³H]-thymidine incorporation for CHO-m2 cells was approximately twice that of CHO-m3 or CHO-m2m3 (B2) cells, 89206 ± 20942 d.p.m. compared to 48581 ± 12457 d.p.m. and 45185 ± 12397 d.p.m. respectively. This perhaps indicates that CHO-m2 cells are less easy to serum-starve and therefore are not as quiescent following 48 h serum-free incubation. Note that total [³H]-thymidine incorporation following 24 h 10% FCS treatment was similar in the three cell lines, 171553 ± 31368 d.p.m, 187101 ± 40748 d.p.m and 168414 ± 36659 d.p.m. for CHO-m2, CHO-m3 and CHO-m2m3 (B2) respectively. Thus, the higher basal incorporation in CHO-m2 cells accounted for the low fold over basal effect observed.

5.3.2 Effects of mACh receptor agonists on [³H]-thymidine incorporation in serum-starved CHO-m2, CHO-m3 and CHO-m2m3 cells

The observed [³H]-thymidine incorporation was differentially modulated following 24 h agonist treatment in the three cell-lines studied under serum-starved conditions. Both MCh (1 mM) and CCh (1 mM) evoked an increase in [³H]-thymidine incorporation in CHO-m2 cells of 1.52 ± 0.09 and 1.57 ± 0.05 fold over basal, respectively, from a basal level of 89206 ± 20942 d.p.m. This compared with an increase of 2.42 ± 0.64 fold over basal stimulated by 10% FCS, (see Figure 5.3, panel A). Despite the modest stimulatory effect of MCh on [³H]-thymidine

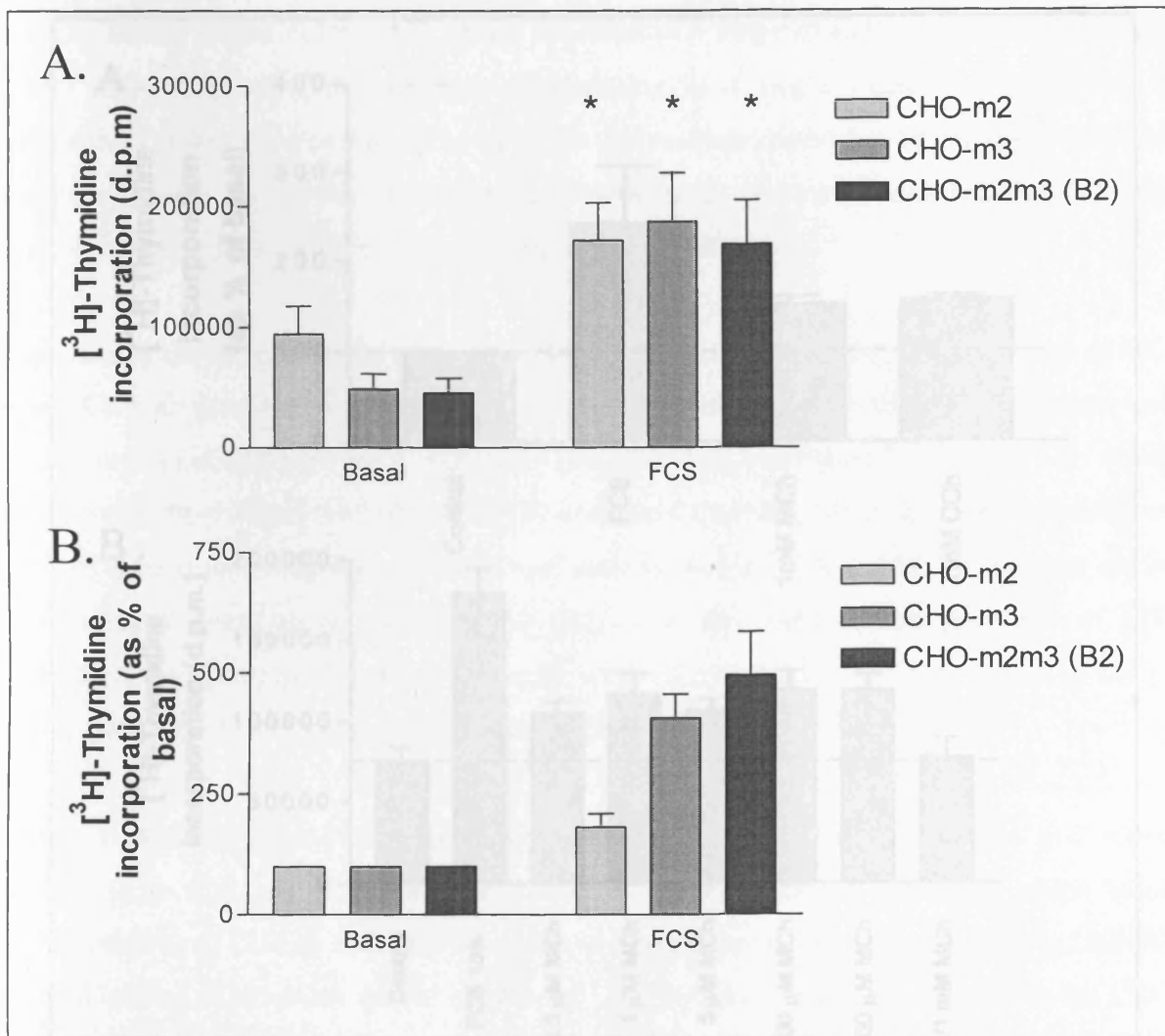


Figure 5.2. A comparison of basal and FCS (10%) stimulated [³H]-thymidine incorporation in CHO-m2, CHO-m3 and CHO-m2m3 (B2) cells. Panel A shows 10% FCS-stimulated [³H]-thymidine incorporation as d.p.m. and panel B plots the same data as % of basal. Data are shown as means ± S.E.M. of at least six separate experiments performed in triplicate. For each cell line FCS (10%) stimulated a significant increase in [³H]-thymidine incorporation (* P<0.01, Student's unpaired *t*-test).

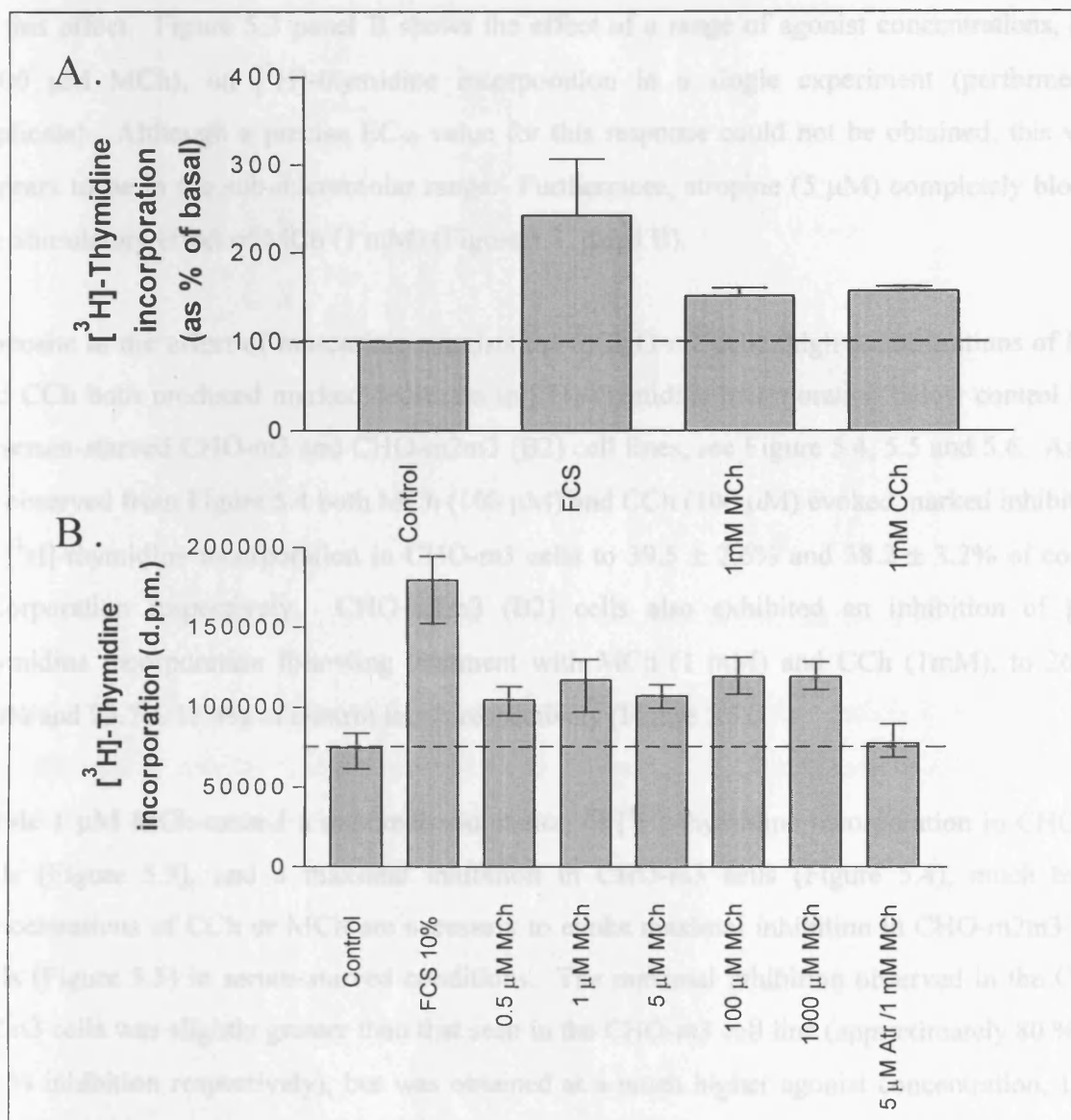


Figure 5.3. Stimulation of [³H]-thymidine incorporation into serum-starved CHO-m2 cells following 24 h stimulation with the muscarinic agonists MCh or CCh (at stated concentrations) and FCS (10%). In panel A data are plotted as means ± S.E.M. % for n=3-5 performed in triplicate. Panel B shows concentration-dependence of this response and data are plotted as means ± range for one experiment performed in triplicate.

incorporation in CHO-m2 cells, an attempt was made to explore the concentration-dependence of this effect. Figure 5.3 panel B shows the effect of a range of agonist concentrations, (0.5-1000 μ M MCh), on [3 H]-thymidine incorporation in a single experiment (performed in triplicate). Although a precise EC₅₀ value for this response could not be obtained, this value appears to be in the sub-micromolar range. Furthermore, atropine (5 μ M) completely blocked the stimulatory effect of MCh (1 mM) (Figure 5.3, panel B).

Opposite to the effect of muscarinic agonists upon CHO-m2 cells, high concentrations of MCh and CCh both produced marked decreases in [3 H]-thymidine incorporation below control level in serum-starved CHO-m3 and CHO-m2m3 (B2) cell lines, see Figure 5.4, 5.5 and 5.6. As can be observed from Figure 5.4 both MCh (100 μ M) and CCh (100 μ M) evoked marked inhibitions of [3 H]-thymidine incorporation in CHO-m3 cells to $39.5 \pm 2.6\%$ and $38.2 \pm 3.2\%$ of control incorporation respectively. CHO-m2m3 (B2) cells also exhibited an inhibition of [3 H]-thymidine incorporation following treatment with MCh (1 mM) and CCh (1mM), to $26.2 \pm 5.0\%$ and $23.7 \pm 13.4\%$ of control levels respectively (Figure 5.5).

While 1 μ M MCh caused a maximal stimulation of [3 H]-thymidine incorporation in CHO-m2 cells (Figure 5.3), and a maximal inhibition in CHO-m3 cells (Figure 5.4), much higher concentrations of CCh or MCh are necessary to evoke maximal inhibition in CHO-m2m3 (B2) cells (Figure 5.5) in serum-starved conditions. The maximal inhibition observed in the CHO-m2m3 cells was slightly greater than that seen in the CHO-m3 cell line (approximately 80 % and 60 % inhibition respectively), but was obtained at a much higher agonist concentration, 1 μ M compared to 1 mM for CHO-m3 and CHO-m2m3 (B2) respectively (Figures 5.4 and 5.5). This difference in concentration-dependency of inhibition in the CHO-m3 and CHO-m2m3 (B2) could be predicted, since CHO-m2m3 (B2) cells would be expected to demonstrate characteristics of both M₂ and M₃ receptors and therefore the resulting signal is a balance between both stimulatory and inhibitory effects. As observed for other responses measured in this project (e.g cAMP, Ca²⁺, IP₃ or JNK see Chapters 3, 4 and 6) the co-expressing CHO-m2m3 (B2) cells 'mask' the M₂ signal component and appear to display many of the characteristics of a CHO-m3 cell line. However a greater maximal inhibition in CHO-m2m3 (B2) would not have been predicted as the M₂ receptor component stimulates DNA synthesis, although this effect is modest.

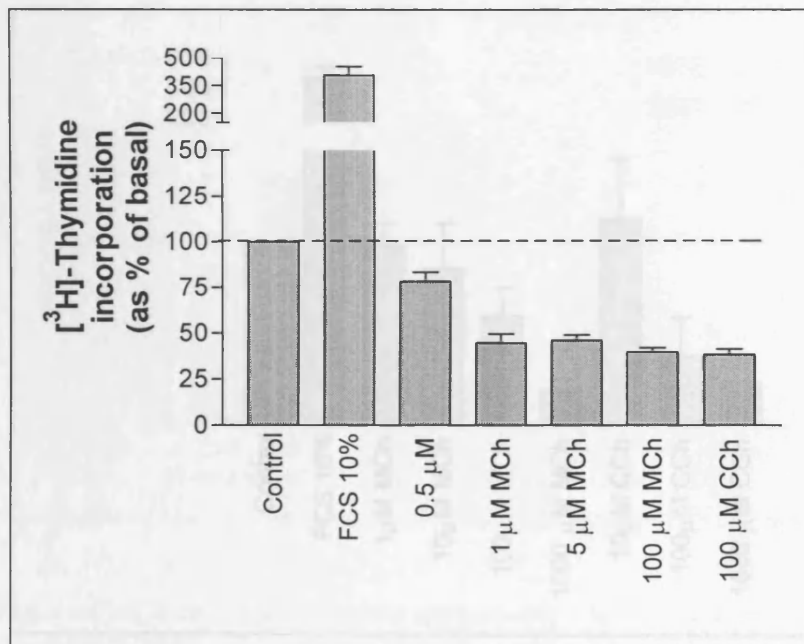


Figure 5.4. Effects of 10% FCS and MCh and CCh (at stated concentrations) upon [³H]-thymidine incorporation in serum-starved CHO-m3 cells. Data are shown as means ± S.E.M. for at least three separate experiments performed in triplicate.

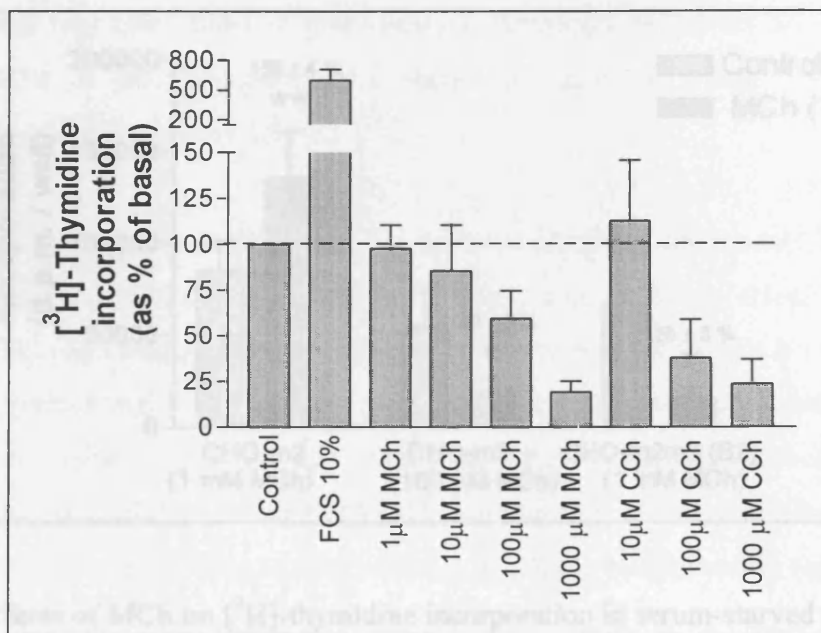


Figure 5.5. Effects of MCh on [³H]-thymidine incorporation in serum-starved CHO-m2, CHO-m3 and CHO-m2m3 (B2) cells. * indicates MCh treatment is statistically different from control.

Figure 5.5 Effects of 10% FCS and MCh and CCh (at stated concentrations) upon [³H]-thymidine incorporation in serum-starved CHO-m2m3 (B2) cells. Data are shown as means ± S.E.M. for at least three separate experiments performed in triplicate.

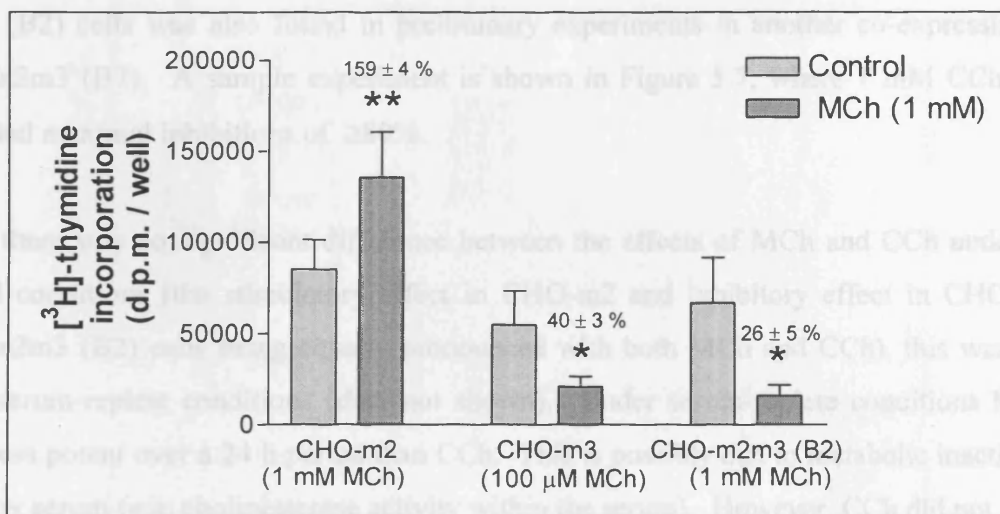


Figure 5.6. Effects of MCh on [³H]-thymidine incorporation in serum-starved CHO-m2, CHO-m3 and CHO-m2m3 (B2) cells. * indicates MCh treatment is statistically different from control, P < 0.05 Student's *t*-test, paired observations, ** indicates P < 0.001.

Nicho *et al.* (1997) showed, through measuring [³H]-thymidine incorporation, that CCh acting at M₁ receptors, expressed in NIH3T3 cells, could cause an increase or decrease in cell proliferation. They demonstrated that CCh could concentration-dependently evoke either a stimulatory or inhibitory effect on [³H]-thymidine incorporation depending on the initial growth state of the cells. In quiescent cells (serum-starved) CCh elicited a stimulatory response, and in growing cells (serum-replete) CCh caused an inhibition of cell growth.

Following this report [³H]-thymidine incorporation in serum-replete cells was ascertained in CHO-m2, CHO-m3 and CHO-m2m3 cells. Full concentration-effect curves were constructed for the three main cell lines being studied (Figures 5.8, 5.9 and 5.10).

Chapter 2 and Section 5.2 describe the protocol for serum-replete experiments. In these experiments control cells were incubated in serum-containing medium throughout the protocol and therefore had an extra 48 h further growing time compared with serum-starved cells. This was reflected in the basal incorporated [³H]-thymidine levels, which were 2.3, 15.2 and 16.7 fold greater in CHO-m2, CHO-m3 and CHO-m2m3 (B2) cell lines in serum-replete conditions.

The observation of agonist-induced inhibition of [³H]-thymidine incorporation in the CHO-m2m3 (B2) cells was also found in preliminary experiments in another co-expressing clone, CHO-m2m3 (B7). A sample experiment is shown in Figure 5.7, where 1 mM CCh or MCh generated maximal inhibitions of ≥80%.

While there was no significant difference between the effects of MCh and CCh under serum-starved conditions (the stimulatory effect in CHO-m2 and inhibitory effect in CHO-m3 and CHO-m2m3 (B2) cells being equally pronounced with both MCh and CCh), this was not true under serum-replete conditions (data not shown). Under serum-replete conditions MCh was much less potent over a 24 h period than CCh. This is possibly due to metabolic inactivation of MCh, by serum (e.g. cholinesterase activity within the serum). However, CCh did not appear to be affected, for this reason CCh was used as the mAChR agonist for serum-replete experiments (see below).

5.3.3 Agonist effects on [³H]-thymidine incorporation in serum-replete CHO-m2, CHO-m3 and CHO-m2m3 cells

Nicke *et al.* (1999) showed, through measuring [³H]-thymidine incorporation, that CCh acting at M₃ receptors, expressed in NIH3T3 cells, could cause an increase or decrease in cell proliferation. They demonstrated that CCh could concentration-dependently evoke either a stimulatory or inhibitory effect on [³H]-thymidine incorporation depending on the initial growth state of the cells. In quiescent cells (serum-starved) CCh elicited a stimulatory response, and in growing cells (serum-replete) CCh caused an inhibition of cell growth.

Following this report [³H]-thymidine incorporation in serum-replete cells was ascertained in CHO-m2, CHO-m3 and CHO-m2m3 cells. Full concentration-effect curves were constructed for the three main cell lines being studied (Figures 5.8, 5.9 and 5.10).

Chapter 2 and Section 5.2 describe the protocol for serum-replete experiments. In these experiments control cells were incubated in serum-containing medium throughout the protocol and therefore had an extra 48 h further growing time compared with serum-starved cells. This was reflected in the basal incorporated [³H]-thymidine levels, which were 7.5, 15.2 and 16.7 fold greater in CHO-m2, CHO-m3 and CHO-m2m3 (B2) cell lines in serum-replete conditions

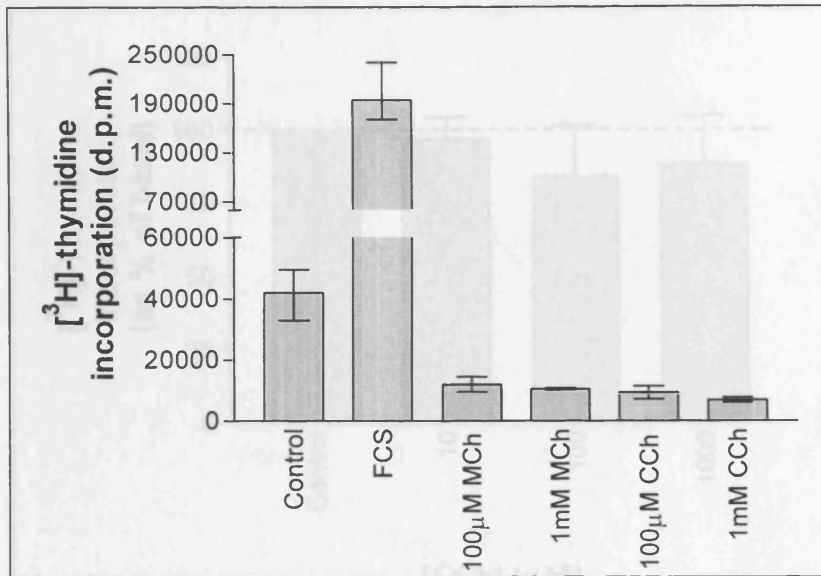


Figure 5.7. Effects of 10% FCS and MCh and CCh (at stated concentrations) upon [³H]-thymidine incorporation in serum-starved CHO-m2m3 (B7) cells. The plot is an example experiment, data are shown as means \pm range for one experiment performed in triplicate. means \pm S.E.M. of three separate experiments performed in triplicate.

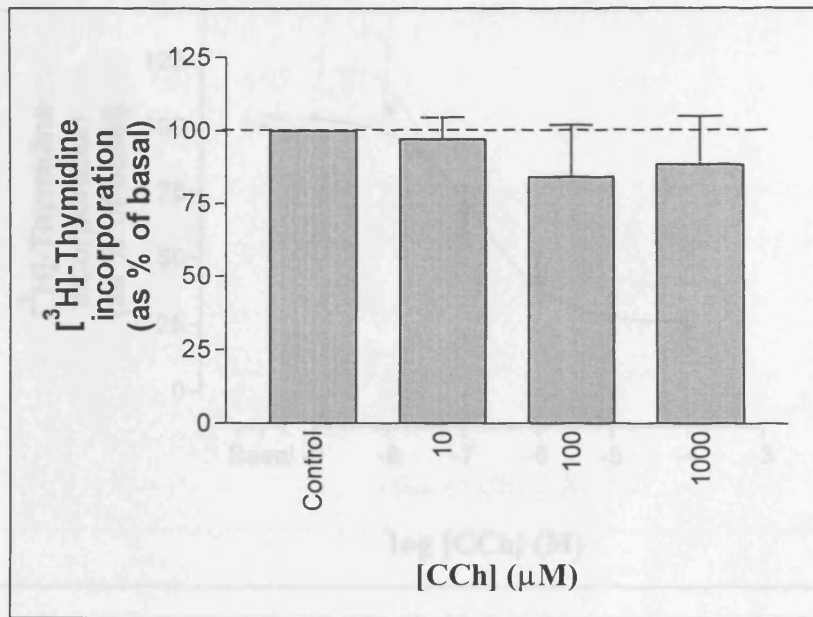


Figure 5.8. Concentration-effect bar graph showing the effect of increasing CCh concentrations upon [^3H]-thymidine incorporation in serum-replete CHO-m2 cells. Data are presented as means \pm S.E.M. of three separate experiments performed in triplicate.

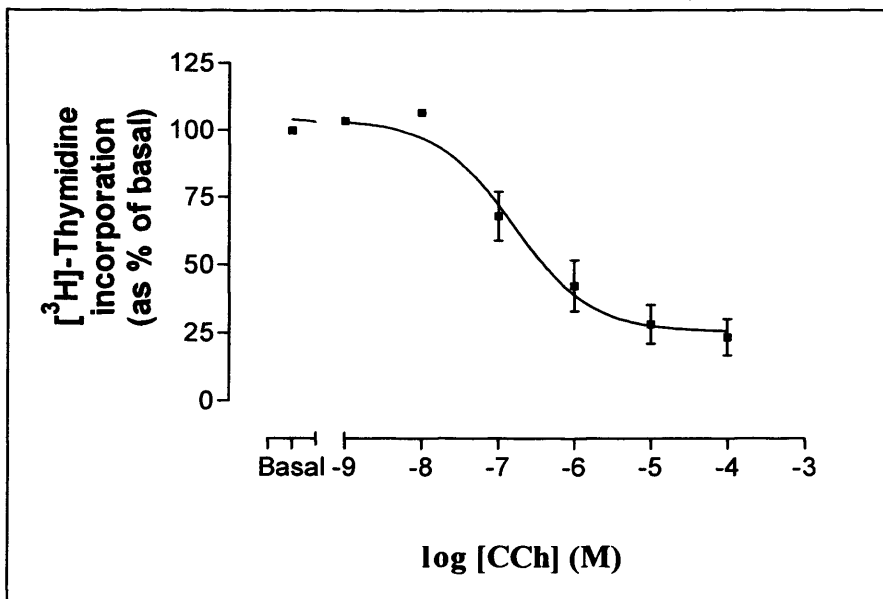


Figure 5.9. Concentration-effect graph showing the effect of increasing CCh concentrations upon $[^3\text{H}]\text{-thymidine}$ incorporation in serum-replete CHO-m3 cells. Data are presented as means \pm S.E.M. of three separate experiments performed in triplicate.

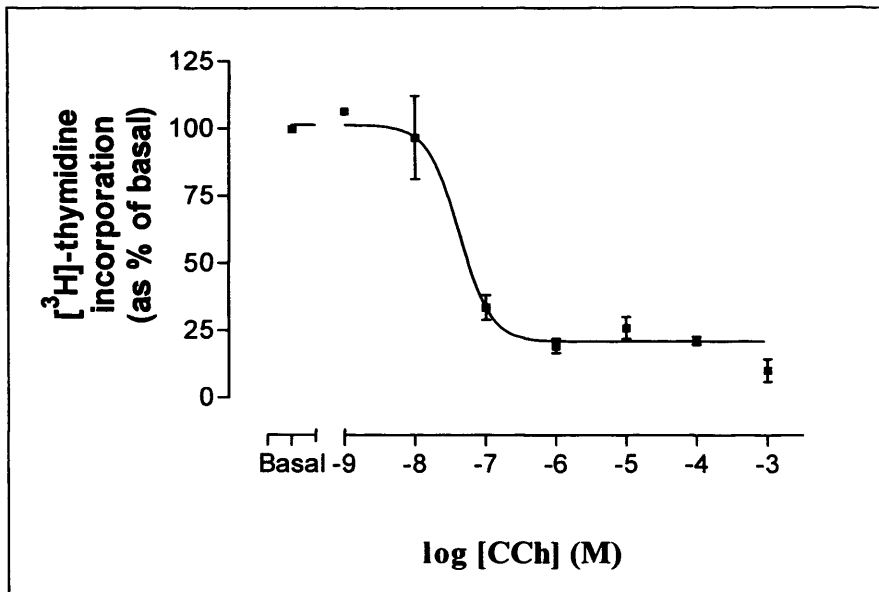


Figure 5.10. Concentration-effect graph showing the effect of increasing CCh concentration upon $[^3\text{H}]$ -thymidine incorporation in serum-replete CHO-m2m3 (B2) cells. Data are presented as means \pm S.E.M. of three separate experiments performed in triplicate.

compared to serum-starved conditions. The basal incorporation in all three serum-replete cell lines, of 666430 ± 274474 , 706526 ± 204136 and 756771 ± 191353 (CHO-m2, CHO-m3 and CHO-m2m3 (B2) respectively) was similar.

Figure 5.3 above showed that in CHO-m2 cells under serum-starved conditions, there is an agonist-induced increase above basal in [^3H]-thymidine incorporation. However, as can be observed in Figure 5.8 under serum-replete conditions CCh (100 μM) produced no apparent difference from basal in [^3H]-thymidine incorporation in CHO-m2 cells. Thus, the observed stimulation in DNA synthesis in CHO-m2 cells under serum-starved conditions was lost in the presence of serum.

The effect of agonist treatment on [^3H]-thymidine incorporation in CHO-m2 cells was very different to that observed in both CHO-m3 and CHO-m2m3 (B2) cells under serum-starved conditions. Whereas there was no effect of agonist in CHO-m2 cells under serum-containing conditions, as for serum-starved conditions, CHO-m3 and CHO-m2m3 (B2) cells showed marked inhibitions of [^3H]-thymidine incorporation upon agonist treatment ($P < 0.05$ Student's *t*-test, paired observations, see Figures 5.8-5.11).

Figure 5.9 shows in CHO-m3 cells under serum-replete conditions inhibition of basal [^3H]-thymidine incorporation with maximal inhibition to $15.6 \pm 6.7\%$ of control was obtained with 100 μM ($-\log \text{IC}_{50}$, 6.8 ± 0.2). Similar to the CHO-m3 cells, the serum-replete CHO-m2m3 (B2) cells showed a marked concentration-dependent inhibition of [^3H]-thymidine incorporation (Figure 5.10) upon 24 h treatment with CCh. Inhibition of basal was observed at CCh concentrations above 10 nM and maximal inhibition to $19.4 \pm 2.6\%$ of control incorporated levels was observed with 1 μM CCh ($-\log \text{IC}_{50}$, 7.4 ± 0.1). It is noteworthy that the CCh concentration-effect curve for serum-replete CHO-m2m3 (B2) cells is steeper than that for CHO-m3 cells, and the IC_{50} value is lower. Directly contrasting to the effects observed in serum-starved conditions, serum-replete CHO-m2m3 (B2) cells appear to require lower agonist concentrations than CHO-m3 to cause maximal inhibitory effects.

Thus, for both serum-starved and serum-replete conditions, agonist produced a decrease in [^3H]-thymidine incorporation in both CHO-m3 and CHO-m2m3 cells. However a modest agonist-

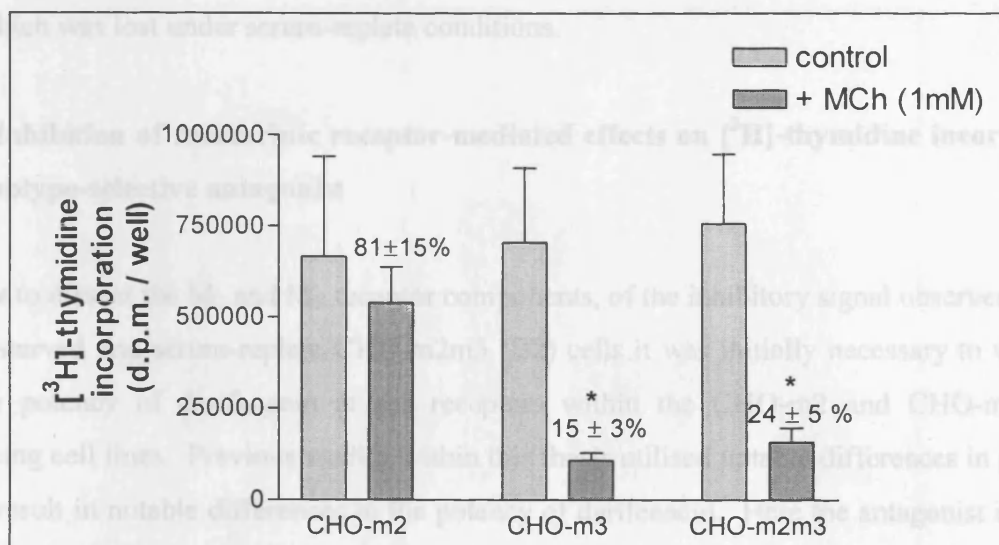


Figure 5.11 Effects of MCh (1 mM) on [³H]-thymidine incorporation in serum-replete CHO-m2, CHO-m3 and CHO-m2m3 (B2) cells. * indicates MCh treatment is statistically different from control, $P < 0.05$ Student's *t*-test, paired observations.

As expected from radioligand binding and cAMP characterization studies using darifenacin (see Figures 3.5 and 3.11) 300 nM was a sufficient concentration to block the 10 μ M CCh inhibitory signal observed in CHO-m3 cells, as seen in the preliminary [³H]-thymidine incorporation experiment represented in Figure 5.13. 10 μ M CCh caused a 28% inhibition which is blocked by 300 nM darifenacin in CHO-m3 cells.

Therefore experiments using 300 nM darifenacin prior to CCh (10 μ M) stimulation under serum-starved conditions in CHO-m2m3 (B2) co-expressing cells would be predicted to block the M_2 component, but not affect the M_3 -mediated component.

As discussed for the experiments above 10 μ M CCh causes a greater inhibition in serum-replete CHO-m3 cells compared with that seen under serum-starved conditions, (67.5 \pm 3.5 % compared to 28 % respectively), as would be expected with the cells in a growing phase. Therefore, it is interesting to note that a higher darifenacin concentration (1000 nM) was required to block entirely the inhibitory effect 10 μ M CCh on [³H]-thymidine incorporation in

induced stimulation of [³H]-thymidine incorporation was observed in serum-starved CHO-m2 cells which was lost under serum-replete conditions.

5.3.4 Inhibition of muscarinic receptor-mediated effects on [³H]-thymidine incorporation by a subtype-selective antagonist

In order to dissect the M₂ and M₃ receptor components, of the inhibitory signal observed, in both serum-starved and serum-replete CHO-m2m3 (B2) cells it was initially necessary to verify the relative potency of darifenacin at the receptors within the CHO-m2 and CHO-m3 single expressing cell lines. Previous studies within this thesis utilised notable differences in protocols which result in notable differences in the potency of darifenacin. Here the antagonist is present in the well for 24.5 h and the cells are exposed to agonist for 24 h and darifenacin may be affected by serum though this chronic exposure. In serum-starved CHO-m2 cells, as can be seen in Figure 5.12, 10 μM CCh caused a doubling of [³H]-thymidine incorporation from a mean basal level of 19158 d.p.m. to 41795 d.p.m., compared to a four fold increase caused by 10% FCS. Under these serum-starved conditions concentrations of darifenacin above 300 nM were required to antagonise this stimulation, 300 nM caused approximately a 50 % inhibition.

As expected from radioligand binding and cAMP characterisation studies using darifenacin (see Figures 3.5 and 3.11) 300 nM was a sufficient concentration to block the 10 μM CCh inhibitory signal observed in CHO-m3 cells, as seen in the preliminary [³H]-thymidine incorporation experiment represented in Figure 5.13. 10 μM CCh caused a 28% inhibition which is blocked by 300 nM darifenacin in CHO-m3 cells.

Therefore experiments using 300 nM darifenacin prior to CCh (10 μM) stimulation under serum-starved conditions in CHO-m2m3 (B2) co-expressing cells would be predicted to block the M₃-component, but not affect the M₂-mediated component.

As discussed for the experiments above 10 μM CCh causes a greater inhibition in serum-replete CHO-m3 cells compared with that seen under serum-starved conditions, (67.5 ± 3.5 % compared to 28 % respectively), as would be expected with the cells in a growing phase. Therefore, it is interesting to note that a higher darifenacin concentration (1000 nM) was required to block entirely the inhibitory effect 10 μM CCh on [³H]-thymidine incorporation in

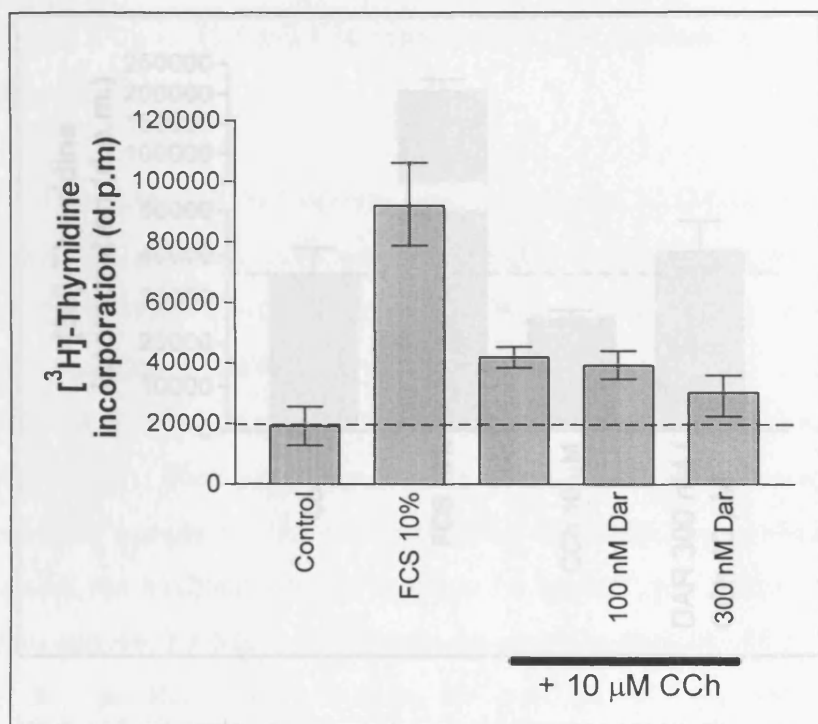


Figure 5.13. Antagonism of CCh (10 μ M) induced inhibition of [³H]-thymidine incorporation

Figure 5.12. A graph of a representative experiment where darifenacin (at stated concentrations) was used to antagonise the CCh (10 μ M) induced stimulation of [³H]-thymidine incorporation in serum-starved CHO-m2 cells. Darifenacin was added to wells 30 min prior to addition of CCh (10 μ M). Data are shown as means \pm range for one experiment performed in triplicate.

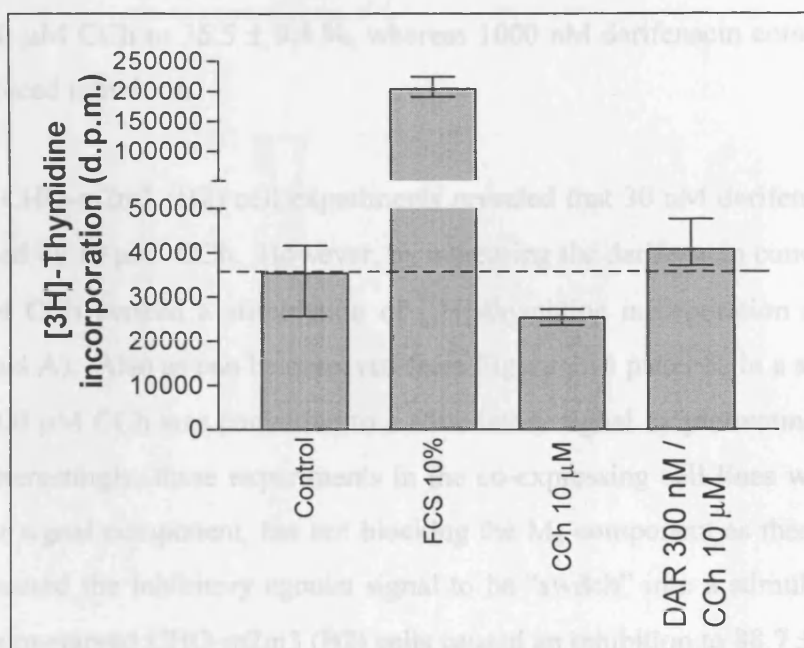


Figure 5.13. Antagonism of CCh (10 µM) induced inhibition of [³H]-thymidine incorporation by darifenacin (300 nM) in serum-starved CHO-m3 cells. Darifenacin was added 30 min prior to addition of CCh (10 µM). Data are presented as means ± range for one experiment performed in triplicate.

Experiments with CHO-m2m3 (B2) cells in serum-replete conditions revealed a difference compared to serum-starved cells in which lower concentrations of CCh are needed to cause 50% inhibition (see Figures 5.5 and 5.10 above, pIC₅₀ values of 7.5 and 7.4 for serum-starved and serum-replete, respectively) (much greater darifenacin concentrations were needed to block the inhibitory signal, since 10 µM CCh had a greater inhibitory effect) (Figure 5.16). In comparison to serum-starved CHO-m2m3 (B2) cells, where inhibition caused by 10 µM CCh was blocked by 10 nM darifenacin, serum-replete cells required 1000 nM antagonist to cause complete block of this inhibition (Figures 5.15 and 5.16). As was observed for serum-replete CHO-m2 cells, since the M₂ signal component of the mixed population of mAChRs in the serum-replete CHO-m2m3 (B2) cells is unmasked, by darifenacin (1000 nM) blocking the M₁ component, there is no modulation of [³H]-thymidine incorporation above control levels.

serum-replete CHO-m3 cells (see Figure 5.14). Darifenacin at 300 nM only blocks the 67.5 % inhibition by 10 μ M CCh to 35.5 ± 9.4 %, whereas 1000 nM darifenacin completely abolishes this agonist-induced inhibition.

Serum-starved CHO-m2m3 (B2) cell experiments revealed that 30 nM darifenacin could block inhibition evoked by 10 μ M CCh. However, by increasing the darifenacin concentration (above 30 nM) 10 μ M CCh evoked a stimulation of [3 H]-thymidine incorporation above basal (see Figure 5.15 panel A). Also as can be observed from Figure 5.15 panel B, in a single experiment inhibition by 100 μ M CCh was converted to a stimulatory signal by pretreatment with 300 nM darifenacin. Interestingly, these experiments in the co-expressing cell lines were antagonising the M_3 receptor signal component, but not blocking the M_2 component as these concentrations of antagonist caused the inhibitory agonist signal to be “switch” into a stimulatory signal. 10 μ M CCh in serum-starved CHO-m2m3 (B2) cells caused an inhibition to 88.7 ± 15.7 % of basal [3 H]-thymidine incorporation levels, but in the presence of 300 nM darifenacin this concentration of CCh caused a 1.45 ± 0.39 fold increase above basal. Figure 5.15 panel A shows that concentrations of darifenacin above 300 nM then begin to block the stimulatory M_2 -component of the signal in serum-starved CHO-m2m3 (B2) cells (as was observed for CHO-m2 cells, see Figure 5.12).

Experiments with CHO-m2m3 (B2) cells in serum-replete conditions revealed a difference compared to serum-starved cells as while lower concentrations of CCh are needed to cause 50 % inhibition (see Figures 5.5 and 5.10 above, pIC_{50} values of >5 and 7.4 for serum-starved and serum-replete, respectively) much greater darifenacin concentrations were needed to block the inhibitory signal, since 10 μ M CCh had a greater inhibitory effect (Figure 5.16). In comparison to serum-starved CHO-m2m3 (B2) cells, where inhibition caused by 10 μ M CCh was blocked by 30 nM darifenacin, serum-replete cells required 1000 nM antagonist to cause complete block of this inhibition (Figures 5.15 and 5.16). As was observed for serum-replete CHO-m2 cells, once the M_2 signal component of the mixed population of mAChRs in the serum-replete CHO-m2m3 (B2) cells is unmasked, by darifenacin (1000 nM) blocking the M_3 component, there is no stimulation of [3 H]-thymidine incorporation above control levels.

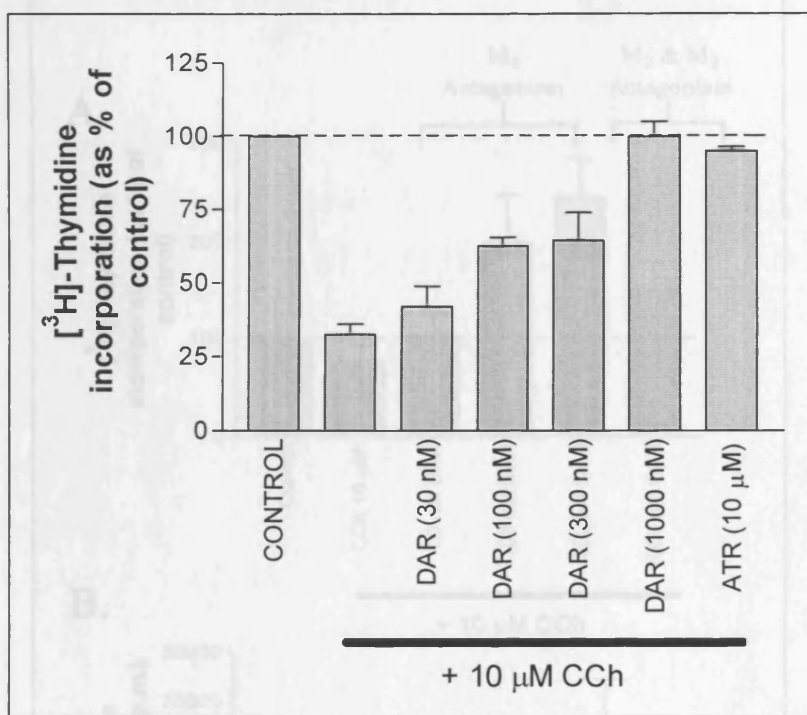


Figure 5.14. Antagonism of CCh (10 μM) induced inhibition of [³H]-thymidine incorporation by darifenacin (stated concentrations) in serum-replete CHO-m3 cells. Darifenacin was added to wells 30 min prior to CCh (10 μM) addition. Data are presented as means ± S.E.M. for three separate experiments performed in triplicate.

Figure 5.15. Antagonism of CCh-induced inhibition of [³H]-thymidine incorporation by darifenacin (stated concentrations) in serum-starved CHO-m3(m2) (B2) cells. Panel A shows darifenacin blocking inhibition by 10 μM CCh and panel B shows 300 nM darifenacin blocking inhibition by 100 μM CCh in one representative experiment. In panel A data are presented as mean ± S.E.M. for four separate experiments performed in triplicate, panel B is means ± range for one experiment performed in triplicate.

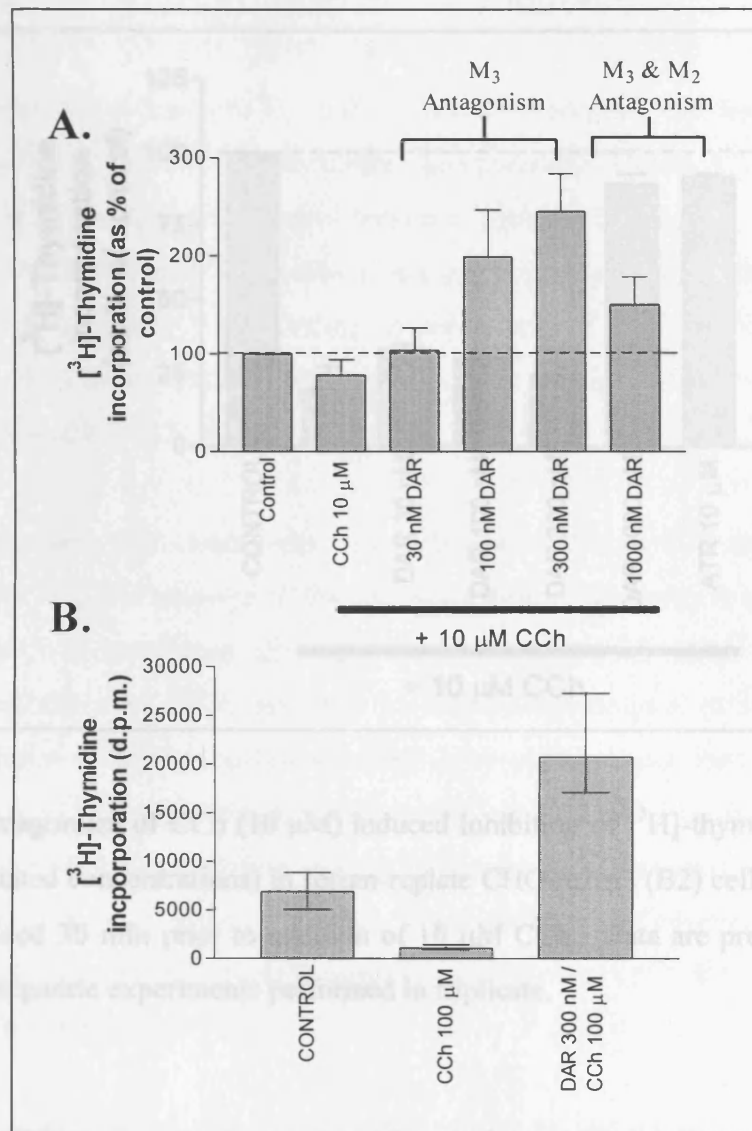


Figure 5.15. Antagonism of CCh-induced inhibition of [³H]-thymidine incorporation by darifenacin (stated concentrations) in serum-starved CHO-m2m3 (B2) cells. Panel A shows darifenacin blocking inhibition by 10 μ M CCh and panel B shows 300 nM darifenacin blocking inhibition by 100 μ M CCh in one representative experiment. In panel A data are presented as mean \pm S.E.M. for four separate experiments performed in triplicate, panel B is means \pm range for one experiment performed in triplicate.

5.4 Discussion

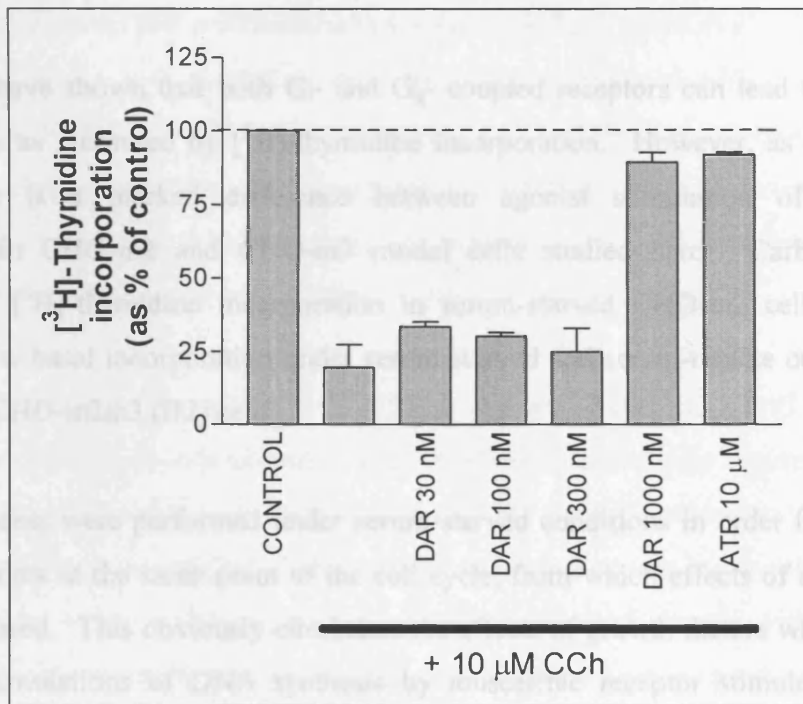


Figure 5.16. Antagonism of CCh (10 μ M) induced inhibition of [³H]-thymidine incorporation by darifenacin (stated concentrations) in serum-replete CHO-m2m3 (B2) cells. Darifenacin and atropine were added 30 min prior to addition of 10 μ M CCh. Data are presented as means \pm S.E.M. for three separate experiments performed in triplicate.

5.4 Discussion

Many studies have shown that both G_i - and G_q - coupled receptors can lead to stimulation of DNA synthesis as measured by [3 H]-thymidine incorporation. However, as this Chapter has reported there is a marked difference between agonist stimulation of [3 H]-thymidine incorporation in CHO-m2 and CHO-m3 model cells studied here. Carbachol evoked a stimulation of [3 H]-thymidine incorporation in serum-starved CHO-m2 cells but a marked inhibition below basal incorporation under serum-starved and serum-replete conditions in both CHO-m3 and CHO-m2m3 (B2) cells.

Initial experiments were performed under serum-starved conditions in order for all cells to be quiescent and thus at the same point of the cell cycle, from which effects of agonist treatment could be measured. This obviously eliminates the effects of growth factors which would mask any modest stimulations of DNA synthesis by muscarinic receptor stimulation. Then, by repeating the agonist strategy experiments under serum-replete conditions, it was possible to study the inhibition of [3 H]-thymidine incorporation observed in CHO-m3 and CHO-m2m3 (B2) cells. Also, it was possible to observe whether the muscarinic receptor effects were cell cycle-dependent as described by Nicke et al. (1999), where activation of M_3 -receptors, expressed in NIH3T3 cells, inhibited [3 H]-thymidine incorporation in growing cells, but caused a stimulation under serum-starved conditions.

Under serum-starved conditions the three cell lines (CHO-m2, CHO-m3 and CHO-m2m3 (B2)) all demonstrated equal levels of [3 H]-thymidine incorporation following 24 h 10% FCS treatment. However, untreated cell [3 H]-thymidine incorporation rates differed, with CHO-m2 cells displaying twice the basal level observed in CHO-m3 or CHO-m2m3 (B2) cells (See Figure 5.2). This could be a clonal difference in which CHO-m2 cells are less easy to serum-starve than the other cell lines. However, it is evident from the amount of [3 H]-thymidine incorporation observed in control cells in all three cell lines and the modest FCS stimulation (1.8 - 4.9 fold over basal, see Figure 5.2) that possibly CHO-cells are difficult to quiesce and require greater than 24 h serum starvation to cease growing.

Few previous studies have reported the phenomenon of chronic activation of mACh receptor causing an inhibition of [3 H]-thymidine incorporation, as observed in CHO-m3 and CHO-m2m3

(B2) cells in this study. However studies have been published on the inhibitory effects of elevated cAMP levels on cell proliferation in smooth muscle (Shapiro et al., 1996; Billington et al., 1999). Billington and colleagues demonstrated that elevated cAMP levels caused an inhibition of PDGF-stimulated growth as measured by [³H]-thymidine incorporation. It has been shown that β_2 -adrenoceptor stimulation mediates an inhibition of human airway smooth muscle proliferation, by elevating cAMP levels, as measured by [³H]-thymidine incorporation (Tomlinson et al., 1995; Stewart et al., 1997).

It was shown in Chapter 3 that stimulation of M₃ mACh receptors in CHO-m3 and CHO-m2m3 cells can increase (forskolin-stimulated) cyclic AMP accumulation (see Figure 3.8). This most likely occurs via a 'promiscuous' coupling of the M₃ mACh receptor to G_s G proteins to stimulate adenylyl cyclase activity. Such a route has been shown previously for the M₁ mACh receptor expressed in the CHO cell background (Burford and Nahorski, 1996). However, it seems unlikely that the inhibitory effects of M₃ mACh receptor stimulation on [³H]-thymidine incorporation rates can be accounted for by changes in adenylyl cyclase activity. In CHO-m3 and CHO-m2m3 cells the cyclic AMP-elevating effects are only seen at high agonist concentrations, whilst at lower agonist concentrations inhibition of (forskolin-stimulated) adenylyl cyclase activity is seen. It is the latter inhibitory effect that coincides with the agonist concentration range necessary to cause maximal inhibitory effects on [³H]-thymidine incorporation under both serum-replete and serum-starved conditions.

In contrast to the observations reported in this study, previous links have been made between mACh receptors linked to PI hydrolysis and increases in cell growth as measured by [³H]-thymidine incorporation (Ashkenazi et al., 1989; Gutkind et al., 1991; Heller-Brown et al., 1997). Ashkenazi and colleagues, studying muscarinic receptors in brain-derived astrocytoma and neuroblastoma cell lines, as well as CHO cells recombinantly expressing M₁-M₄ muscarinic receptors, showed muscarinic receptors to activate DNA synthesis. They proposed a link between PLC activation and DNA synthesis, since those mACh receptors poorly linked to PI hydrolysis (M₂- and M₄-subtypes) weakly activated DNA synthesis, whereas those subtypes (M₁- and M₃-subtypes) that efficiently coupled to PI hydrolysis strongly activated DNA synthesis. Ashkenazi et al. (1989) report a modest activation of PI hydrolysis upon CCh-stimulation of CHO-m2 and CHO-m3 cells and a modest increase in DNA synthesis (2.5 ± 0.3 and 1.5 ± 0.1 fold in CHO-m2 and CHO-m3 cells respectively).

While the findings presented here for serum-starved CHO-m3 cells contradict those reported by Ashkenazi et al. (1989) (60 % CCh-induced inhibition in this report compared to a 50 % stimulation in CHO-m3 cells for Ashkenazi et al.) this could possibly be explained by the apparent large difference in coupling to G_q-mediated PI hydrolysis (2.1 compared to \approx 50 fold for Ashkenazi et al. and this study, respectively). Also, as has been reported previously PLC can be stimulated by G _{$\beta\gamma$} subunits of G_i G-proteins (Blank et al., 1992; Camps et al., 1992). While this may occur in the model studied by Ashkenazi et al. (1989) as they reported M₂ receptors (G_i-coupled) to activate PLC (EC₅₀ 100 μ M carbachol), it has been shown not to be the case in the CHO-m2 cells studied in this thesis (see Chapter 4, Effect of PTX upon [³H]-IP_x accumulation).

In the studies reported in this thesis thus far, measurements in co-expressing CHO-m2m3 cells have largely paralleled those observed in CHO-m3 cells. However, [³H]-thymidine incorporation measurements, under serum-starved conditions, revealed an observable difference between agonist-induced effects in CHO-m3 and CHO-m2m3 (B2) cells; as much greater agonist concentrations were required to evoke a maximal inhibition of [³H]-thymidine incorporation in CHO-m2m3 (B2) cells. In co-expressing cells, DNA synthesis changes would be expected to result from a balance between the observed effects in CHO-m2 (modest stimulation) and CHO-m3 cells (inhibition). However, this stimulatory M₂-component is either absent, or more-likely masked, in serum-replete experiments due to the cells being in growth phase. By using the M₃ > M₂ selective antagonist darifenacin it was possible to recover the agonist-induced M₂-mediated stimulatory component evoked with CCh concentrations that cause a substantial inhibition in serum-starved CHO-m2m3 (B2) cells in the absence of darifenacin. Darifenacin showed good M₃>M₂ selectivity in serum-starved experiments (\leq 300 nM blocked M₃ component in CHO-m3 and CHO-m2m3 (B2) cells, see Figures 5.13 and 5.15 respectively) however apparent lack activity in serum-replete conditions (\geq 1000 nM to block M₃ component, see Figures 5.14 and 5.16). This may raise questions about darifenacin binding to, or being inactivated by, serum over a 24 h period (i.e. not 100% bioavailable).

The marked differences observed at the level of [³H]-thymidine incorporation will be interesting to interpret once the MAPK profiles have been established for all the cell lines. MAPKs have been directly implicated in cell proliferation (Bornfeldt et al., 1997; Brunet et al., 1999; Pagès et al., 1993; Tombes et al., 1998; for review see Gudermann et al., 2000). There have been a

number of studies linking the duration of MAPK activation in determining if a signal results in proliferation or differentiation, often linking transient ERK activation with cell proliferation, and sustained late phase ERK activation with differentiation (for review see Marshall, 1995). Studies by Dent and colleagues using primary hepatocytes have observed increased DNA synthesis via JNK and p38 activation, whereas prolonged ERK activation inhibited DNA synthesis through the induction of the expression of cyclin-dependent kinase inhibitor proteins (e.g. p21^{Cip-1/WAF1} and p16^{INK4a}). However, these workers also reported that this inhibition of DNA synthesis was only observed with chronic ERK activation and an increase in DNA synthesis was observed with transient ERK activation (see also Spector et al., 1997; Auer et al., 1998a and 1998b; Tombes et al., 1998). Upon activation, ERK has been reported to translocate to the nucleus (Chen et al., 1992; Brunet et al., 1999) and influence the activation of transcription factors. Nicke et al. (1999) reported activation of M₃-receptors expressed in NIH3T3 cells causing either a stimulatory (serum-starved) or inhibitory (serum-replete) effect on DNA synthesis depending on context of cellular growth. They showed the observed M₃-mediated effects on DNA synthesis were not dependent on ERK activation, but the inhibitory response observed in serum-replete experiments correlated with decreased cyclin D1 expression and hypophosphorylation of the retinoblastoma gene product (Rb) thus preventing G₀/G₁ cell cycle progression. However, ERK has been shown to mediate cell proliferation or growth inhibition in human arterial smooth muscle cells (SMCs) depending on downstream enzyme targets (Bornfeldt et al., 1997). ERK activation was shown to be essential in PDGF-induced cell proliferation in SMCs that do not secrete growth-inhibitory prostanoids such as PGE₂ but ERK activates a negative feedback pathway via cPLA₂, PGE₂ release and cyclic AMP-dependent protein kinase activation to attenuate the mitogenic response in SMCs that secrete large amounts of inhibitory prostanoids.

Hence, it will be important to characterise the MAPK responses within our cell lines (see Chapter 6) to establish whether they correlate with the [³H]-thymidine incorporation data presented here. Also it would have been interesting to investigate further the M₃-mediated inhibition of [³H]-thymidine incorporation and to establish if this indicator of cell proliferation is related directly to cell number by counting cell number (as shown by Krymskaya et al., 2000). Also it would be interesting to establish if any morphological changes occurred under agonist stimulation in CHO-m3 cells. This could be investigated using pulse-labelling with [³⁵S]-methionine as a measure of total protein synthetic rates within the cell. It should be noted that

throughout the [³H]-thymidine incorporation experiments (0h - 72h) the cells were routinely visualised by microscopy and whereas reduced cell density was apparent, no changes in cell shape or size were observed implying that growth of CHO-m3 cells was inhibited by agonist treatment rather than inducing hypertrophy or cell loss (e.g. apoptosis).

It would also be interesting to establish if the inhibition of DNA synthesis observed in the co-expressing CHO-m2m3 (B2) cells by agonist stimulation parallels that in smooth muscle tissue, showing that the CHO cell model created is a good paradigm for smooth muscle tissue.

Chapter Six: Characterisation of the activation of extracellular signal-regulated kinase and c-Jun NH₂-terminal kinase by M₂- and M₃- mACh receptors in CHO cells and bovine tracheal smooth muscle tissue preparations

6.1 Introduction

At the level of second messenger generation the co-expressing CHO-m2m3 cell lines have recapitulated both the M₂- (cAMP) and M₃- (cAMP, Ca²⁺, IP₃, IP_x) mACh receptor-mediated components in a fashion predicted for single expressing CHO-m2 or CHO-m3 cells (Chapters 3 and 4). Also, CHO-m2m3 cells have been shown to exhibit a balance between M₂- and M₃-receptor-mediated responses at the level of DNA synthesis as measured by [³H]-thymidine incorporation (Chapter 5). However, with the knowledge that activation of M₂- and M₃-receptors lead to opposing effects upon DNA synthesis within the CHO cells, and that ERK activation may be fundamentally involved in the signalling events leading to effects on cell proliferation (Pagès et al., 1993, for review see Gutkind 1998b), it was considered both interesting and important to characterise the MAPK activation profiles of the CHO-m2m3 cells. Work from this Department has previously reported different JNK activation profiles for these receptors, but similar ERK profiles when M₂ and M₃ mACh receptors are expressed alone in CHO cells (Wylie et al., 1999). It will also be interesting to see if changes in ERK and /or JNK activation correlate with the [³H]-thymidine results already reported. As described in the Introduction to this thesis the pathways linking GPCRs to MAPK activation are still not fully defined, but there are numerous putative targets for cross-talk between M₂- and M₃-receptor signalling pathways, both within the MAPK cascade (e.g. MEKK1-3 activating ERK, JNK or p38, as reviewed by Robinson and Cobb, 1997) and upstream of this cascade (e.g. Rac/Cdc42 interactions with Ras, Robinson and Cobb, 1997, as well as G_{βγ} subunits from G_i- linked receptor stimulation activating PLCβ, Blank et al., 1992).

Muscarinic receptor signalling leading to the activation of MAPKs (ERK, JNK and p38) has been studied in many cell types including CHO cells (Budd et al., 1999 (M₃), Wylie et al., 1999 (M₂ and M₃)) human neuroblastoma SK-N-BE(C) cells (Kim et al., 1999 (M₃)), rat 1a fibroblasts (Mitchell et al., 1995 (M₁ and M₂)), COS-7 cells (Crespo et al., 1994 (M₁ and M₂)),

Faure et al., 1994 (M₂)), HEK-293 cells (Yamouichi et al., 1997 (M₁ and M₂), Slack, 2000 (M₃)) and SH-SY5Y cells (Offermans et al., 1993 (M₃)).

Both Wylie et al. (1999) and Mitchell et al. (1995) reported G_i-linked M₂ and G_{q/11}-linked M₁ (Mitchell) or M₃ (Wylie) receptor-mediated increases in ERK activation to be Ca²⁺-independent. Mitchell and colleagues also reported that increases in JNK activity via both M₂- and M₁- (more robust response) receptor stimulation were Ca²⁺-dependent, however Wylie and colleagues only found a modest M₂-receptor mediated increase in JNK activity, whilst the increase in JNK activity mediated by M₃-receptors was only partially Ca²⁺-dependent. The studies by Wylie et al. (1999) and Slack (2000) both demonstrated a PKC-dependence of M₃-mediated ERK responses based on experiments using the PKC inhibitors Ro 31-8220 and GF109203X, respectively.

While the majority of studies performed to investigate the pathways linking GPCRs to the activation of MAPKs have involved immortalised cell lines, some studies have also been based in smooth muscle preparations and it will be important to establish if our model for co-expression of receptors represents a good paradigm for smooth muscle tissue preparations. A study by Kelleher and colleagues compared different mitogens for their ability to activate ERK. They demonstrated both growth factor (PDGF and EGF) and GPCR (5-HT) activation of ERK in bovine tracheal smooth muscle (Kelleher et al., 1995). Carbachol has also been shown to cause an increase in ERK activity in both human airway smooth muscle and canine tracheal smooth muscle through a G_α-subunit-mediated and PTX-sensitive pathway (Emala et al., 1999; Gerthoffer et al., 1997). However, as reported previously cultured airway smooth muscle cells have been shown to rapidly lose the M₃-mACh receptor population present *in vivo*, leaving only M₂-receptors in cultured cells (Yang et al. 1990; Yang et al., 1991; Widdop et al., 1993). BTSM slices prepared as described in Chapter 2 have previously been shown to retain a mixed population of M₂ and M₃ mACh receptors for at least 24 h post mortem (unpublished data).

With the knowledge that both M₂- and M₃- receptors have been shown to activate ERK, and M₃-receptor stimulation has been shown to activate JNK in CHO cells (Wylie et al., 1999, Budd et al., 1999) this Chapter describes the characterisation of these responses using these model cells in comparison to CHO-m2m3 cell activation of MAPKs, to investigate any possible interactions between the receptor signalling pathways. Since stimulation of M₂- and M₃-receptors lead to the

activation of two traditionally very distinct classical second messenger signalling pathways (inhibition of adenylyl cyclase and PLC activation respectively), but with similar concentration-dependency and time-course profiles of ERK activation (Wylie et al. 1999), it will be interesting to investigate any possible cross-talk / interactions of these two co-expressed receptor signalling pathways at the level of MAPKs. Therefore, the aim of this Chapter is to confirm that M₂- and M₃- muscarinic receptors couple to MAPKs, specifically ERK and JNK, in CHO cells and observe the effects of co-activation of these receptors within the same cell to see if there is any evidence for cross-talk in the co-expressing cell lines and to compare these results with those obtained in smooth muscle tissue preparations.

6.2 Methods

ERK and JNK activity assays were performed by either immunoprecipitation with a polyclonal ERK1/2-selective antibody, or using a GST-c-Jun fusion protein, respectively (Wylie et al., 1999), as described above in the Methods section (Chapter 2).

ERK activity was measured in bovine tracheal smooth muscle slice preparations within 24 h of dissection of fresh tissue from a local abattoir. Following initial preparation of the BTSM slices, the tissue was maintained in culture medium overnight (see Chapter 2). Following stimulation with agonist, ERK activity was determined by Western blotting of samples with a phospho-ERK antibody which only binds activated ERK. This approach was necessary as bovine ERK activity could not be recovered by immunoprecipitation using the anti-ERK polyclonal antibody (Santa Cruz) and kinase activity assay using epidermal growth factor (EGF-R) peptide as the substrate. Carbachol (CCh) was used as the muscarinic ACh receptor agonist in BTSM experiments as it is poorly hydrolysed by cholinesterase activity and has been shown to have similar efficacy and potency for activation of M₂- and M₃- receptor signalling pathways compared to MCh (Chapter 4, FLIPR [Ca²⁺]_i).

6.3 Results

6.3.1 Time-course profiles of ERK activation in CHO-m2, CHO-m3 and CHO-m2m3 cell lines

Time-course measurements of ERK activity were performed on the three cell lines under study, CHO-m2, CHO-m3 and CHO-m2m3, and these are shown in Figure 6.1. As can be observed, stimulation of CHO-m2, CHO-m3 and CHO-m2m3 (B2) cells with methacholine (MCh; 100 μ M) evoked rapid increases in ERK activity in each cell-line, peaking, in all cases, at 15-30 fold over basal activity at 5 min, where basal activity values were 199 ± 24 , 239 ± 55 and 353 ± 80 fmol/min/mg protein respectively. However, whereas the ERK activity had largely declined back to basal levels in CHO-m2 and CHO-m3 cells within 30 min of continued MCh exposure, the ERK response was much more sustained in the CHO-m2m3 (B2) cell-line (30 min MCh was statistically different from 30 min control in CHO-m2m3 (B2) cells at $P < 0.05$ by Student's *t*-test, $P > 0.05$ in CHO-m2 and CHO-m3 cells). Thus, the response was still 8.2 ± 0.8 fold over basal ($n=8$) compared to 2.4 ± 0.4 ($n=9$) and 2.5 ± 0.6 ($n=7$) fold over basal at 30 min for CHO-m2 and CHO-m3 respectively, see Figure 6.1.

This more sustained activation of ERK in co-expressing CHO-m2m3 (B2) cells was also observed in another co-expressing CHO-m2m3 clone (B7) in which MCh (100 μ M) stimulated an ERK activation of 7.8 ± 0.9 ($n=3$) fold over basal at 30 min (data not shown). Extended time-course experiments revealed that all cell lines studied returned to basal within 120 min and remained at basal levels up to 6 h with continued agonist exposure (data not shown). However, both the B2 and B7 co-expressing CHO-m2m3 clones showed sustained activity of ≥ 3 fold over basal at 80 min (3.2 and 4.4 fold over basal, respectively, see Figure 6.2).

6.3.2 Concentration-dependency of MCh-stimulated ERK activation in CHO-m2, CHO-m3 and CHO-m2m3 (B2) cells

The effect of varying MCh concentration on ERK activation at 5 min, the peak response time in CHO-m2, CHO-m3 and CHO-m2m3 cell lines, showed interesting results in the co-expressing cell lines (Figure 6.3). Assessment of the concentration-dependence of the ERK response revealed that EC_{50} values for the CHO-m2 and CHO-m3 ERK responses were in the low

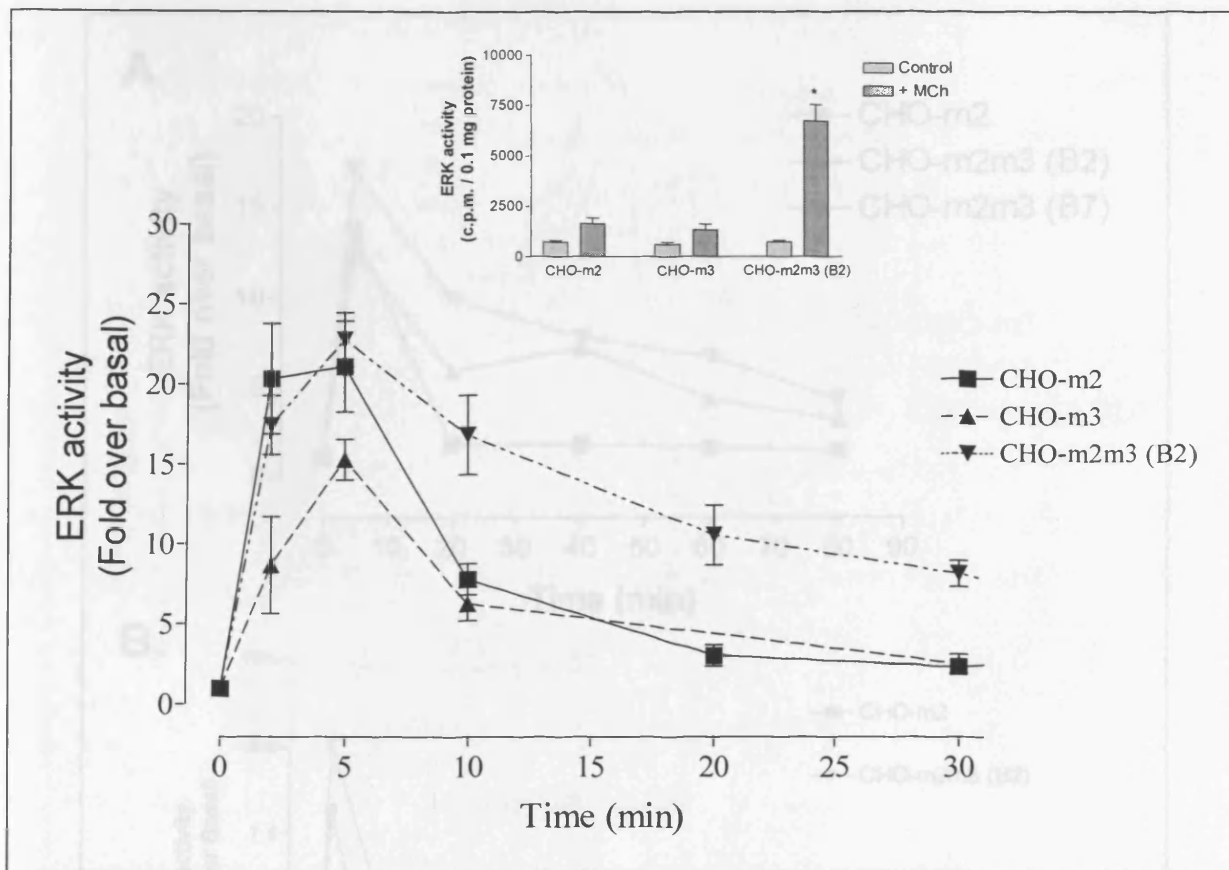


Figure 6.1. ERK activity time-course for CHO-m2, CHO-m3 and CHO-m2m3 (B2) cell-lines following stimulation with 100 μ M MCh. The main graph are expressed as fold-over-basal and the inset shows 30 min control versus MCh challenge. Data are shown as means \pm S.E.M. for at least seven separate experiments. * indicates $P < 0.05$ Student's paired t -test, paired observations.

Figure 6.3 ERK activation time-course, following stimulation with 100 μ M MCh, for CHO-m2, CHO-m2m3-clone B2 and CHO-m2m3-clone B7. Panel A shows sustained activation in both co-expressing cell lines beyond 60 min, data set shown as means for two experiments. In Panel B data are shown as fold over basal for one representative experiment performed in duplicate.

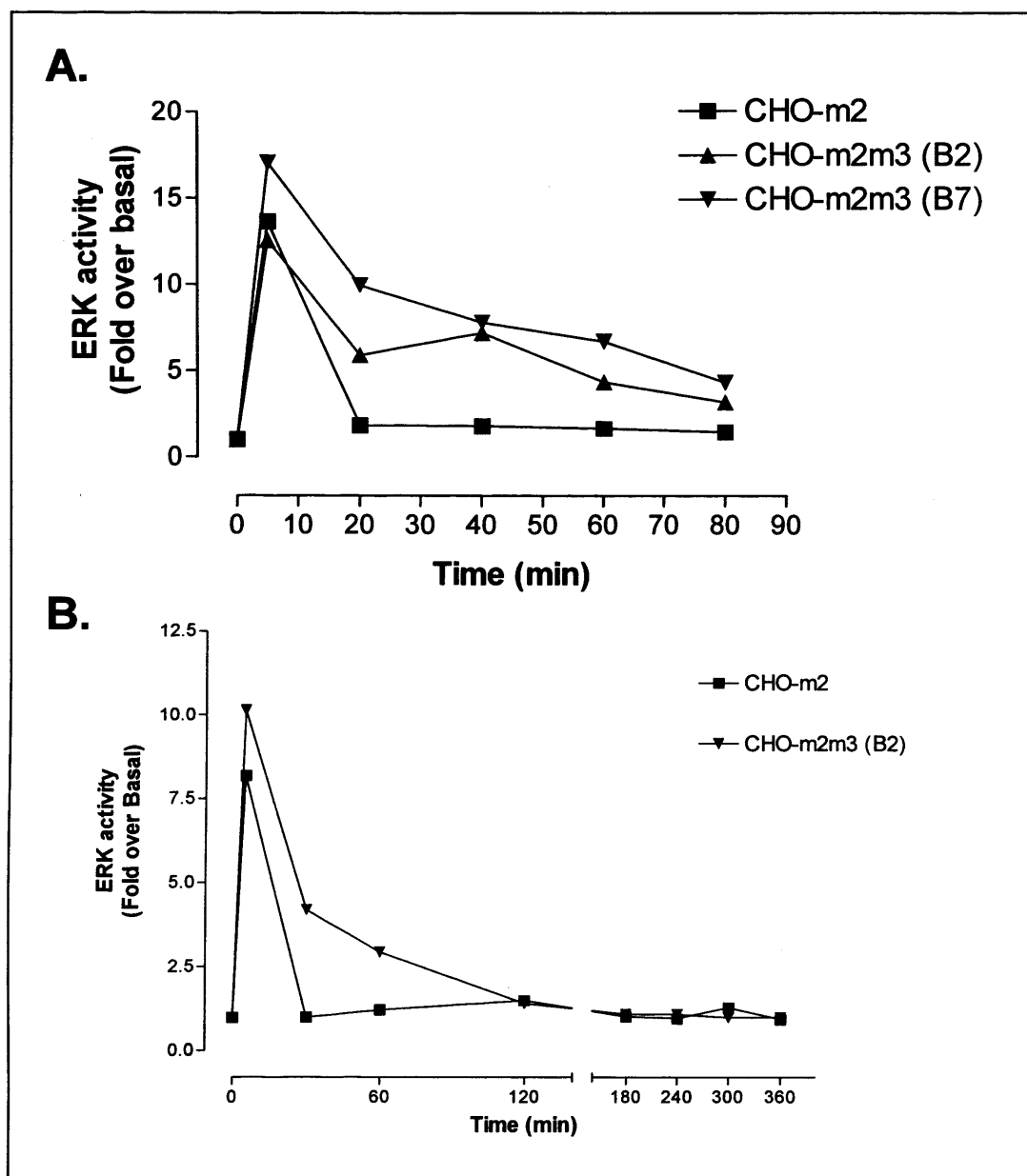


Figure 6.2 ERK activation time-course, following stimulation with 100 μ M MCh, for CHO-m2, CHO-m2m3-clone B2 and CHO-m2m3-clone B7. Panel A shows sustained activation in both co-expressing cell lines beyond 60 min, data are shown as means for two experiments. In Panel B data are shown as fold over basal for one representative experiment performed in duplicate.

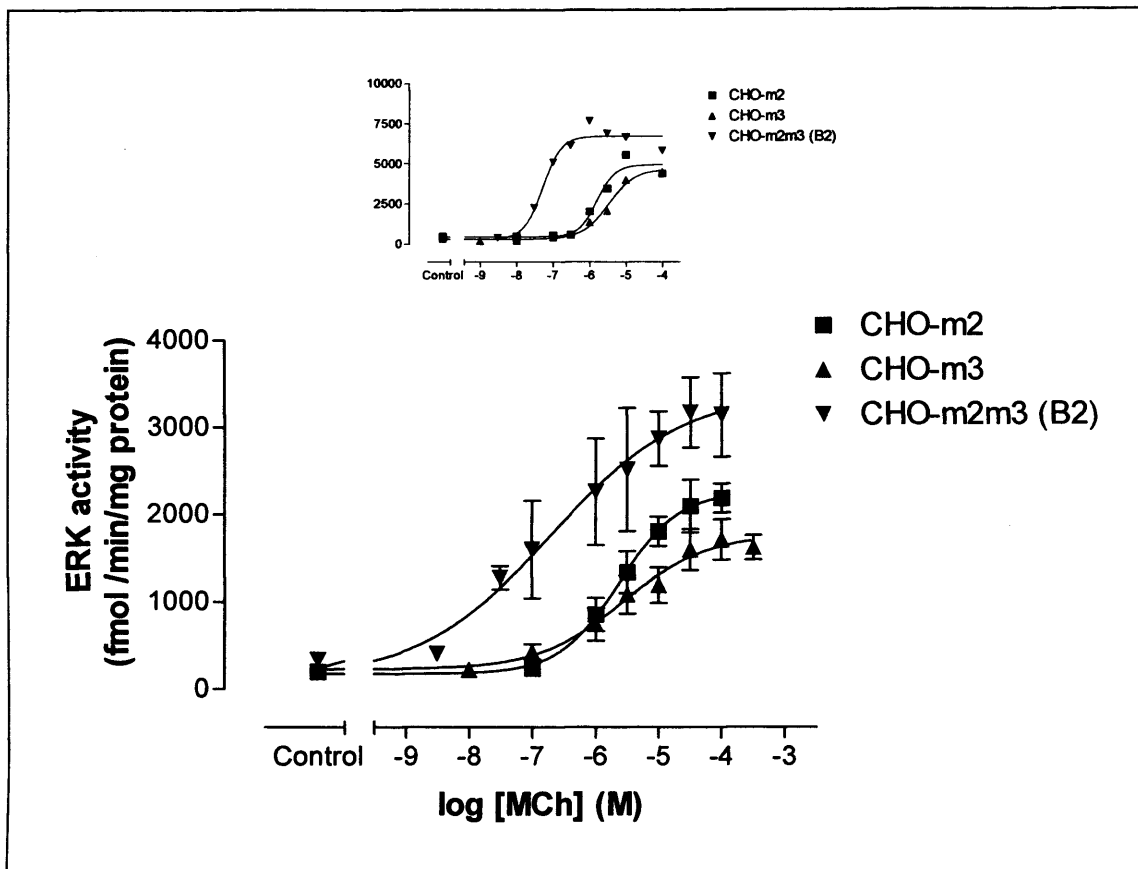


Figure 6.3 Concentration-effect curves for MCh-stimulated ERK activation at 5 min in CHO-m2 (n=4), CHO-m3 (n=5) and CHO-m2m3 (n=6) cells. Data are shown as means \pm S.E.M. The inset shows a single representative experiment.

micromolar range (pEC_{50} , 5.6 ± 0.1 ($n=4$) and 5.7 ± 0.3 ($n=5$) for CHO-m2 and CHO-m3, respectively), which correlated with those previously found (Wylie et al, 1999) in these cells. However, surprisingly, the EC_{50} value for the co-expressing CHO-m2m3 (B2) cell-line was significantly (approximately 50-fold) lower, ranging from 30 to 80-fold between experiments (pEC_{50} , 7.2 ± 0.1 ($n=6$); see Figure 6.3). These values are summarised in Table 6.1. (One-way ANOVA with Tukey's multiple comparison post hoc test showed $P < 0.05$ CHO-m2m3 vs CHO-m2 or CHO-m2m3 vs CHO-m3 and $P > 0.05$ CHO-m2 vs CHO-m3).

The leftward shift of the concentration-dependency curve was also observed in a second co-expressing clone, CHO-m2m3 (B7), ($pEC_{50} = 6.92 \pm 0.04$, $n=3$). Also, as shown in Table 6.1, a second CHO cell line expressing M_3 receptors, CHO-vt9, at a lower receptor density (160 fmol/mg protein) demonstrated a concentration-dependent MCh-stimulated ERK activation with an EC_{50} value lying to the right of both CHO-m2 and CHO-m3 cells ($pEC_{50} = 4.80 \pm 0.13$, $n=3$). Measurements at a 30 min time-point in CHO-m2m3 (B2) cells, where a sustained activity is observed of approximately 8-10 fold, also revealed an EC_{50} value in the 10-100 nM range (pEC_{50} values 7.15 and 6.97, $n=2$).

6.3.3 Time-courses of agonist-stimulated JNK activity in CHO-m2, CHO-m3 and CHO-m2m3 (B2) cells

Preliminary time-course profile experiments revealed that MCh-stimulated increases in JNK activity in CHO-m3 cells were more slowly developing than the ERK time-course profile, reaching a peak between 30-60 min after agonist addition, as reported previously by Wylie and colleagues (Wylie et al., 1999). Also in agreement with previous observations, essentially no stimulation of JNK activity was observed in CHO-m2 cells (Figure 6.4). Responses were similar between the CHO-m3 and m2m3 (B2) cell-lines (peak increases of 5-8 fold over basal, Figure 6.4).

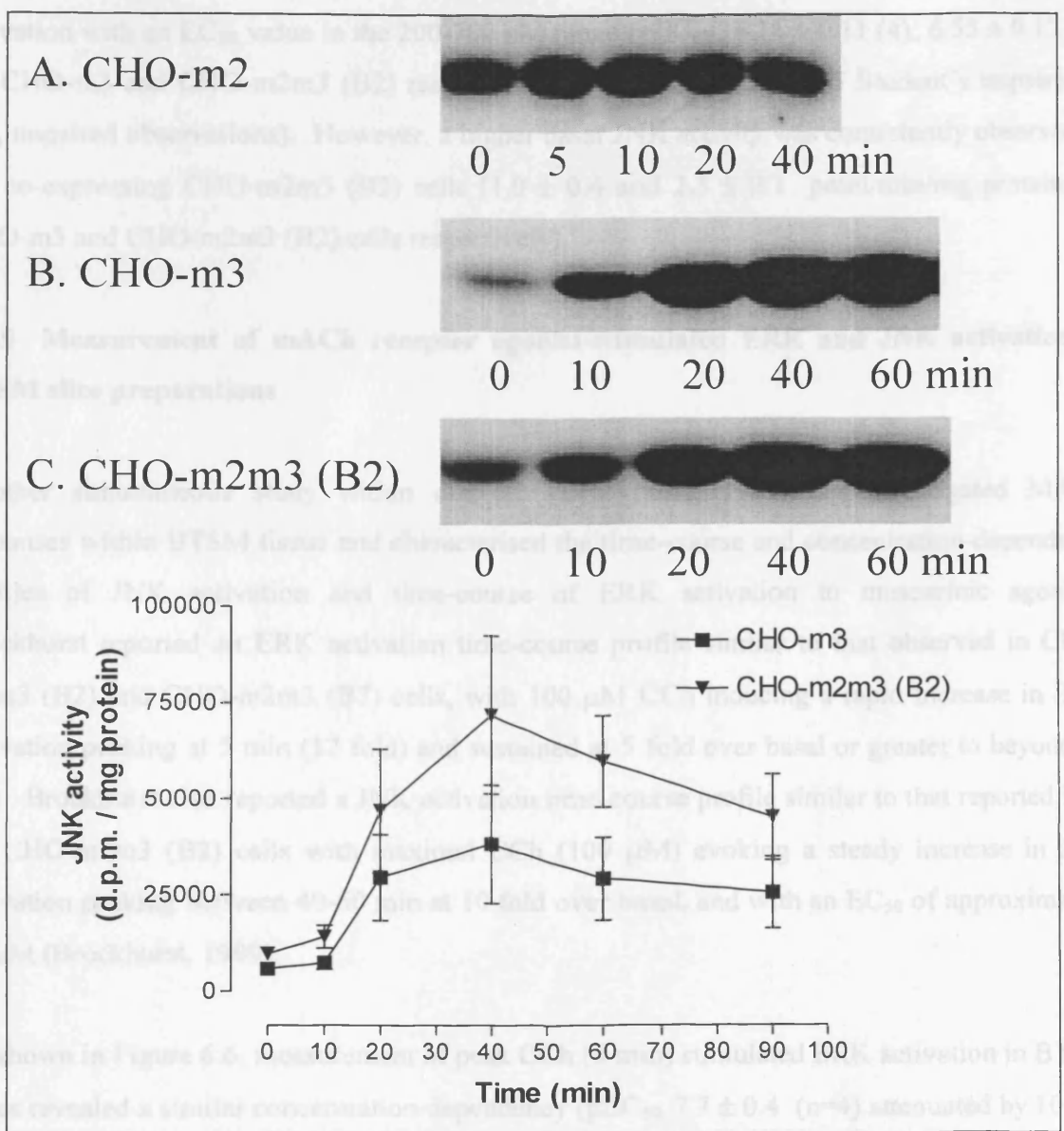
6.3.4 Concentration-dependency of MCh stimulated JNK activation in CHO-m3 and co-expressing CHO-m2m3 (B2) cells

Comparison of the concentration-dependencies for JNK activation by MCh at peak response (30 min) in CHO-m3 and CHO-m2m3 (B2) cells revealed only modest differences (approx. 3 fold).

Cell Line (CHO)	EC₅₀ (peak) (M) Mean	pEC₅₀ mean ± S.E.M.	n
M₂	2.81×10^{-6}	5.58 ± 0.09	4
M₃	5.21×10^{-6}	5.69 ± 0.27	5
M₂M₃ (B2)	7.20×10^{-8}	7.17 ± 0.07	6
M₂M₃ (B7)	5.06×10^{-7}	6.92 ± 0.04	3
(M₃) VT-9	1.70×10^{-5}	4.80 ± 0.13	3
M₂M₃ (B2) (30 min)	8.92×10^{-8}	7.05	2

Table 6.1 Summary of the EC₅₀ values calculated from methacholine concentration-effect curves for peak ERK (5 min) activation in CHO-m2, CHO-m3, CHO-vt-9 and CHO-m2m3 (B2) and CHO-m2m3 (B7) cells, and also 30 min activation in CHO-m2m3 (B2) cells.

Figure 6.4. Time-course profiles of MCh (100 μ M) stimulated JNK activation in CHO-m2, CHO-m3 and CHO-m2m3 cells. Panels A, B and C show representative autoradiographs for CHO-m2, CHO-m3 and CHO-m2m3 (B2) cells respectively. The blots have been developed for different times. The graph shows time-course profiles of JNK activation as measured by [γ - 32 P]-ATP incorporation into c-Jun (see Methods), data are shown as means \pm S.E.M. for at least three separate experiments.



6.4 Discussion

The studies presented in this chapter were undertaken to establish whether cross-talk can occur between M_2 and M_3 mACh receptors to bring about an antagonistic or synergistic activation of MAPK (ERK/JNK) pathways. Time-course studies revealed that MCh (100 μ M) induced a robust (>15 fold) increase in ERK activation in the three main cell lines studied. In each case the peak increase in ERK activity occurred at about 5 min after agonist addition, however, the

As can be observed from Figure 6.5 and Table 6.2 MCh elicited increases in peak JNK activation with an EC₅₀ value in the 200-700 nM range (pEC₅₀, 6.11 ± 0.11 (4); 6.55 ± 0.13 (6), for CHO-m3 and CHO-m2m3 (B2) respectively, see Figure 6.5, P<0.05 Student's unpaired *t*-test, unpaired observations). However, a higher basal JNK activity was consistently observed in the co-expressing CHO-m2m3 (B2) cells (1.0 ± 0.4 and 2.3 ± 0.1 pmol/min/mg protein for CHO-m3 and CHO-m2m3 (B2) cells respectively).

6.3.5 Measurement of mACh receptor agonist-stimulated ERK and JNK activation in BTSM slice preparations

Another simultaneous study within our lab (Brockhurst, 1999) has investigated MAPK responses within BTSM tissue and characterised the time-course and concentration-dependency profiles of JNK activation and time-course of ERK activation to muscarinic agonists. Brockhurst reported an ERK activation time-course profile similar to that observed in CHO-m2m3 (B2) and CHO-m2m3 (B7) cells, with 100 µM CCh inducing a rapid increase in ERK activation peaking at 5 min (12 fold) and sustained at 5 fold over basal or greater to beyond 90 min. Brockhurst also reported a JNK activation time-course profile similar to that reported here for CHO-m2m3 (B2) cells with maximal CCh (100 µM) evoking a steady increase in JNK activation peaking between 40-60 min at 10 fold over basal, and with an EC₅₀ of approximately 15 µM (Brockhurst, 1999).

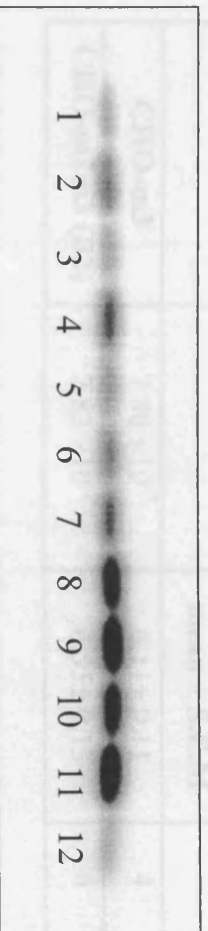
As shown in Figure 6.6, measurement of peak CCh (5 min) stimulated ERK activation in BTSM slices revealed a similar concentration-dependency (pEC₅₀, 7.7 ± 0.4 (n=4) attenuated by 10 µM atropine) to MCh stimulation of CHO-m2m3 (B2) cells, see Figure 6.6 (panels A and B) and Table 6.1.

6.4 Discussion

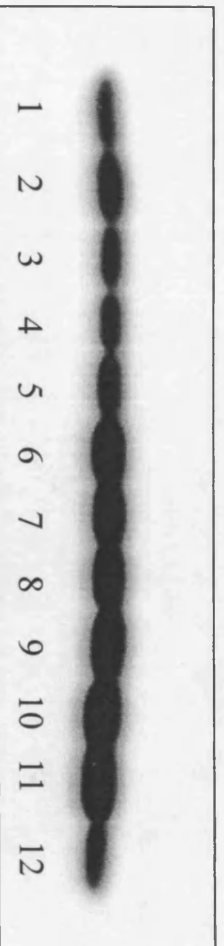
The studies presented in this Chapter were undertaken to establish whether cross-talk can occur between M₂ and M₃ mACh receptors to bring about an antagonistic or synergistic activation of MAPK (ERK/JNK) pathways. Time-course studies revealed that MCh (100 µM) induced a robust (>15 fold) increase in ERK activation in the three main cell lines studied. In each case the peak increase in ERK activity occurred at about 5 min after agonist addition, however, the

Figure 6.5 Concentration-dependency of MCh-stimulated JNK activation in CHO-m3 (n=4) and CHO-m2m3 (n=6) cells, 30 min agonist stimulation. Panels A and B show representative autoradiographs for concentration-dependencies in CHO-m3 and CHO-m2m3 (B2) cells where lanes 1 to 12 represent control, 1 nM, 3 nM, 10 nM, 30 nM, 100 nM, 300 nM, 1 μ M, 3 μ M, 10 μ M, 30 μ M MCh and control respectively. Panel C shows a graph of concentration-dependency of MCh-stimulated JNK activation in CHO-m3 (n=4) and CHO-m2m3 (n=6) cells, 30 min agonist stimulation. Data are shown as means \pm S.E.M.

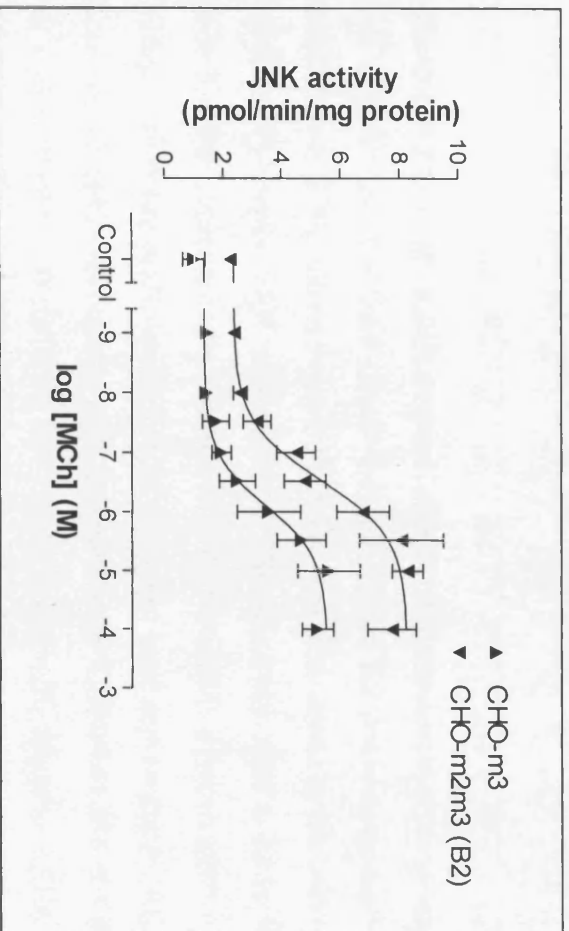
A. CHO-m3



B. CHO-m2m3 (B2)



C.



Cell-Line	Mean EC₅₀ (M)	pEC₅₀ mean ± S.E.M	n
CHO-m3	7.80×10^{-7}	6.11 ± 0.11	4
CHO-m2m3 (B2)	2.83×10^{-7}	6.55 ± 0.13	6

Table 6.2. Summary of MCh-stimulated JNK activation concentration-dependence data in CHO-m3 and CHO-m2m3 (B2) cells.

Largely of the ERK response differs considerably between the cell lines. In both CHO-m2

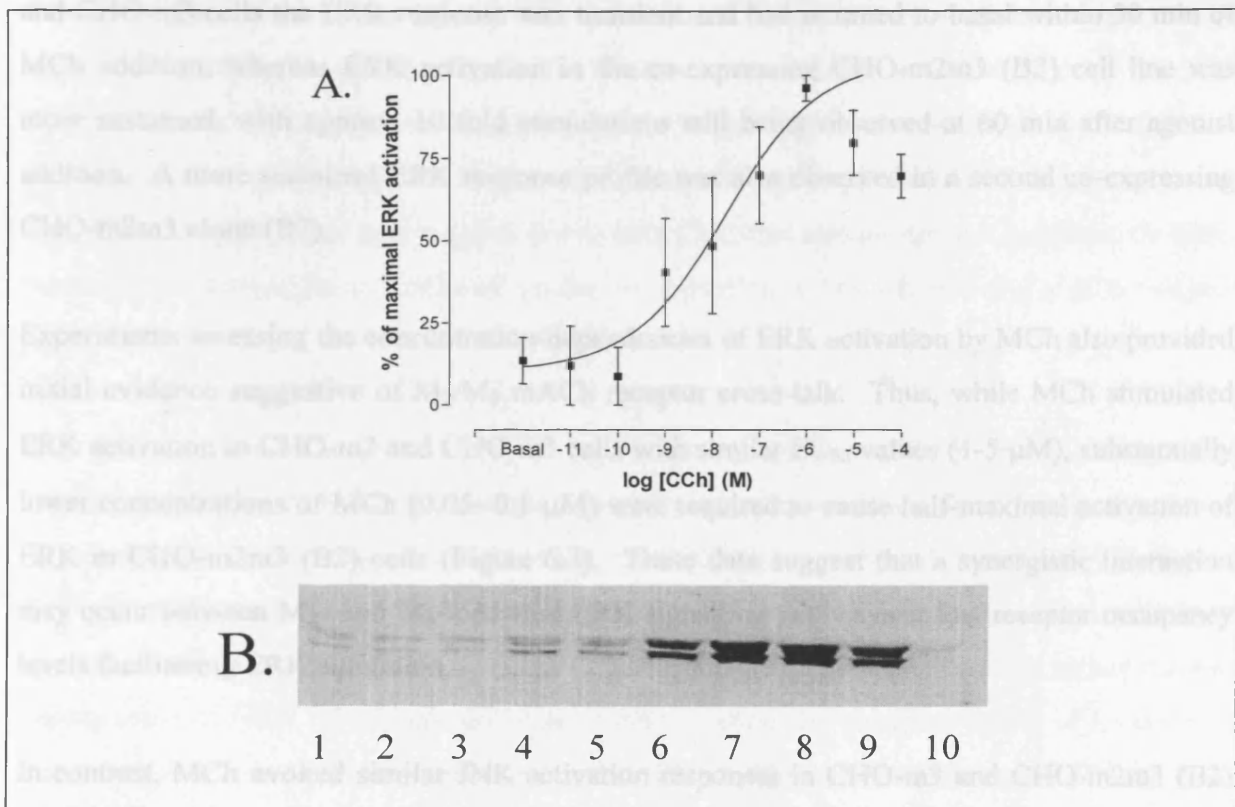


Figure 6.6 Graph and example autoradiograph representing concentration-response effect for 5 min carbachol stimulation of BTSM slices. Panel A shows the concentration-effect curve for CCh-stimulated (5 min) ERK activation in BTSM slices as determined by densitometric analysis of autoradiographs of phospho-ERK Western blots. Data are represented as mean % of maximal ERK activation for four separate experiments \pm S.E.M. Panel B is a representative western blot for BTSM samples showing phospho-ERK with the upper band representing ERK 1 (p44) and the lower panel ERK 2 (p42) following 5 min treatment with KHB, 0.01 nM, 0.1 nM, 1 nM, 10 nM, 100 nM, 1 μ M, 10 μ M, 100 μ M CCh and 10 μ M atropine 30 min prior to 100 μ M CCh, in lanes 1-10 respectively.

reported studies in CHO cells and other recombinant cell lines (Wu-Judd et al., 1995; Budd et al., 1999; Kim et al., 1999; Wyble et al., 1999; Slack, 2000), with previous studies also demonstrating characteristic, rapid (peak at 5 min) M₂ and M₄ mACh receptor-stimulated ERK responses, while ERK activation is typically more slowly developing (peak at 10-60 min) and the M₃ mACh receptor stimulating a much more marked enzyme activation.

Preliminary data have also been presented for the bovine tracheal smooth muscle (BTSM) slice preparation, which co-expresses M₂ and M₃ mACh receptors (total mACh receptor population

longevity of the ERK response differed considerably between the cell lines. In both CHO-m2 and CHO-m3 cells the ERK response was transient and had returned to basal within 30 min of MCh addition, whereas ERK activation in the co-expressing CHO-m2m3 (B2) cell line was more sustained, with approx. 10 fold stimulations still being observed at 60 min after agonist addition. A more sustained ERK response profile was also observed in a second co-expressing CHO-m2m3 clone (B7).

Experiments assessing the concentration-dependencies of ERK activation by MCh also provided initial evidence suggestive of M₂/M₃ mACh receptor cross-talk. Thus, while MCh stimulated ERK activation in CHO-m2 and CHO-m3 cells with similar EC₅₀ values (1-5 μM), substantially lower concentrations of MCh (0.05- 0.1 μM) were required to cause half-maximal activation of ERK in CHO-m2m3 (B2) cells (Figure 6.3). These data suggest that a synergistic interaction may occur between M₂- and M₃-mediated ERK signalling pathways at low receptor occupancy levels facilitating ERK activation.

In contrast, MCh evoked similar JNK activation responses in CHO-m3 and CHO-m2m3 (B2) cells, but no activation in CHO-m2 cells. Thus, co-activation of M₂ mACh receptors has little effect on M₃ receptor-stimulated JNK activation, although it is noteworthy that basal JNK activity in CHO-m2m3 cells was consistently higher than in CHO-m3 cells. Preliminary experiments showed that the basal JNK activities in CHO-m3 or CHO-m2m3 (B2) cells were unaffected by pre-incubation with mACh receptor antagonists (atropine, darifenacin), however, whether the raised basal JNK activity is a clonal difference or a consequence of M₂/M₃ mACh receptor co-expression has not been established.

The ERK and JNK activation profiles reported here in CHO-m2 and CHO-m3 cells correlate well with previously reported studies in CHO cells and other recombinant cell lines (Mitchell *et al.*, 1995; Budd *et al.*, 1999; Kim *et al.*, 1999; Wylie *et al.*, 1999; Slack, 2000), with previous studies also demonstrating characteristic, rapid (peak at 5 min) M₂ and M₃ mACh receptor-stimulated ERK responses, while JNK activation is typically more slowly developing (peak at 30-60 min) and the M₃ mACh receptor stimulating a much more marked enzyme activation.

Preliminary data have also been presented for the bovine tracheal smooth muscle (BTSM) slice preparation, which co-expresses M₂ and M₃ mACh receptors (total mACh receptor population

609 ± 98 fmol/mg protein; approx. 80:20% M₂:M₃ ratio). Robust activations of both ERK and JNK activities were seen in BTSM following CCh stimulation. Interestingly, while concentration-dependency experiments for CCh-stimulated JNK activation yielded an EC₅₀ value of approx 10 μM, increases in phospho-ERK in BTSM was stimulated by much lower concentrations of CCh (EC₅₀, 10-50 nM) reminiscent of that observed in CHO-m2m3 cells (see Figs. 6.3 and 6.6). These data suggest that in both CHO and airways smooth muscle cells ERK, but not JNK activation is facilitated by the co-activation of the M₂ and M₃ mACh receptor populations.

Over the past 10 years a large number of studies have provided evidence for ERK being either causal or contributory to the phenotypic changes evoked in a variety of cell-types by growth factors and a diverse array of stimuli acting via GPCRs (Pouyssegur & Seuwen, 1992; Davis, 1993; Dhanasekaran et al., 1995; Gudermann et al., 2000). A crucial aspect of such signalling appears to be the ability of the stimulus to cause a sufficiently robust and sustained nuclear translocation of ERK (Khokhlatchev et al., 1998) to allow the phosphorylation of a variety of transcription factors and altered gene expression (Weber et al., 1997; Brunet et al., 1999). Thus, the much more sustained time-course of agonist-induced ERK activation seen in M₂ and M₃ mACh receptor co-expressing CHO cells could potentially have important implications for cell fate.

A possible confusion is the fact that different patterns of ERK activation have been associated with proliferative versus non-proliferative (*e.g.* growth arrest/cell differentiation) signalling responses in different cells. Pagès et al. (1993), Alblas et al. (1996) and Weber et al. (1997) have shown that sustained ERK activation is a necessary requirement for fibroblast proliferation, while sustained ERK activation has been associated with growth arrest and cellular differentiation in other cell types (Traverse et al., 1992; Alblas et al., 1996; Tombes et al., 1998; reviewed by Marshall, 1995). It is interesting to note that in human airways smooth muscle (HASM) cells Orsini et al. (1999) have demonstrated that stimuli must cause a prolonged ERK activation to induce mitogenesis. However, the relative roles of ERK and JNK in regulating cell fate has not been established and it may be that the ERK response cannot be considered in isolation, but the relative activations (in terms of concentration-dependency, magnitude and longevity) of ERK versus JNK (and perhaps p38) must be taken into account. ERK activation may be necessary but is not sufficient for cell proliferation.

Considering the potential novelty and importance of the initial findings it was considered necessary to perform a number of further experiments to demonstrate that the observed cross-talk between M_2 and M_3 mACh receptors, at the level of ERK activation, was truly due to receptor co-expression and not due to any clonal differences between cell lines. In serum-starved cells, fetal calf serum (FCS; 0.3-10%) stimulated a concentration-dependent ERK activation which did not differ between the CHO-m2, CHO-m3, CHO-m2m3 (B2) and CHO-m2m3 (B7) cell lines (data not shown). In addition, experiments were also attempted where cDNAs for M_2 , M_3 , or M_2 and M_3 mACh receptors were transiently transfected into CHO-K1 cells (incorporated into a pcDNA3 plasmid and transfected (at concentrations up to $5 \mu\text{g ml}^{-1}$) using FuGene6 72 h prior to agonist stimulation of ERK activity). Unfortunately, these experiments were unsuccessful and there was insufficient time to establish the technical cause of this failure. As an alternative it was decided to adopt a pharmacological approach to attempt to dissect the M_2/M_3 -mediated components of the observed synergy in ERK activation (see Chapter 7).

As to the possible cross-talk mechanism downstream of M_2/M_3 mACh receptor activation, studies by Hawes and colleagues in CHO cells have demonstrated G_i signalling to ERK activation to occur via $G_{\beta\gamma}$ signalling through a PKC-independent and Ras-dependent pathway, while G_q -mediated ERK signalling proceeds via a PKC-dependent and Ras-independent pathway (Hawes et al., 1995). This may imply that cross-talk between M_2 - and M_3 receptor-initiated signalling pathways may occur within the cascade leading to ERK activation, however signalling from GPCRs to MAPKs may not be so simple, as G_q -mediated signalling has also been shown to occur independently of PKC (Crespo et al., 1994; Budd et al., 2001), and G_i signalling can proceed to ERK via Ras-dependent pathways (Winitz et al., 1993; Crespo et al., 1994). Thus, there is much still to learn about the individual pathways linking G_q - or G_i -coupled GPCRs to ERK activation. In the next Chapter a number of approaches will be used to attempt to delineate further the potential cross-talk between M_2 and M_3 mACh receptors to regulate this important cell surface-to-nucleus signalling pathway.

Chapter Seven: Dissection of synergistic ERK activation through co-stimulation of M₂- and M₃-receptors in CHO-m2m3 cells and BTSM tissue preparations

7.1 Introduction

Chapter 6 described how co-stimulation of M₂ and M₃ receptors in CHO-m2m3 cells caused a synergistic ERK activation, as observed by a more sustained time-course profile and left-shift of the concentration-dependency to mACh receptor agonist stimulation. These findings are potentially very important since it has been demonstrated that upon activation ERK translocates to the nucleus where it may contribute to the regulation of gene transcription, influencing phenotypic consequences (Khokhlatchev et al., 1998; Brunet et al., 1999) and ERK has been shown by Pagès et al. (1993) to be essential for proliferative signalling in fibroblasts.

It was important to characterise this 'cross-talk' phenomenon further and dissect the relative contributions of the M₂ (G_i) and M₃ (G_q) components. This has been attempted by using PTX to uncouple M₂-mediated signalling pathways through G α_i protein ADP ribosylation, or by using subtype-selective concentrations of methoctramine or tripitramine (M₂>M₃), or darifenacin (M₃>M₂). Possibly the receptors contribute equally to the enhanced signal, or perhaps the G_q or G_i component is dominant and only a low activation of the other additional pathway is required to observe the synergistic ERK activation. Also, by studying the activation of other G protein-coupled receptors endogenously expressed in the CHO cell model it was possible to investigate whether the observed 'cross-talk' effects on ERK activation are specific to co-activation of mACh receptor signalling pathways, or is a more general phenomenon relating generically to G_q and G_i protein signalling pathways.

7.2 Results

7.2.1 Effects of pertussis toxin (PTX) pre-treatment on the concentration-dependency of ERK activation in CHO-m2, CHO-m3 and CHO-m2m3 (B2) cells

A key objective was to alter or abolish selectively one of the mACh receptor pathways to determine its contribution to the synergy observed in co-expressing cells. This could be achieved through ADP ribosylation of $G_{i/o}$ proteins by PTX, or through pharmacological dissection of the observed ERK responses using mACh receptor subtype-selective antagonists.

Pertussis toxin (PTX, 100 ng/ml, 16 h pre-treatment) completely attenuated the MCh-stimulated ERK activation in CHO-m2 cells (Figure 7.1). In CHO-m3 cells however, there was no effect of PTX pre-treatment on MCh-stimulated ERK activity with high MCh concentrations (above 10 μ M), but there was an augmentation of the ERK activation with concentrations of MCh below 10 μ M. Thus, as can be observed by comparing both Figure 6.3 and 7.2, there was a marked leftward shift (\approx 100 fold) in MCh concentration-dependency in the presence of PTX in CHO-m3 cells, ($P < 0.05$, Student's *t*-test, paired observations; pEC_{50} , 5.69 ± 0.27 ; 7.84 ± 0.20 for -PTX and +PTX conditions respectively, see Figure 7.2). PTX pre-treatment did not affect basal ERK activity in either CHO cell line.

As shown in Figure 7.3, PTX pre-treatment caused no shift in the MCh concentration-response curve for ERK activation in CHO-m2m3 (B2) cells (pEC_{50} , 7.17 ± 0.09 ; 7.93 ± 0.47 for -PTX and +PTX respectively, summarised in Table 7.1, not significantly different $P > 0.05$ Student's *t*-test, paired observations), but reduced the maximal response by approx. 50%. In a single experiment in CHO-m2m3 (B2) cells it was shown that 100 ng/ml PTX caused a maximal inhibition and no further inhibition was obtained with ≥ 16 h pre-treatment with a higher concentration of PTX (Figure 7.4).

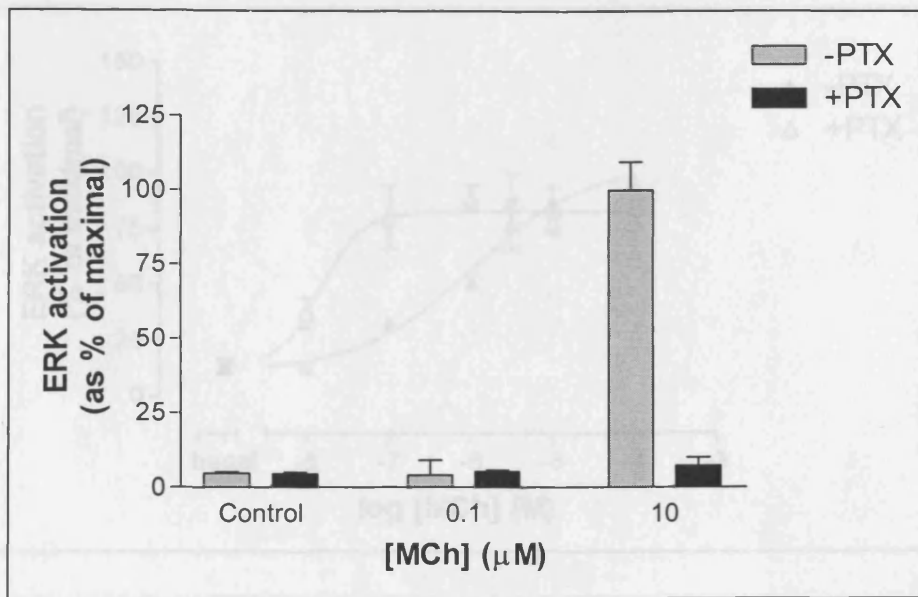


Figure 7.2 Effect of PTX pre-treatment on concentration-response relationship of MCh-

Figure 7.1 Effect of PTX pre-treatment on MCh-stimulated peak ERK (5 min) activation in CHO-m2 cells. Data are shown as means \pm S.E.M. for three separate experiments.

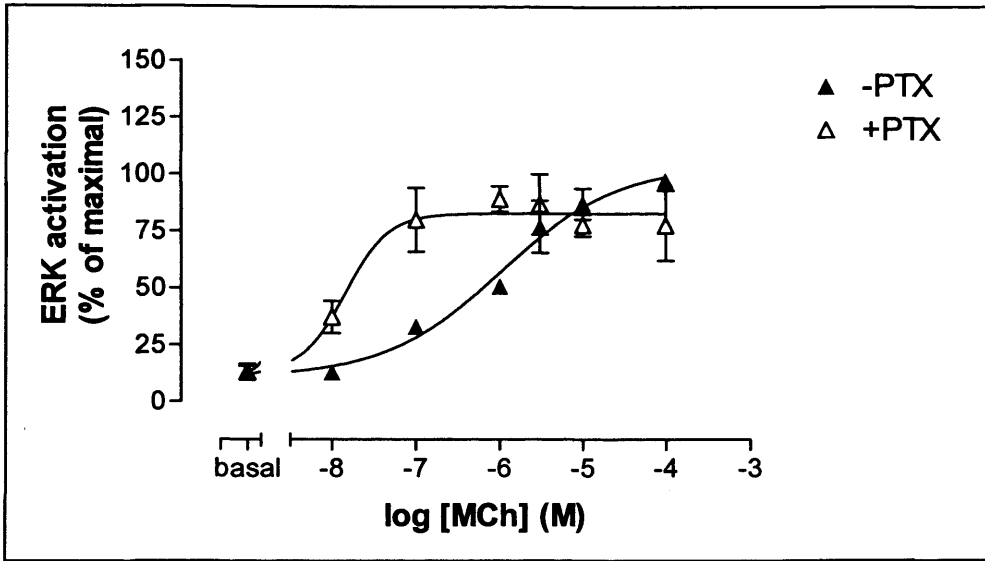


Figure 7.2 Effect of PTX pre-treatment on concentration-response relationship of MCh-stimulated peak ERK (5 min) activation in CHO-m3 cells. Data are shown as means \pm S.E.M. for three separate experiments.

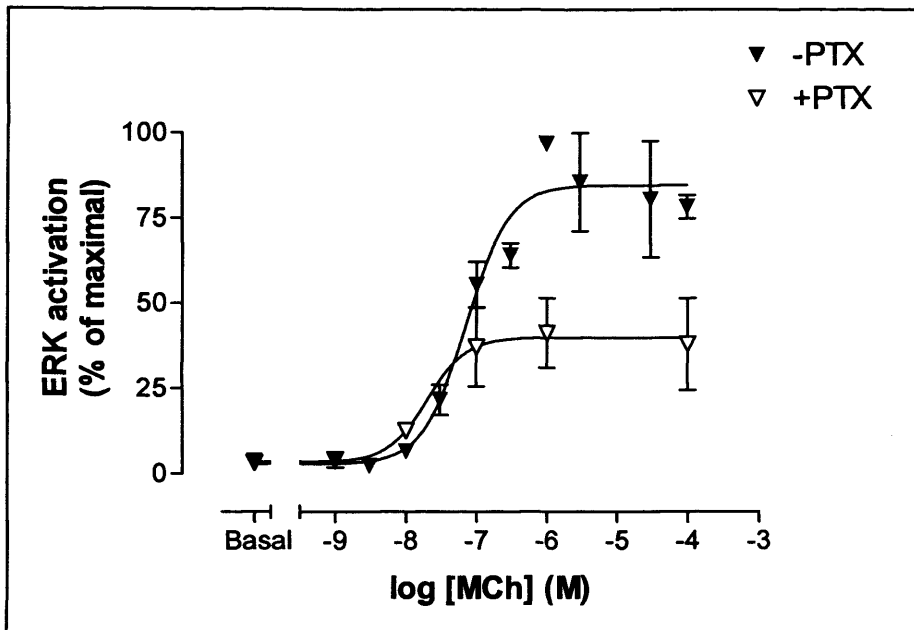


Figure 7.3 Effect of PTX pre-treatment on the concentration-response relationship of MCh-stimulated peak ERK (5 min) activation in CHO-m2m3 (B2) cells. Data are shown as means \pm S.E.M. for three separate experiments.

Cell Line	<u>- PTX</u>		<u>+ PTX</u>	
	pEC ₅₀	S.E.M	pEC ₅₀	S.E.M
CHO-m2 (n=3)	5.58	± 0.09	NA	NA
CHO-m3 (n=3)	5.98	± 0.19	7.84	± 0.20
CHO-m2m3 (B2) (n=3)	7.17	± 0.09	7.93	± 0.47

Table 7.1 A summary of MCh-stimulated peak ERK (5 min) activation pEC₅₀ values determined from concentration-response curves in the presence and absence of PTX.

NA = not applicable as no response.

7.2.3 Pharmacological distinction of M_2 - and M_3 -mACh receptor components of the MCh-stimulated ERK activation in CHO-m2, CHO-m3, CHO-m2m3 (B2) cells and R15M tissue slices

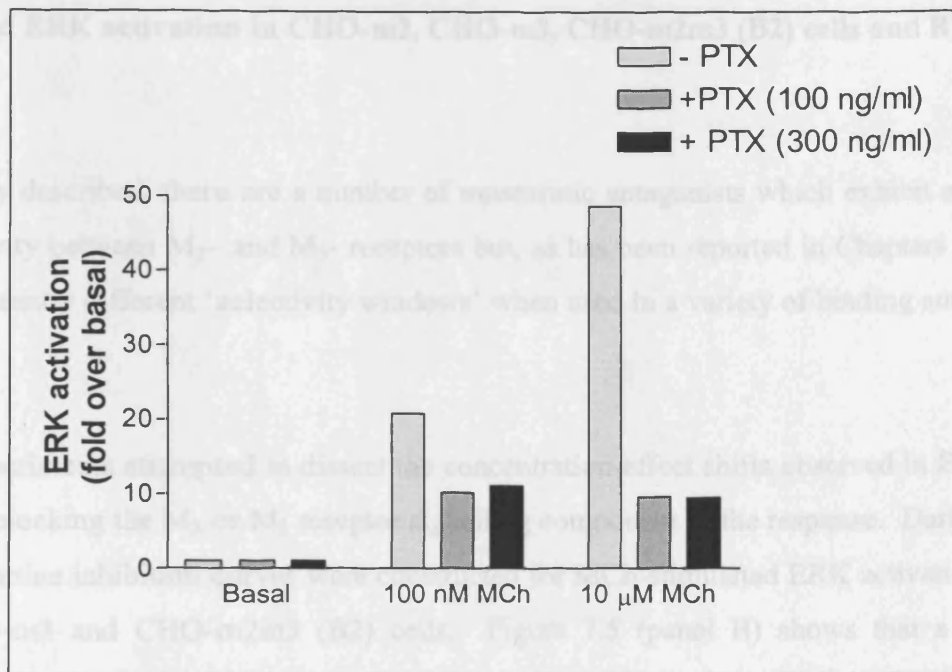


Figure 7.4 Effect of varying PTX concentration on MCh-stimulated peak ERK (5 min) activation in CHO-m2m3 (B2) cells. Data shown represent a single preliminary experiment.

experiments appear that 100 nM or 300 nM darifenacin would be an appropriate concentration to antagonise completely M_2 -receptors without inhibiting the M_3 -receptor population within the CHO-m2m3 cells challenged with MCh (10 μM). However, as Figure 7.5 shows 100 nM darifenacin does not completely block the M_3 -component and also begins to inhibit the M_2 -component (by as much as 40%) in CHO-m3 and CHO-m2 cells, respectively. This can also be observed from an initial experiment (Figure 7.5 panel A) where approx. 10 fold selectivity was observed. This is inefficient M_2/M_3 discrimination to allow complete blockade of one component whilst not compromising the second component.

MCh (10 μM) produced approximately 50% of maximal ERK activation in CHO-m2 and CHO-m3 cells (see Figure 6.2) and, as can be observed from Figure 7.5 (panel B), 10 μM darifenacin completely abrogated this response in both cell lines. Interestingly, 10 μM darifenacin also completely inhibited 10 μM MCh-stimulated ERK activation in CHO-m2m3 (B2) cells. However in a single experiment 100 nM darifenacin completely abrogated 150 nM MCh (EC_{50} response) stimulated ERK activation (Figure 7.6), whereas 100 nM darifenacin only caused approx. 50 % inhibition of EC_{50} ERK activation in CHO-m2 or CHO-m3 cells (Figure 7.5), which may indicate that greater than 50 % activation of the signalling pathway from both

7.2.2 Pharmacological dissection of M₂- and M₃- mACh receptor components of the MCh-stimulated ERK activation in CHO-m2, CHO-m3, CHO-m2m3 (B2) cells and BTSM tissue slices

As already described, there are a number of muscarinic antagonists which exhibit some degree of selectivity between M₂- and M₃- receptors but, as has been reported in Chapters 3, 4, 5 they have apparently different 'selectivity windows' when used in a variety of binding and functional studies.

Initial experiments attempted to dissect the concentration-effect shifts observed in ERK activity by either blocking the M₃ or M₂ receptor signalling component of the response. Darifenacin and methoctramine inhibition curves were constructed for MCh-stimulated ERK activation in CHO-m2, CHO-m3 and CHO-m2m3 (B2) cells. Figure 7.5 (panel B) shows that a 'selectivity window' for M₃- over M₂- antagonism for darifenacin on peak ERK activation (5 min) following stimulation with MCh (10 µM) was not as great as observed previously for cAMP accumulation (approx. 400 fold; see Chapter 3, Figure 3.12). The cAMP accumulation experiments implied that 100 nM or 300 nM darifenacin would be an appropriate concentration to antagonise completely M₃-receptors without inhibiting the M₂-receptor population within the CHO-m2m3 cells challenged with MCh (10 µM). However, as Figure 7.5 shows 100 nM darifenacin does not completely block the M₃- component and also begins to inhibit the M₂- component (by as much as 40%) in CHO-m3 and CHO-m2 cells, respectively. This can also be observed from an initial experiment (Figure 7.5 panel A) where approx. 10 fold selectivity was observed. This is insufficient M₃/M₂ discrimination to allow complete blockade of one component whilst not compromising the second component.

MCh (10 µM) produced approximately 80% of maximal ERK activation in CHO-m2 and CHO-m3 cells (see Figure 6.3) and, as can be observed from Figure 7.5 (panel B), 10 µM darifenacin completely attenuated this response in both cell lines. Interestingly, 10 µM darifenacin also completely inhibited 10 µM MCh-stimulated ERK activation in CHO-m2m3 (B2) cells. However in a single experiment 100 nM darifenacin completely attenuated 250 nM MCh-(EC₈₀ response) stimulated ERK activation (Figure 7.6), whereas 100 nM darifenacin only caused approx. 50 % inhibition of EC₈₀ ERK activation in CHO-m2 or CHO-m3 cells (Figure 7.5), which may indicate that greater than 50 % activation of the signalling pathway from both

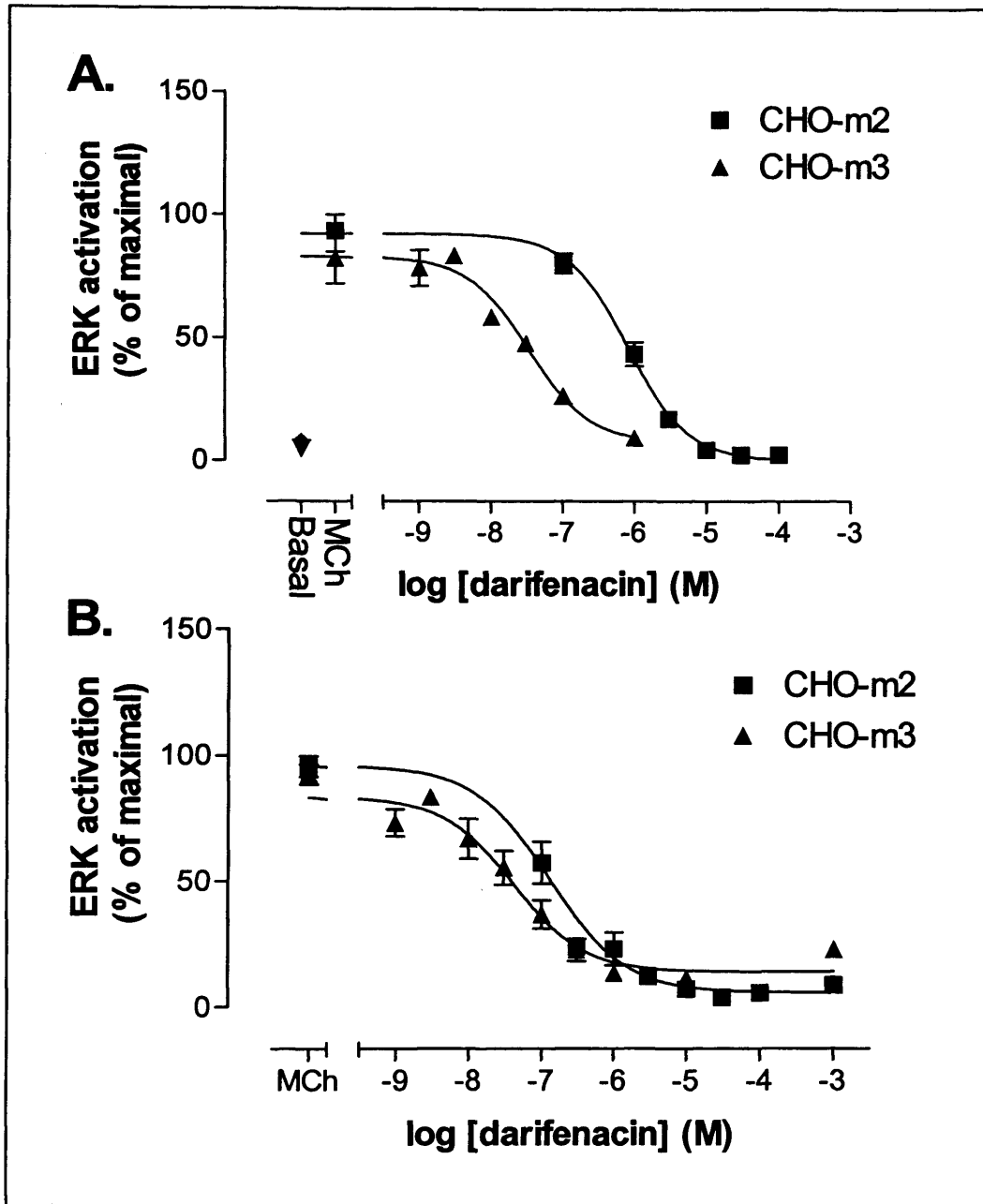


Figure 7.5 Inhibition by darifenacin of MCh (10 μ M) stimulated ERK activation in CHO-m2 and CHO-m3 cells. Panel A shows a representative experiment performed in duplicate, data are means \pm range. In panel B Data are shown as means \pm S.E.M. for three separate experiments performed in duplicate.

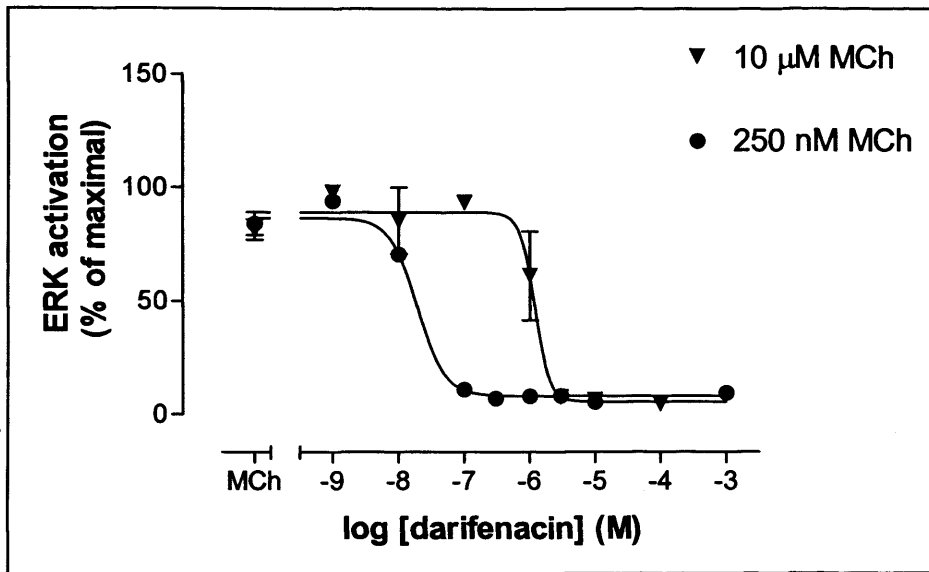


Figure 7.6 Darifenacin inhibition of MCh (10 μ M or 250 nM) stimulated ERK activation in CHO-m2m3 (B2) cells. Data are shown as mean \pm range for two separate experiments for 10 μ M MCh and mean for one experiment for 250 nM MCh, performed in duplicate).

receptors is required in order to observe the synergistic ERK activation. However, Cheng-Prussoff analysis of these different IC_{50} values in CHO-m2m3 (B2) cells reveals pK_i values of 8.38 and 8.09 for EC_{120} and EC_{80} respectively, compared to pK_i values of 7.28 ± 0.38 and 7.97 ± 0.23 for CHO-m2 and CHO-m3 cells, respectively (see Table 7.2).

In a preliminary experiment methoctramine demonstrated a greater selectivity window than darifenacin, pIC_{50} values of 7.72 and 5.92 against 10 μ M MCh-stimulated ERK activation in CHO-m2 and CHO-m3, respectively. Similar to darifenacin, methoctramine inhibition of a supra-maximal MCh (10 μ M) stimulated ERK activity response in CHO-m2m3 (B2) cells lay to the right of both cell lines expressing the receptors singularly ($pIC_{50} = 5.08$) (see Figure 7.7).

Despite the apparent lack of a workable M_2/M_3 selective antagonist, experiments were nevertheless attempted to dissect the concentration-effect shifts observed in ERK activity by using a concentration of darifenacin which was shown to be optimal for blocking M_3 -receptors, but leaving the M_2 -receptor response largely intact. Interestingly, as shown in Figure 7.8, 100 nM darifenacin caused a rightward shift in the MCh-stimulated ERK activation concentration-effect curve in CHO-m2m3 (B2) cells towards that observed in CHO-m2 cells. More thorough characterisation of the ERK activation in CHO-m2m3 cells was attempted by using a variety of darifenacin concentrations (30 - 1000 nM), however inter-experimental variation made these results hard to interpret and hence the use of 100 nM darifenacin provided the only complete dataset. Schild plot analysis (Arunlakshana and Schild, 1959) of the individual experiments in Figure 7.8 revealed pA_2 value of 8.18 ± 0.15 ($n=3$; individual experiments of 8.46, 7.94 and 8.14, respectively).

To explore the possible contributions of M_2 and M_3 mACh receptors to ERK stimulation in airways smooth muscle methoctramine inhibition of CCh-stimulated ERK activation in BTSM slices was assessed and is represented by the blot shown in Figure 7.9. This blot shows that 1 μ M methoctramine completely abolished the ERK response evoked by 1 μ M CCh.

Cell Line	[MCh] μM	<u>darifenacin</u>			<u>methoctramine</u>		
		n	pIC ₅₀	pK _i	n	pIC ₅₀	pK _i
CHO-m2	10	3	6.89 ± 0.11	7.28 ± 0.38	1	7.72	8.40
CHO-m3	10	3	7.38 ± 0.15	7.97 ± 0.23	1	5.92	6.69
CHO-m2m3 (B2)	10	2	5.92	8.38	1	5.10	7.25
CHO-m2m3 (B2)	0.25	1	7.71	8.09	n.d	n.d.	n.d.

Table 7.2. A summary of pIC₅₀ and pK_i values for mACh receptor antagonist inhibition of MCh-stimulated ERK activation. n.d. = not determined.

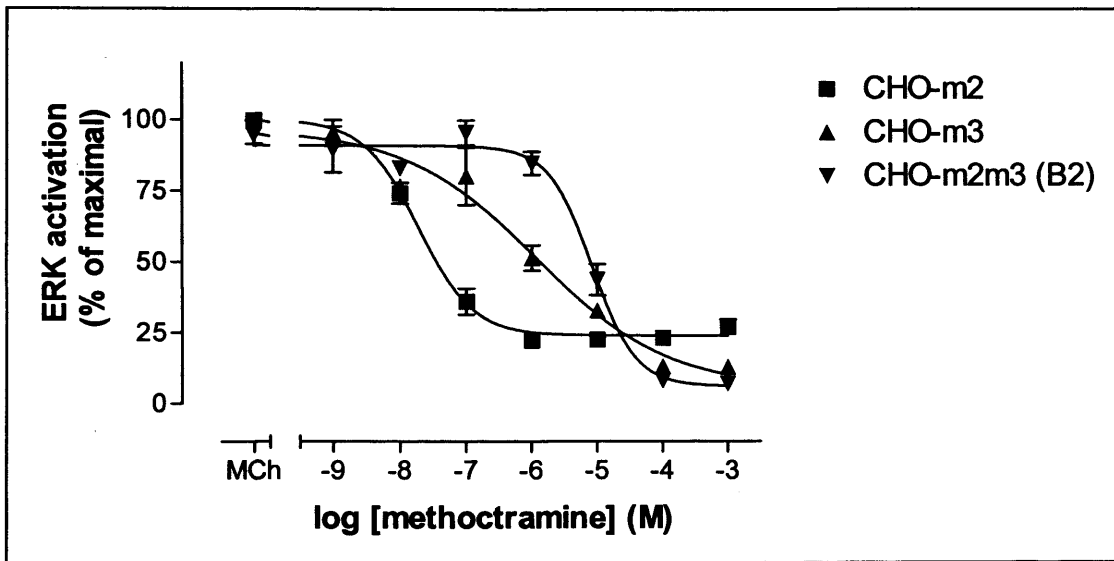


Figure 7.7 Methoctramine inhibition curves of MCh (10 μ M) stimulated ERK activation in CHO-m2, CHO-m3 and CHO-m2m3 (B2) cells. Data are shown as means \pm range for one experiment performed in triplicate.

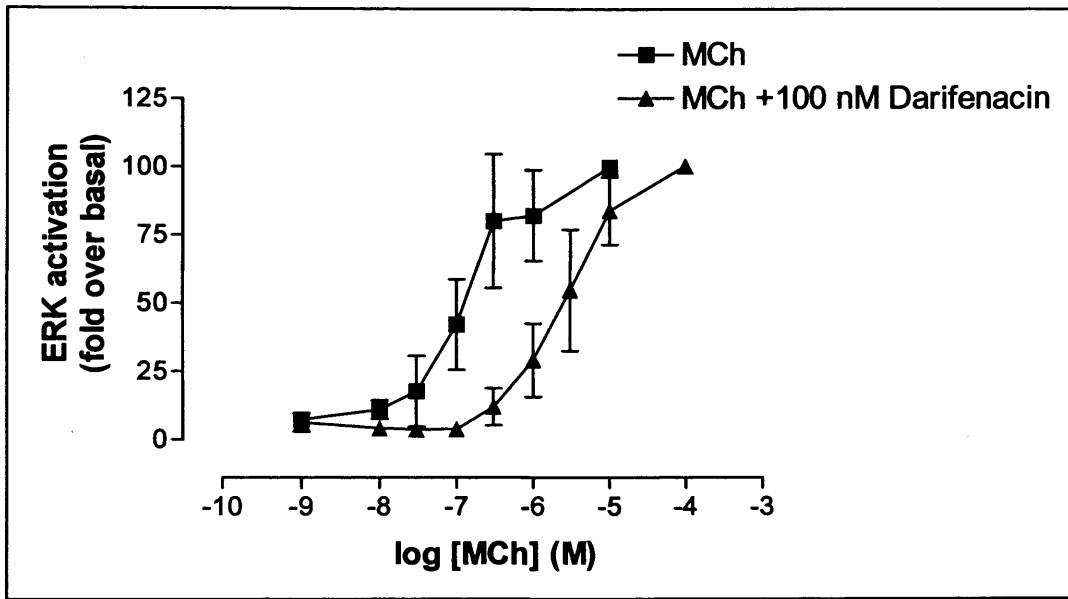


Figure 7.8 Darifenacin (100 nM) antagonism of MCh-stimulated ERK activation in CHO-m2m3 (B2) cells. Data are shown as means \pm S.E.M. for three separate experiments.

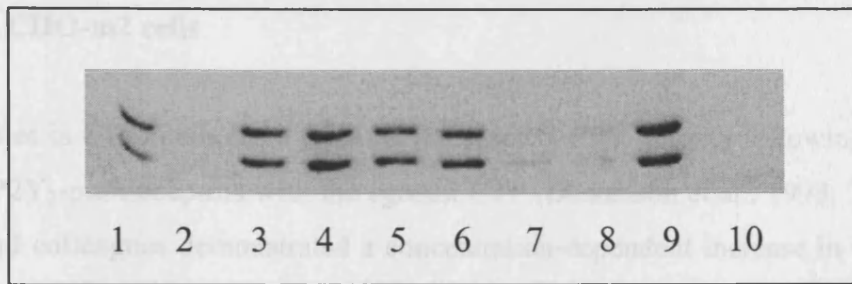


Figure 7. 9 Methoctramine antagonism of CCh (1 μ M, 5 min) stimulated ERK activation in BTSM slices. 1 μ M CCh alone and KHB in lanes 1 and 2, and 1 nM, 10 nM, 100 nM, 300 nM, 1 μ M and 10 μ M methoctramine antagonism of 1 μ M CCh in lanes 3-8 respectively. Lanes 9 and 10 show 1 μ M (duplicate) CCh alone and 10 μ M atropine (30 min prior to agonist) with 1 μ M CCh. Representative autoradiograph of Western blots for BTSM experiment samples showing phospho-ERK with the upper band in both panels representing ERK 1 (p44) and the lower panel ERK 2 (p42). The blot represents three other reproduced experiments with the same result.

the fold over basal, $n=3$). This compares to 100 μ M MCh activation in *in vitro* cells which gave an ERK activation increase of 11.8 ± 1.2 fold over basal ($n=3$).

Addition of UTP (10 μ M) and NCh (10 nM - 100 μ M) simultaneously to CHO-m2 cells caused an elevation in ERK activation (measured at 5 min) and a marked leftward shift of the curve as shown in Figure 7.11 ($P < 0.05$ Student's *t*-test, paired observations). 10 μ M UTP was selected as the concentration to be added simultaneously with MCh in order to investigate the stimulation of both G_{β} and G_{γ} proteins in the activation of ERK since it activated ERK via P2Y₂ receptors (*in vitro*), but caused only 40 % of maximal MCh-stimulated ERK activation.

As can be observed from Figure 7.11, concentration-dependent ERK activation following addition of MCh is significantly left-shifted (approx 10 fold) in the presence of 10 μ M UTP (pEC_{50} 5.43 ± 0.34 ; 6.37 ± 0.37 for MCh and MCh + UTP, respectively in CHO-m2 cells; $P < 0.05$ Student's two tailed *t*-test, paired observations). In these experiments, 10 μ M UTP causes a 2.8 ± 0.9 fold increase in basal ERK activation, and the maximal response to MCh decrease from 10.0 ± 2.2 to 13.9 ± 2.5 fold over basal.

7.2.3 Effects of co-stimulating mACh receptors and endogenous P2Y receptors on ERK activation in CHO-m2 cells

Previous studies in CHO cells have reported increases in ERK activity following stimulation of endogenous P2Y₂-purinoceptors with the agonist UTP (Dickenson et al., 1998; Tu et al., 2000). Dickenson and colleagues demonstrated a concentration-dependent increase in UTP-stimulated ERK activation and a time-course profile similar to that reported here for MCh stimulation of CHO-m2 or CHO-m3 cells, namely a rapid increase to peak activation at 5 min and a return to basal between 20-30 min. Therefore, by stimulating endogenous G_q-coupled P2Y₂ receptors with UTP in CHO-m2 cells it was possible to investigate whether co-stimulation of G_i- and G_q-coupled receptors in CHO cells caused 'sensitisation' of ERK activation, and hence a leftward shift of the concentration-response curve.

As can be observed from Figure 7.10, UTP elicited an increase in ERK activity at concentrations above 1 μ M in a concentration-dependent manner (pEC₅₀, 5.4 \pm 0.3 and a peak increase of 5.0 \pm 0.5 fold over basal, n=3). This compares to 100 μ M MCh activation in these cells which gave an ERK activation increase of 11.8 \pm 1.2 fold over basal (n=3).

Addition of UTP (10 μ M) and MCh (10 nM - 100 μ M) simultaneously to CHO-m2 cells caused an elevation in ERK activation (measured at 5 min) and a marked leftward shift of the curve as shown in Figure 7.11 (P < 0.05 Student's *t*-test, paired observations). 10 μ M UTP was selected as the concentration to be added simultaneously with MCh in order to investigate the stimulation of both G_i- and G_q- proteins in the activation of ERK since it activated ERK via P2Y₂ receptors (\approx EC₉₀), but caused only 40 % of maximal MCh-stimulated ERK activation.

As can be observed from Figure 7.11, concentration-dependent ERK activation following addition of MCh is significantly left-shifted (approx 10 fold) in the presence of 10 μ M UTP (pEC₅₀, 5.43 \pm 0.34; 6.51 \pm 0.31 for MCh and MCh + UTP, respectively in CHO-m2 cells; P < 0.05 Student's two tailed *t*-test, paired observations). In these experiments, 10 μ M UTP causes a 2.8 \pm 0.9 fold increase in basal ERK activation, and the maximal response to MCh increase from 10.0 \pm 2.2 to 13.9 \pm 2.5 fold over basal.

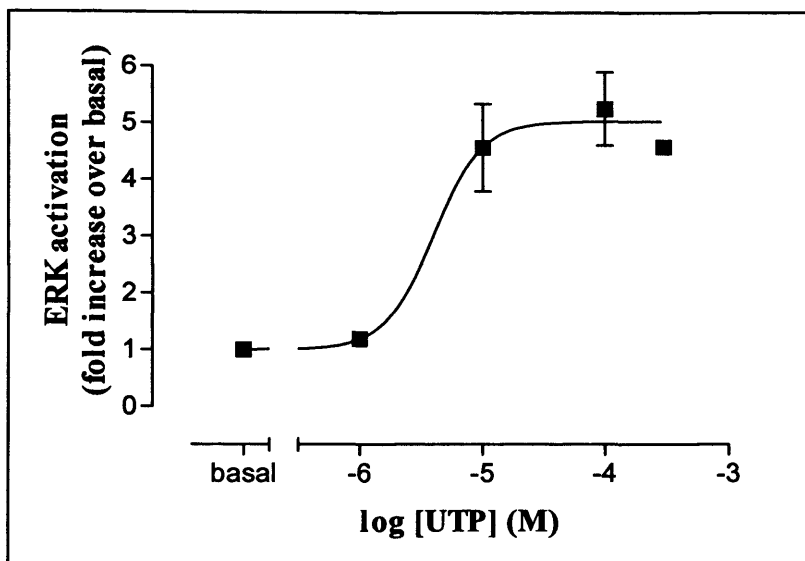


Figure 7.10 Concentration-response curve of ERK activation (5 min) following UTP stimulation in CHO-m2 cells, expressed as fold increase over basal. Data are shown as means \pm S.E.M for three separate experiments. Basal ERK activity was 403 ± 31 fmol ATP/min/mg

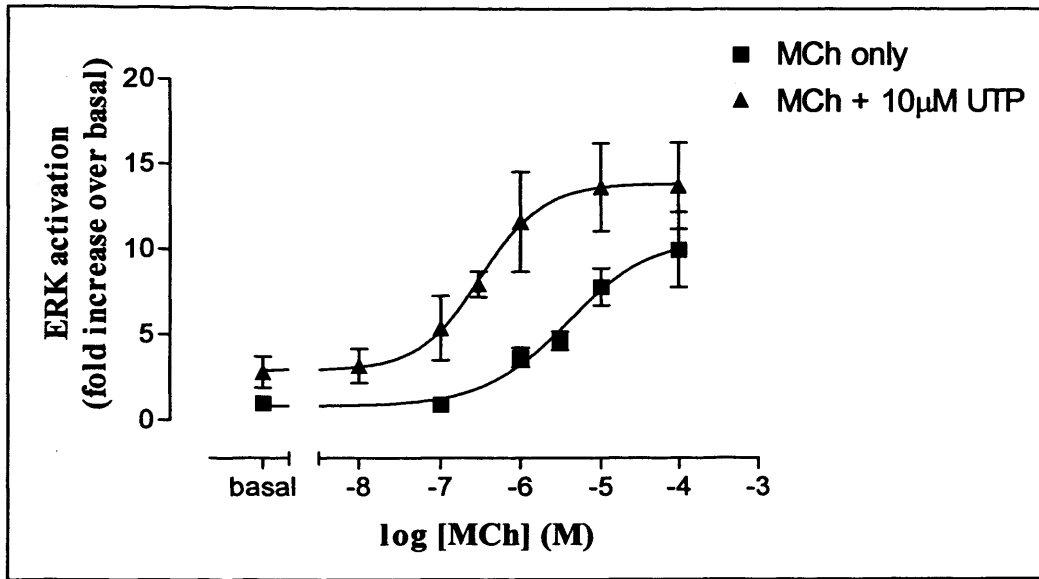


Figure 7.11 Concentration-response curves of peak ERK activation following MCh stimulation in the presence and absence of 10 μ M UTP in CHO-m2 cells, expressed as fold increase over basal. Data are represented as means \pm S.E.M. for three separate experiments.

Interestingly, the initial findings in the converse experiment, where the MCh concentration was kept constant and UTP concentrations varied, revealed only a slight leftward shift in the concentration-response relationship of peak ERK activation in CHO-m2 cells. However, further experiments will be needed to determine the true extent of this shift (Figure 7.12).

The UTP concentration-response curve was constructed in the presence of 500 nM or 1 μ M MCh since, as shown in Figure 7.11, these concentrations evoked an increase in ERK activation (\approx EC₃₀) which did not exceed the maximum increase observed for UTP alone. While the shift in EC₅₀ value is very modest (3.95 μ M, 1.35 μ M and 1.06 μ M for UTP, UTP + 500 nM MCh and UTP + 1 μ M MCh conditions respectively) it is possible to observe from Figure 7.12 that 1 μ M UTP alone evokes no increase in ERK activation in CHO-m2 cells (n=3), but in the presence of 500 nM MCh or 1 μ M MCh evoked an approx. half-maximal response.

Addition of MCh in the presence of 10 μ M UTP had no apparent effect on the ERK activation concentration-response relationship in CHO-m2m3 (B2) cells (n=1, data not shown). UTP (10 μ M) did not cause a leftward shift in the concentration-dependency relationship in CHO-m2m3 (B2) cells and this adds evidence to the fact that this synergy in ERK activation is cross-talk between G_i- and G_q-coupled receptors.

7.3 Discussion

The experiments summarised within this Chapter pharmacologically characterised the reported synergy in ERK activation upon co-activation of M₂ and M₃ receptors, and in the process uncovered some unexpected characteristics of the signalling pathways.

Effects of pertussis toxin pre-treatment on concentration-dependency of ERK activation

To establish whether the observed left shift of concentration-dependency in co-expressing CHO-m2m3 cells was due to cross-talk between M₂ and M₃ mACh receptors, CHO-m2m3 (B2) cells were PTX pre-treated to uncouple the M₂ (G_i) receptor. Using CHO-m2 cells, data confirmed that PTX completely abolished ERK activation by the m2 receptor. PTX pre-treatment of co-expressing cells (Figure 7.3) shows that the maximal ERK activation in CHO-m2m3 (B2) cells

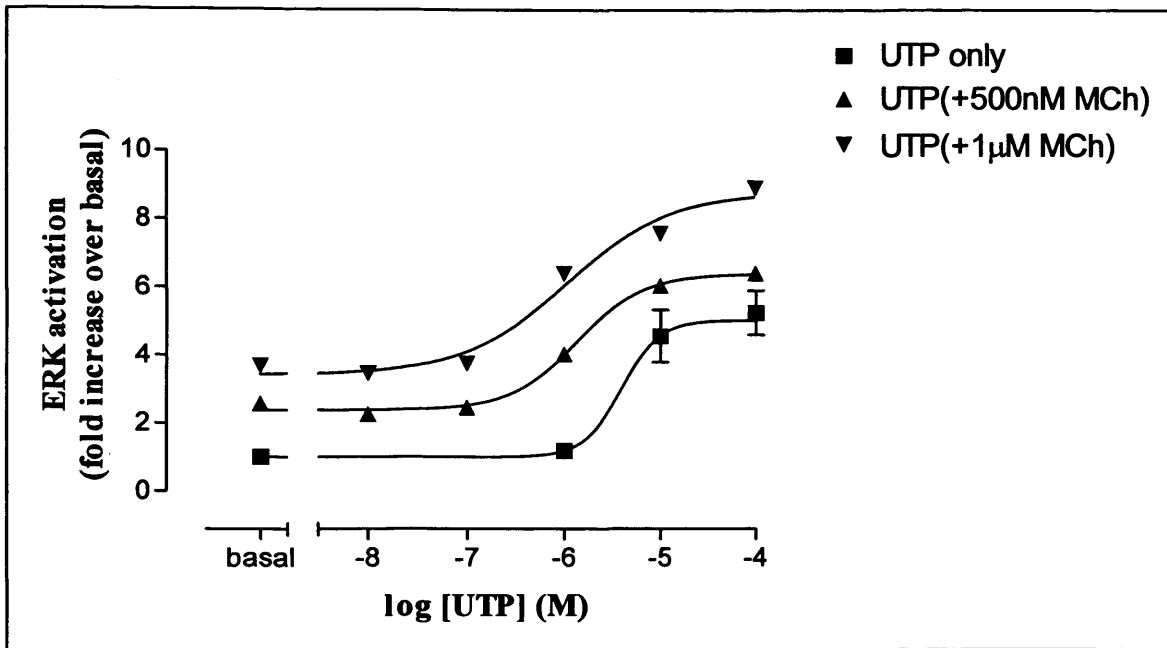


Figure 7.12 Concentration-response curves of peak ERK activation following UTP stimulation in the presence and absence of 500 nM or 1 μ M MCh in CHO-m2 cells, expressed as fold increase over basal. Data are shown as means \pm S.E.M. for UTP (n=3), and are mean from one preliminary experiment for UTP + 500 nM MCh and UTP + 1 μ M MCh.

appeared to be a summation of M_2 - and M_3 - mediated ERK responses. Surprisingly, although PTX treatment of CHO-m2m3 (B2) cells reduced the maximal ERK activation to a similar level to that in PTX-untreated or -treated CHO-m3 cells it did not rightward shift the MCh-stimulated ERK activation EC_{50} value, towards that for M_3 -mediated response (pEC_{50} , -PTX, 7.17 ± 0.09 ; +PTX, 7.93 ± 0.47 in CHO-m2m3 (B2) cells). However, this result could be explained by analysis of PTX pre-treatment upon MCh-induced ERK activation in CHO-m3 cells (Figure 7.2) which revealed another surprising result. At maximally effective MCh concentrations ($100 \mu\text{M}$) the ERK activation was partially inhibited (10-40% across 4 experiments) by PTX treatment in CHO-m3 cells. This correlated with Wylie et al. (1999) who reported maximal MCh ($100 \mu\text{M}$) stimulated ERK activation in CHO-m3 cells to be partly PTX-sensitive ($\approx 50\%$). Although Budd et al. (1999) reported MCh (1 mM) stimulated ERK activation in CHO-m3 cells to be PTX-insensitive, re-analysis of Figure 5 in their paper revealed a decrease (33%) in basal ERK activation in PTX pre-treated cells; taking this decrease into account it could be estimated that an approx. 50 % decrease in ERK activation levels actually occurred correlating with the data of Wylie et al. (1999). Although, G_q -coupled ERK activation by the M_3 receptor appears to be partly PTX-sensitive at high agonist concentration, van Biesen et al. (1996) also reported that activation of the M_1 receptor, classically coupled to $G_{q/11}$, activates ERK via G_o protein (PTX sensitive) in a PKC-dependent, Ras-independent manner in CHO cells. It has also been shown in these CHO-m3 cells that MCh stimulates activation of $G_{q/11}$ and $G_{i/o}$ proteins (particularly $Gi3\alpha$, Akam et al., 2001).

Observation of the effect of PTX on the complete concentration-dependency curve for MCh-stimulated ERK activation in CHO-m3 cells reveals a more complex signalling pathway than can be explained by a simple promiscuity of M_3 receptors coupling to both $G_{q/11}$ and $G_{i/o}$ proteins (Figure 7.2). At sub-maximal MCh concentrations there was a marked enhancement of ERK activation following PTX pre-treatment, manifested as an approx. 70 fold leftward shift of EC_{50} value. These data suggest that uncoupling of $G_{i/o}$ proteins 'sensitises' ERK activation to M_3 receptor stimulation. Hence $G_{i/o}$ activity stimulated by M_3 receptor activation may have an inhibitory effect on M_3 receptor $G_{q/11}$ -mediated ERK activation.

This unexpected effect of PTX in CHO-m3 cells may account for the effect of PTX treatment in CHO-m2m3 (B2) cells. Concentration-dependency curves for MCh-stimulated ERK activation in PTX pre-treated CHO-m3 and PTX-untreated CHO-m2m3 (B2) cells overlies each other

(pEC₅₀, 7.84 ± 0.20 and 7.93 ± 0.47 for CHO-m3 +PTX and CHO-m2m3 (B2) respectively). It is also noteworthy, that PTX-treatment did not affect maximal peak ERK activation (5 min) in CHO-m3 cells but decreased the maximal MCh-stimulated ERK activation increase in CHO-m2m3 (B2) cells to same levels as CHO-m3 cells (approx. 15 fold over basal, c.f. Figures 6.3, 7.2 and 7.3). Therefore the co-activation of M₂ receptors and M₃ receptors (in CHO-m2m3 (B2) cells) appears to result in the same ERK activation as stimulation of PTX pre-treated CHO-m3 cells. Activation of the M₂ receptors potentially 'traffics' G_i protein towards other effector outcomes than M₃ receptor activation of G_i proteins. Activation of M₂ receptors in CHO-m2m3 cells may actually 'sequester' the G_i protein from activated M₃ receptors and therefore exert a functional effect similar to PTX treatment in CHO-m3 cells. A diagram summarising this theory is shown in Figure 7.13.

Akam et al. (2001), using [³⁵S]-GTPγS binding/immunoprecipitation methodology, showed that MCh activated Gα_{i1/2/3} but not Gα_o or Gα_{q/11} in CHO-m2 cells and they also showed MCh activated Gα_{q/11} and Gα_{i3/0} but not Gα_{i1/2} or Gα_o proteins in CHO-m3 cells. Based on these observations, it is possible to suggest that G_{i3} proteins mediate the MCh-stimulated pathway inhibiting ERK activation in CHO-m3 cells. Blaukat et al. (2000), studied co-operation of Gα_{q/11} and Gα_{i/0} signalling in ERK activation by bradykinin and M₃ receptors in HEK293 cells, and concluded that co-activation of Gα₁₁ and Gα_{i2} caused the greatest ERK activation. Future investigations should include studying the effects of PTX on MCh-stimulated [³⁵S]-GTPγS binding in CHO-m3 cells to determine whether G protein coupling preferences of M₃ receptors are altered by PTX treatment. However, Wylie et al. (1999) reported no effect of PTX (24 h, 100 ng/ml) on M₃ receptor-mediated IP₃ mass accumulation, indicating PTX pretreatment does not result in more efficient coupling to G_q, at least with respect to PLC regulation.

Pharmacological dissection of M₂- and M₃- receptor components of MCh-stimulated ERK activation in CHO-m2, CHO-m3, CHO-m2m3 (B2) cells and BTSM tissue slices

As an alternative to PTX-treatment, selective muscarinic antagonists were used in an attempt to dissect the contribution of M₂ and M₃ receptors to ERK activation in CHO-m2m3 (B2) cells. Cheng-Prusoff analysis of darifenacin inhibition of MCh (10 μM) stimulated ERK activation

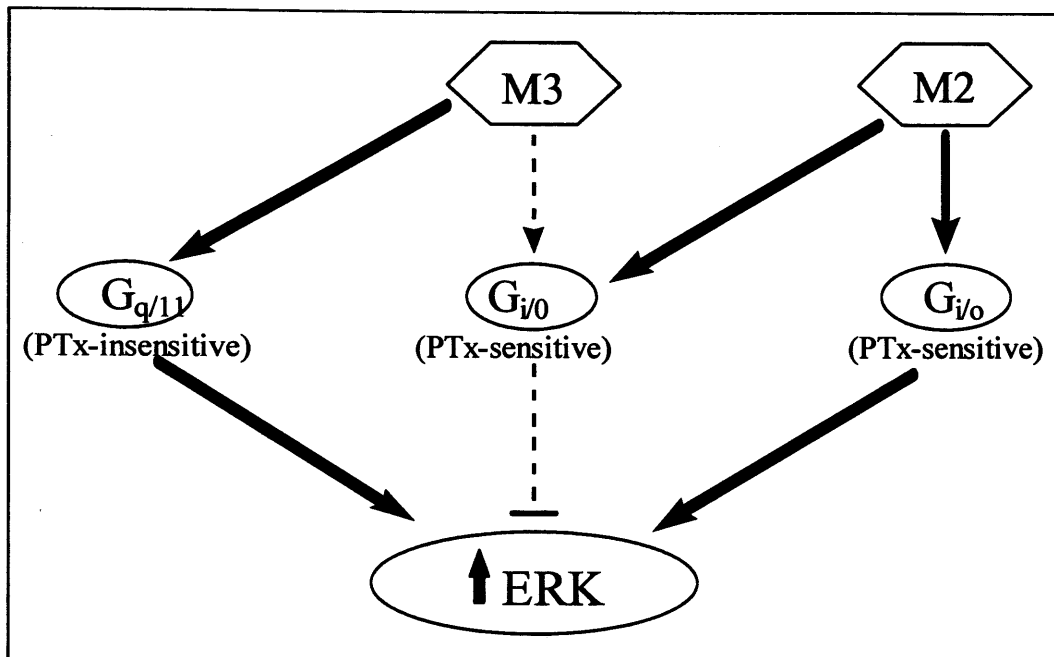


Figure 7.13 Diagram summarising the potential pathways linking M₂ and M₃ receptor activation and G protein subtype and ERK activation, and the effect of PTX treatment. Dashed lines represent proposed promiscuous coupling of M₃ receptors to G_i proteins following agonist challenge. Solid lines represent classical preferential G-protein coupling.

revealed a modest 'selectivity window' between CHO-m2 and CHO-m3 cells (pK_i 7.28 ± 0.38 and 7.97 ± 0.23 for CHO-m2 and CHO-m3 cells, respectively). Studies in CHO-m2m3 (B2) cells revealed pK_i values more similar to those from CHO-m3 cells (8.38 and 8.09 for experiments using 10 μ M and 250 nM MCh, respectively).

By observing Figures 7.6 and 7.7 it is possible to see that supra-maximal MCh (10 μ M) stimulated ERK activation in CHO-m2m3 (B2) cells was completely inhibited by darifenacin at concentrations above 1 μ M, however 0.1 μ M darifenacin caused $\approx 50\%$ inhibition of EC_{80} (10 μ M MCh) response in CHO-m2 and CHO-m3 cells, but complete attenuation of the EC_{80} response (250 nM MCh) in CHO-m2m3 (B2) cells. These data appear to suggest that greater than 50% contributions from each receptor activation are required for synergistic effects to be observed.

An initial experiment, investigating the sustained time-course, involved inhibition of the M_2 -mediated component of the ERK response by tripitramine in the CHO-m2m3 (B2) cells. Results suggested that although the 5 min peak was partially attenuated, the sustained response at 30 min was not affected by 100 nM tripitramine (data not shown). This result may imply that only partial activation of the M_2 signalling pathway simultaneously with M_3 activation of ERK was sufficient for the sustained time-course. It will therefore be intriguing to observe what occurs when the reciprocal experiment is performed using an M_3 over M_2 selective antagonist (darifenacin) to observe the effect on the sustained response.

Despite some tantalising glimpses of the possible mechanisms underlying M_2/M_3 interactions in CHO-m2m3 (B2) cells it must be concluded that the mACh receptor antagonists used here did not (and perhaps could not) satisfactorily separate the contributions of the two receptor components.

Effects of co-stimulating mACh receptors and endogenous P2Y receptors on ERK activation in CHO-m2 and CHO-m2m3 (B2) cells

UTP stimulation of CHO-m2 cells caused a concentration-dependent ERK activation which correlated well with previously published data (pEC_{50} , 5.80, 5.40 ± 0.34 , and approx. E_{max} . 4 and 5 fold for Dickenson et al. (1998) and this study respectively). Co-activation of both

endogenous PTX-insensitive P2Y₂ receptors and M₂ receptors enhanced the ERK signal. Analysis of this concentration-dependence showed a marked left shift (≈ 10 fold) of the EC₅₀ value for MCh-stimulated ERK activation in the presence of UTP (1 μ M) compared to MCh alone.

Dickenson et al. (1998) reported synergistic increases in ERK activation in CHO-A1 cells upon co-activation of G_i (adenosine A₁) and G_q (P2Y₂) coupled receptors, where maximal ERK activation from co-stimulation of A₁ adenosine and P2Y₂ receptors was greater than the sum of the two individual signals. Interestingly, they also reported partial PTX sensitivity of maximal ERK activation from P2Y₂ receptors (traditionally preferentially G_q coupled) as previously reported for M₃ receptors in CHO cells (Wylie et al., 1999; Budd et al., 1999). However Tu and colleagues demonstrated a PTX-insensitive P2Y₂-mediated ERK activation in C6 glioma cells (Tu et al., 2000). It would be interesting to observe if PTX pre-treatment affected the UTP concentration-response curve, as it may be expected to left-shift if P2Y₂ receptors mimic M₃ receptor coupling. These UTP findings, together with the result that UTP did not shift the EC₅₀ for MCh-stimulated ERK activation in CHO-m2m3 (B2) cells showed the observed synergy in ERK activation is due to cross-talk between G_i- and G_q-mediated signalling pathways and is not specific to M₂ receptor interactions with M₃ receptors .

The augmentation of ERK activation in CHO-m3 cells by uncoupling the M₃ receptor from G_i protein interaction, by using PTX, reveals that the synergy observed in co-expressing CHO-m2m3 (B2) cells involves a complicated balance between G protein effects upon MAPK signalling. It would be interesting to study the effect of PTX in a second M₃-expressing CHO clone (CHO-m3vt-9) with a lower receptor expression to observe if the observed promiscuous coupling of M₃ receptors is a consequence of over-expression in this model or is an inherent property of all M₃ receptors.

It is important to discover the mechanism by which the M₂ and M₃ signalling pathways interact to facilitate ERK activation. Chapters 3 and 4 revealed no evidence for synergy in second messenger generation in CHO-m2m3 (B2) cells and Wylie et al. (1999) reported no effect of PTX on IP₃ generation (time-course or concentration-response) in CHO-m3 cells, implying that the M₃ signalling via G_i protein apparently to suppress ERK activation at low agonist concentrations does not suppress G_q coupling to PLC activation. Thus, the increased potency of

MCh in PTX-treated cells appears to be selective for the ERK pathway and independent of PLC activation.

Interestingly, the potency of MCh-induced ERK activation in PTX-treated CHO-m3 cells is similar to that observed in non-PTX-treated CHO-m2m3 (B2) cells. Thus, co-expression of the M₂ receptors appears to have a similar effect on M₃ receptor-mediated ERK activation as PTX treatment alone. One possibility is that co-expression of the M₂ receptor effectively uncouples the M₃ receptor from G_i proteins in the cell, thereby enabling the M₃ receptor exclusively to link to G_q protein. This appears to allow the M₃ receptor to couple more effectively to the ERK pathway via PTX-insensitive G proteins. G_i-coupling to the M₃ receptor is therefore functionally inhibitory to M₃ mediated ERK activation. However, this is in contrast to M₂ receptor-mediated activation of ERK, which is entirely G_{i/o} mediated.

Clearly, it is necessary to establish the biochemical route by which M₂ and M₃ receptors activate ERK. One point of potential convergence of the M₂- and M₃-mediated signalling pathways is at the level of PKC. For example, Wylie et al. (1999) reported that MCh-stimulated ERK activation in CHO-m2 and CHO-m3 cells is PKC-dependent. Co-activation of these receptors may therefore facilitate a more complete activation of one or more isoforms of PKC at agonist concentrations that are submaximal when only one receptor subtype is activated. Clearly, in order to test this hypothesis, it would be necessary to characterise the PKC isoforms expressed in CHO cells and to determine which translocate to the plasma membrane at low agonist concentrations in CHO-m2m3 cells. However, synergistic ERK activation by P2Y₂ and A1 receptors in CHO cells appears to be PKC-independent (Dickenson et al., 1998), suggesting that alternative mechanisms may account for the cross-talk observed in CHO-m2m3 cells.

It has previously been reported that Raf activation by Ras is an important point of convergence of G_i- and G_q-coupled receptor co-activation of ERK (Adomeit et al., 1999; Blaukat et al., 2000). Assays are available to measure activation of Ras and isoforms of Raf, and these would provide important clues to the mechanism of ERK activation by M₂ and M₃ receptors in CHO-m2m3 cells. It is important to note that PKC can enhance GTP loading on Ras and activate Raf in a number of cell types (Marais et al., 1998). Identification of the PKC isoforms activated by M₂ and M₃ receptors may well reveal the mechanism by which co-activation of these muscarinic receptors enhances Ras-Raf activation of the ERK cascade.

Chapter 8: Final discussion

The aims of the studies described in this Thesis were to investigate whether agonist-induced co-activation of M₂ and M₃ muscarinic acetylcholine receptors, when co-expressed in CHO cells, differed from the summation of their activation when each receptor is individually expressed. It was hoped that these studies would provide an insight into possible interactions / cross-talk occurring between M₂ and M₃ receptor signalling when co-expressed, as occurs in a number of smooth muscle tissues.

[³H]-NMS displacement radioligand binding studies, with subtype-selective antagonists, revealed M₂ and M₃ sub-populations in a 1:3 (M₂:M₃) ratio in the CHO-m2m3 (B2) cells. Measurements of cAMP accumulation and IP₃ mass demonstrated CHO-m2m3 (B2) cells to contain functionally coupled M₂ and M₃ receptors, and importantly, single cell Ca²⁺ imaging provided clear evidence for the successful M₃ co-transfection and expression into all the parent CHO-m2 cells.

Agonist-activation of CHO-m2 cells evoked increases in [Ca²⁺]_i, [³H]-IP_x accumulation, [³H]-thymidine incorporation, ERK activation and an inhibition of cAMP accumulation. In comparison agonist-activation of CHO-m3 cells induced increases in IP₃ mass and [³H]-IP_x accumulations, [Ca²⁺]_i, ERK and JNK activation, a biphasic cAMP accumulation and an inhibition of [³H]-thymidine incorporation into DNA. Studies in co-expressing CHO-m2m3 (B2) cells revealed-agonist induced responses which largely recapitulated those mediated by M₃-receptor activation with respect to IP₃ mass and [³H]-IP_x accumulation, ERK and JNK activation. Studies in CHO-m2m3 (B2) cells of agonist-induced inhibition of [³H]-thymidine incorporation demonstrated a balance between M₂-mediated stimulatory and M₃-mediated inhibitory signalling effects, with greater concentrations of mACh receptor agonist required to evoke maximal inhibition under serum-starved conditions.

Measurements of MCh effects on forskolin (FK) stimulated cAMP accumulation and ERK activation in CHO-m2m3 (B2) cells provided some evidence for cross-talk between M₂ and M₃ receptor-stimulated signalling pathways. MCh stimulation of CHO-m2m3 (B2) cells caused a biphasic modulation of FK-stimulated cAMP accumulation (inhibition at low agonist concentrations and stimulation at high agonist concentrations). It was shown that the M₂

inhibitory component is synergised at low agonist concentrations by a M_3 -receptor mediated increase in intracellular Ca^{2+} causing an inhibition of adenylyl cyclase (potentially through Ca^{2+} -inhibited AC subtypes V and VI, Sunahara et al., 1996).

There was no evidence for cross-talk between co-expressed M_2 and M_3 receptors at the level of Ca^{2+} release, with CHO-m2m3 cells exhibiting the same characteristics as CHO-m3 cells (rapid, large agonist-induced increase in intracellular Ca^{2+}), compared to a modest agonist-induced response in CHO-m2 cells. However, it was noteworthy that M_2 -mediated Ca^{2+} release does not appear to be PLC-mediated and is *inhibited* in the presence of a normal extracellular Ca^{2+} concentration. Since PIP_2 hydrolysis does not appear to be involved, it will be interesting to determine the exact mechanism of Ca^{2+} release in CHO-m2 cells, (one possibility is the involvement of sphingosine kinase) and also if the mechanism is the same in both the presence and absence of Ca^{2+} .

The clearest evidence for cross-talk between co-expressed M_2 - and M_3 -receptors was observed in measurements of ERK activation. MCh stimulated a sustained ERK response in CHO-m2m3 (B2) cells, which remained elevated beyond 60 min, and mimicked the time-course profile of CCh-induced ERK activation in BTSM slice preparations. Measurements of the concentration-dependence of ERK activation also revealed a marked leftward shift in EC_{50} value (≈ 50 fold) in CHO-m2m3 (B2) cells compared to that found in either CHO-m2 or CHO-m3 cells. Importantly, the sustained ERK activation and low EC_{50} value observed in CHO-m2m3 cells were also characteristics of agonist activation of mACh receptors co-expressed in BTSM tissue. This leftward shift observed in CHO-m2m3 cells was shown not to be specific to M_2 - and M_3 -receptor cross-talk, but potentially a more general phenomenon of G_i and G_q protein co-activation, as G_i/G_q co-stimulation of CHO-m2 cells with MCh and UTP (fixed concentration) respectively, co-activating M_2 (G_i -coupled) and endogenous P2Y (G_q -coupled) receptors, also caused a leftward shift in the concentration-dependence relationship. The lower EC_{50} value observed in CHO-m2m3 (B2) was similar to that observed in BTSM slice preparations ($EC_{50} < 100$ nM) where M_2 and M_3 receptors are endogenously co-expressed. Interesting unexpected signalling phenomena were also unmasked with respect to ERK activation in PTX-treated cells. As expected, PTX completely attenuated MCh-stimulated ERK activation in CHO-m2 cells. In CHO-m2m3 (B2) cells, PTX pre-treatment reduced maximal ERK activation by agonist, but did not affect the concentration-dependency. However, MCh-stimulated ERK activation in CHO-

m3 cells was markedly left-shifted following PTX pre-treatment and the concentration-dependency relationship shifted over that for untreated CHO-m2m3 (B2) cells. Hence, the M₃-mediated activation of ERK appears to have a PTX-sensitive (G_i) inhibitory component, which is overcome by a PTX-insensitive (G_q-driven) signal at higher agonist concentrations. It is known that over-expressed receptors can couple promiscuously to G proteins (Gudermann et al., 1997). Akam et al. (2001) reported M₃ receptors could couple to both G_{q/11} and G_{i3} proteins, (determined using [³⁵S]-GTPγS binding and immunoprecipitation techniques) when expressed in CHO cells at similar levels to those reported in this thesis (2.5 ± 0.1 and 3.7 ± 0.4 pmol/ mg protein for Akam et al. (2001) and this report, respectively).

Therefore, future studies investigating PTX treatment in lower expressing M₃ clones (e.g. CHO-m3vt-9, 160 ± 8 fmol/mg protein) could reveal if the PTX-sensitive component of the M₃-mediated ERK activation is due to high expression receptor promiscuity, since it has been proposed that over-expression may cause receptor-G protein coupling infidelity (Gudermann et al., 1997). Also Cordeaux et al. (2000), reported Adenosine A₁ (traditionally G_i-coupled) receptor stimulation of IP_x accumulation via both pertussis toxin-sensitive and -insensitive G proteins in an expression level-dependent manner when expressed in CHO cells.

The point of interaction between the M₂ and M₃ receptor signalling pathways leading to synergistic ERK activation could occur at many loci in the downstream cascade (see Figure 8.1). This Thesis has provided evidence for both M₂ and M₃ signalling pathways mediating intracellular Ca²⁺ release, cAMP accumulation, IP_x accumulation and ERK activation, indicating that the signalling from these receptors is not as simple as classically reported (with respect to regulation of AC and PLC, respectively). However, there was no evidence of sensitisation /synergy of the responses at the level of traditional second messenger molecule production (cAMP, IP_x or Ca²⁺) implying that the position of interaction/ cross-talk is further downstream between second messenger generation and the MAPK cascade or indeed is independent of traditional second messenger generation.

GPCR signalling to activation of MAPKs has been reported to be cell type and receptor-specific, utilising Ras-dependent or -independent mechanisms (for reviews see Malarkey et al., 1995; Gutkind, 1998; Lopez-Illasca, 1998). It has been shown that G_i-coupled receptors can activate ERK through PTX-sensitive pathways by utilising Gβγ subunits (Crespo et al., 1994b; Hawes et

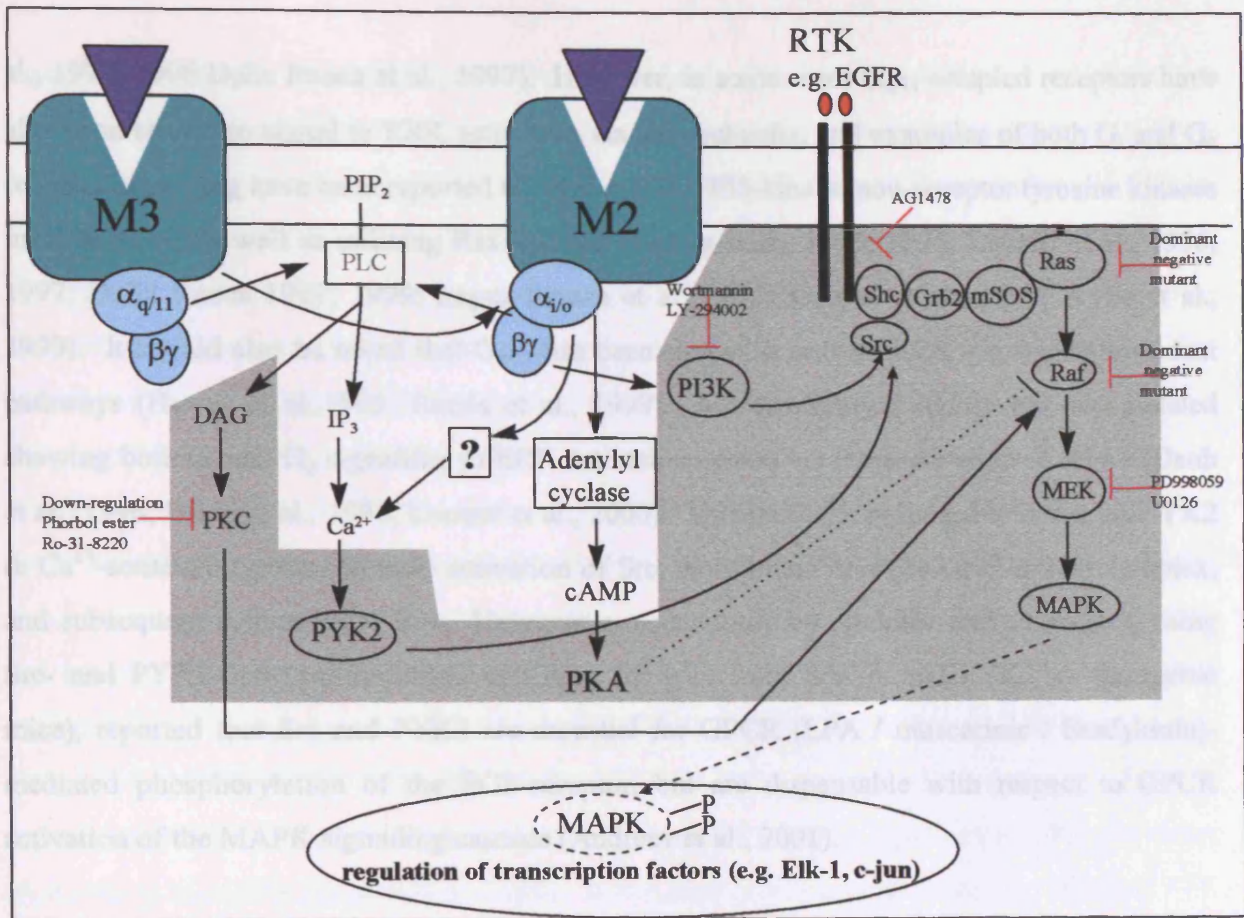


Figure 8.1. Possible points of interaction (shaded area) for convergence of activated M₂ and M₃ signalling pathways leading to synergistic ERK activation. Red lines indicate potential areas for future studies to further dissect these GPCR to MAPK pathways and synergistic ERK response.

With this plethora of possibilities for interactions between the pathways from M₂ and M₃ receptors, it will be important firstly to define the exact pathways utilised by the receptors (see Figure 8.1), and then to accumulate evidence to define the point of cross-talk between the two

al., 1995; 1996 Della Rocca et al., 1997). However, in some cases $G_{q/11}$ -coupled receptors have also been shown to signal to ERK activation via $G\beta\gamma$ subunits, and examples of both G_i and G_q receptor signalling have been reported to involve PKC, PI3-kinase, non-receptor tyrosine kinases including Src, as well as utilising Ras and Raf (Hawes et al., 1995; 1996; Luttrell et al., 1996; 1997; Della Rocca 1997; 1999; Lopez-Illasaca et al., 1997; Graneß et al., 1998; Wylie et al., 1999). It should also be noted that $G_{q/11}$ has been shown to activate ERK via Ras-independent pathways (Hawes et al., 1995; Emala et al., 1999). More recently evidence has accumulated showing both G_i and G_q signalling to ERK activation occurs via transactivation of RTKs (Daub et al., 1996; Dikic et al., 1996; Leserer et al., 2000). This has been proposed to occur via PYK2 (a Ca^{2+} -sensitive tyrosine kinase) activation of Src, recruitment of a Src-Grb2-mSOS complex, and subsequent activation of Ras. However a recent study by Andreev and colleagues, using Src- and PYK2-deficient fibroblast cell-lines (derived from Src $-/-$ and PYK2 $-/-$ transgenic mice), reported that Src and PYK2 are essential for GPCR (LPA / muscarinic / Bradykinin)-mediated phosphorylation of the EGF-receptor, but are dispensable with respect to GPCR activation of the MAPK signalling cascade (Andreev et al., 2001).

More specifically, studies of muscarinic receptor activation of MAPK have demonstrated similar trends to those detailed for GPCRs in general, with some contradictory evidence. PTX-insensitive muscarinic receptor activation (M_1 or M_3) has demonstrated $G_{q/11}$ signalling to ERK activation via PKC-dependent or independent, Ca^{2+} -independent mechanisms and involving Ras and / or transactivation of EGF receptors (Crespo et al., 1994a; Hawes et al., 1995; Mitchell et al., 1995; Tsai et al., 1997; Felsch, 1998; Kim et al., 1999; Wylie et al., 1999; Slack, 2000; Budd et al., 2001). Studies of PTX-sensitive muscarinic receptor (M_2) mechanisms have reported G_i -mediated ERK activation by $G\beta\gamma$ subunit-, PI3-kinase and /or PKC-dependent, Ras and Raf dependent pathways (Crespo et al., 1994b; Mitchell et al., 1995; Kim et al., 1999; Wylie et al., 1999). However, it is now thought that GPCR signalling to MAPK may be more complicated than described above, as M_3 receptors have been reported to signal to ERK activation by two pathways, including a PKC-dependent and -independent component (Slack, 2000; Budd et al., 2001; Adomeit et al., 1999).

With this plethora of possibilities for interaction(s) between the pathways from M_2 and M_3 receptors, it will be important firstly to define the exact pathways utilised by the receptors (see Figure 8.1), and then to accumulate evidence to define the point of cross-talk between the two

signalling pathways. This can be achieved by extension of the present studies to measurements of Raf-1 kinase and MEK activity which may disclose if the synergy is occurring within the MAPK cascade, or more likely it will be important to examine the involvement of (i) PKC / PI3-kinase (PKC inhibited by Ro-31-8220 or down-regulation by chronic phorbol ester treatment; PI3-kinase inhibited by wortmannin or LY294002), (ii) transactivation (by measuring phosphorylation of the EGFR or inhibition by AG1478), as well as utilising Ras and Raf dominant-negative mutants. It will be important to investigate the activation of Raf-1 because although it has been reported to be phosphorylated and activated by PKC isoforms (Kolch et al., 1993) it is also known that PKA activity may inhibit ERK signalling through PKA inhibition of Raf-1 kinase activity (for reviews see Houslay and Kolch, 2000; Kolch, 2000). Hence, it will also be interesting to establish the contribution of cAMP levels and hence PKA activity in M₂ and M₃ receptor-stimulated ERK activation as both receptors were shown to modulate cAMP accumulation. PKA phosphorylates Raf-1 on Ser-43 and this is believed to inhibit Ras-Raf interaction and hence activation (Wu et al., 1993). It has also been reported that the Ras-Raf complex is a point for convergence of G_i- and G_q- coupled receptor signalling to ERK activation (Adomeit et al., 1999; Blaukat et al. 2000). It will also be valuable to assess the effect of PTX treatment on the time-course of MCh-stimulated ERK activation in CHO-m3 cells, since PTX caused a leftward shift in concentration-response in CHO-m3 cells to overlie CHO-m2m3 cells. Hence it will be important to determine if the sustained time-course is a phenomenon of M₃/G α_q stimulation of ERK, which is suppressed by G α_i co-activation.

The phenomenon of muscarinic receptor cross-talk at the level of ERK activation is potentially very important because the longevity of ERK activation has been implicated in determining cell fate (for review see Marshall, 1995). Marshall discussed the possibility that transient ERK activation causes cell proliferation, whereas sustained ERK activation results in differentiation in some cell types. However, it appears as though these important cell fate decisions are unlikely to be attributable simply to the longevity of ERK activation reported in Chapter 6. Thus, while agonist-stimulation of CHO-m2 and CHO-m3 cells induced very similar transient ERK activation profiles, these receptors mediate opposing effects on cell proliferation (as measured by [³H]-thymidine incorporation into DNA, see Chapters 5 and 6). It is noteworthy that in those cell lines exhibiting agonist-induced JNK activation (CHO-m3 and CHO-m2m3 (B2)), agonist-induced inhibition of [³H]-thymidine incorporation is also observed. Although, at present there are no commercially available JNK inhibitors, two compounds have recently been

reported specifically to inhibit JNK, namely CEP-1347 (Maroney et al., 1998; 1999) and SP 600125 (Xia et al., 2000) and these compounds, along with the p38 inhibitor SB 203580, may prove to be useful tools in determining the potential roles of JNK and p38 activation in cell cycle progression.

Future studies should include assessment of the effects of inhibition of ERK activation (through MEK1 inhibition using U0126 or PD98059) on cell proliferation ($[^3\text{H}]$ -thymidine incorporation), as JNK activation may be causing an inhibition of cell proliferation countering ERK-mediated cell proliferation. Hence, M_2 -mediated increases in $[^3\text{H}]$ -thymidine incorporation may be mediated by ERK activation. Recent work by Kao and colleagues, in PC12 cells, has shown that differences in cell proliferation and differentiation responses from EGF and PDGF stimulation are caused by differential phosphorylation of scaffold proteins mediating Rap1 activation, and subsequent activation of ERK mediated by B-Raf (Kao et al., 2001).

Assessment of pharmacological agents

As Table 8.1 summarises, the selectivity window for the mACh receptor antagonists studied here varied markedly between the different assays performed. Antagonist dissection of ERK activation proved problematic, and although tripitramine appears to have the greatest selectivity window (M_2 over M_3 , binding) other antagonists provided a workable discrimination in some assays (e.g. darifenacin pIC_{50} for cAMP, 5.6 and 8.0 at M_2 and M_3 , respectively). However, it should be noted that selectivity with darifenacin was particularly poor in $[\text{Ca}^{2+}]$ FLIPR experiments, where it was not possible to use this agent to discriminate between M_2 and M_3 receptors.

These differences in selectivity between assays may be due to differences in experimental protocols and hence agonist/antagonist incubation times. In experiments with greater than 20 min agonist/antagonist interaction time (binding, cAMP accumulation, thymidine incorporation) antagonists affinities are closest to their published displacement binding pK_i values (Maggio et al., 1994; Eglen and Watson, 1996b; Hedge et al., 1997). However, these values deviate further from reported values (where interaction time is ≥ 1 h) with less agonist / antagonist interaction time, for example ERK activation (5 min) or $[\text{Ca}^{2+}]_i$ release (measured at 3-15 s) compared to

binding (≥ 1 h). Meloy et al. (2001) studied an extensive range of muscarinic receptor antagonists in rat submaxillary gland and noted difficulties with data generated with darifenacin. They reported pseudo-irreversible antagonism with darifenacin after observe a collapse of concentration-effect curves with decreased E_{max} values with higher darifenacin concentrations, which could be overcome with multiple exposures to agonist over a long period of time.

While it was possible to use these pharmacological antagonists for displacement binding studies and for dissection of cAMP and [3 H]-thymidine responses, they are not sufficiently selective to achieve satisfactory discrimination in studies to delineate the mechanisms of M_2 and M_3 receptor cross-talk. Future work to investigate the observed cross-talk could involve selective alkylation of one receptor subtype (e.g. protect M_2 receptor population with tripitramine), however these experiments would be laborious due to the need for careful receptor population determination. A more sophisticated protocol would be to use expression of an inducible M_3 receptor within the parent CHO-m2 cell line (using e.g. LacSwitch, Hermans et al., 1999) allowing varied expression levels (theoretically from zero to very high expression levels) of one receptor to aid dissection of the contributory components of the two receptors.

In summary this Thesis has provided new evidence for cross-talk between M_2 and M_3 receptor signalling pathways causing synergistic effects in both longevity and concentration-dependence of ERK activation, and further work is required to elucidate the downstream significance and mechanisms of regulation of the observed effects, as well as establishing whether the model utilised has provided a paradigm for tissues co-expressing M_2 and M_3 mACh receptors.

Assay	Ligand	n ≥	CHO-m2	CHO-m3	CHO-m2m3
Binding	tripitramine	3	9.35 ± 0.15	6.75 ± 0.25	high 9.43 ± 0.07 low 6.97 ± 0.15
	methoctramine	3	8.00 ± 0.18	5.60 ± 0.21	high 7.90 ± 0.11 low 5.80 ± 0.20
	darifenacin	3	7.30 ± 0.15	8.34 ± 0.04	low 7.11 ± 0.06 high 8.38 ± 0.01
cAMP	tripitramine	3	n.d.	*6.04 ± 0.12	n.d.
	darifenacin	3	n.d.	*8.01 ± 0.14	*low 5.60 ± 0.10 *high 8.01 ± 0.23
Ca ²⁺	tripitramine	3	9.25 ± 0.47	7.59 ± 0.54	7.94 ± 0.33
	atropine	3	10.76 ± 0.61	10.09 ± 0.42	10.57 ± 0.38
	darifenacin	3	8.48 ± 0.1	8.98 ± 0.54	8.85 ± 0.25
Thymidine	darifenacin	3	n.d.	8.06 ±	8.40 ±
ERK	darifenacin	3	7.28 ± 0.38	7.97 ± 0.23	8.38 / 8.09
	methoctramine	1	8.40	6.69	7.25

Table 8.1 Summary of antagonist affinity values, calculated according to the method of Cheng and Prusoff (1973), in a variety of assays. n = minimum number of separate experiments contributing to mean ± S.E.M. pK_i value; n.d.= not determined; * = value quoted as pIC₅₀

Appendix:

Materials

List of reagents and suppliers.

Synthetic peptide corresponding to amino acids 662-681 of the epidermal growth factor receptor (EGFR) sequence:

R R E L V E P L T P S G E A P N Q A L L

was purchased from Proteins and Nucleic Acid Chemistry Laboratory (PNAACL, MRC Toxicology Unit, University of Leicester).

C-Jun-GST beads were also a kind gift from Dr Jonathan L. Blank, University of Leicester.

Initially tripitramine tetraoxalate was purchased from RBI chemicals Ltd, MA, USA. and subsequently was obtained as a kind gift from Dr C. Melchiorre, University Of Bologna, Italy. Darifenacin was a kind gift from Pfizer Central Research, Sandwich, UK.

From Amersham International PLC, Aylesbury, Bucks, England

ECL reagent

[³H]-Inositol

D-*myo*-[³H]-Inositol (1,4,5) trisphosphate ([³H]-IP₃)

N-methyl-[³H]-scopolamine ([³H]-NMS)

Glutathione SepharoseTM 4B

Hyperfilm MP

Protein A Sepharose

[³H]-Thymidine

From Calbiochem Novachem Ltd Nottingham, England

Hygromycin B

Fura-2

From Fisher, Loughborough, Leics, England

Acetone

D-Glucose

Hydrochloric acid
Potassium Chloride
Sodium Chloride
Sodium hydroxide
Trichloroacetic acid

From Gibco.Brl (now Invitrogen), Paisley, Scotland

Foetal calf serum
Fungizone (amphotericin B)
MEM- α (without ribonucleosides and deoxyribonucleosides)
New Born Calf Serum
Penicillin-streptomycin

**From New England Nuclear (N.E.N.) Ltd, (now Perkin Elmer Life Science products),
Stevenage, Herts, England**

[^3H]-Adenosine 3'-5'-cyclic monophosphate ([^3H]-cAMP)
[γ - ^{32}P]-Adenosine 5'-Triphosphate ([γ - ^{32}P]-ATP)

From Packard Ltd, UK

Emulsifier Safe
Scintillation Plus

From Promega, UK

Anti-active MAPK antibody

From Research Biochemicals International (R.B.I.), Poole, Dorset

Methocramine tetrahydrochloride

From Santa Cruz Biotechnology Inc, Santa Cruz, CA, USA

Rabbit ERK 1 polyclonal antibody (C-16)

From Sigma Chemical company Limited, Poole, Dorset, England

α -rabbit secondary antibody
acetyl- β -methylcholine chloride (Methacholine)
adenosine 3'5'-cyclic monophosphate (cAMP)

ammonium persulphate
ampicillin
aprotinin
atropine (sulfate salt)
 β -glycerophosphate
bovine serum albumin (BSA; fraction V)
charcoal
Carbamylcholine chloride (carbachol)
Disodium hydrogen phosphate
Dithiothreitol (DTT)
Ethanol
Ether
Ethylenediaminetetra-acetic acid (EDTA)
Ethylene glycol-bis(β -aminoethyl ether)-N,N,N',N'-tetraacetic acid (EGTA)
Folin-Ciocalteu's phenol reagent
Forskolin
HEPES
Imidazole
Isopropyl β -D-thiogalactopyranoside (IPTG)
Leupeptin
Low weight Molecular markers
Methacholine chloride
NP-40
Orthophosphoric acid
Pertussis Toxin
Phenylethanolamine-N-methyltransferase (PMSF)
Ponceau Red
Serva Blue G
Sodium Orthovanadate (Na_2VO_4)
1,1,2-Trichlorotrifluoroethane (Freon)
Tri-n-octylamine
Tryptone
Tween-20
Yeast extract

From Teflabs, Austin, Texas, USA

Fluo-3AM

From Whatman, UK

p81 paper

SDS -PAGE gel compositions:

12% (w/v) -for JNK bead preparation and JNK assay

10 % (w/v) - for Western blotting (phospho-ERK assay on BTSM preparations)

The following are sufficient to produce one large gel:

Solution	10% Resolving gel	12% Resolving gel	Stacking gel
Acrylamide (30 % w/v)	10 ml	12 ml	1.6 ml
3× running buffer	10 ml	10 ml	-
Milli Q H ₂ O	10 ml	8 ml	6.4 ml
Imidazole buffer	-	-	4 ml
Ammonium Persulphate 10% (w/v)	160 µl	160 µl	100 µl
TEMED	40 µl	40 µl	16 µl

(3× running buffer composition; 825 mM Tris HCl, 115 mM SDS, 6.4 M glycine, filtered.

Imidazole buffer composition; 110 mM Tris HCl, 700 mM imidazole, 10 mM SDS, filtered, pH 6.8)

REFERENCES

- Adomeit, A., Graness, A., Gross, S., Seedorf, K., Wetzker, R. and Liebmann, C. (1999) Bradykinin B2 receptor-mediated Mitogen-activated protein kinase activation in COS-7 cells requires dual signaling via both protein kinase C pathway and epidermal growth factor receptor transactivation. *Mol. Cell. Biol.* **19**, 5289-5297
- Andreev, J., Galisteo, M.L., Kranenburg, O., Logan, S.K., Chui, E.S., Okigaki, M., Cary, L.A., Moolenaar, W.H. and Schlessinger, J. (2001) Src and Pyk2 mediate G-protein-coupled receptor activation of epidermal growth factor receptor (EGFR) but are not required for coupling to the mitogen-activated protein (MAP) kinase signaling cascade. *J. Biol. Chem.* **276**, 20130-20135
- Akam, E.C., Challiss, R.A.J. and Nahorski, S.R. (2001) G_{q/11} and G_{i/o} profiles in CHO cells expressing human muscarinic acetylcholine receptors: dependence on agonist as well as receptor-subtype. *Br. J. Pharmacol.* **132**, 950-958
- Alblas, J., van Etten, I. and Moolenaar, W.H. (1996) Truncated, desensitization-defective neurokinin receptors mediate sustained MAP kinase activation, cell growth and transformation by a Ras-independent mechanism. *EMBO J.* **15**, 3351-3360
- Anderson, N. G., Maller, J. L., Tonks, N.K. and Sturgill, T. W. (1990) Requirement for integration of signals from two distinct phosphorylation pathways for activation of MAP kinase. *Nature* **343**, 651-653
- Anderson, N.G., Li, P., Marsden, L.A., Williams, N., Roberts, T.M. and Sturgill, T.W. (1991) Raf-1 is a potential substrate for mitogen-activated protein kinase *in vivo*. *Biochem. J.* **277**, 573-576
- Arunlakshana, O. and Schild, H.O. (1959) Some quantitative uses of drug antagonists. *Br. J. Pharmacol. Chemother.* **14**, 48-58
- Ashkenazi, A., Ramachandran, J. and Capon, D.J. (1989) Acetylcholine analogue stimulates DNA synthesis in brain-derived cells via specific muscarinic receptor subtypes. *Nature* **340**, 146-150
- Auer, K.L., Park, J-S., Seth, P., Coffey, R.J., Darlington, G., Abo, A., McMahon, M., Depinho, R.A., Fisher, P.B. and Dent, P. (1998a) Prolonged activation of the mitogen-activated protein kinase pathway promotes DNA synthesis in primary hepatocytes from p21^{Cip-1/WAF1}-null mice, but not in hepatocytes from p16^{INK4a}-null mice. *Biochem. J.* **336**, 551-560
- Auer, K.L., Contressa, J., Brenz-verca, S., Pirola, L., Rusconi, S., Cooper, G., Abo, A., Wymann, M.P., Davis, R.J., Birrer, M. and Dent, P. (1998b) *Mol. Cell. Biol.* **9**, 561-573
- Batzer, N.L., Daly, R., Yajnik, V., Skolnik, E., Chardin, P., Bar-Sagi, D., Margolios, B. and Schlessinger, J. (1993) Guanine-nucleotide-releasing factor hSos1 binds to Grb2 and links receptor tyrosine kinases to Ras signalling. *Nature* **363**, 85-87
- Berridge, M.J. (1993) Inositol trisphosphate and calcium signalling. *Nature*. **361**, 315-325

- Berridge, M.J. (1998) Neuronal calcium signalling. *Neuron*. **21**, 13-26
- Berridge, M.J., Bootman, M.D. and Lipp, P. (1998) Calcium- a life and death signal. *Nature*. **395**, 645-648
- Berridge, M.J., Lipp, P. and Bootman, M.D. (2000) The versatility and universality of calcium signalling. *Nature. Mol. Cell. Biol.* **1**,11-21
- Berstein, G., Blank, J.L., Jhon, D-Y., Exton, J.H., Rhee, S.G. and Ross, E.M. (1992) Phospholipase C- β 1 is a GTPase-activating protein for $G_{q/11}$ its physiologic regulator. *Cell*. **70**, 411-418
- Bhagal, R. H. (2000) Interactive regulation of ERK and JNK signalling pathways by the M3-muscarinic receptor and β 2-adrenoceptor co-expressed in CHO cells. Intercalated BSc dissertation. University of Leicester, England.
- Billington, C.K., Joseph, S.K., Swan, C., Scott, M.G.H., Jobson, T.M. and Hall, I.P. (1999) Modulation of human airway smooth muscle proliferation by type 3 phosphodiesterase inhibition. *Am. J. Physiol.* **276**, L412-L419
- Birdsall, N.J., Hulme, E.C., Stockton, J., Burgen, A.S. Berrie, C.P., Hammer, R., Wong, E. H. and Zigmond, M.J. (1983) Muscarinic receptor subclasses: evidence from binding studies. *Adv. Biochem. Psychopharmac.* **37**: 323-329
- Birdsall, N.J.M., Nathanson, N.M. and Schwarz, R.D. (2001) Muscarinic receptors: it's a knockout. *Trends. Pharm. Sci.* **22**, 215-219
- Birnbaumer, L., Abramowitz, J. and Brown, A.M. (1990) Receptor-effector coupling by G-proteins. *Biochimica et Biophysica Acta.* **1031**, 163-224
- Blank, J.L., Ross, A. H. and Exton, J.H. (1991) Purification and characterization of two G-proteins that activate the β 1 isozyme of phosphoinositide-specific phospholipase C. *J. Biol. Chem.* **266**, 18206-18216
- Blank, J.L., Brattain, K.A. and Exton, J.H. (1992) Activation of cytosolic phosphoinositide phospholipase C by G-protein $\beta\gamma$ subunits. *J. Biol. Chem.* **267**, 23069-23075
- Blank, J.L., Gerwins, P., Elliott, E.M., Sather, S. and Johnson, G.L. (1996) Molecular cloning of mitogen-activated protein/ERK kinase kinases (MEKK) 2 and 3. *J. Biol. Chem.* **271**, 5361-5368
- Blaukat, A., Ivankovic-Dikic, I., Grönroos, E., Dolfi, F., Tokiaw, G., Vuori, K. and Dikic, I. (1999) Adaptor proteins Grb2 and Crk couple Pyk2 with activation of specific mitogen-activated protein kinase cascades. *J. Biol. Chem.* **274**, 14893-14901
- Blaukat, A., Barac, A., Cross, M.J., Offermans, S. and Dikic, I. (2000) G protein-coupled receptor-mediated mitogen-activated protein kinase activation through cooperation of $G\alpha_q$ and $G\alpha_i$ signals. *Mol. Cell. Biol.* **20**, 6837-6848
- Blenis, J. (1993) Signal transduction via the MAP kinases: proceed at your own RSK. *Proc. Natl. Acad. Sci. USA.* **90**, 5889-5892

Bohmann, D., Bos, T.J., Admon, A., Nishimura, T., Vogt, P.K. and Tjian, R. (1987) Human proto-oncogene c-jun encodes a DNA binding protein with structural and functional properties of transcription factor AP-1. *Science* **238**, 1386-1392

Bondeva, T., Pirola, L., Bulgarelli-Leva, G., Rubio, I., Wetzker, R. and Wymann, M.P. (1998) Bifurcation of lipid and protein kinase signals of PI3K to the protein kinases PKB and MAPK. *Science*. **282**, 293-296

Bonner, T.I., Buckley, N.J., Young, A.C. and Brann, M.R. (1987) Identification of a family of muscarinic acetylcholine receptor genes. *Science*. **237**, 527-532

Bonner, T.I., Buckley, N.J., Young, A.C. and Brann, M.R. (1988) Cloning and expression of the human and rat m5 muscarinic acetylcholine receptor genes. *Neuron*. **1**, 403-410

Bornfeldt, K.E., Campbell, J.S., Koyama, H., Argast, G.M., Leslie, C.C., Raines, E.W., Krebs, E.G. and Ross, R. (1997) The mitogen-activated protein kinase pathway can mediate growth inhibition and proliferation in smooth muscle cells. *J. Clin. Invest.* **100**, 875-885

Boxall, D. K. (1998) Muscarinic receptor signalling in model cells and smooth muscle. PhD thesis. University of Leicester, England.

Bradford, M.M. (1976) A rapid and sensitive method for the quantitation of microgram quantities of protein using the principle of protein-dye binding. *Anal. Biochem.* **72**, 248-254

Brockhurst, I. (1999) Regulation of mitogenic signalling pathways by G protein-coupled and cytokine receptors in airways smooth muscle. Intercalated BSc dissertation. University of Leicester, England.

Brown, B.L., Albano, J.D.M., Elkins, R.P., Sgherzi, A.M. and Tampion, W. (1971) A simple and sensitive saturation assay method for the measurement of adenosine 3',5'-cyclic monophosphate. *Biochem. J.* **121**, 561-563

Brunet, A., Pagès, G., Pouyssegur, J. (1994) Growth factor-stimulated MAP kinase induces rapid retrophosphorylation and inhibition of MAP kinase kinase (MEK1). *FEBS Letters* **346**, 299-303

Brunet, A., Roux, D., Lenormand, P., Dowd, S., Keyse, S. and Pouyssegur, J. (1999) Nuclear translocation of p42/p44 mitogen-activated protein kinase is required for growth factor-induced gene expression and cell cycle entry. *EMBO J.* **18**, 664-674

Buday, L. and Downward, J. (1993) Epidermal growth factor regulates p21ras through the formation of a complex of receptor, Grb2 adapter protein, and Sos nucleotide exchange factor. *Cell* **73**, 611-620

Budd, D.C., Rae, A. and Tobin, A.B. (1999) Activation of the mitogen-activated protein kinase pathway by a G_{q/11}-coupled muscarinic receptor is independent of receptor internalisation. *J. Biol. Chem.* **274**, 12355-12360

Budd, D.C., Willars, G.B., McDonald, J.E. and Tobin, A.B. (2001) Phosphorylation of the G_{q/11}-coupled M₃-muscarinic receptor is involved in receptor activation of the ERK-1/2 mitogen-activated protein kinase pathway. *J. Biol. Chem.* **276**, 4581-4587

Burford, N.T. and Nahorski, S.R. (1996) Muscarinic M₁ receptor-stimulated adenylate cyclase activity in Chinese hamster ovary cells is mediated by G(s)-alpha and is not a consequence of phosphoinositidase C activation. *Biochem. J.* **315**, 883-888

Burford, N.T., Tobin, A.B. and Nahorski, S.R. (1995) Coupling of muscarinic m₁, m₂ and m₃ acetylcholine receptors expressed in Chinese hamster ovary cells to pertussis toxin-sensitive/insensitive guanine nucleotide-binding proteins. *Eur. J. Pharm.* **289**, 343-351

Burrack, W.R. and Shaw, A.S. (2000) Signal transduction: hanging on a scaffold. *Current Opin. Cell. Biol.* **12**, 211-216

Camps, M., Carozzi, A., Schnabel, P., Scheer, A., Parker, P.J. and Gierschik, P. (1992) Isozyme-selective stimulation of phospholipase C-β₂ by G protein βγ-subunits. *Nature.* **360**, 684-689

Carroll, R.C. and Peralta, E.G. (1998) The m₃ muscarinic acetylcholine receptor differentially regulates calcium influx and release through modulation of monovalent cation channels. *EMBO J.* **17**, 3036-3044

Carruthers, A.M., Challiss, R.A.J., Mistry, R., Saunders, R., Thomsen, C. and Nahorski, S.R. (1997) Enhanced type 1α metabotropic glutamate receptor-stimulated phosphoinositide signalling after pertussis toxin treatment. *Mol. Pharmacol.* **52**, 406-414

Caulfield, M.P. (1993) Muscarinic receptors- characterization, coupling and function. *Pharmac. Ther.* **58**, 319-379

Caulfield, M.P. and Birdsall, N.J.M. (1998) International union of pharmacology. XVII. Classification of muscarinic acetylcholine receptors. *Pharmacological Reviews.* **50**, 279-290

Ceresa, B.P. and Schmid, S.L. (2000) Regulation of signal transduction by endocytosis. *Curr. Opin. Cell. Biol.* **12**, 204-210

Challiss, R.A.J., Batty, I.H. and Nahorski, S.R. (1989) Mass measurements of inositol 1,4,5-trisphosphate in rat cerebral cortex slices using a radioreceptor assay: effects of neurotransmitters and depolarization. *Biochem. Biophys. Res. Commun.* **157**, 684-691

Challiss, R.A.J., Chilvers, E.R., Willcocks, A.L. and Nahorski, S.R. (1990) Heterogeneity of [³H]inositol 1,4,5-trisphosphate binding sites in adrenal-cortical membranes: Characterization and validation of a radioreceptor assay. *Biochem. J.* **265**, 421-427

Challiss, R.A.J., Patel, N. and Arch, J.R.S. (1992) Comparative effects of BRL 38227, nitrendipine and isoprenaline on carbachol- and histamine-stimulated phosphoinositide metabolism in airway smooth muscle. *Br. J. Pharmacol.* **105**, 997-1003.

Challiss, R.A. and Blank, J.L. (1997) CRC Press. Chapter 2. Muscarinic acetylcholine receptor signalling pathways in smooth muscle. *Muscarinic receptor subtypes in smooth muscle.* pp 39-85 Ed. Eglen, R.M.

Chan, J.S.C., Lee, J.W.M., Ho, M.K.C. and Wong, Y.H. (2000) Preactivation permits subsequent stimulation of phospholipase C by G_i-coupled receptors. *Mol. Pharmacol.* **57**, 700-708

- Chang, L. and Karin, M. (2001) Mammalian MAP kinase signalling cascades. *Nature* **410**, 37-40
- Chen, R.-H., Sarnecki, C., and Blenis, J. (1992) Nuclear localization and regulation of erk- and rsk-encoded protein kinases. *Mol. Cell. Biol.* **12**, 915-927
- Chen, Y.-H., Grall, D., Salcini, A.E., Pelicci, P.G., Pouyssegur, J. and Van Obberghen-Schilling E. (1996) Shc adaptor proteins are key transducers of mitogenic signaling mediated by the G protein-coupled thrombin receptor. *EMBO Journal.* **15**, 1037-1044
- Cheng, Y.-C. and Prusoff, W.H. (1973). Relationship between the inhibitor constant (K_i) and the concentration of inhibitor which causes 50 percent inhibition of an enzymatic reaction. *Biochem. Pharmacol.* **22**, 3099-3108.
- Chiarini, A., Budriesi, R., Bolognesi, A., Minarini, A. and Melchoirre, C. (1995) *In vitro* characterisation of tripitramine, a polymethylene tetraamine displaying high selectivity and affinity for muscarinic M2 receptors. *Br. J. Pharmacol.* **114**, 1507-1517
- Choppin, A., Stepan, G.J., Loury, D., Watson, N. and Eglen, R.M. (1999) Effect of ovariectomy on muscarinic receptors in rat isolated uterus in vitro. *Br. J. Pharmacol.* **127**, 1551-1558
- Cobb, M. H. and Goldsmith, E. J. (1995) How MAP kinases are regulated. *J. Biol. Chem.* **270**, 14843-14846
- Cobb, M. H. and Goldsmith, E. J. (2000) Dimerization in MAP-kinase signaling. *Trends. Biochem. Sci.* **25**, 7-9
- Cook, S.J., Rubinfeld, B., Albert, I. and McCormick, F. (1993a) RapV12 antagonizes Ras-dependent activation of ERK1 and ERK2 by LPA and EGF in Rat-1 fibroblasts. *EMBO J.* **12**, 3475-85
- Cook, S.J. and McCormick, F. (1993b) Inhibition by cAMP of Ras-dependent activation of Raf. *Science.* **262**, 1069-1072
- Cook, S.J., Aziz, N. and McMahon, M. (1999) The repertoire of Fos and Jun proteins expressed during the G1 phase of the cell cycle is determined by the duration of mitogen-activated protein kinase activation. *Mol. Cell. Biol.* **19**, 330-341
- Cooper, D.M., Mons, N. and Karpen, J.W. (1995) Adenylyl cyclases and the interaction between calcium and cAMP signalling. *Nature.* **374**, 421-424
- Cordeaux, Y., Briddon, S.J., Megson, A.E., McDonnell, J., Dickenson, J.M. and Hill, S.J. (2000) Influence of receptor number on functional responses elicited by agonists acting at the human adenosine A₁ receptor: evidence for signalling pathway-dependent changes in agonist potency and relative intrinsic activity. *Mol. Pharmacol.* **58**, 1075-1084
- Coso, O.A., Chiariello, M., Yu, J.-C., Teramoto, H., Crespo, P., Xu, N., Miki, T. and Gutkind, J.S. (1995a) The small GTP-Binding proteins Rac1 and Cdc42 regulate the activity of the JNK/SAPK signaling pathway. *Cell* **81**, 1137-1146

- Coso, O.A., Chiariello, M., Kalinec, G., Kyriakis, J.M., Woodgett, J. and Gutkind, J.S. (1995b) Transforming G protein-coupled receptors potently activate JNK (SAPK). *J. Biol. Chem.* **270**, 5620-5624
- Coso, O.A., Teramoto, H., Simonds, W.F. and Gutkind, J.S. (1996) Signaling from G protein-coupled receptors to c-Jun kinase involves β subunits of heterotrimeric G proteins acting on a Ras and Rac1-dependent pathway. *J. Biol. Chem.* **271**, 3963-3966
- Crespo, P., Xu, N., Daniotti, J.L., Troppmair, J., Rapp, U.R. and Gutkind, J.S. (1994a) Signaling through transforming G protein-coupled receptors in NIH 3T3 cells involves c-Raf activation. *J. Biol. Chem.* **269**, 21103-21109
- Crespo, P., Xu, N., Simonds, W.F. and Gutkind, J.S. (1994b) Ras-dependent activation of MAP kinase pathway mediated by G-protein β subunits. *Nature* **369**, 418-420
- Crespo, P., Cachero, T.G., Xu, N. and Gutkind, J.S. (1995) Dual effect of β -adrenergic receptors on mitogen-activated protein kinase. *J. Biol. Chem.* **270**, 25259-25265
- Daaka, Y., Luttrell, L.M., Ahn, S., Della Rocca, G.J., Ferguson, S.S.G., Caron, M.G. and Lefkowitz, R.J. (1998) Essential role for G protein-coupled receptor endocytosis in the activation of mitogen-activated protein kinase. *J. Biol. Chem.* **273**, 685-688
- Daub, H., Weiss, F.U., Wallasch, C., and Ullrich, A. (1996) Role of transactivation of the EGF receptor in signalling by G-protein-coupled receptors. *Nature*. **379**, 557-560
- Daub, H., Wallasch, C., Lankenau, A., Kerrlich, A. and Ullrich, A. (1997) Signal characteristics of G protein-transactivated EGF receptor. *EMBO J.* **16**, 7032-7044
- Davis, R.J. (1993) The mitogen-activated protein kinase signal transduction pathway. *J. Biol. Chem.* **268**, 14553-14556
- Davis, R.J. (1994) MAPKs: new JNK expands the group. *Trends. Biochem. Sci.* **19**, 470-473
- Davis, R.J. (2000) Signal transduction by the JNK group of MAP kinases. *Cell.* **103**, 239-252
- De Vries, L. and Farquhar, M.G. (1999) RGS proteins: more than just GAPs for heterotrimeric G proteins. *Trends. Cell Biol.* **9**, 138-144
- Deacon, K. and Blank, J.L. (1997) Characterization of the mitogen-activated protein kinase kinase 4 (MKK4)/c-Jun NH₂-terminal kinase 1 and MKK3/p38 pathways regulated by MEK kinase 2 and 3. *J. Biol. Chem.* **272**, 14489-14496
- Deacon, K. and Blank, J.L. (1999) MEK Kinase 3 Directly Activates MKK6 and MKK7, Specific Activators of the p38 and c-Jun NH₂-terminal Kinases. *J. Biol. Chem.* **274**, 16604-16610
- Del Río, E., Nicholls, D.G. and Downes, C.P. (1994) Involvement of calcium influx in muscarinic cholinergic regulation of phospholipase C in cerebellar granule cells. *J Neurochem.* **63**, 535-543

Della Rocca, G.J., van Biesen, T., Daaka, Y., Luttrell, D.K., Luttrell, L.M. and Lefkowitz, R.J. (1997) Ras-dependent mitogen-activated protein kinase activation by G protein-coupled receptors. *J. Biol. Chem.* **272**, 19125-19132

Della Rocca, G.J., Maudsley, S., Daaka, Y., Lefkowitz, R.J. and Luttrell, L.M. (1999) Pleiotropic coupling of G protein-coupled receptors to the mitogen-activated protein kinase cascade. *J. Biol. Chem.* **274**, 13978-13984

Denhardt, D.T. (1996) Signal-transducing protein phosphorylation cascades mediated by Ras/Rho proteins in the mammalian cell: the potential for multiplex signalling. *Biochem. J.* **318**, 729-747

Dent, P., Haser, W., Haystead, T.A.J., Vincent, L.A., Roberts, T.M. and Sturgill, T.W. (1992) Activation of mitogen-activated protein kinase by v-Raf in NIH 3T3 cells and in vitro. *Science*. **257**, 144-1407

Della Rocca, G. J., van Biesen, T., Daaka, Y., Luttrell, D.K., Luttrell, L.M. and Lefkowitz, R.J. (1997) Ras-dependent mitogen-activated protein kinase activation by G protein-coupled receptors. *J. Biol. Chem.* **272**, 19125-19132

Della Rocca, G. J., Maudsley, S., Daaka, Y., Lefkowitz, R.J. and Luttrell, L.M. (1999) Pleiotropic coupling of Gprotein-coupled receptors to the mitogen-activated protein kinase cascade. *J. Biol. Chem.* **274**, 13978-13984

Dérijard, B., Hibi, M., Wu, I-H., Barrett, T., Su, B., Deng, T., Karin, M. and Davis, R.J. (1994) JNK1: a protein kinase stimulated by UV light and Ha-Ras that binds and phosphorylates the c-Jun activation domain. *Cell* **76**, 1025-1037

Dhanasekaran, N., Heasley, L.E. and Johnson, G.L. (1995) G protein-coupled receptor systems involved in cell growth and oncogenesis. *Endocrine Reviews*. **16**, 259-270.

Dhanasekaran, N., Tsim, S-T., Dermott, J.M. and Onesime, D. (1998) Regulation of cell proliferation by G proteins. *Oncogene* **17**, 1383-1394

Dickens, M., Rogers, J.S., Cavanagh, J., Raitano, A., Xia, Z., Halpern, J.R., Greenberg, M.E., Sawyers, C.L. and Davis, R.J. (1997) A cytoplasmic inhibitor of the JNK signal transduction pathway. *Science* **277**, 693-696

Dickenson, J.M., Blank, J.L. and Hill, S.J. (1998) Human adenosine A₁ receptor and P2Y₂-purinoceptor-mediated activation of the mitogen-activated protein kinase cascade in transfected CHO cells. *Br. J. Pharmacol.* **124**, 1491-1499

Dikic, I., Tokiwa, G., Lev, S., Courtneidge, S.A. and Sclessinger, J. (1996) A role for Pyk2 and Src in linking G-protein-coupled receptors with MAP kinase activation. *Nature*. **383**, 547-550

Duckworth, B.C. and Cantley, L.C. (1997) Conditional inhibition of the mitogen-activated protein kinase cascade by wortmannin. *J. Biol. Chem.* **272**, 27665-27670

Edelman, J.L., Kajimura, M., Woldemussie, E. and Sachs, G. (1994) Differential effects of carbachol on calcium entry and release in CHO cells expressing the m3 muscarinic receptor. *Cell calcium*. **16**, 181-193

- Eglen, R.M., Reddy, H., Watson, N. and Challiss, R.A.J. (1994) Muscarinic acetylcholine receptor subtypes in smooth muscle. *Trends Pharmacol. Sci.* **15**, 114-119
- Eglen, R. M., Hedge, S.S. and Watson, N. (1996a) Muscarinic receptor subtypes and smooth muscle function. *Pharmacological Reviews.* **48**, 531-565
- Eglen, R.M. and Watson, N. (1996b) Selective muscarinic receptor agonists and antagonists. *Pharmacol. and Toxicol.* **78**, 59-68
- Eglen, R.M. and Nahorski, S.R. (2000) The muscarinic M5 receptor: a silent or emerging subtype? *Br. J. Pharmacol.* **130**, 13-21
- Emala, C. W., Liu, F. and Hirshman, C.A. (1999) G_iα but not G_qα is linked to activation of p21^{ras} in human airway smooth muscle cells. *Am. J. Physiol.* **276**, L564-L570
- Exton, J. H. (1993) Role of G proteins in activation of phosphoinositide phospholipase C. *Advances in second messengers and phosphoprotein research.* **28**, 65-72
- Exton, J.H. (1996) Regulation of phosphoinositide phospholipases by hormones, neurotransmitters, and other agonists linked to G proteins. *Annu. Rev. Pharmacol. Toxicol.* **36**, 481-509
- Faure, M., Voyno-Yasenetskaya, T. A. and Bourne, H. R. (1994) cAMP and βγ subunits of heterotrimeric G proteins stimulate the mitogen-activated protein kinase pathway in COS-7 cells. *J. Biol. Chem.* **269**, 7851-7854
- Felsch, J.S., Cachero, T.G. and Peralta, E.G. (1998) Activation of protein tyrosine kinase PYK2 by the m1 muscarinic acetylcholine receptor. *Proc. Natl. Acad. Sci. USA.* **95**, 5051-5056
- Felder, C.C. (1995) Muscarinic acetylcholine receptors: signal transduction through multiple effectors. *FASEB J.* **9**, 619-625
- Ferguson, S.S.G., (2001) Evolving concepts in G protein-coupled receptor endocytosis: the role in receptor desensitisation and signaling. *Pharmacol. Rev.* **53**, 1-24
- Fernandes, L.B., Fryer, A.D., and Hirshman, C.A. (1992) M₂ muscarinic receptors inhibit isoproterenol-induced relaxation of canine airway smooth muscle. *J. Pharmacol. Exp. Ther.* **262**, 119-126
- Fukuda, M., Gotoh, Y. and Nishida, E. (1997) Interaction of MAP kinase with MAP kinase kinase: its possible role in the control of nucleocytoplasmic transport of MAP kinase. *EMBO J.* **16**, 1901-1908
- Gale, N.W., Kaplan, S., Lowenstein, E.J., Sclessinger, J. and Bar-Sagi, D. (1993) Grb2 mediates the EGF-dependent activation of guanine nucleotide exchange on Ras. *Nature* **363**, 88-92
- Garrington, T.P. and Johnson, G.L. (1999) Organisation and regulation of mitogenic-activated protein kinase signalling pathways. *Current Opin. Cell. Biol.* **11**, 211-218
- Gerthoffer, W.T., Yamboliev, I.A., Pohl, J., Haynes, R., Dang, S. and Mchugh, J. (1997) Activation of MAP kinases in airway smooth muscle. *Am. J. Physiol.* **272**, L244-L252

Gille, H., Sharrocks, A.D. and Shaw, P.E. (1992) Phosphorylation of transcription factor p62(TCF) by MAP kinase stimulates ternary complex formation at c-fos promoter. *Nature*. **358**, 414-417.

Gomez, J., Shannon, H., Kostenis, E., Felder, C., Zhang, L., Brodtkin, J., Grinberg, A., Sheng, H. and Wess, J. (1999) Pronounced pharmacologic deficits in M2 muscarinic acetylcholine receptor knockout mice. *Proc. Natl. Acad. Sci. USA*. **96**, 1692-1697

Gould, K.L. and Hunter, T. (1998) Platelet-derived growth factor induces multisite phosphorylation of pp60 (c-src) and increases its protein-tyrosine kinase activity. *Molecular & Cellular Biology*. **8**, 3345-3356

Graneß, A., Adomeit, A., Heinze, R., Wetzter, R. and Liebmann, C. (1998) A novel mitogenic signalling pathway of bradykinin in the human colon carcinoma cell line Sw-480 involves sequential activation of a G_{q/11} protein, phosphatidylinositol 3-kinase β and protein kinase C ϵ . *J. Biol. Chem.* **273**, 32016-32022

Griffin, M.T. and Ehlert, F.J. (1992) Specific inhibition of isoproterenol-stimulated cyclic AMP accumulation by M2 muscarinic receptors in rat intestinal smooth muscle. *J. Pharmacol. Exp. Ther.* **263**, 221-225

Gudermann, T., Kalbrenner, F., and Schultz, G. (1996) Diversity and selectivity of receptor-G protein interaction. *Annu. Rev. Pharmacol. Toxicol.* **36**, 429-459

Gudermann, T., Grosse, R. and Schultz, G. (2000) Contribution of receptor/G protein signaling to cell growth and transformation. *Naunyn-Schmiedeberg's Arch. Pharmacol.* **361**, 345-362

Gupta, S., Barrett, T., Whitmarsh, A.J., Cavanagh, J., Sluss, H.K., Derijard, B. and Davis, R.J. (1996) Selective interaction of JNK protein kinase isoforms with transcription factors. *EMBO J.* **15**, 2760-2770.

Gutkind, J.S., Novotny, E.A., Brann, M.R. and Robbins, K.C. (1991) Muscarinic acetylcholine receptor subtypes as agonist-dependent oncogenes. *Proc. Natl. Acad. Sci.* **88**, 4703-4707

Gutkind, J.S., Crespo, P., Coso, O.A., Kilinec, G. and Xu, N. (1995) Proliferative signalling through muscarinic receptors: a model for receptors coupled to heterotrimeric G proteins. Chapter 7. *Molecular Mechanisms of muscarinic acetylcholine receptor function*. ED Jurgen Wess. R.G. Landes Company.

Gutkind, J.S. (1998a) The pathways connecting G protein-coupled receptors to the nucleus through divergent mitogen-activated protein kinase cascades. *J. Biol. Chem.* **273**, 1839-1842

Gutkind, J.S. (1998b) Cell growth control by G protein-coupled receptors: from signal transduction to signal integration. *Oncogene* **17**, 1331-1342

Hall, R.A., Premomnt, R.T. and Iefkowitz, R.J. (1999) Heptahelical receptor signaling beyond the G protein paradigm. *J. Cell Biol.* **145**, 927-932

Hamilton, S.E., Loose, M.D., Qi, M., Levey, A.I., Hille, B., McKnight, G.S., Idzerda, R. L. and Nathanson, N.M. (1997) Disruption of the m1 receptor gene ablates muscarinic

- receptor-dependent M current regulation and seizure activity in mice. *Proc. Natl. Acad. Sci. USA.* **94**, 13311-13316
- Hammer, R., Berrie, C.P., Birdsall, N.J.M., Burgen, A.S.V. and Hulme, E.C. (1980) Pirenzepine distinguishes between different subclasses of muscarinic receptors. *Nature.* **283**, 90-92
- Hawes, B.E., van Biesen, T., Koch, W.J., Luttrell, L.M. and Lefkowitz, R.J. (1995) Distinct pathways of G_i- and G_q-mediated mitogen-activate protein kinase activation. *J. Biol. Chem.* **270**, 17148-17153
- Hawes, B.E., Luttrell, L.M., van Biesen, T. and Lefkowitz, R.J. (1996) Phosphatidylinositol 3-kinase is an early intermediate in the G $\beta\gamma$ -mediated mitogen-activated protein kinase signaling pathway. *J. Biol. Chem.* **271**, 12133-12136
- Hedge, S.S., Choppin, A., Bonhaus, D., Briaud, S., Loeb, M., Moy, T.M., Loury, D. and Eglen, R.M. (1997) Functional role of M2 and M3 muscarinic receptors in the urinary bladder of rats in vitro and in vivo. *Br. J. Pharmacol.* **120**, 1409-1418
- Heldin, C.H. (1995) Dimerization of cell surface receptors in signal transduction. *Cell* **80**, 213-223
- Heller-Brown, J., Sah, V., Moskowitz, S., Ramirez, T., Collins, L., Post, G. and Goldstein, D. (1997) pathways and roadblocks in muscarinic receptor-mediated growth regulation. *Life Sci.* **60**, 1077-1084
- Hermans, E., Challiss, R.A.J. and Nahorski, S.R. (1999) Effects of varying the expression level of recombinant human mGlu1 α receptors on the pharmacological properties of agonists and antagonists. *Br. J. Pharmacol.* **126**, 873-882
- Hildebrandt, J.D. (1997) Role of subunit diversity in signaling by heterotrimeric G proteins. *Biochem. Pharm.* **54**, 325-339
- Hill, C.S. and Treisman, R. (1995) Transcriptional regulation by extracellular signals: mechanisms and specificity. *Cell* **80**, 199-211
- Hirshman, C.A. and Emala, C.W. (1999) Actin reorganization in airway smooth muscle cells involves G_q and G_{i,2} activation of Rho. *Am J. Physiol.* **277**, L653-L661
- Hornigold, D.C., Blank, J.I., Eglen, R.M. and Challiss, R.A.J. (2000a) Cross-talk between M₂- and M₃-muscarinic receptors co-expressed in CHO cells at the level of mitogen-activated protein kinase regulation. *Proc. Aust. Soc. Clin. Exp. Pharmacol. Toxicol.* **7**, 16
- Hornigold, D.C., Blank, J.I., Eglen, R.M. and Challiss, R.A.J. (2000b) Muscarinic receptor crosstalk in the regulation of ERK and JNK activities in CHO-m2m3 cells. *Biochem Soc Trans.* **28**, A429, 1567
- Hornigold, D.C., Blank, J.L. and Challiss R.A.J. (2001) Interaction between M₂- and M₃-muscarinic acetylcholine receptors to regulate extracellular-signal regulated kinase and c-Jun N-terminal kinase in Chinese Hamster ovary cells and airways smooth muscle. *In preparation.*

- Hordijk, P.L., Verlaan, I., Jalink, K., van Corven, E.J. and Moolenaar, W.H. (1994) cAMP abrogates the p21ras-mitogen-activated protein kinase pathway in fibroblasts. *J. Biol. Chem.* **269**, 3534-3538
- Houslay, M.D. and Kolch, W. (2000) Cell-type specific integration of cross-talk between extracellular signal-regulated kinase and cAMP signaling. *Mol. Pharm.* **58**, 659-668
- Hulme, E.C., Birdsall, N.J.M. and Buckley, N.J. (1990) Muscarinic receptor subtypes. *Annu. Rev. pharmacol. Toxicol.* **30**, 633-673
- Inouye, K., Mizutani, S., Koide, H. and Kaziro, Y. (2000) Formation of the Ras dimer is essential for raf-1 activation. *J. Biol. Chem.* **275**, 3737-3740
- Kalbrener, F., Abel, A., Wittau, N. and Schultz, G. (1999) Promiscuity and fidelity in receptor-G-protein coupling: cell cycle-dependent coupling of the vasopressin V₁ receptor. *Biochem. Soc. Trans.* **27**, 158-163
- Karin, M. and Hunter, T. (1995) Transcriptional control by protein phosphorylation: signal transmission from the cell surface to the nucleus. *Current Biology* **5**, 747-757
- Kelleher, M.D., Abe, M.K., Chao, T.S.O., Jain, M., Green, J.M., Solway, J., Rosner, M.R. and Hershenson, M.B. (1995) Role of MAP Kinase activation in bovine tracheal smooth muscle mitogenesis. *Am. J. Physiol.* **268**, L894-L901
- Keyse, S.M. (2000) Protein phosphatases and the regulation of the mitogen-activated protein kinase signalling. *Curr. Opin. Cell Biol.* **12**, 186-192
- Khokhlatchev, A.V., Canagarajah, B., Wilsbacher, J., Robinson, M., Atkinson, M., Goldsmith, E. and Cobb, M. (1998) Phosphorylation of the MAP kinase ERK2 promotes its homodimerization and nuclear translocation. *Cell* **93**, 605-615
- Kim, J.Y., Yang, M.S., O.H., C.D., Kim, K.T., Ha, M.J., Kang, S.S. and Chun, J.S. (1999) Signalling pathway leading to an activation of mitogen-activated protein kinase by stimulating M₃ muscarinic receptor. *Biochem. J.* **337**, 275-280
- Kolch, W., Heidecker, G., Kochs, G., Hummel, R., Vahidi, H., Mischak, H., Finkenzeller, G., Marme, D. and Rapp UR. (1993) Protein kinase C alpha activates Raf-1 by direct phosphorylation. *Nature.* **364**, 249-252
- Kolch, W. (2000) Meaningful relationships: the regulation of the Ras/ Raf/ MEK/ ERK pathway by protein interactions. *Biochem. J.* **351**, 289-305
- Kotlikoff, M.I., Dhulipala, P. and Wang, Y-X. (1999) M₂ signalling in smooth muscle cells. *Life Sciences.* **64**, 437-442
- Kozasa, T., Jiang, X., Hart, M.J., Sternweis, P.M., Singer, W.D., Gilman, A.G., Bollag, G. and Sternweis, P.C. (1998) p115 RhoGEF, a GTPase activating protein for G α_{12} and G α_{13} . *Science.* **280**, 2109-2111
- Krymskaya, V.P., Orsini, M.J., Estzerhas, A.J., Brodbeck, K.C., Benovic, J.L., Panettieri Jr, R.A. and Penn, R.B. (2000) Mechanism of proliferation synergy by receptor tyrosine kinase and G protein-coupled receptor activation in human airway smooth muscle. *Am. J. Respir. Cell. Mol. Biol.* **23**, 546-554

- Kubo, T., Fukuda, Mikami, A., Maeda, A., Takahashi, H., Mishina, A., Haga, K., Ichiyama, A., Kangawa, K., Kojima, M., Matsuo, H., Hirose, T. and Numa, S. (1986) Cloning, sequencing and expression of complementary DNA encoding the muscarinic acetylcholine receptor. *Nature*. **323**, 411-416
- Kyriakis, J.M., App, H., Zhang, X-F., Banerjee, P., Brautigan, Rapp, U.R. and Avruch, J. (1992) Raf-1 activates MAP kinase-kinase. *Nature* **358**, 417-421
- Kyriakis, J.M. and Avruch, J. (1996) Sounding the Alarm: Protein Kinase Cascades Activated by Stress and Inflammation. *J. Biol. Chem.* **271**, 24313-24316
- Lallemant, D., Ham, J., Garbay, S., Bakiri, L., Traincard, F., Jeannequin, O., Pfarr, C.M. and Yaniv, M. (1998) Stress-activated protein kinases are negatively regulated by cell density. *EMBO Journal*. **17**, 5615-5626
- Lambert, D.G., Ghataorje, A.S. and Nahorski, S.R. (1989) Muscarinic receptor binding characteristics of a human neuroblastoma SK-N-SH and its clones SH-SY5Y and SH-EP11. *Eur. J. Pharmacol.* **165**, 71-77
- Lambert, D.G. and Nahorski, S.R. (1990) Muscarinic-receptor-mediated changes in intracellular Ca²⁺ and inositol 1,4,5-trisphosphate mass in a human neuroblastoma cell line, SH-SY5Y. *Biochem. J.* **265**, 555-562
- Leaney, J.L. and Tinker, A. (2000) The role of members of the pertussis toxin-sensitive family of G proteins in coupling receptors to the activation of the G protein-gated inwardly rectifying potassium channel. *Proc. Natl. Acad. Sci.* **97**, 5651-5656
- Lenormand, P., Brondello, J-M., Brunet, A. and Pouyssegur, J. (1998) Growth factor-induced p42/p44 MAPK nuclear translocation and retention requires both MAPK activation and neosynthesis of nuclear anchoring proteins. *J. Cell Biol.* **142**, 625-633
- Lefkowitz, R.J. (1998) G protein-coupled receptors. *J. Biol. Chem.* **273**, 18677-18680
- Leserer, M., Gschwind, A. and Ullrich, A. (2000) Epidermal growth factor receptor signal transactivation. *IUBMB Life* **49**, 405-409
- Lev, S., Moreno, H., Martinez, R., Canoll, P., Peles, E., Musacchio, J.M., Plowman, G.D., Rudy, B. and Schlessinger, J. (1995) Protein tyrosine kinase PYK2 involved in Ca²⁺-induced regulation of ion channel and MAP kinase functions. *Nature*. **376**, 737-745.
- Levine, J.S., Koh, J.S., Triaca, V. and Lieberthal, W. (1997) Lysophosphatidic acid: A novel growth and survival factor for renal proximal tubular cells. *Am. J. Physiol.* **273**, F575-F585
- Linesman, D.A., Hofmann, F. and Fisher, S.K. (2000) A role for the small molecular weight GTPases, Rho and Cdc42, in muscarinic receptor signaling to focal adhesion kinase. *J. Neurochem.* **74**, 2010-2020
- Lopez-Illasaca, M., Crespo, P., Pellici, P.G., Gutkind, J.S. and Wetzker, R. (1997) Linkage of G protein-coupled receptors to the MAPK signaling pathway through PI 3-kinase γ . *Science* **275**, 394-397

- Lopez-Illasaca, M. (1998) Signaling from G-protein-coupled receptors to mitogen-activated protein (MAP)-kinase cascades. *Biochem. Pharmacol.* **56**, 269-277
- Lowry, O.H., Rosebrough, N.J., Farr, A.L. and Randall, R.J. (1951) Protein measurement with the folin phenol reagent. *J. Biol. Chem.* **193**, 265-275
- Lowy, D.R. and Willumsen, B.M. (1993) Function and regulation of Ras. *Annu. Rev. Biochem.* **62**, 851-891
- Luttrell, L.M., Hawes, B.E., van Biesen, T., Luttrell, D.K., Lansing, T.J. and Lefkowitz, R.J. (1996) Role of c-Src tyrosine kinase in G protein-coupled receptor- and G $\beta\gamma$ subunit-mediated activation of mitogen-activated protein kinases. *J. Biol. Chem.* **271**, 19443-19450
- Luttrell, L.M., Della Rocca, G.J., van Biesen, T., Luttrell, D.K. and Lefkowitz, R.J. (1997) G $\beta\gamma$ subunits mediate Src-dependent phosphorylation of the epidermal growth factor receptor. *J. Biol. Chem.* **272**, 4637-4644
- Luttrell, L.M., Daaka, Y. and Lefkowitz, R.J. (1999) Regulation of tyrosine kinase cascades by G-protein-coupled receptors. *Curr. Opin. Cell. Biol.* **11**, 177-183
- Maggio, R., Barbier, P., Bolognesi, M.L., Minarini, A., Tedeschi, D. and Melchiorre, C. (1994) Binding profile of the selective muscarinic antagonist tripitramine. *Eur. J. Pharmacol.* **268**, 459-462
- Malarkey, K., Belham, C.M., Paul, A., Graham, A., McLees, A., Scott, P.H. and Plevin, R. (1995) The regulation of tyrosine kinase signalling pathways by growth factor and G-protein-coupled receptors. *Biochem. J.* **309**, 361-375
- Marais, R., Light, Y., Mason, C., Paterson, H., Olsen, M.F. and Marshall, C.J. (1998) Requirement of Ras-GTP complexes for activation of Raf-1 by protein kinase C. *Science.* **280**, 109-112
- Maroney, A.C., Glicksman, M.A., Basma, A.N., Walton, K.M., Knight Jnr, E., Murphy, C.A., Bartlett, B.A., Finn, J.P., Angeles, T., Matsuda, Y., Neff, N.T., and Dionne, C. A. (1999) Motoneuron apoptosis is blocked by CEP-1347 (KT 7515), a novel inhibitor of the JNK signalling pathway. *J. Neurochem.* **18**, 104-111
- Maroney, A.C., Finn, J.P., Bozyczko-Coyne, D., O'Kane, T.M., Neff, N.T., Tolkovsky, A.M., Park, D.S., Yan, C.Y.I., Troy, C.M. and Greene, L.A. (1999) CEP-1347 (KT7515), an inhibitor of JNK activation, rescues sympathetic neurons and neuronally differentiated PC12 cells from death evoked by three distinct insults. *J. Neurochem.* **73**, 1901-1912
- Marshall, C.J. (1995) Specificity of receptor tyrosine kinase signaling: transient versus sustained extracellular signal-regulated kinase activation. *Cell.* **80**, 179-185
- Masgrau, R., Servitja, J.M., Sarri, E., Young, K.W., Nahorski, S.R. and Picatoste, F. (2000) Intracellular Ca²⁺ stores regulate muscarinic receptor stimulation of phospholipase C in cerebellar Granule cells. *J. Neurochem.* **74**, 818-826
- Matsui, M., Motomura, D., Karasawa, H., Fujikawa, T., Jiang, J., Komiya, Y., Takahashi, S-I., and Taketo, M.M. (2000) Multiple functional defects in peripheral autonomic organs in mice lacking acetylcholine receptor gene for the M3 subtype. *Proc. Natl. Acad. Sci. USA.* **97**, 9579-9584

McKenzie, F.R. and Pouyssegur, J. (1996) cAMP-mediated growth inhibition in fibroblasts is not mediated via mitogen-activated protein (MAP) kinase (ERK) inhibition. cAMP-dependent protein kinase induces a temporal shift in growth factor-stimulated MAP kinases. *J. Biol. Chem.* **271**, 13476-13483

Megson, A.C., Dickenson, J.M., Townsend-Nicholson, A. and Hill, S.J. (1995) Synergy between the inositol phosphate responses to transfected human adenosine A1-receptors and constitutive P2-purinoceptors in CHO-K1 cells. *Br. J. Pharmacol.* **115**, 1415-1424

Meloy, T.D., Daniels, D.V., Hedge, S.S., Eglen, R.M. and Ford, A.P.W. (2001) Functional characterisation of rat submaxillary gland muscarinic receptors using microphysiometry. *Br. J. Pharmacol.* **132**, 1606-1614

Meyer zu Heringdorf, D. Lass, H., Alemany, R., Laser, K.T., Neumann, E., Zhang, C., Schmidt, M., Rauen, U., Jakobs, K.H. and van Koppen, C.J. (1998) Sphingosine kinase-mediated Ca²⁺ signalling by G-protein-coupled receptors. *EMBO J.* **17**, 2830-2837

Minden, A., Lin, A., McMahon, M., Lange-Carter, C., Dérijard, B., Davis, R.J., Johnson, G.L. and Karin, M. (1994) Differential activation of ERK and JNK mitogen-activated protein kinases by Raf-1 and MEKK. *Science* **266**, 1719-1723

Minden, A., Lin, A., Claret, F-X., Abo, A. and Karin, M. (1995) Selective activation of the JNK signaling cascade and c-Jun transcriptional activity by the small GTPases Rac and Cdc42Hs. *Cell* **81**, 1147-1157

Minden, A. and Karin, M. (1997) Regulation and function of the JNK subgroup of MAP kinases. *Biochim. Biophys Acta.* **1333**, F85-F104

Mistry, R., Hornigold, D.C., Boxall, D.K., Eglen, R.M. and Challiss, R.A.J. (2000) Synergistic and antagonistic regulation of cyclic AMP levels in CHO cells by recombinant M₂- and M₃-muscarinic receptors. *Proc. Aust. Soc. Clin. Exp. Pharmacol. Toxicol.* **7**, 23

Mistry, R., Hornigold, D.C., Boxall, D.K., Eglen, R.M. and Challiss R.A.J. (2001) Regulation of adenylyl cyclase activity by crosstalk between M₂- and M₃-muscarinic acetylcholine receptors co-expressed in Chinese hamster ovary cells. *Submitted.*

Mitchell, F., Russell, M. and Johnson, G.L. (1995) Differential calcium dependence in the activation of c-Jun kinase and mitogen-activated protein kinase by muscarinic acetylcholine receptors in Rat 1a cells. *Biochem. J.* **309**, 381-384

Mochizuki, N., Ohba, Y., Kiyokawa, E., Kurata, T., Murakami, T., Ozaki, T., Kitabatake, A., Nagashima, K. and Matsuda, M. (1999) Activation of the ERK/MAPK pathway by an isoform of rap1GAP associated with Gα_i. *Nature* **400**, 891-894

Moriguchi, T., Toyoshima, F., Masuyama, N., Hanafusa, H., Gotoh, Y. and Nishida, E. (1997) A novel SAPK/JNK kinase, MKK7, stimulated by TNFα and cellular stresses. *EMBO J.* **16**, 7045-7053

Mukhin, Y.V., Garnovskaya, M.N., Collinsworth, G., Grewal, J.S., Pendergrass, D., Naga, T., Pinckney, S., Greene, E.L. and Raymond, J.R. (2000) 5-Hydroxytryptamine(1A) receptor/G(i)betagamma stimulates mitogen-activated protein kinase via NAD(P)H oxidase

- and reactive oxygen species upstream of Src in Chinese hamster ovary fibroblasts. *Biochem. J.* **347**, 61-67
- Nagoa, M., Yamauchi, J., Kaziro, Y. and Itoh, H. (1998) Involvement of protein kinase C and Src family tyrosine kinase in *Gαq/11*-induced activation of c-Jun N-terminal kinase and p38 mitogen-activated protein kinase. *J. Biol. Chem.* **273**, 22892-22898
- Nahorski, S.R., Ragan, C.I. and Challiss, R.A.J. (1991) Lithium and the phosphoinositide cycle: an example of uncompetitive inhibition and its pharmacological consequences. *Trends Pharmacol Sci.* **12**, 297-303
- Nahorski, S.R., Tobin, A.B. and Willars, G.B. (1997) Muscarinic M₃ receptor coupling and regulation. *Life Sci.* **60**, 1039-1045
- Nebrada, A.R. and Porras, A. (2000) p38 MAP kinases: beyond the stress response. *Trends. Bioc. Sci.* **25**, 257-260
- Neubig, R.R. (1998) Specificity of receptor-G protein coupling: protein structure and cellular determinants. *Seminars in Neuroscience.* **9**, 189-197
- Nicke, B., Detjen, K. and Logsdon, C.D. (1999) Muscarinic cholinergic receptors activate both inhibitory and stimulatory growth mechanisms in NIH3T3 cells. *J. Biol. Chem.* **274**, 21701-21706
- Northwood, I.C. , Gonzalez, F.A., Wartmann, M., Raden, D.L. and Davis, R.J. (1991) Isolation and characterization of two growth factor-stimulated protein kinases that phosphorylate the epidermal growth factor receptor at threonine 669 *J. Biol. Chem.* **266**, 15266-15276
- Offermans, S., Bombien, E. and Schultz, G. (1993) Stimulation of tyrosine phosphorylation and mitogen-activated-protein (MAP) kinase activity in human SH-SY5Y neuroblastoma cells by carbachol. *Biochem J.* **294**, 545-550
- Offermans, S. (1999) New insights into the in vivo function of heterotrimeric G-proteins through gene deletion studies. *Naunyn-Schmiedeberg's Arch. Pharmacol.* **360**, 5-13
- Orsini, M.J., Krymskaya, V.P., Esterhas, A.J., Benovic, J.L., Panettieri Jr, R.A. and Penn, R.B. (1999) MAPK superfamily activation in human airway smooth muscle: mitogenesis requires prolonged p42/p44 activation. *Am. J. Physiol.* **277**, L479-L488
- Pagès, G., Lenormand, P., L'Alemain, G., Chambard, J-C., Meloche, S. and Pouyssegur, J. (1993) Mitogen-activated protein kinases p42^{mapk} and p44^{mapk} are required for fibroblast proliferation. *Proc. Natl. Acad. Sci. USA.* **90**, 8319-8323
- Peralta, E.G., Winslow, J.W., Ashkenazi, A., Smith, D.H., Ramachandran, J. and Capon, D.J. (1987) Structural basis of muscarinic acetylcholine receptor subtype diversity. *Trends Pharmacol. Sci.* **8**, 6-11
- Pelicci, G., Lanfrancone, L., Grignani, F., McGlade, J., Cavallo, F., Forni, G., Nicoletti, I., Grignani, F., Pawson, T. and Pelicci, P.G. (1992) A novel transforming protein (SHC) with an SH2 domain is implicated in mitogenic signal transduction. *Cell.* **70**, 93-104

- Pouyssegur, J. and Seuwen, K. (1992) Transmembrane receptors and intracellular pathways that control cell proliferation. *Ann. Rev. Physiol.* 54, 195-210
- Pronk, G.J. and Bos, J.L. (1994) The role of p21^{ras} in receptor tyrosine kinase signalling. *Biochimica et Biophysica Acta*. 1198,131-147
- Quitterer, U. and Lohse, M.J. (1999) Cross-talk between G α I- and G α q-coupled receptors is mediated by G β y exchange. *Proc. Natl. Acad. Sci. USA*. 96, 10626-10631
- Rasmussen, H., Tokuwa, Y. and Park, S. (1987) Protein kinase c in the regulation of smooth muscle contraction. *FASEB, J.* 1, 177-185.
- Ray, L.B. and Sturgill, T.W. (1987) Rapid stimulation by insulin of a serine/threonine kinase in 3T3-L1 adipocytes that phosphorylates microtubule-associated protein 2 *in vitro*. *Proc. Natl. Acad. Sci. USA*. 84, 1502-1506
- Rhee, S.G. and Dennis, E.A. (1996) Chapman and Hall. In *Signal Transduction* Ed Heldin, C-H and Purton, M. Chapter 12. Function of Phospholipases in signal transduction. pp173-188
- Robinson, M. J., and Cobb, M.H., (1997) Mitogen-activated protein kinase pathways. *Curr. Opin. Cell. Biol.* 9,180-186
- Roffel, A.F., Elzinga, C.R.S., Van Amsterdam, R.G.M., De Zeeuw, R.A. and Zaagsma, J. (1988) Muscarinic M2 receptor in bovine tracheal smooth muscle: Discrepancies between binding and function. *Eur. J. Pharmacol.* 153, 73-82
- Roseberry, A.G., Bünnemann, M., Elavunkal, J. and Hosey, M.M. (2001) Agonist-dependent delivery of M2 muscarinic acetylcholine receptors to the cell surface after pertussis toxin treatment. *Mol. Pharmacol.* 59, 1256-1268
- Rozakis-Adcock, M., McGlade, J., Mbamalu, G., Pelicci, G., Daly, R., Li, W., Batzer, A., Thomas, S., Brugge, J., Pelicci, P.G., Schlessinger, J. and Pawson, T. (1992) Association of the Shc and Grb2/Sem5 SH2-containing proteins is implicated in activation of the Ras pathway by tyrosine kinases. *Nature*. 360, 689-692
- Rozakis-Adcock, M., Fernley, R., Wade, J., Pawson, T. and Bowtell, D. (1993) The SH2 and SH3 domains of mammalian Grb2 couple the EGF receptor to the Ras activator mSOS1. *Nature* 363, 83-85
- Sambrook, J., Fritsch, E.F. and Maniatis, T. (1989) in *Molecular Cloning, a laboratory manual*. Cold spring Harbor: Cold Spring Harbor Press.
- Sawyer, G.W. and Ehlert, F.J. (1999) Muscarinic M₃ receptor inactivation reveals a pertussis toxin-sensitive contractile response in the guinea pig colon: evidence for M₂/M₃ receptor interactions. *Mol. Pharmacol.* 289, 464-476
- Scatchard, G (1949) The attractions of proteins for small molecules and ions. *Ann. N.Y. Acad. Sci.* 51, 660-672
- Schmidt, M., Bienek, C., Van Koppen, C., Michel, M.C. and Jakobs, K.H. (1995) Differential calcium signalling by m2 and m3 muscarinic acetylcholine receptors in a single cell type. *Naunyn-Schmiedeberg's Arch. Pharmacol.* 352, 469-476

- Schonwasser, D.C., Marais, R.M., Marshall, C.J. and Parker, P.J. (1998) Activation of the mitogen-activated protein kinase/extracellular signal-regulated kinase pathway by conventional, novel and atypical protein kinase C isoforms. *Mol. Cell. Biol.* **18**, 790-798
- Selbie, L.A., King, N.V., Dickenson, J.M. and Hill, S.J. (1997) Role of G-protein $\beta\gamma$ subunits in the augmentation of P2Y₂ (P_{2U}) receptor-stimulated responses by neuropeptide Y Y₁ G_{i/o}-coupled receptors. *Biochem. J.* **328**, 153-158
- Selbie, L.A. and Hill, S.J. (1998) G protein-coupled-receptor cross-talk: the fine tuning of multiple receptor-signalling pathways. *Trends Pharmacol. Sci.* **19**, 87-93
- Shapiro, P.S., Evans, J.N., Davis, R.J. and Posada, J.A. (1996) The seven-transmembrane-spanning receptors for endothelin and thrombin cause proliferation of airway smooth muscle cells and activation of the extracellular regulated kinase and c-Jun NH₂-terminal kinase groups of mitogen-activated protein kinases. *J. Biol. Chem.* **271**, 5750-5754
- Short, S.M., Boyer, J.L. and Juliano, R.L. (2000) Integrins regulate the linkage between upstream and downstream events in G protein-coupled receptor signalling to mitogen-activated protein kinase. *J. Biol. Chem.* **275**, 12970-12977
- Simmonds, W.F. (1999) G protein regulation of adenylate cyclase. *Trends. Pharmacol. Sci.* **20**, 66-73
- Slack, B.E. (2000) The m3 muscarinic acetylcholine receptor is coupled to mitogen-activated protein kinase via protein kinase C and epidermal growth factor receptor kinase. *Biochem. J.* **348**, 381-387
- Stengel, P.W., Gomeza, J., Wess, J. and Cohen, M.L. (2000) M₂ and M₄ receptor knockout mice: muscarinic receptor function in cardiac and smooth muscle in vitro. *J. Pharm. Exp. Ther.* **292**, 877-885
- Stewart, A.G., Tomlinson, P.R. and Wilson, J.W. (1997) Beta 2-adrenoceptor agonist-mediated inhibition of human airway smooth muscle cell proliferation: importance of the duration of beta 2- adrenoceptor stimulation. *Br. J. Pharmacol.* **121**, 361-368
- Stokoe, D., Macdonald, S.G., Cadwallader, K., Symons, M. and Hancock, J.F. (1994) Activation of Raf as a result of recruitment to the plasma membrane. *Science* **264**, 1463-1467
- Strader, C.D., Fong, T.M., Tota, M.R. and Underwood, D. (1994) Structure and function of G protein-coupled receptors. *Annu. Rev. Biochem.* **63**, 101-132
- Sunahara, R.K., Dessauer, C.W. and Gilman, A.G. (1996) Complexity and diversity of mammalian adenylyl cyclases. *Annu. Rev. Pharmacol. Toxicol.* **36**, 461-480
- Tobin, A.B., Lambert, D.G. and Nahorski, S.R. (1992) Rapid desensitization of muscarinic m3 receptor-stimulated polyphosphoinositide responses. *Mol. Pharmacol.* **42**, 1042-1048
- Tobin, A.B., Keys, B. and Nahorski, S.R. (1996) Identification of a novel receptor kinase that phosphorylates a phospholipase C-linked muscarinic receptor. *Journal of Biological Chemistry.* **271**, 3907-3916

- Tombes, R.M., Aver, K.C., Mikkelsen, R., Valerie, K., Wymann, P., Marshall, C.J., McMahon, M. and Dent, P. (1998) The mitogen-activated protein (MAP) kinase cascade can either stimulate or inhibit DNA synthesis in primary cultures of rat hepatocytes depending upon whether its activation is acute/phasic or chronic. *Biochem. J.* **330**, 1451-1460
- Tomlinson, P.R., Wilson J.W. and Stewart A.G. (1995) Salbutamol inhibits the proliferation of human airway smooth muscle cells grown in culture: Relationship to elevated cAMP levels. *Biochem. Pharmacol.* **49**, 1809-1819
- Tournier, C., Whitmarsh, A.J., Cavanagh, J., Barrett, T. and Davis, R.J. (1997) Mitogen-activated protein kinase kinase 7 is an activator of the c-Jun NH₂-terminal kinase. *Proc. Natl. Acad. Sci.* **94**, 7337-7342
- Traverse, S., Gomez, N., Paterson, H., Marshall, C. and Cohen, P. (1992) Sustained activation of the mitogen-activated protein (MAP) kinase cascade may be required for differentiation of PC12 cells. *Biochem. J.* **28**, 351-355
- Treisman, R. (1996) Regulation of transcription by MAP kinase cascades. *Curr. Opin. Cell Biol.* **8**, 205-215
- Tu, M.T., Luo, S.F., Wang, C.C, Chien, C.S., Chiu, C.T., Liu, C.C. and Yang, C.M. (2000) P2Y₂ receptor-mediated proliferation of C6 glioma cells via activation of Ras/Raf/MEK/MAPK pathway. *Br. J. Pharmacol.* **129**, 1481-1489
- Van Biesen, T., Hawes, B.E., Raymond, J.R., Lutrell, L.M., Koch, W.J. and Lefkowitz, R.J. (1996) Go-protein α -subunits activate mitogen-activated protein kinase via a novel protein kinase C-dependent mechanism. *J. Biol. Chem.* **271**, 1266-1269
- Van der Geer, P., Hunter, T. and Lindberg, R.A. (1994) Receptor protein-tyrosine kinases and their signal transduction pathways. *Annu. Rev. Cell. Biol.* **10**, 251-337
- Vossler, M.R., Yao, H., York, R.D., Pan, M-G., Rim, C.S. and Stork, P.J.S. (1997) cAMP activates MAP kinase and Elk-1 through a B-Raf and Rap1-dependent pathway. *Cell* **89**, 73-82
- Wang, Y-X, Fleischmann, B.K., and Kotlikoff, M.I. (1997) M₂ receptor activation of nonselective cation channels in smooth muscle cells: calcium and G_i/G_o requirements. *Am. J. Physiol.* **273**, C500-C508
- Wang, Y-X, Dhulipala, P.D.K., Li, L., Benovic, J.L. and Kotlikoff, M.I. (1999) Coupling of M₂ muscarinic receptors to membrane ion channels via phosphoinositide 3-kinase γ and atypical protein kinase C. *J. Biol. Chem.* **274**, 13859-13864
- Waskiewicz, A.J. and Cooper, J.A. (1995) Mitogen and stress response pathways: MAP kinase cascades and phosphatase regulation in mammals and yeast. *Curr. Opin. Cell Biol.* **7**, 798-805
- Watkins, D.C., Moxham, C.M., Morris, A.J. and Malbon, C.C. (1994) Suppression of G α ₂ enhances phospholipase C signalling. *Biochem. J.* **299**, 593-596

Weber, J.D., Raben, D.M., Phillips, P.J. and Baldassare, J.J. (1997) Sustained activation of extracellular-signal-regulated kinase 1 (ERK1) is required for the continued expression of cyclin D1 in G₁ phase. *Biochem. J.* **326**, 61-68

Wess, J. (1993) Molecular basis of muscarinic acetylcholine receptor function. *Trends. Pharm. Sci.* **14**, 308-313

Whitmarsh, A.J., Cavanagh, J., Tournier, C., Yasuda, J. and Davis, R.J. (1998) A mammalian scaffold complex that selectively mediates MAP kinase activation. *Science* **281**, 1671-1674

Widdop, S., Daykin, K. and Hall, I.P. (1993) Expression of muscarinic M2 receptors in cultured human airway smooth muscle cells. *Am. J. Respir. Cell Mol. Biol.* **9**, 541-546

Williams, N.G., Zhong, H. and Minneman, K.P. (1998) Differential coupling of α_1 -, α_2 -, and β -adrenergic receptors to mitogen-activated protein kinase pathways and differentiation in transfected PC12 cells. *J. Biol. Chem.* **273**, 24624-24632

Winitz, S., Russell, M., Qian, N-X., Gardner, A., Dwyer, L. and Johnson, G.L. (1993) Involvement of Ras and Raf in the G_i-coupled acetylcholine muscarinic m2 receptor activation of mitogen-activated protein (MAP) kinase kinase and Map kinase. *J. Biol. Chem.* **268**, 19196-19199

Wu, J., Dent, P., Jelinek, T., Wolfman, A., Weber, M.J. and Sturgill, T.W. (1993) Inhibition of the EGF-activated MAP kinase signaling pathway by adenosine 3',5'-monophosphate. *Science.* **262**, 1065-1069

Wylie, P.G., Challiss, R.A.J. and Blank, J.L. (1999) Regulation of extracellular-signal regulated kinase and c-Jun N-terminal kinase by G-protein-linked muscarinic acetylcholine receptors. *Biochem. J.* **338**, 619-628

Wylie, P.G. (2000) Characterisation of extracellular signal regulated protein kinase 1/2 (ERK 1/2) and c-Jun NH₂-Terminal kinase (JNK/SAPK) in CHO cells expressing the muscarinic m2 and m3 receptors. PhD thesis. University of Leicester, England.

Xia, Z., Dickens, M., Raingeaud, J., Davis, R.J. and Greenberg, M.E. (1995) Opposing effects of ERK and JNK-p38 MAP kinases on apoptosis. *Science.* **270**, 1326-1331

Xia, Y., Makris, C., Su, B., Li, E., Yang, J., Nemerow, G.R. and Karin, M. (2000) MEK kinase 1 is critically required for c-Jun N-terminal kinase activation by proinflammatory stimuli and growth factor-induced cell migration. *Proc. Natl. Acad. Sci. USA.* **97**, 5243-5248

Yamada, M., Miyakawa, T., Duttaroy, A., Yamanaka, A., Moriguchi, T., Makita, R., Ogawa, M., Chou, C.J., Xia, B., Crawley, J.N., Felder, C.C., Deng, C-X, Wess, J. (2001) Mice lacking the M3 muscarinic acetylcholine receptor are hypophagic and lean. *Nature.* **410**, 207-212

Yamauchi, J., Kaziro, Y. and Itoh, H. (1997a) C-terminal mutation of G protein beta subunit affects differentially extracellular signal-regulated kinase and c-Jun N-terminal kinase pathways in human embryonal kidney 293 cells. *J. Biol. Chem.* **272**, 7602-7607

- Yamauchi, J., Nagao, M., Kaziro, Y. and Itoh, H. (1997b) Activation of p38 mitogen-activated protein kinase by signalling through G protein-coupled receptors. *J. Biol. Chem.* **272**, 27771-27777
- Yang, C-M., Dwyer, T.M., Mohan, P.M., IK, H. and Farley, J.M. (1990) Down-regulation of muscarinic receptors in the striatum of organophosphate-treated swine. *Toxicology and Applied Pharmacology.* **104**, 375-385
- Yang, C.M., Chou, S.P., Sung, T.S. and Chien, H.J. (1991) Regulation of functional muscarinic receptor expression in tracheal smooth muscle cells. *Am. J. Physiol.* **261**, C1123-C1129
- Young, K.W., Challiss, R.A.J., Nahorski, S.R. and Mackrill, J.J. (1999) Lysophosphatidic acid-mediated Ca²⁺ mobilization in human SH-SY5Y neuroblastoma cells is independent of phosphoinositide signalling, but dependent on sphingosine kinase activation. *Biochem. J.* **343**, 45-52
- Yung, Y., Yao, Z., Hanoch, T. and Seger R. (2000) ERK1b, a 46-kDa ERK isoform that is differentially regulated by MEK. *J. Biol. Chem.* **275**, 15799, 15808
- Zheng, C.F. and Guan, K.L. (1994) Activation of MEK family kinases requires phosphorylation of two conserved Ser/Thr residues. *EMBO J.* **13**, 1123-1131
- Zholos, A.V. and Bolton T.B. (1997) Muscarinic receptor subtypes controlling the cationic current in guinea-pig ileal smooth muscle. *Br. J. Pharmacol.* **122**, 885-893
- Zhou, G., Zhao, Q.B. and Dixon, J.E. (1995) Components of a new human protein kinase signal transduction pathway. *J. Biol. Chem.* **270**, 12665-12669